Contributions to Commodity Geology Research

U.S. GEOLOGICAL SURVEY BULLETIN 1877

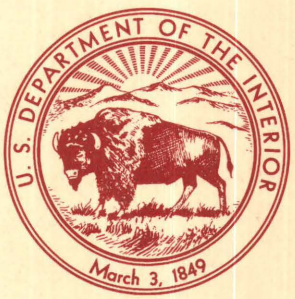

AVAILABILITY OF BOOKS AND MAPS OF THE U.S. GEOLOGICAL SURVEY

Instructions on ordering publications of the U.S. Geological Survey, along with prices of the last offerings, are given in the current-year issues of the monthly catalog "New Publications of the U.S. Geological Survey." Prices of available U.S. Geological Survey publications released prior to the current year are listed in the most recent annual "Price and Availability List." Publications that are listed in various U.S. Geological Survey catalogs (**see back inside cover**) but not listed in the most recent annual "Price and Availability List" are no longer available.

Prices of reports released to the open files are given in the listing "U.S. Geological Survey Open-File Reports," updated monthly, which is for sale in microfiche from U.S. Geological Survey Book and Open-File Report Sales, Box 25425, Denver, CO 80225. Reports released through the NTIS may be obtained by writing to the National Technical Information Service, U.S. Department of Commerce, Springfield, VA 22161; please include NTIS report number with inquiry.

Order U.S. Geological Survey publications **by mail** or **over the counter** from the offices given below.

BY MAIL

Books

Professional Papers, Bulletins, Water-Supply Papers, Techniques of Water-Resources Investigations, Circulars, publications of general interest (such as leaflets, pamphlets, booklets), single copies of Earthquakes & Volcanoes, Preliminary Determination of Epicenters, and some miscellaneous reports, including some of the foregoing series that have gone out of print at the Superintendent of Documents, are obtainable by mail from

U.S. Geological Survey, Book and Open-File Report Sales
Box 25425
Denver, CO 80225

Subscriptions to periodicals (Earthquakes & Volcanoes and Preliminary Determination of Epicenters) can be obtained ONLY from the

Superintendent of Documents
Government Printing Office
Washington, D.C. 20402

(Check or money order must be payable to Superintendent of Documents.)

Maps

For maps, address mail orders to

U.S. Geological Survey, Map Sales
Box 25286
Denver, CO 80225

Residents of Alaska may order maps from

U.S. Geological Survey, Map Sales
101 Twelfth Ave. - Box 12
Fairbanks, AK 99701

OVER THE COUNTER

Books

Books of the U.S. Geological Survey are available over the counter at the following U.S. Geological Survey Public Inquiries Offices, all of which are authorized agents of the Superintendent of Documents:

- **ANCHORAGE, Alaska**—Rm. 101, 4230 University Dr.
- **ANCHORAGE, Alaska**—Federal Bldg., Rm. E–146, 701 C St.
- **DENVER, Colorado**—Federal Bldg., Rm. 169, 1961 Stout St.
- **LAKEWOOD, Colorado**—Federal Center, Bldg. 810
- **MENLO PARK, California**—Bldg. 3 (Stop 533), Rm. 3128, 345 Middlefield Rd.
- **RESTON, Virginia**—503 National Center, Rm. 1C402, 12201 Sunrise Valley Dr.
- **SALT LAKE CITY, Utah**—Federal Bldg., Rm. 8105, 125 South State St.
- **SAN FRANCISCO, California**—Customhouse, Rm. 504, 555 Battery St.
- **SPOKANE, Washington**—U.S. Courthouse, Rm. 678, West 920 Riverside Ave.
- **WASHINGTON, D.C.**—Main Interior Bldg., 2600 corridor, 18th and C Sts., NW.

Maps

Maps may be purchased over the counter at the U.S. Geological Survey offices where books are sold (all addresses in above list) and at the following U.S. Geological Survey offices:

- **ROLLA, Missouri**—1400 Independence Rd.
- **DENVER, Colorado**—Map Distribution, Bldg. 810, Federal Center
- **FAIRBANKS, Alaska**—New Federal Bldg., 101 Twelfth Ave.

Contributions to Commodity Geology Research

JOHN H. DeYOUNG, Jr., and JANE M. HAMMARSTROM, editors

This volume is published as chapters A–K. These chapters are not available separately

U.S. GEOLOGICAL SURVEY BULLETIN 1877

U.S. DEPARTMENT OF THE INTERIOR
MANUEL LUJAN, Jr., Secretary

U.S. GEOLOGICAL SURVEY
Dallas L. Peck, Director

UNITED STATES GOVERNMENT PRINTING OFFICE: 1992

For sale by
Book and Open-File Report Sales
U.S. Geological Survey
Box 25425
Denver, CO 80225

Library of Congress Cataloging in Publication Data

Contributions to commodity geology research.
(U.S. Geological Survey bulletin ; 1877)
Bibliography: p.
Supt. of Docs. no. : I 19.3:1877
1. Geology, Economic. 2. Mines and mineral resources. I. DeYoung, John H., Jr. II. Hammarstrom, Jane Marie. III. Series. IV. Series: U.S. Geological Survey bulletin ; 1877.
QE75.B9 no. 1877 557.3 s [553] 88–600424
[TN260]

CONTENTS

[Letters designate the chapters]

Introduction

By John H. DeYoung, Jr.

What is commodity geology? It is defined here as the application of geologic science to the understanding of the geologic and economic aspects of resources of mineral commodities. The research results contributed to this bulletin provide some examples of the variety of geologic approaches to mineral-resource research. As an introduction to these studies, the following brief historical perspective on commodity geology is presented.

Some understanding of mineral-resource distribution in North America was a goal of early explorers who came to the New World with a mandate to search for gold and other precious metals. When the United States was founded and started to experience economic growth, concern about mineral resources and other raw materials became a concern of the Government. In 1833, geologist G.W. Featherstonhaugh wrote to the Secretary of War to recommend that "a geological chart, upon which all the metallic and mineral resources of each of the States should be accurately delineated, would be a labor productive of great advantages to the nation, and would be well received by it" (Featherstonhaugh, 1833, p. 5).

These ideas on a map of geology and mineral deposits were an early recognition of the importance of geologic science in national materials policy. In 1879, following a recommendation by the National Academy of Sciences, Congress combined the activities of four Territorial Surveys, which had been directed to explore the Western United States, into the U.S. Geological Survey (USGS). The USGS was charged to classify the public lands and to examine the geological structure, mineral resources, and products of the national domain.

Commodity geology became the essential role of geologists in the USGS Division of Mineral Resources; these geologists also collected statistics on production and resources of minerals for the annual publication "Mineral Resources of the U.S." In 1925, responsibility for the publication of "Mineral Resources of the U.S." (today's "Minerals Yearbook") and the attendant statistical collection was transferred to the Bureau of Mines (USBM), which had been established in 1910 (National Research Council, 1982, p. 129–131). Since that time, USGS commodity geologists have teamed up with commodity specialists in the USBM for several important studies of the national mineral position. Examples include the 1948 book "Mineral Resources of the United States" (USBM and USGS, 1948) and the basic report on Reserves and Potential Resources for the Paley Commission (President's Materials Policy Commission, 1952). Resource information from USGS geologists is a regular contribution to the annual publication of "Mineral Commodity Summaries" by the USBM.

Geologic studies of mineral resources, including descriptive and quantitative models of mineral deposits, research concerning the genesis and geologic setting of deposits, the distribution of elements among earth materials, and the investigation of possibilities for occurrence of undiscovered mineral resources continue to be important responsibilities of the USGS. Summaries of the geology and resources of mineral and energy commodities were published in 1973 in a benchmark USGS Professional Paper titled "United States Mineral Resources" (Brobst and Pratt, 1973). More recently, USGS work on models of mineral-deposit types has been published in a single volume, "Mineral Deposit Models," with 87 deposit models that include data from over 3,900 mineral deposits around the world (Cox and Singer, 1986).

Results of the diverse types of research included under the rubric of commodity geology are often abstracted in compendium-type publications, but more complete accounts of these studies are published in a variety of scientific journals and technical report series. This bulletin assembles several examples of commodity geology research. These examples do not comprehensively cover the range of geologic research applications to mineral commodity problems, but they do offer a sampling or flavor of the diversity of important questions about resource occurrences, questions that underlie frequently expressed concerns about minerals availability.

Four general research approaches are represented by the 11 papers. Two of these approaches are based on models of mineral-deposit types. Genetic models of mineral deposits offer interpretations of the geologic origin of deposits, thus making regional geologic history an important factor in predicting areas where undiscovered resources might occur. This type of genetic deposit model research is represented

Manuscript approved for publication September 28, 1988.

by the studies of Clark (barite) and Rytuba and Heropoulos (mercury). Quantitative models of the size of mineral deposits (grade and tonnage models) are constructed from the collection and analysis of statistics from well-explored deposits. The methods used in these studies can be applied in estimating the size of undiscovered resources in geologically favorable areas and in comparing the importance of different geologic mineral-deposit types in analyzing possibilities for mineral supply. Grade and tonnage model approaches are used in the papers by Orris (barite); Cox and Singer (gold); and Menzie, Jones, and Elliott (tungsten).

Descriptive accounts of the regional distribution of mineral commodities are a traditional economic geology approach to resource analysis. The reports of Williams (sand and gravel offshore the United States) and Elliott (tungsten in southeastern China) are representative of this type of study.

Less traditional, but of increasing importance as mineral production from certain conventional deposit types declines, is the study of different modes of occurrence for mineral commodities, either as different or lower grade deposit types having the sought-after commodity as a main product or as a potential byproduct in deposits of other minerals. Four examples of this type of research are presented here—Foose (nickel in laterites); Page, Briskey, and Mei (platinum-group elements in porphyry copper deposits); Page, Bagby, Madrid, and Moring (platinum-group elements in gold deposits); and Breit (vanadium in fossil-fuel deposits).

Concerns about the adequacy of future mineral supplies stimulate inquiry into mineral resources, but these concerns are not universally shared. For instance, the 33 specialists who constituted a Unesco Advisory Panel on Science, Technology and Society in the early 1980's were in large part optimistic about production and use of resources. They believed that inequities in population growth and resource availability could be ameliorated by "mandates." Two geologists at a 1986 Dahlem Workshop on Resources and World Development had a more supportive view of mineral-resource research, regarding "the issues of resource abundance and availability to be of vital importance to societal health," and concluding that inequities cannot be resolved "without major efforts to do so." (McLaren and Skinner, 1987, p. 1). In addition, some lessons of that Dahlem Workshop serve to temper the expectations that may be created by the title of this bulletin:

> All problems connected with resources and the environment involve many disciplines in science, technology, and socioeconomics; all issues are multifaceted and none is the prerogative of a single group of specialists.
>
> Science and technology can discover, describe and assess resources and the distribution of resources can be outlined, but scientists and technologists can say distressingly little about the economic viability of future resources. (McLaren and Skinner, 1987, p. 3.)

REFERENCES

Brobst, D.A., and Pratt, W.P., eds., 1973, United States mineral resources: U.S. Geological Survey Professional Paper 820, 722 p.

Cox, D.P., and Singer, D.A., eds., 1986, Mineral deposit models: U.S. Geological Survey Bulletin 1693, 379 p.

Featherstonhaugh, G.W., 1833, Letter dated January 12, 1833, to Lewis Cass, Secretary of War, *in* Public documents of the Senate of the United States, 22d Congress, 2d Session, v. I, document 35, p. 5–7.

McLaren, D.J., and Skinner, B.J., 1987, Introduction, *in* McLaren, D.J., and Skinner, B.J., eds., Resources and world development: Chichester, England, John Wiley and Sons, p. 1–12.

National Research Council, Committee on National Statistics, 1982, A review of the statistical program of the Bureau of Mines: Washington, D.C., National Academy Press, 210 p.

President's Materials Policy Commission, 1952, Resources for freedom, v. II, The outlook for key commodities: Washington, D.C., U.S. Government Printing Office, 210 p.

[U.S.] Bureau of Mines and [U.S.] Geological Survey, 1948, Mineral resources of the United States: Washington, D.C., Public Affairs Press, 212 p.

Chapter A

Barite—A Model for Deposition from Stratified Seawater Based on Barite Nodules in Paleozoic Shale and Mudstone of the Appalachian Basin

By SANDRA H.B. CLARK

U.S. GEOLOGICAL SURVEY BULLETIN 1877

CONTRIBUTIONS TO COMMODITY GEOLOGY RESEARCH

CONTENTS

FIGURES

Barite—A Model for Deposition from Stratified Seawater Based on Barite Nodules in Paleozoic Shale and Mudstone of the Appalachian Basin

By Sandra H.B. Clark

Abstract

Barite nodules occur in Ordovician and Devonian shales and mudstones of the Appalachian basin at numerous localities. Characteristics of some nodules, such as those having alternate layers of concentric calcite and barite, suggest that the nodules formed during early diagenesis as chemical conditions varied. Comparison of lithologies and environments of deposition at several localities suggests that these barite nodules formed at or near times of maximum sea level in mostly stagnant, oxygen-deficient marine environments and in association with calcareous and pyritic concretions. Some barite nodules occur in strata that record dysaerobic bottom conditions, which are between lithologies that represent aerobic and anaerobic bottom conditions. The characteristics of the nodules and enclosing shale and mudrock suggest that variations in Eh and pH conditions associated with the margins of anoxic seawater could result in the precipitation of barium from pore waters of the sediments. Although not enough barium is present in normal seawater to allow formation of significant amounts of barium precipitate, anoxic seawater of low to normal pH can contain substantial dissolved barium. Barite that reached deeper anoxic waters, possibly through the marine biological cycle, could dissolve and be concentrated at margins of anoxic water bodies. The model for concentration of barite from anoxic seawater at reduction-oxidation interfaces provides a feasible alternative to models that show barium derived from submarine-exhalative sources or other forms of hydrothermal fluids.

INTRODUCTION

Occurrences of barite in marine sedimentary rocks are widespread, and in some areas the accumulations are thick enough to constitute economically important bedded or stratiform barite deposits. In some deposits, for example those in Nevada and Arkansas, barite is dominant; in others, for example Meggen in Germany and Ballynoe in Ireland, barite is peripheral or laterally gradational into base-metal deposits. Because of possible economic significance, barite in marine sedimentary rocks is of interest as a potential indicator of associated stratiform deposits. A study of barite nodules in several localities from Ordovician and Devonian shale and mudstone of the Appalachian basin has led to a model of how barite could have been deposited from seawater in a stratified water body without introduction of barium from hydrothermal sources such as submarine springs. The objective of this paper is to present this model as a feasible alternative explanation for the occurrence of barite in marine shale and mudstone in the absence of evidence for submarine-exhalative activity.

I thank Eric R. Force, Wallace de Witt, Jr., Frank R. Ettensohn, Michael P. Cecile, Kevin L. Shelton, Walter E. Dean, Laurence M. Nuelle, and Forrest G. Poole for valuable comments and suggestions; Elizabeth E. Good for editing; and Sylvia M. Heinrich and Karen L. Cinsavich for assisting in the fieldwork.

CHARACTERISTICS OF THE NODULES

Barite nodules have been reported from Middle Ordovician shales in Tennessee, from Lower to Middle Devonian shales in Virginia, West Virginia, and Pennsylvania, and from Upper Devonian shales in New York (Carpenter and Fagan, 1969; de Witt, 1974; Way and Smith, 1983; Pepper and others, 1985; Nuelle and Shelton, 1986) (fig. 1).

The nodules commonly consist of acicular, bladed crystals oriented radially to a small central mass of equant barite crystals. Nodules of this type, called rosettes, may be hollow in the core and generally contain interstitial clay and other impurities in increasing amounts from core to rim. Another common type of nodule is composed of unoriented, irregularly shaped barite crystals in which clay fills interstices. Many of the nodules are spherical or oblate and commonly coalesce into irregular bulbous masses. The barite nodules are associated with pyritic concretions or with calcareous nodules and concretions or both at many localities. Laminae in the enclosing shale or mudstone

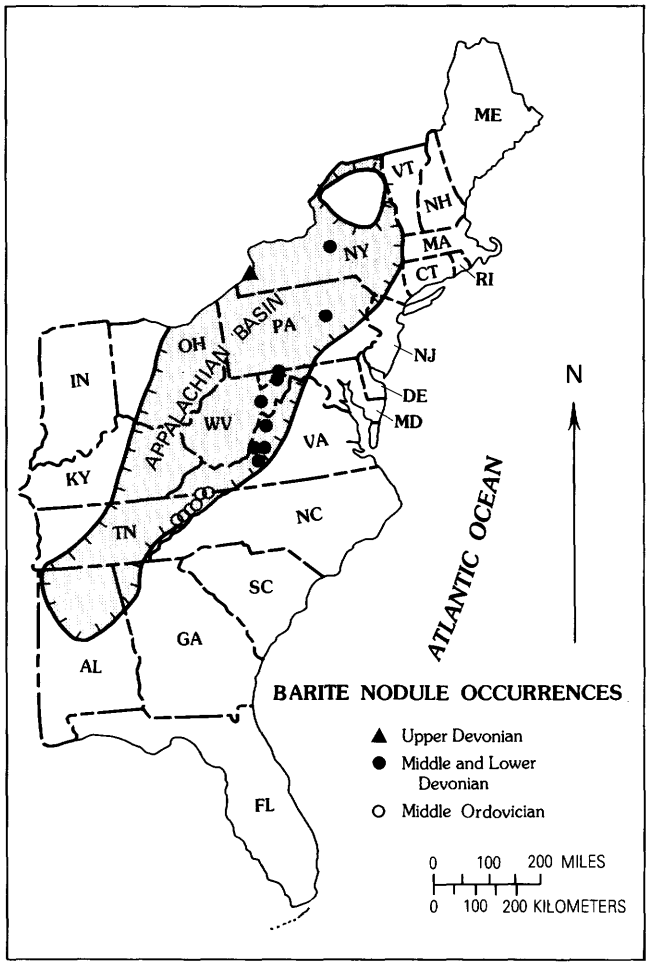

Figure 1. Places in the Eastern United States where barite nodules have been found in rocks of the Appalachian basin.

curve conformably around the nodules in little-deformed areas. Concentric calcareous and barite layers alternate in concretions, some of which are more than 12 cm in diameter, near Williamsville, Bath County, Va. Barite also fills shrinkage fractures in barite nodules as well as in septarian pyritic and calcareous concretions. Calcite, pyrite, and sphalerite are associated with barite in some of the fracture-filling veinlets.

Barite rosettes occur along bedding in mudstone and shale, which are compacted around the rosettes, near Silver Creek, Chautauqua County, N.Y. Barite fills the chambers of a large undeformed fossil cephalopod, and barite rosettes occur in a surrounding calcareous nodule (Pepper and others, 1985). The barite rosettes in the carbonate nodule are similar in size and form to rosettes in the main body of the rock.

The symmetric compaction of laminae around nodules, the association of barite with carbonate and pyrite, and the fact that barite fills chambers of undeformed fossils enclosed in calcareous nodules suggest that the barite formed early in diagenesis in response to slight fluctuations in reduction-oxidation potential and pH during development.

GEOLOGIC SETTING AND PALEOENVIRONMENT

Barite nodules in the western part of Virginia occur in the Lower to Middle Devonian Needmore Shale (fig. 2*A*), which represents prodeltaic deposition (Dennison, 1971) in a basin deep enough to restrict vertical circulation (Ettensohn and Barron, 1981). The shale and mudstone associated with the barite nodules in the Needmore Shale near Clifton Forge, Alleghany County, Va., were deposited in a basin of stratified stagnant water from water having different oxygen contents. Shale beneath the barite-nodule zone is dark gray to grayish black, fissile, carbonaceous, and mostly nonfossiliferous except for rare imprints of *Lingula*, suggesting deposition in an anaerobic environment. Barite nodules are in light- to medium-gray, olive-gray or yellowish-gray mudstone that contains sparse pelagic fossils (styliolinids and tentaculitids) and no benthic fossils. The lack of fissility in the mudstone in contrast to the fissility of the underlying and overlying shales is probably the result of bioturbation. This mudstone probably formed under dysaerobic conditions. Overlying the zone of barite nodules is light- to medium-gray and olive-gray silty mudstone containing abundant fossils, including several species of brachiopods, ostracods, and trilobites in addition to pelagic forms. This part of the section accumulated in oxidized water although still in a rather restricted deep-water facies. Barite nodules occur near Williamsville, Va., in a similar but less complete sequence and extend into the base of the highly fossiliferous aerobic zone. Geochemical profiles show slight enrichment of manganese, nickel, and cobalt in matrix shale of the dysaerobic and aerobic zones relative to those of the anaerobic zone and the opposite pattern for lead and silver (Clark and Mosier, 1989).

Barite nodules also occur in shales overlying the Needmore Shale (fig. 2*A*) that contain calcareous concretions and lenses: the Purcell Member of Cate (1963) of the Marcellus Shale in West Virginia, Maryland, and Pennsylvania (de Witt, 1974; Way and Smith, 1983; Nuelle and Shelton, 1986), the Chittenango Member of the Marcellus Shale in New York, beds containing calcareous concretions in the Millboro Shale in Virginia, and the Tully Limestone Member of the Harrell Shale in West Virginia (Nuelle and Shelton, 1986). Matrix shales for the barite nodules associated with calcareous lenses and concretions are mostly nonfossiliferous, fissile, carbonaceous, and pyritic and probably formed in anaerobic to dysaerobic environments.

Barite nodules near Silver Creek in western New York formed in a similar setting (Pepper and others, 1985). They occur mostly in the lower part of the Upper Devonian

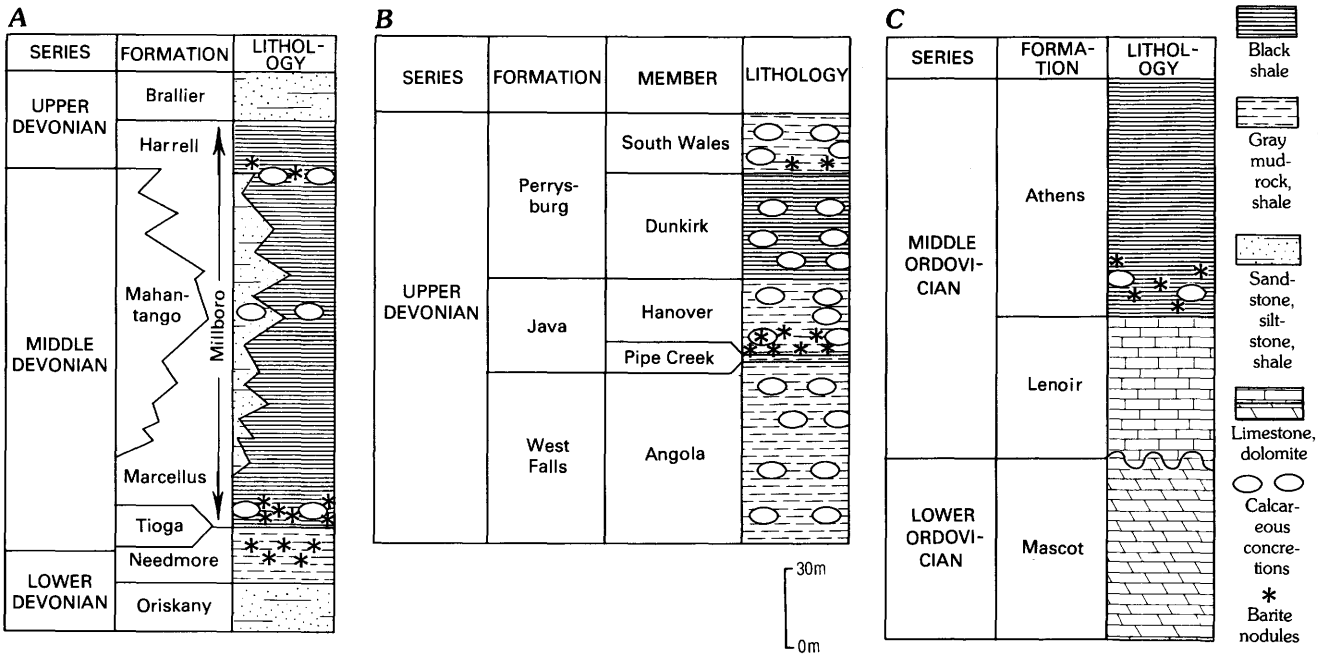

Figure 2. Generalized stratigraphic sections for barite-nodule localities: *A*, In Virginia, West Virginia, Maryland, Pennsylvania, and central New York; *B*, In western New York; *C*, In southern Virginia and Tennessee.

Hanover Shale Member of the Java Formation, although some are present in the South Wales Member of the overlying Perrysburg Formation (fig. 2*B*). The Hanover Shale Member, like the South Wales Member, is composed predominantly of gray mudrock that contains many calcareous concretions and nodules. It overlies a thin, fissile, black shale, the Pipe Creek Shale Member of the Java Formation. Similarly, the South Wales Member overlies a predominantly black-shale unit, the Dunkirk Shale Member of the Perrysburg Formation. The depositional setting was prodeltaic, and mud accumulated in a low-energy reducing environment.

Barite nodules in northeastern Tennessee and southern Virginia occur in the lower part of the Middle Ordovician Athens Shale (Carpenter and Fagan, 1969) (fig. 2*C*). The Athens Shale, which is predominantly dark gray to black, fissile, carbonaceous, and pyritic, probably formed in an anaerobic environment. It overlies the Lenoir Limestone, and nodular beds of limestone are locally interbedded in the lower part of the Athens Shale but are not present in all the barite-nodule localities.

Comparison of the lithologies containing barite nodules and their paleoenvironments shows that a common characteristic is nodule formation in shale and mudstone that were deposited in mostly anaerobic to dysaerobic environments in basinal prodeltaic settings. Some localities yield evidence of variation in reduction-oxidation potential in stratified waters; barite nodules occur in lithologies that were deposited under dysaerobic water columns, stratigraphically between lithologies formed under aerobic and anaerobic conditions. The barite-nodule zone may either underlie or overlie black shale. In other localities, barite is associated with carbonate nodules in dark-gray to black shale, suggesting that there may have been a local increase in pH that effected both the precipitation of calcium carbonate from solution (Blome and Albert, 1985) and the precipitation of barium sulfate to form nodules. The Devonian units in which the barite nodules occur represent sedimentation during or near maximum marine transgression (Johnson and others, 1985; Dennison, 1986).

Evidence for hot spring or other forms of hydrothermal activity such as feeder or fracture zones, crosscutting mineralization, or alteration has not been seen in the areas studied.

DISCUSSION

Several mechanisms have been suggested for barite formation in a marine environment. Submarine springs or exhalations are thought to be the source of barium in many deposits (Cecile and others, 1983; Brobst, 1984; Papke, 1984; Nuelle and Shelton, 1986). Connate brine and ground water have been suggested as fluids that transported barium to sites of precipitation on the sea floor (Hanor and Baria, 1977; Nuelle and Shelton, 1986). Deposition of barite in a sequence of carbonate rocks in northeastern British Columbia was attributed to mixing of anoxic seawater with meteoric ground water near the seaward edge of a coastal aquifer (Morrow and others, 1978). Miller and others

(1977) proposed sedimentary models for precipitation of barite in an anoxic environment; the models were based on studies of the organic fraction from black, bedded-barite samples. The possibility of biogenic concentration of barite was discussed by Shawe and others (1969). Puchelt (1967) suggested that barite may precipitate directly from seawater during evaporation when the volume of seawater is reduced to between one-third and one-fifth of its original volume, corresponding to the last stages of carbonate deposition and the initial stages of calcium sulfate precipitation.

Barite has been reported from deep-sea sediments in many localities (Dean and Schreiber, 1978). Although most is microcrystalline, locally nodules, rosettes, lenses, and laminae are common. Hydrothermal activity associated with rift zones was proposed as a source of the barium (Revelle and Emery, 1951; Arrhenius and Bonatti, 1965) as were biogenic processes (Church, 1979). Dean and Schreiber (1978) proposed that barite had a diagenetic origin at contacts between oxidizing and reducing environments and that the main source of barium was oxidation of organic matter.

The characteristics of the barite nodules described in this paper and their paleoenvironmental setting suggest that they formed by slow growth during diagenesis at or near reduction-oxidation interfaces in a stratified water column or locally near areas of increased pH.

Although barite is relatively insoluble under oxidizing conditions, it is fairly soluble in reducing conditions (fig. 3). Eh and pH values in the field of barite solubility can occur either within sediment on the sea floor with anoxic pore waters, or within anoxic seawater. With an increase in Eh or pH, or both, precipitation of barium sulfate and calcium carbonate would be predicted.

Barium introduced into seawater from hot springs could precipitate in the vicinity of the vent if the Eh of the water were in the stability range for sulfate (Cecile and others, 1983). In this situation, thick deposits of barite might form. A submarine spring venting into anoxic seawater would result in precipitation of sulfides near the vent and sulfates and oxides farther away at sites where the anoxic waters abut oxidized water. Although introduction of barium from submarine springs is a feasible mechanism to explain large accumulations of bedded barite and barite associated with stratiform submarine-exhalative base-metal deposits, the occurrence of barite nodules, lenses, and laminae can be explained by other models that do not involve introduction of barium in hydrothermal fluids or connate brines. In addition to the mechanisms discussed by other researchers, precipitation from anoxic water is a possibility that should be considered.

Although barium is undersaturated by a factor of about one-half in normal seawater (Church and Wolgemuth, 1972), barium can be concentrated in waters having the compositional range of anoxic seawater, as mentioned above. The geologic relations of barite nodules in the

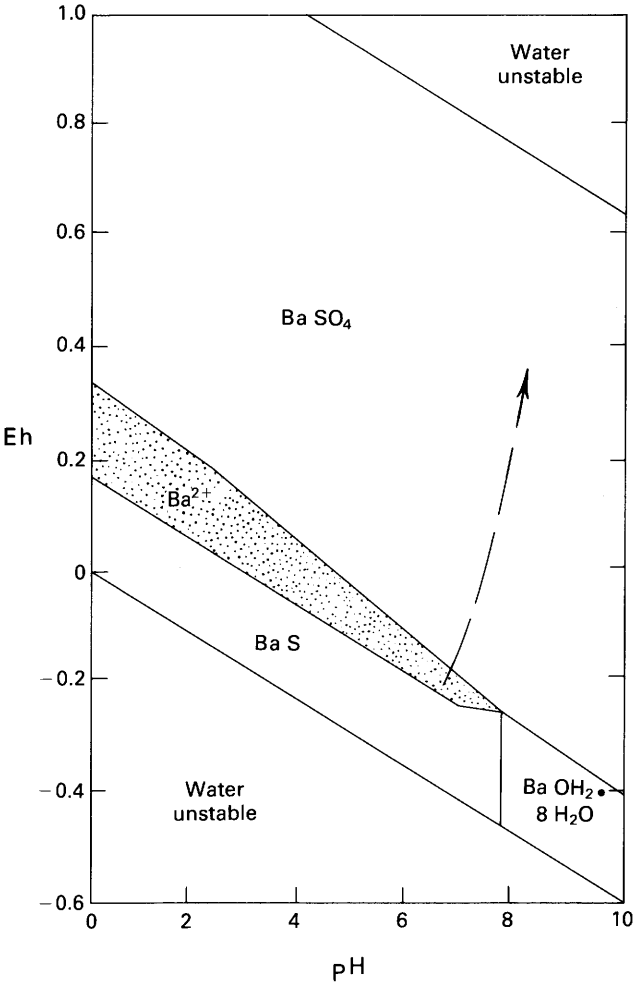

Figure 3. Eh-pH diagram for the system Ba-S-H_2O at 25 °C; 1 atmosphere total pressure; and total dissolved sulfur species=10^{-1}. Adapted from Schmitt (1962). The shaded area is the field of soluble Ba; the long arrow (from Cannon and Force, 1983) shows the change in Eh-pH conditions of water from the Black Sea going from deep anoxic bottom water to oxidized surface water.

Appalachian basin show that reduction-oxidation interfaces are indeed loci of barite-nodule formation. Barium may also be concentrated at interfaces with waters of slightly increased pH in anoxic zones, thus providing an explanation for the association of barite with calcareous and pyritic nodules in dark-gray to black carbonaceous shale.

Concentration of barium by organisms is well known. Bowen (1956) reported barium concentrations ranging from 450 to 4,400 times that in seawater in a wide variety of marine organisms. Observations of Chow and Goldberg (1960), Arrhenius and Bonatti (1965), Dean and Schreiber (1978), and Church (1979) show that involvement of organisms can be important in barite formation.

A model for the concentration of barite from anoxic seawater shown in figure 4 is proposed to explain features in the barite-nodule localities described above. The model is

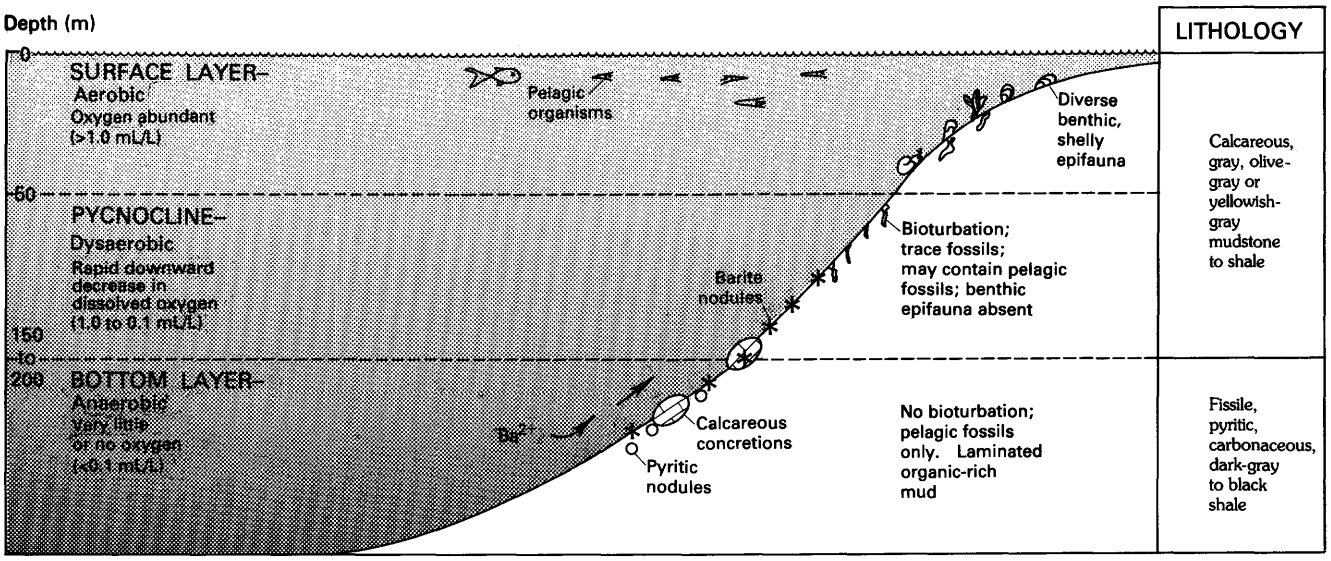

Figure 4. Model for the formation of barite from stratified water. Model of stratified water adapted from Rhoads and Morse (1971), Byers (1977), Ettensohn and Barron (1981), and Ettensohn (1985).

similar and related to the "bathtub ring" model for the formation of shallow marine sedimentary manganese deposits (Cannon and Force, 1983; Force and Cannon, 1988). Eh-pH relations suggest that barite precipitates at lower levels of oxidation than do manganese oxides; thus, barite is more likely to precipitate in the dysaerobic facies than are manganese oxides. However, the Eh-pH relations also suggest that barite might be associated with manganese carbonates, and, indeed, the association of barite with some manganese deposits has been noted by Force and Cannon (1988). The pattern of enrichment of trace amounts of manganese along with cobalt, zinc, and nickel (which could be adsorbed on manganese oxides) in the shale and mudstone in barite nodule zones in western Virginia also supports the suggestion of the relation between barium and manganese deposition (Clark and Mosier, 1989).

In the absence of independent evidence of a submarine exhalative or other hydrothermal source for barium, I suggest the following origin: Barite nodules, layers, or laminae in shales or mudstones that formed at or near times of maximum sea level in dysaerobic to aerobic zones of basins of stratified water or that are associated with carbonate concretions or lenses in anaerobic to dysaerobic zones could have resulted from precipitation of barium dissolved in anoxic pore water.

REFERENCES CITED

Arrhenius, Gustaf, and Bonatti, Enrico, 1965, Neptunism and vulcanism in the ocean, *in* Sears, Mary, ed., Progress in oceanography, v. 3: New York, Pergamon Press, p. 7–22.

Blome, C.D., and Albert, N.R., 1985, Carbonate concretions—An ideal sedimentary host for microfossils: Geology, v. 13, p. 212–215.

Bowen, H.J.M., 1956, Strontium and barium in sea water and marine organisms: Marine Biology Association (United Kingdom) Journal, v. 35, p. 451–460.

Brobst, D.A., 1984, The geologic framework of barite resources: Institution of Mining and Metallurgy Transactions, sec. A, v. 93, p. A123–A130.

Byers, C.W., 1977, Biofacies patterns in euxinic basins—A general model: Society of Economic Paleontologists and Mineralogists Special Publication 25, p. 5–17.

Cannon, W.F., and Force, E.R., 1983, Potential for high-grade shallow-marine manganese deposits in North America, *in* Shanks, W.C., III, ed., Cameron volume on unconventional mineral deposits: New York, American Institute of Mining, Metallurgical and Petroleum Engineers, Society of Mining Engineers, p. 175–189.

Carpenter, R.H., and Fagan, J.M., 1969, Barite nodules in the Athens Shale in northeastern Tennessee and southwest Virginia: Southeastern Geology, v. 10, no. 1, p. 17–29.

Cate, A.S., 1963, Lithostratigraphy of some Middle and Upper Devonian rocks in the subsurface of southwestern Pennsylvania: Pennsylvania Topographic and Geological Survey, General Geology Report G39, p. 229–240.

Cecile, M.P., Shakur, M.A., and Krouse, H.R., 1983, The isotopic composition of western Canadian barites and the possible derivation of oceanic sulphate $\delta^{34}S$ and $\delta^{18}O$ age curves: Canadian Journal of Earth Sciences, v. 20, no. 10, p. 1528–1535.

Chow, T.J., and Goldberg, E.D., 1960, On the marine geochemistry of barium: Geochimica et Cosmochimica Acta, v. 20, p. 192–198.

Church, T.M., 1979, Marine barite, *in* Burns, R.G., ed., Marine minerals: Mineralogical Society of America Short Course Notes, v. 6, p. 175–209.

Church, T.M., and Wolgemuth, Kenneth, 1972, Marine barite saturation: Earth and Planetary Science Letters, v. 15, no. 1, p. 35–44.

Clark, S.H.B., and Mosier, E.L., 1989, Barite nodules in Devonian shale and mudstone of western Virginia: U.S. Geological Survey Bulletin 1880, 30 p.

Dean, W.E., and Schreiber, B.C., 1978, Authigenic barite, Leg 41 Deep Sea Drilling Project, *in* California University, Scripps Institution of Oceanography, La Jolla, Initial reports of the Deep Sea Drilling Project, v. XLI: Washington, D.C., National Science Foundation, p. 915–931.

Dennison, J.M., 1971, Petroleum related to Middle and Upper Devonian deltaic facies in the Central Appalachians: American Association of Petroleum Geologists Bulletin, v. 55, p. 1179–1193.

———1986, Devonian sea-level curve for Virginia and West Virginia compared with eustatic curve of Johnson, Klapper, and Sandberg (1985): Geological Society of America Abstracts with Programs, v. 18, no. 3, p. 218.

de Witt, Wallace, Jr., 1974, Geologic map of the Beans Cove and Hyndman quadrangles and part of the Fairhope quadrangle, Bedford County, Pennsylvania: U.S. Geological Survey Miscellaneous Investigations Series Map I–801, scale 1:24,000.

Ettensohn, F.R., 1985, Controls on development of Catskill Delta complex basin-facies, *in* Woodrow, D.L., and Sevon, W.D., eds., The Catskill Delta: Geological Society of America Special Paper 201, p. 65–77.

Ettensohn, F.R., and Barron, L.S., 1981, Depositional model for the Devonian-Mississippian black shales of North America—A paleoclimatic-paleogeographic approach, *in* Roberts, T.G., ed., GSA Cincinnati '81 field trip guidebooks, v. 2: Falls Church, Virginia, American Geological Institute, p. 344–361.

Force, E.R., and Cannon, W.F., 1988, Depositional model for shallow-marine manganese deposits around black shale basins: Economic Geology, v. 83, p. 93–117.

Hanor, J.S., and Baria, L.R., 1977, Controls on the distribution of barite deposits in Arkansas, *in* Stone, C.G., ed., Symposium on the geology of the Ouachita Mountains, v. 2: Little Rock, Arkansas Geological Commission, p. 42–49.

Johnson, J.G., Klapper, Gilbert, and Sandberg, C.A., 1985, Devonian eustatic fluctuations in Euramerica: Geological Society of America Bulletin, v. 96, no. 5, p. 567–587.

Miller, R.E., Brobst, D.A., and Beck, P.C., 1977, The organic geochemistry of black sedimentary barite—Significance and implications of trapped fatty acids: Organic Geochemistry, v. 1, p. 11–26.

Morrow, D.W., Krouse, H.R., Ghent, E.D., Taylor, G.C., and Dawson, K.R., 1978, A hypothesis concerning the origin of barite in Devonian carbonate rocks of northeastern British Columbia: Canadian Journal of Earth Sciences, v. 15, p. 1391–1406.

Nuelle, L.M., and Shelton, K.L., 1986, Geologic and geochemical evidence of possible bedded-barite deposits in Devonian rocks of the Valley and Ridge province, Appalachian Mountains: Economic Geology, v. 81, p. 1408–1430.

Papke, K.G., 1984, Barite in Nevada: Nevada Bureau of Mines and Geology Bulletin 98, 125 p.

Pepper, J.F., Clark, S.H.B., and de Witt, Wallace, Jr., 1985, Nodules of diagenetic barite in Upper Devonian shales of western New York: U.S. Geological Survey Bulletin 1653, 11 p.

Puchelt, Harald, 1967, Zur Geochemie des Bariums im exogenen Zyklus: New York, Springer-Verlag, 205 p.

Revelle, Roger, and Emery, K.O., 1951, Barite concretions from the ocean floor: Geological Society of America Bulletin, v. 62, p. 707–724.

Rhoads, D.C., and Morse, J.W., 1971, Evolutionary and ecologic significance of oxygen-deficient marine basins: Lethaia, v. 4, p. 413–428.

Schmitt, H.H., ed., 1962, Equilibrium diagrams for minerals at low temperature and pressure: Cambridge, Massachusetts, Geological Club of Harvard, 199 p.

Shawe, D.R., Poole, F.G., and Brobst, D.A., 1969, Newly discovered bedded barite deposits in East Northumberland Canyon, Nye County, Nevada: Economic Geology, v. 64, no. 3, p. 245–254.

Way, J.H., and Smith, R.C., II, 1983, Barite in the Devonian Marcellus Formation, Montour County: Pennsylvania Geology, v. 14 no. 1, p. 4–9.

Chapter B

Barite—A Comparison of Grades and Tonnages for Bedded Barite Deposits with and without Associated Base-Metal Sulfides

By GRETA J. ORRIS

U.S. GEOLOGICAL SURVEY BULLETIN 1877

CONTRIBUTIONS TO COMMODITY GEOLOGY RESEARCH

CONTENTS

FIGURES

TABLES

Barite—A Comparison of Grades and Tonnages for Bedded Barite Deposits with and without Associated Base-Metal Sulfides

By Greta J. Orris

Abstract

Bedded barite mineralization may occur in distinct deposits or in deposits intimately associated with stratiform base-metal sulfide deposits that occur in a similar geologic environment. Analysis of grade, tonnage, and contained barite from the two styles of bedded barite mineralization shows that they can be treated as a single deposit type for the purpose of estimating barite resources.

INTRODUCTION

Basic geologic and descriptive data were collected for 93 deposits classified as bedded or stratiform barite deposits in the geologic literature; the majority of these data have been released as a U.S. Geological Survey Open-File Report (Orris, 1985). Many of the major deposits in this classification, including Meggen, West Germany (Krebs, 1981), and Ballynoe, Ireland, the barite deposit associated with the Silvermines base-metal deposit (Taylor and Andrew, 1978), are associated with stratiform zinc-lead sulfide mineralization. Other deposits, recently the dominant producers of barite, are not spatially associated with base-metal sulfides (Brobst, 1984). These latter deposits include all the known bedded deposits in the Nevada bedded barite belt of Papke (1984) and deposits in Arkansas, the Cuddapah district of India, and some of the deposits in the Selwyn Basin of the Canadian Yukon.

Previous work (Singer and others, 1975; Foose and others, 1980; Singer and DeYoung, 1980) has shown that the lognormal distribution closely approximates observed distributions of ore tonnage, grade, and contained metal for deposits grouped by geologic deposit type. Inclusion of this information from deposits not belonging to the specified deposit type may result in deviations from lognormal distribution. Failure of normality may be identified by using standard statistical techniques or may commonly be observed on frequency distribution plots as breaks or changes in slope. In this study, these techniques were used to identify differences in grade, tonnage, or contained barite between bedded barite deposits with and without associated base-metal sulfide mineralization.

GEOLOGIC SETTING

Barite deposits have routinely been classified within three major deposit types: veins and cavity fillings, residual deposits, and bedded deposits (Brobst, 1984). The bedded deposits include all stratiform bodies within layered, generally sedimentary, sequences of rock or the metamorphic equivalents that have barite as the principal mineral but are not residual deposits or karst fillings. Bedded barite generally occurs in rocks of mid-Paleozoic age, but deposits have been reported in rocks as old as Archean and as young as Cretaceous (Orris, 1985). The host rock sequences are diverse; they most commonly contain chert, argillite, shale, and (or) limestone but can also be composed of dolomite, slate, tuff and volcaniclastic rocks, sandstone, quartzite, greenstone, phyllite, and (or) schist. The host rocks and the contained barite are commonly gray to black because of included organic material but have been reported in colors as diverse as white, cherry red, and green (Orris, 1985).

Many bedded barite deposits exhibit primary depositional and diagenetic features such as graded bedding or crossbedding, rhythmic layering, large-scale interbedding of chert or shale and barite, bending of shale layers around barite nodules, and stylolite seams at the base of baritic layers (Zimmermann and Amstutz, 1964; Zimmermann, 1969, 1976). Some deposits show replacement features including baritized fossils, inclusions of host chert or limestone in the barite, and crosscutting of host rock texture by blades and rosettes of barite (Ketner, 1965, 1975). Evidence of both primary depositional and replacement processes is present in many deposits and typically is explained by the proposal of a submarine-exhalative genesis for the deposit (Zimmermann and Amstutz, 1964; Dawson and Orchard, 1982; Papke, 1984).

In general, the commercial bedded barite deposits are composed of fetid, gray to black, fine-grained barite that occurs either as massive lenses or in beds that vary from thinly laminated to over 15 m thick. Conglomeratic beds, barite rosettes or nodules, and barite cement are common in some deposits. Most of the ore exceeds 50 percent barite and may contain quartz, calcite, organic matter, secondary iron oxide, and some clay or mica. Pyrite is the most abundant sulfide and occurs in over 50 percent of the deposits. Base-metal sulfides are reported in trace to economic quantities in, or closely associated with, over 40 percent of the deposits (Orris, 1985).

Bedded barite deposits may occur as essentially monomineralic deposits such as those in Nevada (Papke, 1984). However, in other areas, stratiform barite deposits commonly have been reported in association with most types of stratiform base-metal deposits including massive sulfide mineralization in felsic to intermediate volcanics (Singer, 1986) and sediment-hosted exhalative zinc-lead deposits (Large, 1981, 1983; Briskey, 1986). Other bedded barite deposits are peripheral, or laterally gradational, to manganese deposits, bedded iron, phosphate, or evaporitic sequences of gypsum and anhydrite. Most of the economic bedded barite deposits occur in sequences of rocks similar to those of sediment-hosted exhalative zinc-lead deposits, but some deposits are in sequences containing abundant volcaniclastic rocks and associated with volcanic-hosted massive sulfides; other deposits occur in limestone or dolomite and are associated with carbonate-hosted deposits.

GRADE-TONNAGE DATA

Deposit size and grade data are available for the 30 bedded barite deposits listed in table 1. Grades are average grades for each deposit, and for some deposits the average percentage of $BaSO_4$ was calculated from reported average densities of the ore. Sizes of deposits are estimates consisting of reported reserves and any known production. Reserve data for these deposits may be calculated on the basis of gravity studies, drilling, or geologic inference, but the method and level of certainty of the estimation are rarely specified. Thirty-two percent of these deposits have associated lead-zinc sulfide mineralization; five of them (Ballynoe, Ireland; Cirque and Mel, Canada; Meggen and Rammelsberg, Germany) are considered principally base-metal sulfide deposits. Barite deposits with associated lead-zinc sulfides are under-represented in the grade-tonnage data set; only 45 percent of the 93 deposits examined in this study report the presence of any base-metal sulfides.

The grades collected for most bedded barite deposits range from 50 percent to 90 percent barite with a mean of 84 percent for the compiled grade data. In barite-lead-zinc deposits, these grades generally reflect a barite-rich lens or zone peripheral to the base-metal sulfide mineralization (Brobst, 1984; Briskey, 1986). Lower grades, generally less than 30 percent, have been reported for some barite that is associated with lead-zinc mineralization; for instance, Carne (1979) reports 25 percent $BaSO_4$ at the Tom lead-zinc deposit in the Canadian Yukon, and the Canada Department of Energy, Mines and Resources (1980) lists 28 percent barite in a stratiform body in schist at the Homestake mine in British Columbia. There is a distinct absence of reported barite grades between 30 and 50 percent. The lower grades of barite may reflect barite present as gangue within lead-zinc deposits and recovered only as a byproduct or a barite grade determined using total base-metal plus barite ore tonnage rather than a barite grade determined solely for the barite-enriched portion(s) of the deposit.

The sample population of 30 barite grades does not have a normal distribution; this is shown by an equivalent of the Shapiro-Wilks test of normality (Shapiro, 1980; Ryan and others, 1982). The correlation factors produced by this test and other summary statistics are presented in table 2. The lack of normality is visually apparent in the convex shape of the inverse cumulative frequency distribution plot of grades (fig. 1). The grade distribution of bedded barite can be attributed to what might be termed the mineralogical limit of barite; it is not possible to have greater than 100 percent barite ore to round out the distribution.

Grade populations of bedded barite deposits with and without associated base-metal sulfides were plotted and compared to determine if there were significant differences in grade between the two sample populations. (Summary statistics are available in table 2.) The distribution of the subset of deposits with base-metal sulfides cannot be shown to be different from a normal distribution, probably because of the small sample size (n=9), and a Mann-Whitney comparison (Ryan and others, 1982) of the medians of the subsets does not show them to be significantly different at the 5-percent level. Therefore, bedded barite with associated base-metal sulfides cannot be shown to be different from bedded barite without associated base-metals on the basis of grade. Because the shapes of the grade curves for the subsets are similar, the frequency distribution is considered appropriate for estimating the occurrence of undiscovered deposit grades even though the population is not normal.

Unlike grade, tonnage shows a lognormal frequency distribution for bedded barite deposits (fig. 2, table 2). Again, a Mann-Whitney comparison of the medians of the two sample populations composed of barite with and without associated base-metals fails to show that the tonnage sample populations are different. Ore tonnages for the 30 bedded barite deposits range from approximately 40,000 metric tons to over 55,000,000 metric tons with a median of 2,600,000 metric tons (fig. 3). Correlation of tonnage with grade is not significantly different than zero; grade neither increases nor decreases in a predictable way with tonnage.

Table 1. Bedded barite deposits used for grade and tonnage models

Name	Location	Age, host rocks
Ballynoe	Ireland	Carboniferous carbonaceous shale, dolostone, and minor chert and limestone.
Ban Thimontha	Thailand	Ordovician-Silurian shale and sandstone.
Barite (Moose)	Yukon Territory, Canada	Devonian-Mississippian black carbonaceous argillite, black chert, and conglomerate.
Barite Valley	South Africa	Archean chert, shale, and tuffites.
Baw Hin Khao	Thailand	Devonian-Mississippian dolomite and minor shale.
Brookfield	Nova Scotia, Canada	Mississippian ferruginous shale and siltstone.
Camamu Bay	Brazil	Cretaceous arkosic sandstone and shale with conglomerate and limestone.
Castle Island	Alaska, United States	Siliceous metasedimentary rock, pillow lavas.
Cathy (Walt)	Yukon Territory, Canada	Devonian argillite, shale, limestone, chert, and conglomerate.
Cirque	British Columbia, Canada	Devonian black carbonaceous shale, siliceous argillite, and chert.
Foss-Ben Eagach	Great Britain	Proterozoic schist.
Greystone	Nevada, United States	Devonian black chert with minor black argillite, gray shale, and limestone(?).
Gurrunda	New South Wales, Australia	Silurian tuffaceous sandstone, shale, and volcanic rocks.
Kempfield	New South Wales, Australia	Silurian siltstone, shale, and volcanic rocks.
Khuzdar	Pakistan	Jurassic gray limestone and shale.
Magnet Cove	Arkansas, United States	Mississippian shale, sandstone.
Mangampeta (2 deposits)	India	Cambrian(?) carbonaceous shale, dolostone, and quartzite.
Meggen	Germany	Middle Devonian slate, limestone, and shale.
Mel	Yukon Territory, Canada	Cambrian-Ordovician limey shale, limestone, and phyllite.
Mountain Springs	Nevada, United States	Devonian black chert with minor argillite and shale.
Nimiuktuk	Alaska, United States	Upper Mississippian black carbonaceous shale and chert.
Phu Mai Tong	Thailand	Ordovician-Devonian(?) shale.
Rammelsberg	Germany	Devonian carbonaceous black shale and slate with sandstone, limestone, and tuff.
Savercool	California, United States	Carboniferous limestone, slate, and quartzite.
Schoonoord	South Africa	Chert.
Snake Mountains	Nevada, United States	Ordovician chert, shale, argillite, conglomerate, limestone, greenstone, and siltstone.
Tea	Yukon Territory, Canada	Lower Mississippian black argillite, shale, siltstone, chert, and limestone.
Uribe	Washington, United States	Paleozoic siliceous siltstone and argillite with intercalated limestone.
Weekaroo	South Australia, Australia	Archean.

A Shapiro-Wilks equivalent test of normality (table 2) shows that contained barite tonnages have normal distribution for the base-metal-sulfide and no base-metal-sulfide subsets, as well as for the data set as a whole. Contained barite is the total amount of barite contained within a deposit, approximated by the product of the deposit tonnage and average grade. As with grade and ore tonnage, a Mann-Whitney comparison failed to show that the subsets were significantly different from each other. Contained barite has a high (r=0.99) positive correlation with ore tonnage, but its correlation with grade is not significantly different from zero. The strong correlation between contained metal and deposit tonnage was observed by Singer and DeYoung (1980) to be typical for the deposit types they investigated, as was the lack of correlation between contained metal and grade. The strong correlation between contained metal and deposit tonnage suggests the observed lack of correlation between grade and tonnage.

SUMMARY

The grade, tonnage, and contained barite content of bedded barite deposits show that stratiform deposits with and without base-metal sulfides may be treated statistically as a single deposit type when estimating barite resources. The independence of grade and tonnage for bedded barite deposits is convenient for modeling grades and tonnages of undiscovered deposits in the manner described by Singer and others (1975) for porphyry copper deposits.

Table 2. Summary statistics for bedded barite grade, tonnage, and contained barite

[All statistics generated by using MINITAB (Ryan and others, 1982) on an IBM personal computer; *n*, number; t, metric ton]

	n	Mean	Median	Standard deviation	Shapiro-Wilks correlation	Comment
Grades						
All deposits	30	84.6%	90.0%	0.123	0.923	not lognormal
Barite ± pyrite	21	87.1%	90.3%	.098	.928	not lognormal
Barite ± base-metal sulfides	9	78.6%	85.0%	.159	.938	normal
Tonnages						
All deposits	30	1,663,000 t	2,606,000 t	.903	.984	lognormal
Barite ± pyrite	21	1,641,000 t	2,723,000 t	.901	.981	lognormal
Barite ± base-metal sulfides	9	1,714,000 t	2,500,000 t	.961	.974	lognormal
Contained barite						
All deposits	30	1,390,000 t	2,307,000 t	.901	.981	lognormal
Barite ± pyrite	21	1,419,000 t	2,323,000 t	.912	.980	lognormal
Barite ± base-metal sulfides	9	1,321,000 t	2,123,000 t	.930	.963	lognormal

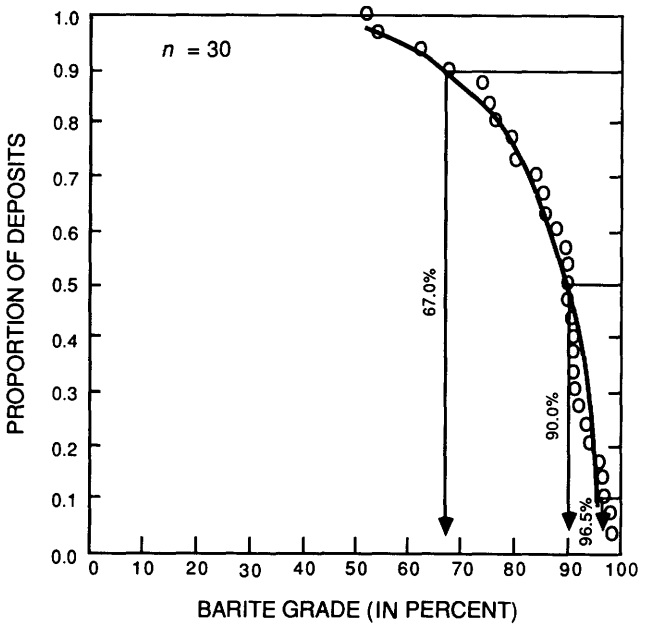

Figure 1. Inverse cumulative frequency plot of grades for 30 bedded barite deposits.

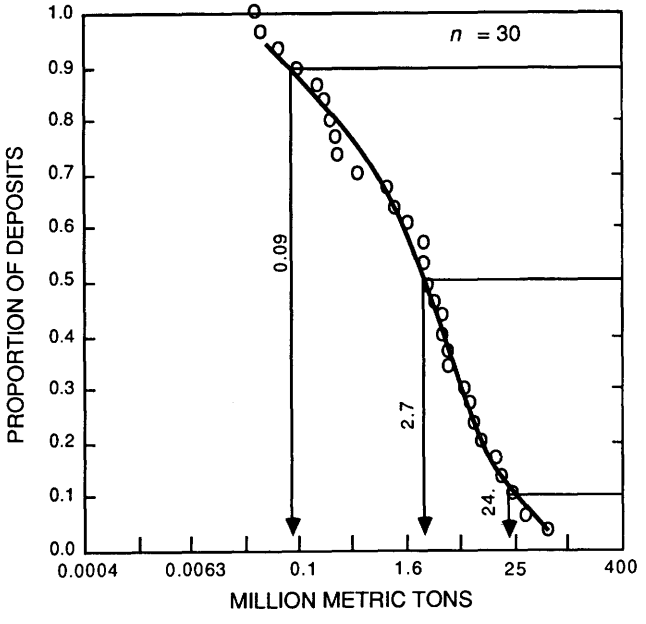

Figure 2. Inverse cumulative frequency plot of deposit tonnage for 30 bedded barite deposits.

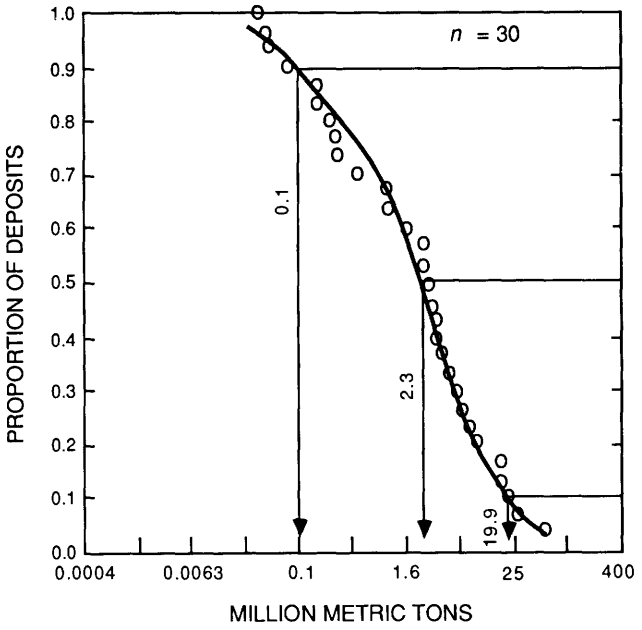

Figure 3. Inverse cumulative frequency plot of contained barite for 30 bedded barite deposits.

REFERENCES CITED

Briskey, J.A., 1986, Descriptive model of sedimentary exhalative Zn-Pb, *in* Cox, D.P., and Singer, D.A., eds., Mineral deposit models: U.S. Geological Survey Bulletin 1693, p. 211–212.

Brobst, D.A., 1984, The geological framework of barite resources: Institution of Mining and Metallurgy Transactions, sec. A, v. 93, p. A123–A130.

Canada Department of Energy, Mines and Resources, 1980, Canadian mineral deposits not being mined in 1980: Mineral Policy Sector Internal Report MRI 80/7, 294 p.

Carne, R.C., 1979, Geological setting and stratiform mineralization Tom claims, Yukon Territory: Canada Department of Indian Affairs Northern Development Open-File Report EGS–1979–4, 30 p.

Dawson, K.M., and Orchard, M.J., 1982, Regional metallogeny of the northern cordillera: biostratigraphy, correlation and metallogenic significance of bedded barite occurrences in eastern Yukon and western District of Mackenzie: Canada Geological Survey Paper 82–1C, p. 31–36.

Foose, M.P., Menzie, W.D., Singer, D.A., and Hanley, J.T., 1980, The distributions and relationships of grade and tonnage among some nickel deposits: U.S. Geological Survey Professional Paper 1160, 14 p.

Ketner, K.B., 1965, Economic geology, *in* Gilluly, James, and Gates, Olcott, eds., Tectonic and igneous geology of the northern Shoshone Range, Nevada: U.S. Geological Survey Professional Paper 475–B, p. B38–B41.

———1975, Replacement barite deposit, southern Independence Mountains, Nevada: U.S. Geological Survey Journal of Research, v. 3, no. 5, p. 547–551.

Krebs, Wolfgang, 1981, The geology of the Meggen ore deposit, *in* Wolf, K.H., ed., Handbook of strata-bound and stratiform ore deposits: New York, Elsevier, v. 9, p. 509–549.

Large, D.E., 1981, Sediment-hosted submarine exhalative lead-zinc deposits—A review of their geological characteristics and genesis, *in* Wolf, K.H., ed., Handbook of strata-bound and stratiform ore deposits: New York, Elsevier, v. 9, p. 469–508.

———1983, Sediment-hosted massive sulfide lead-zinc deposits: An empirical model, *in* Sangster, D.F., ed., Sediment-hosted stratiform lead-zinc deposits: Mineralogical Association of Canada Short Course Handbook, v. 8, p. 1–30.

Orris, G.J., 1985, Bedded/stratiform barite deposits—Geologic and grade-tonnage data including a partial bibliography: U.S. Geological Survey Open-File Report 85–447, 32 p.

Papke, K.G., 1984, Barite in Nevada: Nevada Bureau of Mines and Geology Bulletin 98, 125 p.

Ryan, T.A., Jr., Joiner, B.L., and Ryan, B.F., 1982, MINITAB reference manual: Pennsylvania State University, Statistics Department, 156 p.

Shapiro, S.S., 1980, How to test normality and other distributional assumptions: Milwaukee, Wisconsin, American Society for Quality Control, 78 p.

Singer, D.A., 1986, Descriptive model of Kuroko massive sulfide, *in* Cox, D.P., and Singer, D.A., eds., Mineral deposit models: U.S. Geological Survey Bulletin 1693, p. 189–190.

Singer, D.A., Cox, D.P., and Drew, L.J., 1975, Grade and tonnage relationships among copper deposits: U.S. Geological Survey Professional Paper 907–A, 11 p.

Singer, D.A., and DeYoung, J.H., Jr., 1980, What can grade-tonnage relations really tell us?, *in* Guillemin, Claude, and Lagny, Phillipe, eds., Ressources minérales—Mineral resources: [France] Bureau of Recherches Geologiques et Minières Mémoir 106, p. 91–101.

Taylor, S., and Andrew, C.J., 1978, Silvermines orebodies, County Tipperary, Ireland: Institution of Mining and Metallurgy Transactions, sec. B, v. 87, p. B111–B124.

Zimmermann, R.A., 1969, Strata-bound barite deposits in Nevada: Mineralium Deposita, v. 4, p. 401–409.

———1976, Rhythmicity of barite-shale and of Sr in strata-bound deposits in Arkansas, *in* Wolf, K.H., ed., Handbook of strata-bound and stratiform ore deposits: New York, Elsevier, v. 1, p. 339–353.

Zimmermann, R.A., and Amstutz, G.C., 1964, Small scale sedimentary features in the Arkansas barite district, *in* Amstutz, G.C., ed., Sedimentology and ore genesis; proceedings of a symposium held during the Sixth International Sedimentological Congress, 6th, Delft–1963: New York, Elsevier, p. 157–163.

Chapter C

Gold—Distribution of Gold in Porphyry Copper Deposits

By DENNIS P. COX and DONALD A. SINGER

U.S. GEOLOGICAL SURVEY BULLETIN 1877

CONTRIBUTIONS TO COMMODITY GEOLOGY RESEARCH

CONTENTS

FIGURES

TABLES

Gold—Distribution of Gold in Porphyry Copper Deposits

By Dennis P. Cox *and* Donald A. Singer

Abstract

Analysis of 55 porphyry copper deposits demonstrates a continuum between porphyry copper-gold deposits emplaced at a median depth of 1 km, with a median size of 160 million metric tons of copper ore and a median content of 2.6 percent magnetite in the potassic alteration zone, and porphyry copper-molybdenum deposits emplaced at a median depth of 3.6 km, with a median size of 500 million metric tons and little magnetite. Molybdenum commonly occurs in low-grade peripheral zones outside the copper orebody in the porphyry copper-gold-type deposits. Gold grades are less than 0.05 ppm in the porphyry copper-molybdenum deposits. Between these end members is an economically important group containing significant amounts of both gold and molybdenum.

INTRODUCTION

This paper expands and refines ideas about the distribution of gold in porphyry copper deposits. Previous contributors in this area are Kesler (1973) who plotted gold, molybdenum, and copper content of porphyry ores on a triangular coordinate system and related gold and molybdenum content to tectonic environment; Sillitoe (1979, 1982) who noted the correlation between gold grade and magnetite content in the potassic alteration zones of porphyry copper deposits; and Sinclair and others (1982) who noted other factors, such as deposit morphology, that are correlated with gold content.

In this paper we review information on gold distribution within certain individual well-studied deposits and compare these data to information on a group of 55 deposits for which we have data on tonnage and on grade of copper, gold, and molybdenum (table 1). These data came partly from files of the U.S. Bureau of Mines (R. Rosencranz, written commun., 1983) and partly from other proprietary sources. Estimated premining tonnages, average grades, and the lowest available cutoff grades of well-explored deposits were used. Because of the proprietary nature of some of these data, it is not possible for us to present them in a way that permits identification of individual deposit grades.

Table 1. Porphyry copper deposits examined in this study and classified by their gold and molybdenum content

Porphyry copper deposit type		
Porphyry copper-gold	Porphyry copper-gold-molybdenum	Porphyry copper-molybdenum
Afton, British Columbia	Ajo, Arizona	Berg, British Columbia
Basay, Philippines	Andacolla, Chile	Bethlehem, British Columbia
Bell, British Columbia	Bingham, Utah	Brenda, British Columbia
Caribou Bell, British Columbia	Brenmac-Sultan, Washington	Gambier Island, British Columbia
Copper Mountain, British Columbia	Cash, Yukon Territory	Gibraltar, British Columbia
Dos Pobres, Arizona	Casino, Yukon Territory	Highmont, British Columbia
Fish Lake, British Columbia	Cerro Colorado, Panama	Huckleberry, British Columbia
Frieda River, Papua New Guinea	Copper Flat, New Mexico	Inspiration, Arizona
Galore Creek, British Columbia	Dexing, China	Lornex, British Columbia
Ingerbelle, British Columbia	Granisle, British Columbia	Morenci, Arizona
Mamut, Malaysia	Island Copper, British Columbia	Ray, Arizona
Marcopper, Philippines	Kalamazoo, Arizona	Sierrita-Esperanza, Arizona
Ok Tedi, Papua New Guinea	Morrison, British Columbia	Tyrone, New Mexico
Panguna, Papua New Guinea	Poison Mountain, British Columbia	Twin Buttes, Arizona
Red Chris, British Columbia	Ruth, Nevada	Valley Copper, British Columbia
Rio Vivi, Puerto Rico	Shaft Creek, British Columbia	
Saindak South, Pakistan	Sipalay, Philippines	
Star Mountain, Papua New Guinea	Yandera, Papua New Guinea	
Tanama, Puerto Rico	Santa Rita, Arizona	
Taysan, Philippines		

The deposits include 20 examples here classified as porphyry copper-gold deposits (PCD-Au) (typified by the Dos Pobres deposit in Arizona), 19 classified as porphyry copper-gold-molydenum deposits (PCD-Au-Mo) (of which Bingham, Utah, is a good example), and 16 classified as porphyry copper-molybdenum deposits (PCD-Mo)(typified

by Sierrita-Esperanza, Ariz.). The classification (following Kesler, 1973) is based on distribution of the deposits on a triangular coordinate plot showing their copper grade in percent, molybdenum content in percent times 10, and gold grade in parts per million (ppm) (fig. 1). Our conclusions are that the three types differ significantly in metal content, magnetite content, deposit morphology, depth of emplacement, and tonnage.

FACTORS RELATED TO GOLD CONTENT OF PORPHYRY COPPER DEPOSITS

Copper-Molybdenum Content

In this paper we define the porphyry copper-gold model as having high gold and low molybdenum grade in a magnetite-rich potassic alteration zone of a porphyry copper deposit. Excluded are gold-rich copper skarn orebodies and porphyry systems where gold mineralization was clearly epithermal, younger, or distally related to the intrusion. Because of the gradational variation of gold content and its interdependence with molybdenum, it is not possible to define PCD-Au systems on the basis of gold content alone. Most of the deposits contain 0.3 to 0.7 ppm gold, but some deposits containing less than 0.2 ppm fit the model in other ways such as mineralogy and alteration zoning. The PCD-Au model can be defined more precisely in terms of gold and molybdenum grades according to the relation:

$$\frac{\text{Au}}{\text{Mo}} \geq 30 \qquad (1)$$

where gold is in parts per million and molybdenum is in percent. Equation 1 is plotted on the triangular coordinate plot in figure 1 and separates a group of 20 deposits on the right-hand side that are all good examples of the PCD-Au model.

Gold occurs in porphyry copper deposits in various forms: micron-size particles of free gold were described at Ingerbelle, B.C. (J. McCue, Newmont Mines Ltd., unpublished report, 1980); free gold is associated mainly with bornite, partly with chalcopyrite, and negligibly with pyrite at Panguna, Papua New Guinea (Baldwin and others, 1978); small grains of electrum containing 11.5 to 18.5 percent silver are associated with bornite-gangue grain boundaries at Granisle, B.C., and with chalcopyrite and pyrite at Bell, B.C. (Carson and others, 1970; Cuddy and Kesler, 1982); and inclusions of sylvanite and hessite occur in bornite at Dos Pobres, Ariz. (Langton and Williams, 1982).

Gold content is positively correlated with copper grade within some deposits such as Ingerbelle, B.C. (J. McCue, Newmont Mines Ltd., unpublished report, 1980), and Sapo Alegre, Puerto Rico (Cox and others, 1975). Cuddy and Kesler (1982) found a high correlation of gold grade with bornite content at Granisle, B.C. In some deposits, such as Tanama, Puerto Rico (Cox, 1986), gold and copper grades are independent. For the 55 deposits used in this study, gold and copper average grades are independent at the 1-percent level of significance. Median copper grade for the data set is 0.48 percent.

Within many porphyry deposits, gold grade is negatively correlated with molybdenum grade as pointed out by Popov (1977) and Sillitoe (1982). The low molybdenum content of porphyry copper-gold deposits is related to the fact that in many systems molybdenum is distributed as a peripheral zone outside the copper-gold orebody that itself has a low molybdenum grade. At Dos Pobres (Langton and Williams, 1982), 0.005 to 0.015 percent molybdenum occurs in a quartz-sericite-pyrite alteration zone lying partly within the outer fringe of the > 0.5-percent-copper orebody and partly outside of the orebody. A similar relation is cited by Sillitoe (1979) at Saindak, Pakistan; Bajo de Alumbrera, Argentina; and Dizon, Philippines.

This antipathetic relationship of gold and molybdenum, although not so well developed in other PCD-Au deposits, gives rise to an overall negative correlation of the two metals when data from all 55 deposits in the population are studied. The correlation coefficient between gold and molybdenum is low ($r=-0.45$) but is significant at the 1-percent level.

Of the 48 deposits for which a silver grade also was available, no correlation was found between silver content and that of gold, molybdenum, or copper (fig. 2). Median silver grade for the data set is 1.5 ppm.

Magnetite Content

Magnetite in veinlets makes up more than 1 percent by volume of most porphyry copper-gold orebodies (Saegart and Lewis, 1977; Sillitoe, 1979). Magnetite forms stable assemblages with any of the minerals that characterize potassic or feldspar-stable alteration: chalcopyrite, biotite, anhydrite, K-feldspar, chlorite, or actinolite. Excluded from this general rule are magnetite-rich skarn orebodies and relict magnetite in replacement orebodies in mafic igneous rocks such as those found at Ray, Ariz. The converse of this rule—that magnetite in porphyry copper orebodies is positively correlated with gold content—has numerous exceptions. Magnetite is mentioned as a rare mineral at Poston Butte (Nason and others, 1982) and Sacaton (Cummings, 1982), Ariz. No gold grade is reported for these deposits. At Bethlehem, B.C., secondary magnetite appears as clusters with K-feldspar in the potassic alteration zone without attendant gold mineralization (J.A. Briskey, oral commun., 1984). At Mineral Park, Ariz. (Wilkinson and others, 1982), a late magnetite-chalcopyrite-chlorite vein system cuts early quartz-K-feldspar-biotite-molybdenite veins. These veins form a

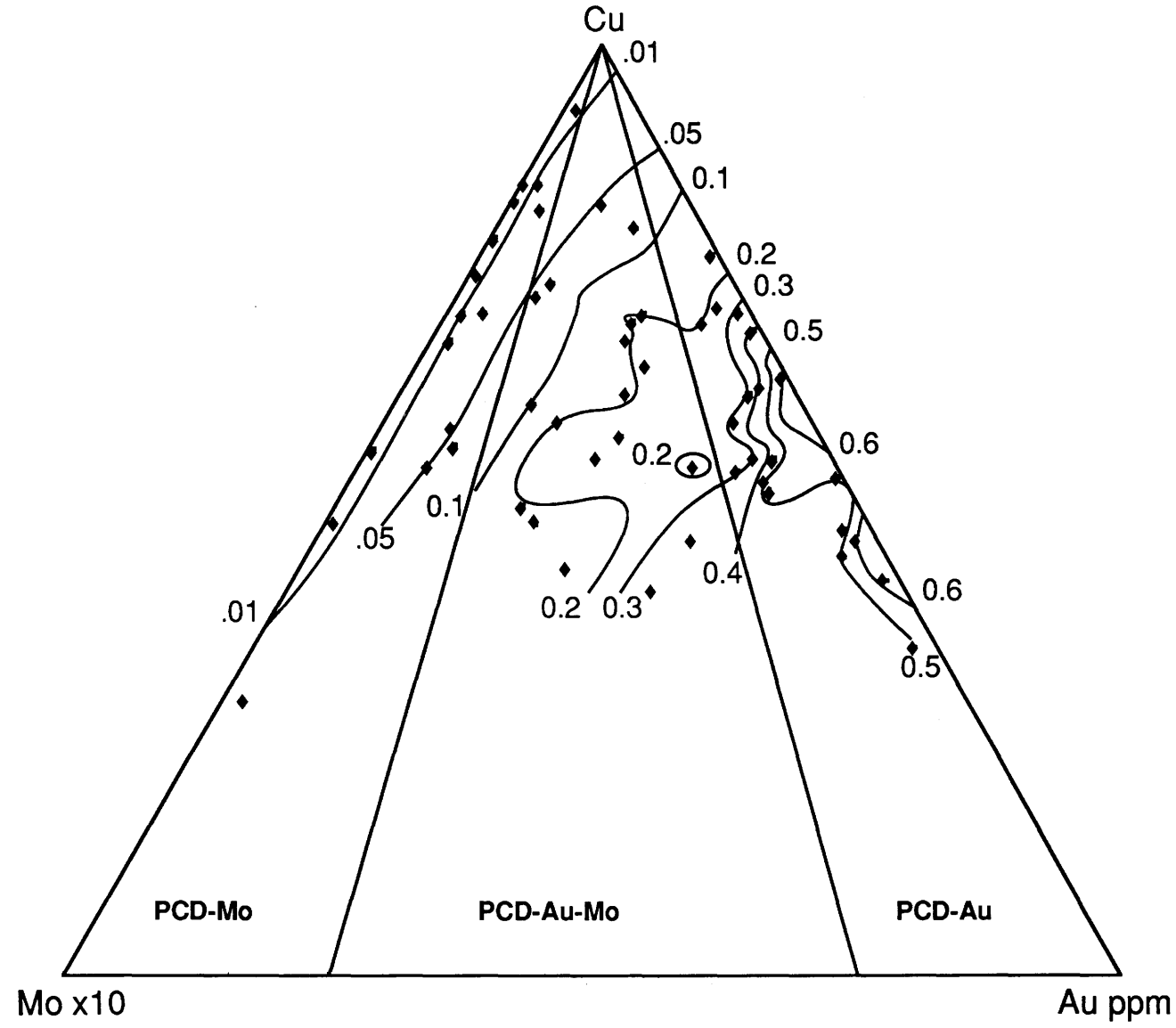

Figure 1. Fifty-five porphyry copper deposits plotted according to their copper, gold, and molybdenum content following Kesler (1973). Diamond symbols represent individual deposits. Contour lines represent gold content of deposits in grams per metric ton. PCD-Mo = Porphyry copper-molybdenum; PCD-Au-Mo = Porphyry copper-gold-molybdenum; and PCD-Au = Porphyry copper-gold.

low-grade copper zone (average 0.069 percent Cu) roughly coextensive with the molybdenum orebody containing >0.03 percent molybdenum. According to Luis Vega (written commun., 1984), the Mineral Park porphyry system contains essentially no gold. Magnetite-chlorite veins are also associated with molybdenum mineralization in the Malala district of Sulawesi (Taylor and Van Leeuwen, 1980). Magnetite and molybdenite form fracture fillings in quartz porphyry. The Malala deposit contains 0.24 percent MoS_2 and subordinate amounts of copper.

Despite these exceptions, magnetite content is positively correlated with gold grade in the deposits included in this study. Where magnetite content is not given in percent in deposit descriptions, word descriptors were converted to numerical estimates according to the following scheme:

trace, rare	0.05
present	1
abundant	3

Magnetite content is plotted on the triangular diagram in figure 3 and versus gold in figure 4. The correlation coefficient (r=0.68) is significant at the 1-percent level for 26 deposits for which an estimated magnetite content greater than zero was known (fig. 4). The deposit represented by the point having high gold and low magnetite content (upper left side of the field) had an original high

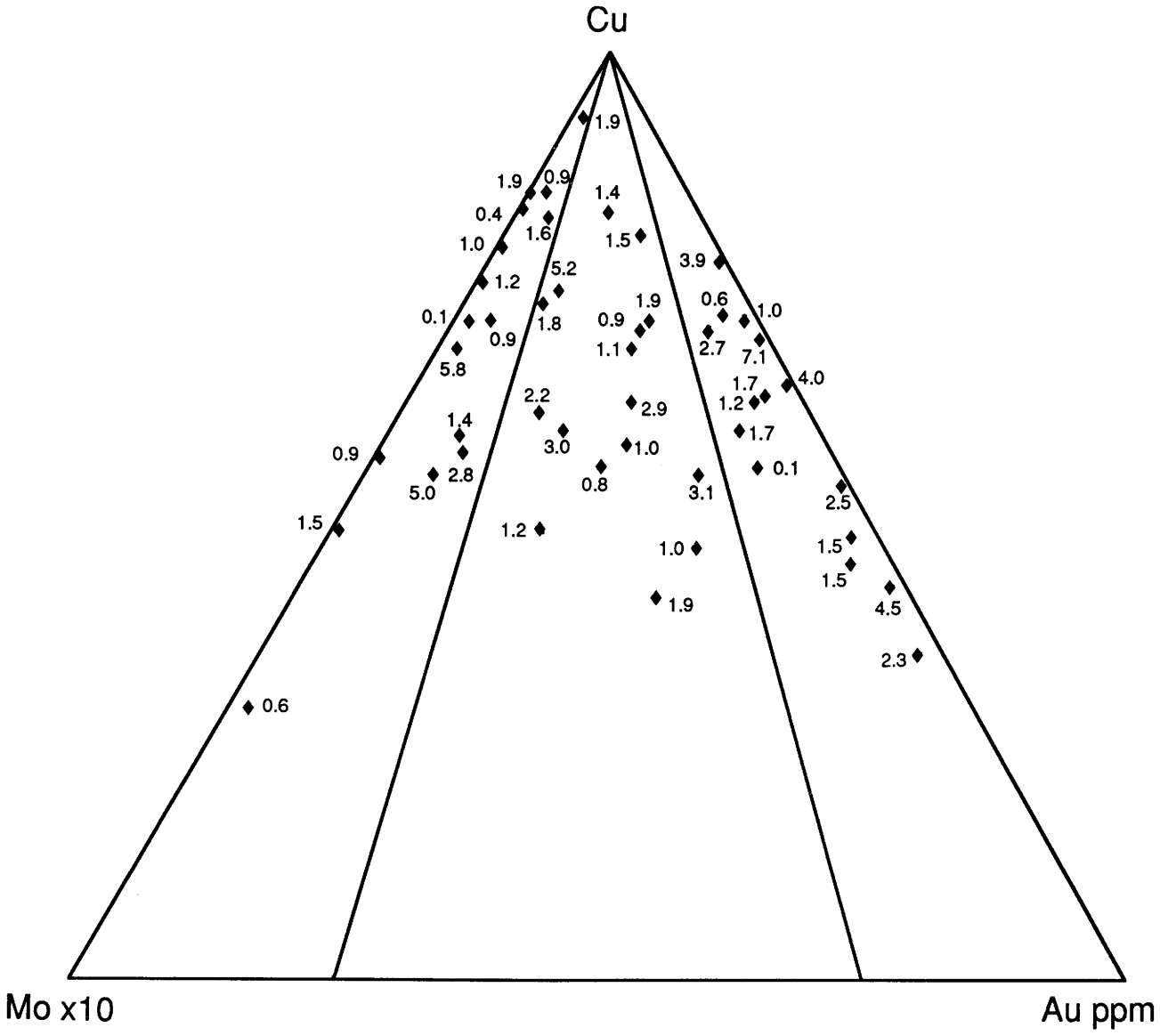

Figure 2. Silver grade of porphyry copper deposits in ppm. Positions of data points represent their copper, gold, and molybdenum content as shown in figure 1. No systematic variation is observed.

content of magnetite that was largely replaced by pyrite during late-stage phyllic alteration.

Deposit Morphology

Sinclair and others (1982) applied the porphyry classification scheme of Sutherland Brown (1976) to a group of porphyry deposits in British Columbia and found that porphyry copper-gold deposits tend to be in classic- and volcanic-type intrusive systems. According to Sutherland Brown, classic-type deposits are centered around small cylindrical plutons. They are commonly associated with breccia pipes and have concentric zones of alteration and mineralization. Coeval volcanic rocks are commonly absent in these deposits. Volcanic-type deposits are related to irregular or dikelike igneous bodies that have intruded "a coeval and at least partly, consanguineous volcanic pile" (Sutherland Brown, 1976, p. 46). We have plotted on figure 5 all deposits of volcanic type plus all those known to have coeval volcanic rocks exposed at or within a kilometer of the deposit. These deposits show a strong concentration on the PCD-Au side of the diagram. In contrast, plutonic-type porphyry deposits, characterized by mineralization in integral zones of medium-sized plutons having phanerocrystalline textures (Sutherland Brown, 1976, p. 48–49), are concentrated on the high-molybdenum, low-gold side of the diagram.

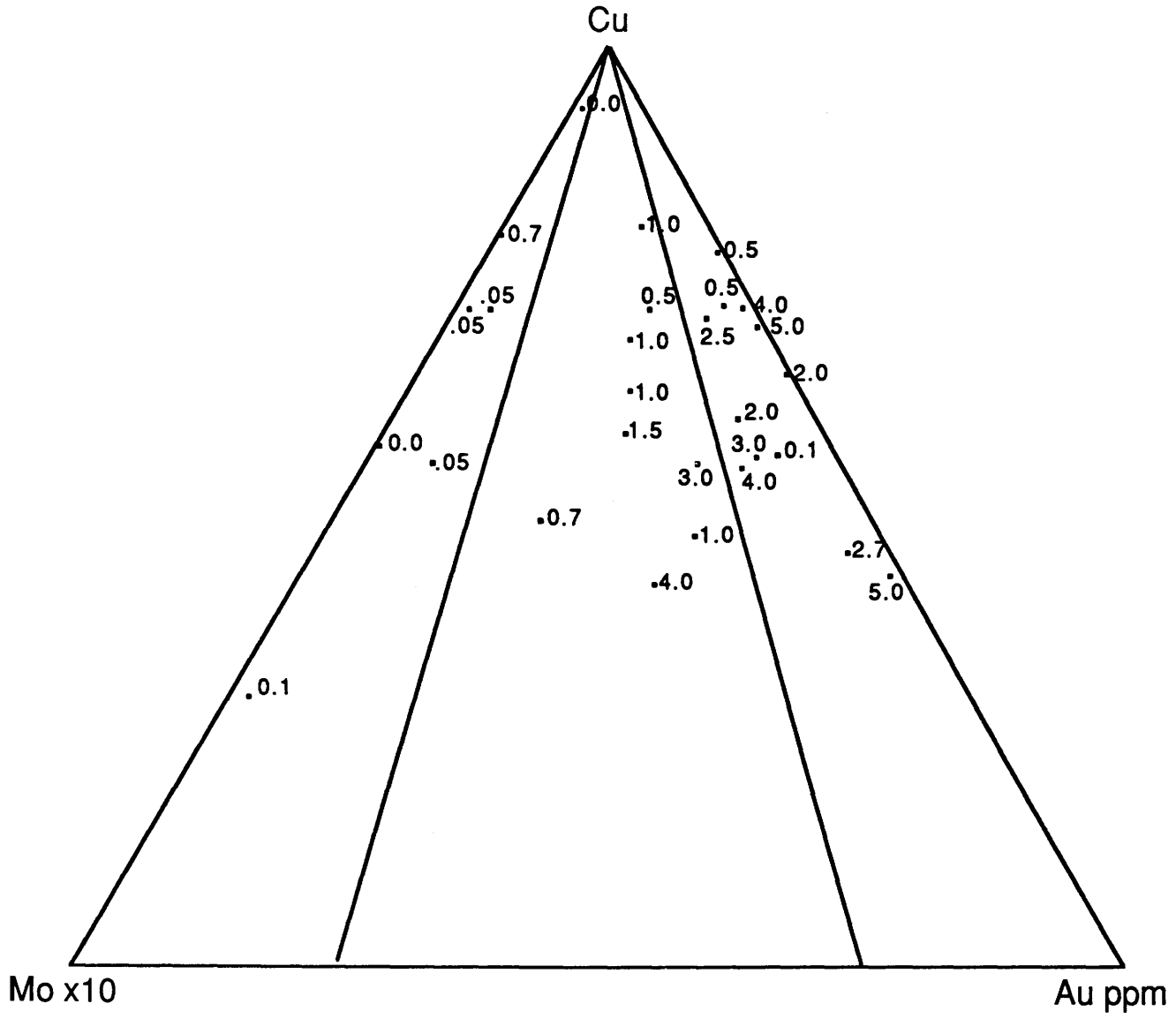

Figure 3. Magnetite content in volume percent in potassic alteration zones in porphyry copper deposits. Position of data points as in figure 1.

Depth of Emplacement

Estimates of depth of emplacement, shown in figure 6, were taken from geologic reports on individual deposits and from Sutherland Brown (1976, fig. 1). The estimates show a negative correlation with gold grade of −0.90, which is significant at the 1-percent level for 18 deposits (fig. 7). Given the close relation between gold content and deposit classification, this correlation is expected because volcanic-type deposits tend to be emplaced at shallow levels in the crust and because the deep erosion required to expose plutonic-type deposits emplaced at deep levels in the crust commonly removes all traces of supracrustal volcanic rocks.

Deposit Tonnage

Sillitoe (1979) noted no relation between deposit tonnage and gold grade in his set of 16 deposits having gold grade greater than or equal to 0.4 ppm. For our set of 55 deposits, which includes a wider range of gold grades, however, there is a low correlation of −0.42 between deposit tonnage and gold grade; this correlation is significant at the 1-percent level. Median tonnage of the PCD-Mo type is roughly three times that of PCD-Au type (table 2), and the tonnages are significantly different. Tonnage classes plotted on figure 8 show a preponderance of small deposits on the high-gold side and a concentration of large deposits on the high-molybdenum side. This correlation is

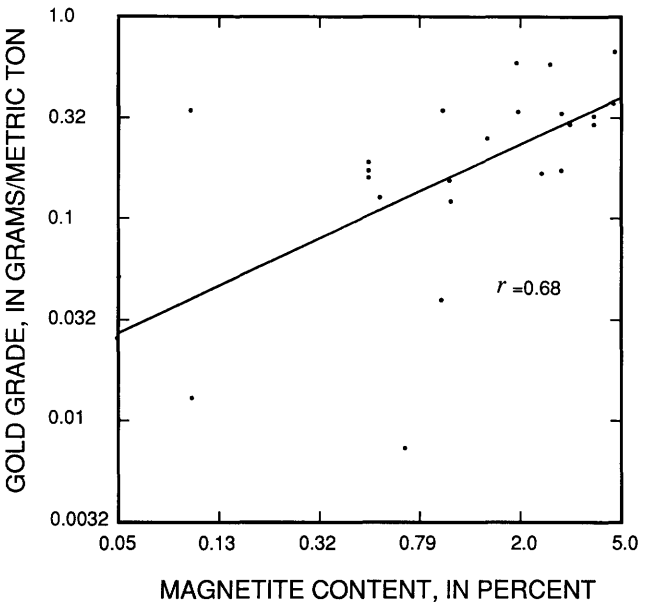

Figure 4. Magnetite content vs. gold grade for 26 porphyry copper deposits. Correlation is 0.68, which is significant at the 1-percent level.

probably closely related to an inherent difference in tonnage between volcanic and plutonic types of deposits.

Associated Igneous Rocks

Descriptions of rock types believed to be genetically related to porphyry copper deposits were taken from the literature and converted into standard rock terminology (Streckeisen, 1973). These types are plotted on figure 9. Of the 20 PCD-Au systems, 8 occur with tonalite or quartz diorite, 6 with syenite or monzonite, and 6 with granodiorite or monzogranite. Of the 16 PCD-Mo systems, 12 occur with monzogranite and granodiorite, 3 with tonalite, and 1 is undetermined. Of 19 deposits classified as PCD-Au-Mo type, 13 were associated with monzogranite and granodiorite, 4 with tonalite, and 2 were undetermined.

We agree with Sillitoe (1979) that associated rock type is not a good descriptor of porphyry copper-gold deposits. There is possibly a general tendency, not shown in the above data, for PCD-Au systems to be associated with the rocks rich in mafic minerals and for PCD-Mo and PCD-Au-Mo systems to occur with monzogranite and granodiorite having low mafic-mineral content.

CHARACTERISTICS OF PORPHYRY COPPER-GOLD DEPOSITS

Porphyry copper-gold deposits have Au:Mo satisfying equation 1 and median gold grades of 0.38 g/t

Table 2. Median grades, tonnages, and depths by type of porphyry copper deposit

	Porphyry copper-gold type	Porphyry copper-gold-molybdenum type	Porphyry copper molybdenum type
Number of deposits	20	19	16
Metric tons $\times 10^6$	160	390	500
Copper (percent)	.55	.48	.41
Molybdenum (percent)	.003	.015	.016
Gold (g/t)	.38	.15	.012
Silver (g/t)	1.69	1.63	1.22
Magnetite content (percent)	2.6	1.0	.05
Depth (km)	1.0	.9	3.6

(table 2). The richest deposits contain 0.9 g/t (Sillitoe, 1979). Median molybdenum grades are 0.003 percent within copper-gold orebodies, but peripheral zones reaching 0.01 percent molybdenum may occur outside the copper-gold orebody. Median deposit tonnage is 160 million metric tons. The largest deposit, Panguna, Papua New Guinea, exceeds 1 billion metric tons.

Porphyry copper-gold deposits tend to form in and around dike swarms or cylindrical plutons of tonalite or syenite-monzonite intruding coeval volcanic rocks (fig. 10). The ore-related intrusions may also be of granodiorite and monzogranite composition. In deposits for which depths of emplacement have been estimated, the median depth is about 1 km. All deposits that have not been affected by pervasive late-stage phyllic alteration and pyritization have magnetite as a stable member of the potassic alteration assemblage. The median magnetite content is 2.6 percent.

CHARACTERISTICS OF PORPHYRY COPPER-GOLD-MOLYBDENUM DEPOSITS

Deposits of the PCD-Au-Mo type have gold and molybdenum contents that satisfy the relation:

$$3 > \frac{\text{Au}}{\text{Mo}} < 30, \qquad (2)$$

where molybdenum and gold are each measured as in equation 1. Median gold grade for this deposit type is 0.15 g/t, and median molybdenum content is 0.015 percent Mo. Median tonnage is 390 million metric tons (table 2). This deposit type includes some large-tonnage deposits that, with their correspondingly high production rates, are important gold producers. Bingham, the largest deposit in this type class, was for many years the second-ranking gold producer in the United States.

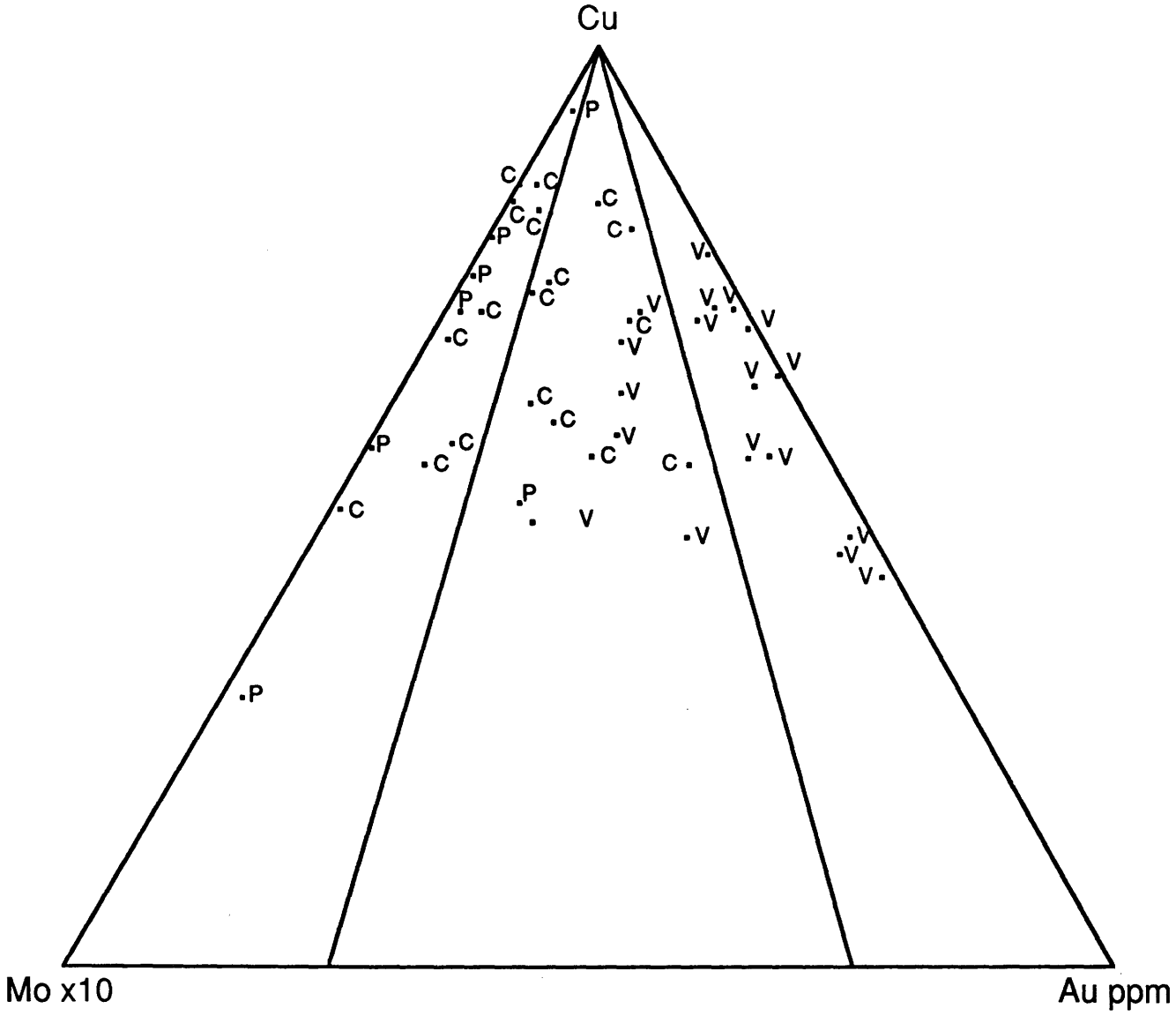

Figure 5. Porphyry copper deposits according to their morphologic class following Sutherland Brown (1976). V's represent volcanic-type plus some classic-type deposits in which coeval volcanic rocks are abundant near the deposit. C is classic type and P is plutonic type.

Both classic- and volcanic-types of deposits contain gold together with molybdenum in copper orebodies. In the classic type, gold is contained in both the intrusive porphyry and in related gold-rich skarn deposits such as at Bingham, Utah; Ruth, Nev.; and Santa Rita, N.M. (fig. 11). Most deposits are related to intrusions of monzogranite and granodiorite composition. Magnetite is commonly present in the potassic alteration assemblage, and the median magnetite content for nine of these deposits is 1 percent. PCD-Au-Mo systems may have important additional gold mineralization in peripheral vein or replacement-type deposits (fig. 11).

CHARACTERISTICS OF PORPHYRY COPPER-MOLYBDENUM DEPOSITS

Deposits of the PCD-Mo system have gold and molybdenum content defined by the relation:

$$\frac{\text{Au}}{\text{Mo}} \geq 3 \qquad (3)$$

where molybdenum and gold are measured as in equation 1. Median molybdenum grade for this type of deposits is not significantly different from that of the PCD-Au-Mo deposit

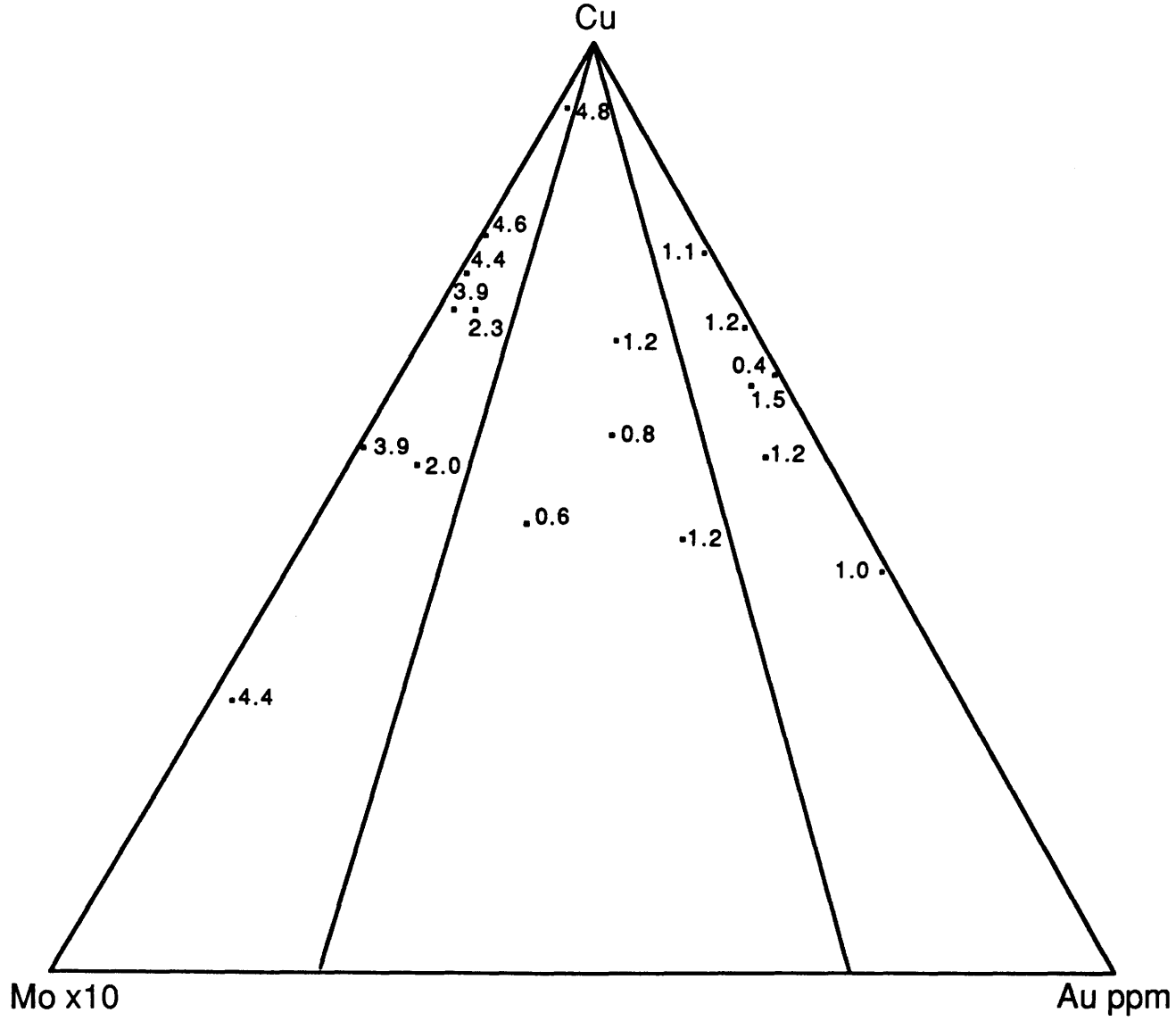

Figure 6. Porphyry copper deposits according to their estimated depth of emplacement in kilometers.

type. Median gold values are 0.012 g/t. Median deposit tonnage is 500 million metric tons.

Classic-type porphyry copper deposits dominate the PCD-Mo deposit type in the United States, and plutonic-type porphyry deposits are important in British Columbia. Figure 12 is a diagram showing characteristics of the latter type. Median depth of emplacement is 3.6 km (table 2). Intrusions associated with ore deposition are mainly monzogranite in the United States and granodiorite or tonalite in British Columbia. Median magnetite content of potassic alteration zones is 0.05 percent. Some deposits have important gold-bearing vein, carbonate replacement, or skarn deposits arranged peripherally around the porphyry intrusion.

GEOCHEMICAL INTERPRETATION

Data presented by Chaffee (1982) for San Manuel, Ariz., show that gold is concentrated in two environments, one within the porphyry copper orebody and the other about 1,200 m outward from the orebody in the propylitic alteration zone. This arrangement implies that two transport-deposition processes may be necessary to explain gold distribution in porphyry systems. One possible suggestion is that gold is deposited from gold complexes at high temperature in the interior of the system and that this gold is partly remobilized at lower temperature and relatively higher f_{S_2} conditions as thiocomplex ions and is transported to peripheral parts of the system. As Sillitoe

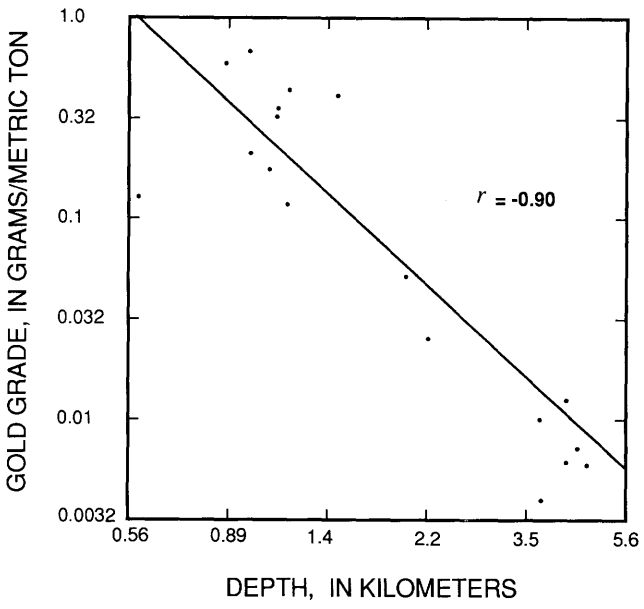

Figure 7. Estimated depth of emplacement vs. gold grade for 18 porphyry copper deposits. The correlation is −0.90, which is significant at the 1-percent level.

(1982) has pointed out, high f_{O_2}/f_{S_2}, as evidenced by high magnetite-to-pyrite ratios in PCD-Au systems, seem, in most cases, to be responsible for trapping gold in the copper-rich part of the system. Where the magnetite-pyrite ratio is low in the potassic alteration stage, sufficient sulfide ions may have been present to cause gold to remain mobile as gold thiocomplex ions during falling temperatures (Henley, 1973). In such chemical environments, gold would migrate outward to form peripheral gold vein-type deposits. One possible mechanism for maintaining high f_{O_2}/f_{S_2} during the early gold-deposition stage might be the dissociation of H_2O to H_2 and O_2. This reaction would be favored by the high temperatures and low pressures that would be associated with tonalite and other more mafic intrusions emplaced at high levels in the crust. Escape of the smaller hydrogen molecules would result in the high f_{O_2}/f_{S_2} required to form magnetite and restrict gold mobilization.

Molybdenum is dispersed under high f_{O_2}/f_{S_2} conditions and is deposited where sulfide ions are concentrated both within copper orebodies in PCD-Mo systems and within the peripheral pyrite zones around PCD-Au systems. This dispersal is expected in view of work by Cao and others (1988) showing that molybdenum can be transported as the complex MoOCl° in solutions buffered by Fe_3O_4-Fe_2O_3-FeS_2 at 350 °C to 400 °C and with NaCl concentrations of 0.1 to 4.5 *M*. These conditions are reasonable for the magnetite-bearing copper ore zone PCD-Au systems.

In this paper we recognize an economically important intermediate type of gold- and molybdenum-rich copper deposits in which neither the gold dispersal nor the molybdenum dispersal process has worked effectively.

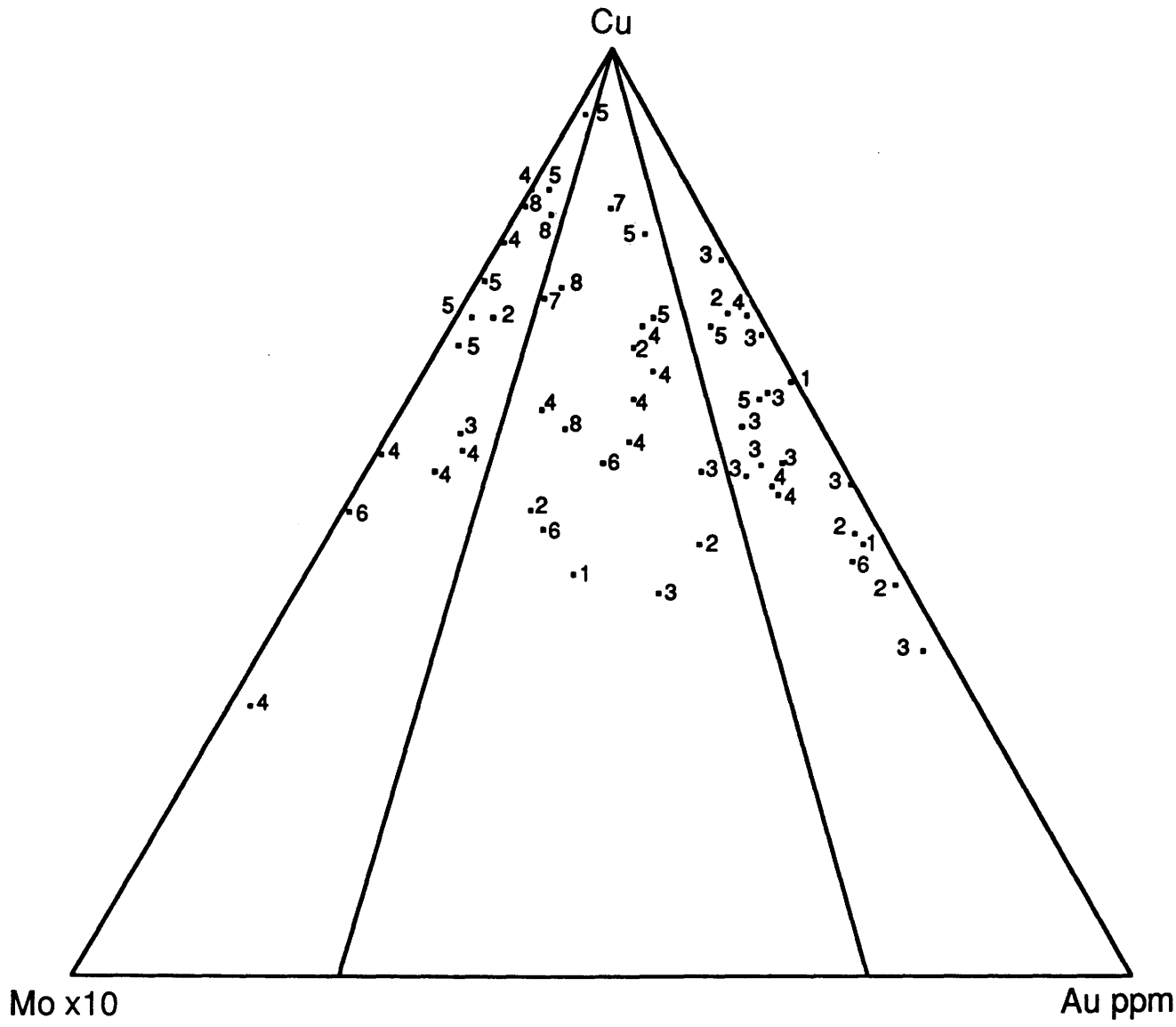

Figure 8. Tonnage classes for porphyry copper deposits, which are defined in millions of metric tons as follows:

1=0 to 50	5=401 to 800
2=51 to 100	6=801 to 1,600
3=101 to 200	7=1,601 to 3,200
4=201 to 400	8=3,201 to 6,400

Correlation of gold content with tonnage is −0.42, which is significant at the 1-percent level.

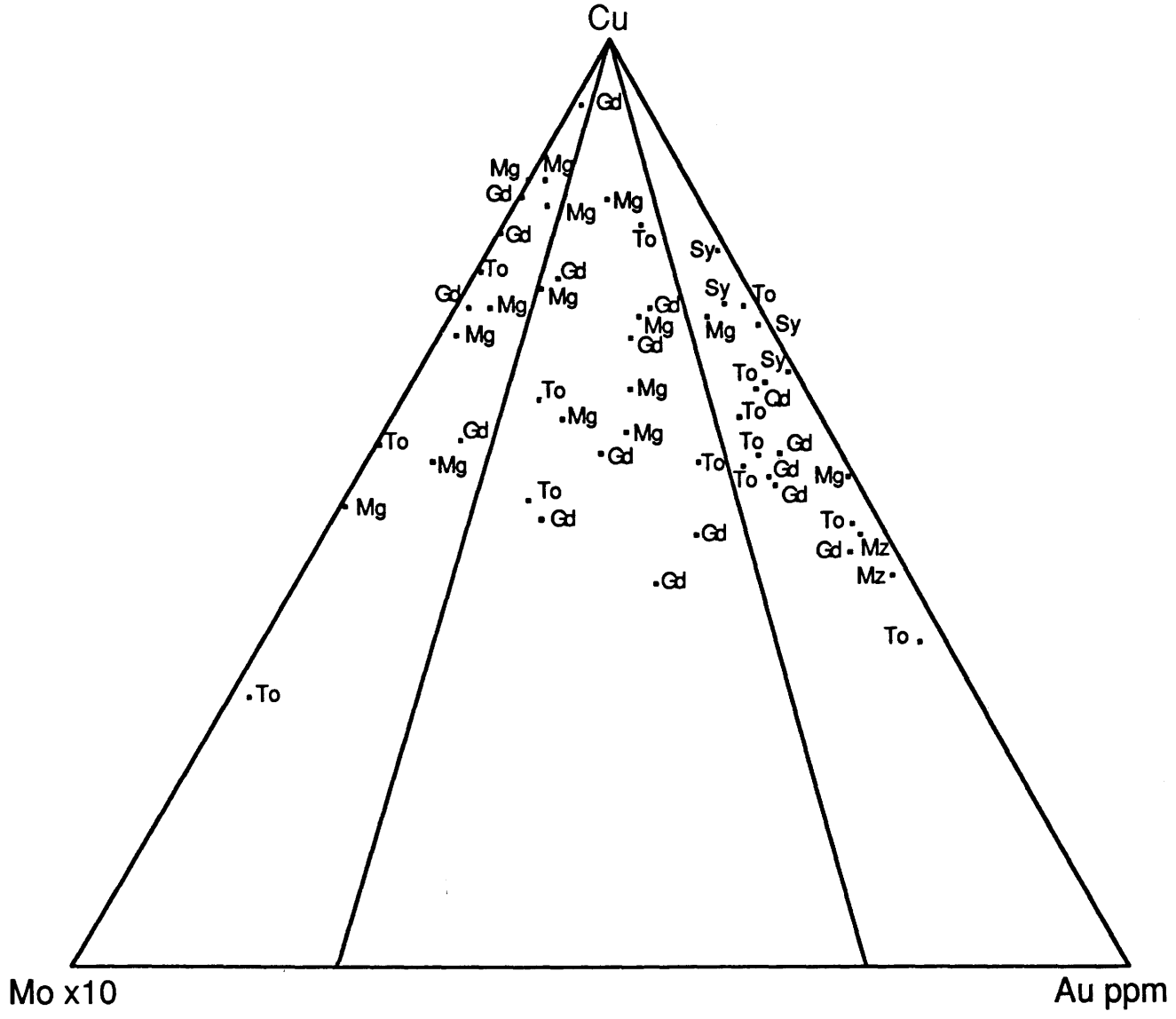

Figure 9. Type of ore-related intrusive rock in porphyry copper deposits. Mg, monzogranite; Gd, granodiorite; To, tonalite; Qd, quartz diorite, Mz, monzonite; Sy, syenite.

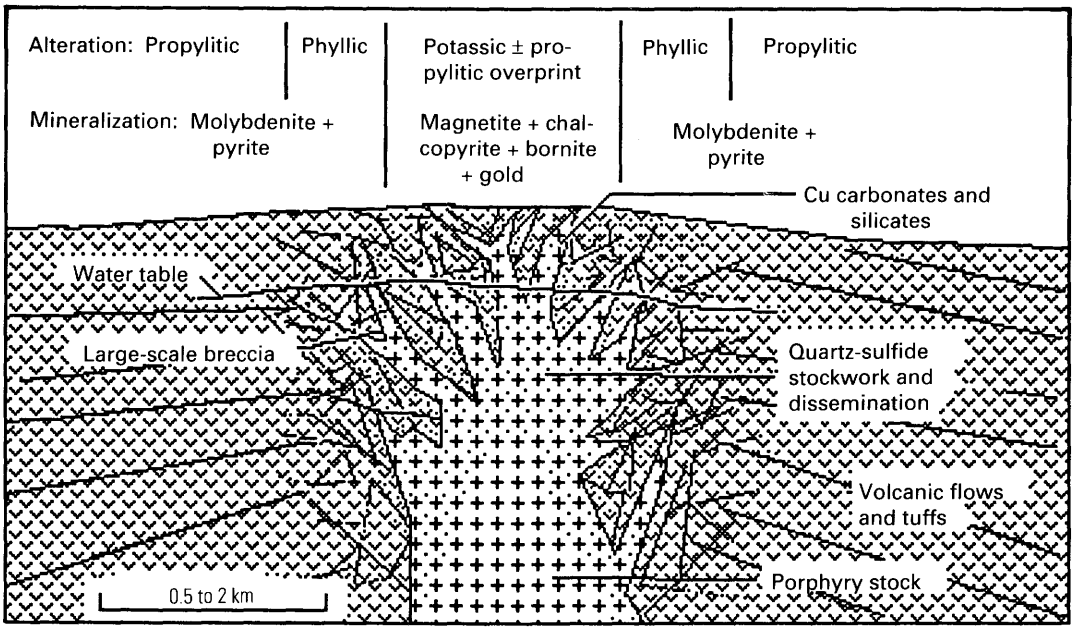

Figure 10. Cross section of porphyry copper-gold deposit as typified by the Dos Pobres deposit in Arizona. Modified from Langton and Williams (1982).

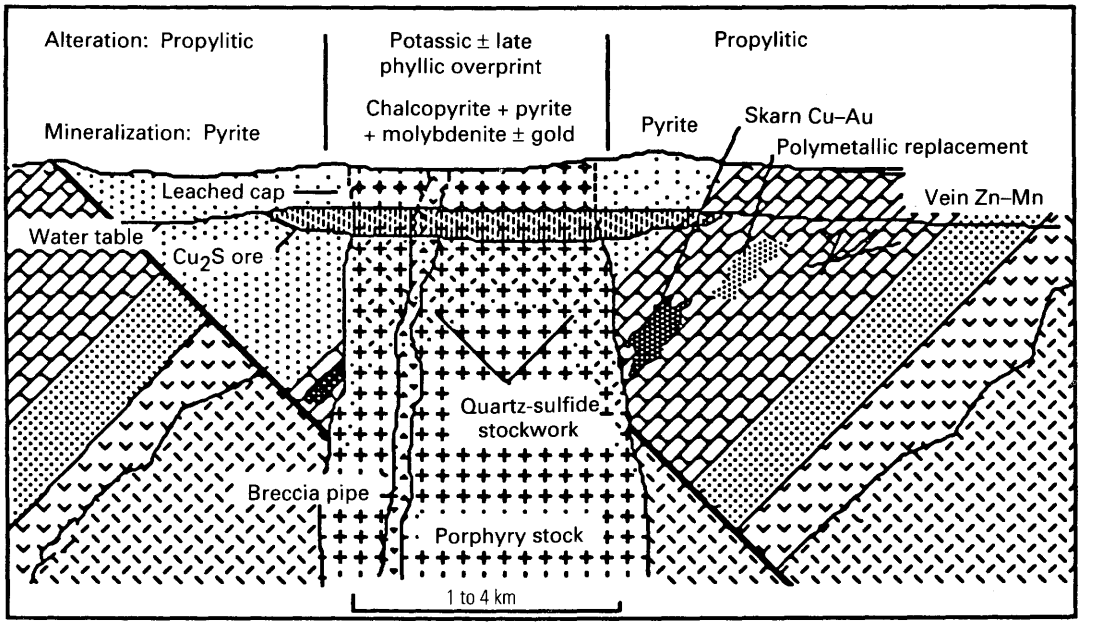

Figure 11. Cross section of a typical porphyry copper-gold-molybdenum deposit.

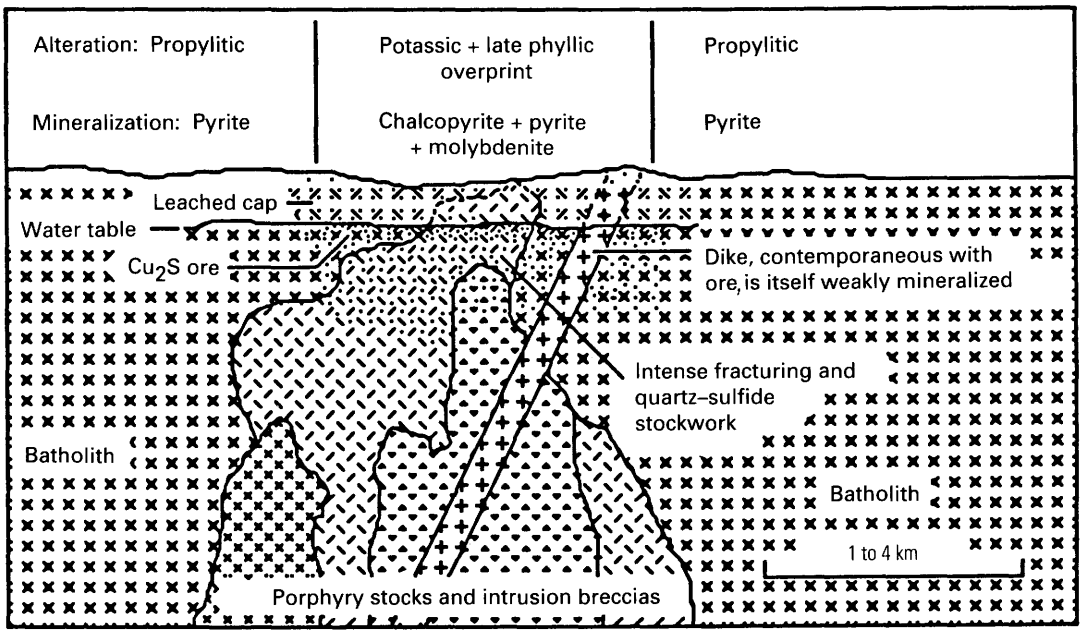

Figure 12. Cross section of a typical porphyry copper-molybdenum deposit.

REFERENCES CITED

Baldwin, J.T., Swain, H.D., and Clark, G.H., 1978, Geology and grade distribution of the Panguna porphyry copper deposit, Bougainville, Papua New Guinea: Economic Geology, v. 73, no. 5, p. 690–702.

Cao, Xiaoyun, Richardson, S.M., and Richardson, C.K., 1988, Solubility of molybdenite (MoS_2) in hydrothermal solutions: Geological Society of America Abstracts with Programs, v. 20, no. 7, p. A43.

Carson, D.J.T., Jambor, J.L., Ogryzlo, P., and Richards, T.A., 1970, Bell copper—Geology, geochemistry and genesis of a supergene enriched biotized porphyry copper deposit with a superimposed phyllic zone, *in* Sutherland Brown, A., ed., Porphyry deposits of the Canadian Cordillera: Canadian Institute of Mining and Metallurgy Special Volume 15, p. 245–263.

Chaffee, M.A., 1982, A geochemical study of the Kalamazoo porphyry copper deposit, *in* Titley, S.R., ed., Advances in geology of the porphyry copper deposits, southwestern North America: Tucson, University of Arizona Press, p. 375–386.

Cox, D.P., 1986, Geology of the Tanama and Helecho porphyry copper deposits and their vicinity, Puerto Rico: U.S. Geological Survey Professional Paper 1327, 59 p.

Cox, D.P., Perez Gonzales, I., and Nash, J.T., 1975, Geology, geochemistry and fluid inclusion petrography of the Sapo Alegre porphyry copper prospect and its metavolcanic wallrocks, west central Puerto Rico: U.S. Geological Survey Journal of Research, v. 3, no. 3, p. 313–327.

Cuddy, A.S., and Kesler, S.E., 1982, Gold in the Granisle and Bell porphyry copper deposits, British Columbia, *in* Levinson, A.A., ed., Precious metals in the Northern Cordillera: Rexdale, Ontario, Association of Exploration Geochemists, p. 157–172.

Cummings, R.B., 1982, Geology of the Sacaton porphyry copper deposit, *in* Titley, S.R., ed., Advances in geology of the porphyry copper deposits, southwestern North America: Tucson, University of Arizona Press, p. 375–386.

Henley, R.W., 1973, Solubility of gold in hydrothermal chloride solutions: Chemical Geology, v. 11, p. 73–87.

Kesler, S.E., 1973, Copper, molybdenum and gold abundances in porphyry copper deposits: Economic Geology, v. 68, no. 1, p. 106–112.

Langton, J.M., and Williams, S.A., 1982, Structural, petrological, and mineralogical controls for the Dos Pobres orebody, *in* Titley, S.R., ed., Advances in geology of the porphyry copper deposits, southwestern North America: Tucson, University of Arizona Press, p. 335–352.

Nason, P.W., Shaw, A.V., and Aveson, K.D., 1982, Geology of the Poston Butte porphyry copper deposit, *in* Titley, S.R., ed., Advances in geology of the porphyry copper deposits, southwestern North America: Tucson, University of Arizona, p. 375–386.

Popov, V.S., 1977, Geologiia i genezis medno- i molybden-porfirovykh mestorozhdenii (Geology and genesis of copper-and-molybdenum-porphyry deposits): Akademiya Nauk SSSR, Ministerstvo geologii SSSR, Institut Mineralogii, geokhimii i kristallokhimii redkikh elementov; Isdatel'stvo "Nauka," Moskow, 203 p. [Translated for U.S. Geological Survey by Dorothy B. Vitaliano, May 1978.]

Saegart, W.E., and Lewis, D.E., 1977, Characteristics of Philippine porphyry copper deposits and summary of current production and reserves: Transactions Society of Mining Engineers of AIME, v. 262, p. 199–209.

Sillitoe, R.H., 1979, Some thoughts on gold-rich porphyry copper deposits: Mineralium Deposita, v. 14, p. 161–174.

———1982, Unconventional metals in porphyry deposits: Society of Mining Engineers of AIME, preprint no. 82–63, 13 p.

Sinclair, A.J., Drummond, A.D., Carter, N.C., and Dawson, K.M., 1982, A preliminary analysis of gold and silver grades of porphyry-type deposits in western Canada, *in* Levinson, A.A., ed., Precious metals in the Northern Cordillera: Association of Exploration Geochemists, Rexdale, Ontario, p. 157–172.

Streckeisen, A., 1973, Classification and nomenclature of plutonic rocks: Geologische Rundschau, v. 63, p. 773–786.

Sutherland Brown, A., 1976, Morphology and classification, *in* Sutherland Brown, A., ed., Porphyry deposits of the Canadian Cordillera: Canadian Institute of Mining and Metallurgy Special Volume 15, p. 44–51.

Taylor, D., and Van Leeuwen, T., 1980, Porphyry-type deposits in Southeastern Asia, *in* Ishihara, S., and Takenouchi, S., eds., Granitic magmatism and related mineralization: Mining Geology Special Issue, no. 8, p. 95–116.

Wilkinson, W.H., Jr., Vega, L.A., and Titley, S.R., 1982, Geology and ore deposits at Mineral Park, Mohave County, Arizona, *in* Titley, S.R., ed., Advances in geology of the porphyry copper deposits, southwestern North America: Tucson, University of Arizona Press, p. 523–541.

Chapter D

Mercury—An Important Byproduct in Epithermal Gold Systems

By JAMES J. RYTUBA and CHRIS HEROPOULOS

U.S. GEOLOGICAL SURVEY BULLETIN 1877

CONTRIBUTIONS TO COMMODITY GEOLOGY RESEARCH

CONTENTS

FIGURES

TABLE

Mercury—An Important Byproduct in Epithermal Gold Systems

By James J. Rytuba *and* Chris Heropoulos

Abstract

Mercury has been recovered as a byproduct from six sediment-hosted precious-metal deposits and three volcanic-related deposits in the Western United States. The largest byproduct mercury production comes from volcanic-related deposits; the Paradise Peak deposit in Nevada is the largest producer. Mercury generally occurs as cinnabar in sediment-hosted deposits, but mercury selenides and oxides have also been reported. In volcanic-related systems, corderoite ($Hg_3S_2Cl_2$) and (or) cinnabar are the main phases, and mercury oxides, chlorides, and silver mercury sulfides are also locally present.

In epithermal gold systems, mercury can be transported in a fluid phase as Hg^0 or $HgS^=$ complex below the ground-water table and as a vapor above the ground-water table. Because mercury is the only ore metal that can be transported in significant amounts as a vapor, the trace-element content of cinnabar can be used to distinguish vapor-deposited cinnabar from fluid-deposited cinnabar. Cinnabar deposited from a vapor is chemically pure and contains very low amounts of trace elements (in ppm): antimony, ≤15; arsenic, ≤20; silver, <0.7; gold, ≤0.5; copper, ≤70; molybdenum, ≤7; lead, ≤30; tin, ≤15; and zinc, ≤200. Cinnabar deposited from a fluid has high concentrations of antimony (>150) or arsenic (>100 ppm); high-antimony samples contain 1–300 ppm silver, and high-arsenic samples contain 0.51 to 1 ppm gold. One or more of the base metals (copper, lead, zinc) generally exceeds concentrations of 300 ppm.

During the evolution of a volcanic-related, epithermal system, mercury is initially introduced into the near surface by the degassing of an intrusive, and the resulting mercury geochemical anomaly is centered on the intrusive. In the subsequent development of a hydrothermal system, mercury is remobilized from the site of the geochemical anomaly and transported in the fluid phase as Hg^0 or $HgS^=$. In the upper levels of the hydrothermal system, cinnabar and (or) mercurian-stibnite and (or) silver-mercury sulfide are deposited, and other ore elements within the solution are incorporated into the cinnabar structure. Above the ground-water table, chemically pure cinnabar is deposited from a vapor and occurs in association with kaolinite, alunite, and native sulfur (forming the "sulfurous type" of mercury deposit). During the waning stage of the system, lowering of the ground-water table exposes previously deposited sulfides to vapors continuing to effervesce from the hydrothermal system. In this oxidizing acid environment, mercurian stibnite is oxidized to antimony oxide, and the mercury released from the stibnite structure combines with $H_2S(g)$ and $Cl_2(g)$ effervescing from the hydrothermal solution to form corderoite. If $Cl_2(g)$ is low, only cinnabar or mercury oxides will form. The Paradise Peak deposit records the entire complex record of mercury deposition expected in an epithermal system.

INTRODUCTION

Exploration for epithermal, precious-metal deposits in the Western United States has caused renewed interest in many inactive mercury deposits and occurrences. This interest has recently led to the discovery of precious metals in several mercury districts and has resulted in the production of mercury as a byproduct from many of these deposits. The recently discovered Paradise Peak gold-silver deposit in Nevada has become the second largest producer of mercury in the United States. The chemical behavior of mercury in epithermal systems is summarized in this paper, and the distribution of mercury in the Paradise Peak deposit is discussed in detail.

BYPRODUCT MERCURY PRODUCTION

Mercury occurs in trace to significant amounts in most epithermal precious-metal deposits. Mercury content of the precious-metal ore generally ranges from 0.1 to 50 ppm (Bagby and Berger, 1985; Berger, 1985), but concentrations may vary considerably within individual deposits. Byproduct production from individual deposits ranges from 10 to 350 flasks (a flask equals 76 pounds) of mercury per year. Volcanic-related and volcanic-hosted precious-metal deposits, especially those related to opalite-type mercury occurrences, produce considerably more byproduct mercury than sediment-hosted gold deposits. The largest U.S. producers of byproduct mercury are volcanic-related deposits: Paradise Peak, Nev., producing 350 flasks per year;

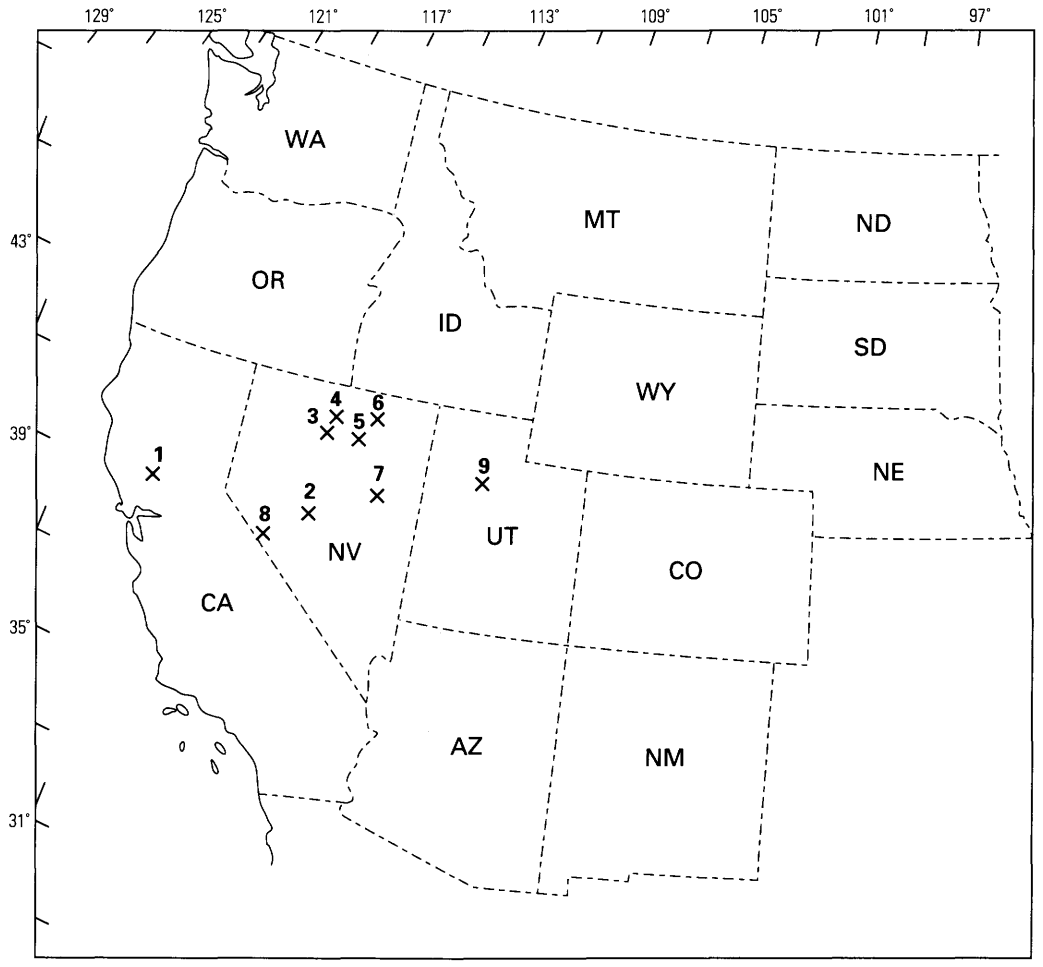

Figure 1. Location of epithermal precious-metal deposits that have produced byproduct mercury. 1, McLaughlin; 2, Paradise Peak; 3, Pinson; 4, Preble; 5, Carlin; 6, Jerritt Canyon; 7, Alligator Ridge; 8, Borealis; and 9, Mercur.

McLaughlin, Calif., producing 200 flasks per year; and Borealis, Nev., producing 4 flasks (fig. 1). Most sediment-hosted precious-metal deposits have produced byproduct mercury, but the production has been low, generally a few flasks per month. These deposits include Alligator Ridge, Carlin, Jerritt Canyon, Pinson, and Preble in Nevada and Mercur in Utah (fig. 1).

In volcanic-hosted deposits, mercury occurs as cinnabar but may also be present as corderoite ($Hg_3S_2Cl_2$), as mercury oxide, and in stibnite. Mercury in sediment-hosted deposits is generally present as cinnabar (Bagby and Berger, 1985; Radtke, 1985). In the Preble deposit, however, a mercury selenide and oxide as well as cinnabar have been identified (Raul Madrid, oral commun., 1989).

MERCURY IN HOT-SPRING SYSTEMS

In the hot-springs system models (see White and Roberson, 1962; Buchanan, 1981; White, 1981; Berger, 1982, 1985; Berger and Eimon, 1983; and Henley and Ellis, 1983), mercury is considered to be deposited at the surface and near-surface environment, with gold, arsenic, and antimony sulfides being deposited at deeper levels in the hydrothermal system (fig. 2). In near-surface hydrothermal systems, the position of the paleoground-water table is an important control on the deposition of mineral phases. Below the ground-water table, transport and deposition of ore metals occur in an aqueous phase. Above the ground-water table, transport and deposition occur from a vapor phase, except in areas where faults and fissures provide channels for fluid flow from the ground-water table to the surface. Unlike silver, gold, arsenic, antimony, and base

Figure 2. *A*, Schematic distribution of mercury from degassing magmas. *B*, Hot-spring system features overprinted on the mercury flux from degassing magma. *C*, Features of the waning stage of a hot-spring system showing overprinting of vapor-dominated alteration and mercury deposition on earlier hypogene ore due to lowering of the paleoground-water table. ▶

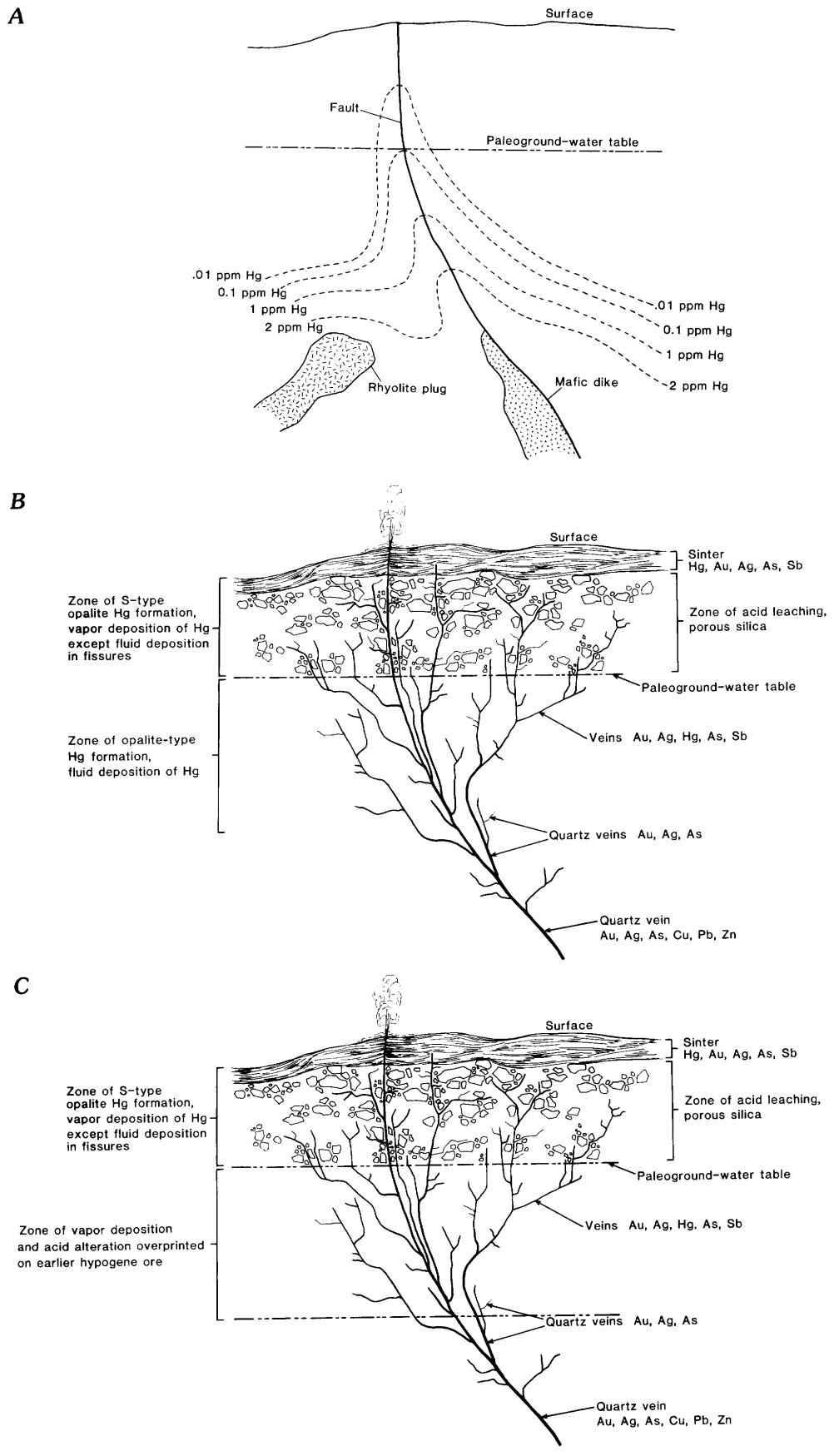
A
Surface
Fault
Paleoground-water table
.01 ppm Hg
0.1 ppm Hg
1 ppm Hg
2 ppm Hg
.01 ppm Hg
0.1 ppm Hg
1 ppm Hg
2 ppm Hg
Rhyolite plug
Mafic dike
B
Surface
Sinter
Hg, Au, Ag, As, Sb
Zone of S-type opalite Hg formation, vapor deposition of Hg except fluid deposition in fissures
Zone of acid leaching, porous silica
Paleoground-water table
Zone of opalite-type Hg formation, fluid deposition of Hg
Veins Au, Ag, Hg, As, Sb
Quartz veins Au, Ag, As
Quartz vein
Au, Ag, As, Cu, Pb, Zn
C
Surface
Sinter
Hg, Au, Ag, As, Sb
Zone of S-type opalite Hg formation, vapor deposition of Hg except fluid deposition in fissures
Zone of acid leaching, porous silica
Paleoground-water table
Zone of vapor deposition and acid alteration overprinted on earlier hypogene ore
Veins Au, Ag, Hg, As, Sb
Quartz veins Au, Ag, As
Quartz vein
Au, Ag, As, Cu, Pb, Zn

Table 1. Trace-element content of cinnabar deposited from vapor or fluid in 28 Nevada mercury deposits

[Analysis by emission spectroscopy. C. Heropoulos, analyst]

Deposit	Deposit type	Ag	As	Au	Cu	Mo	Pb	Sb	Sn	Zn
Vapor-deposited cinnabar										
Buckskin Peak	Opalite	<0.7	2	<0.5	7	<2	<7	2	5	50
Canyon Creek	Mafic volcanic	<.7	5	<.5	70	3	20	<1	<2	200
Castle Peak	Opalite	<.7	2	<.5	50	<2	30	15	<2	70
Cordero	Opalite	<.7	10	<.5	15	7	10	<1	<2	150
Goldbanks	Opalite	<.7	<1	<.5	5	<2	30	15	<2	<15
Red Rose	Opalite	<.7	<1	<.5	1.5	5	20	20	7	<15
Ruby	Sedimentary	<.7	<1	<.5	3	<2	<7	15	<2	<15
Thompson	Opalite	<.7	<1	<.5	7	<2	30	15	15	<15
Fluid-deposited cinnabar										
A and B	Opalite	<0.7	500	<0.5	1	20	150	15	<2	30
Antelope	Limestone	2	15	<.5	.7	<2	15	300	<2	<15
Cahill	Limestone	7.0	30	2.0	50	<2	10	500	15	1,000
Governor	Opalite	1.0	1.5	<.5	<.7	50	30	70	150	<15
Hagen Hegen	Opalite	2.0	100	<.5	7	<2	50	200	3	20
M & M	Opalite	1	150	.5	100	<2	30	100	<2	30
Mammoth	Sedimentary	1	1	1	7	<2	15	15	<2	20
McCoy	Sedimentary	.7	300	<.5	20	<2	150	700	<2	300
Nevada Cinnabar	Opalite	7.0	30	<.5	10	<2	50	200	30	<15
Nevada Sulfur	Opalite	1.5	3	<.5	5	<2	15	150	15	70
Nevada Quicksilver	Limestone	5	70	<.5	15	<2	10	300	>2	30
Pershing	Sedimentary	2	7	1.0	5	<2	300	300	<2	2,000
Red Bird RB1	Limestone	7	10	<.5	3	<2	300	700	<2	300
Red Bird RB2	Limestone	50	3	<.5	1,000	5	>50,000	>50,000	7	>50,000
San Pedro	Opalite	300	700	<.5	500	20	15,000	300	70	7,000
Steamboat Springs	Opalite	5	<1	<.5	700	<2	70	150	7	70
Stockton	Opalite	1	2	<.5	7	3	10	150	<2	<15
Teapot	Opalite	2	1,500	<.5	7	3	20	500	3	30
White Caps	Sedimentary Au	1	30	<.5	30	2	70	1,000	<2	1,000
Van Ness	Metamorphic	2	200	<.5	7	7	<7	50	3	50

metals, mercury can be transported both below the ground-water table (in a hydrothermal fluid) and above the ground-water table (as a vapor).

The control of the paleoground-water table on the deposition of ore elements has been documented at the Buckskin precious-metal deposit (Vikre, 1985) in Nevada. High-mercury contents occur above the paleoground-water table where mercury was deposited from a vapor and below the paleoground-water table where it was deposited from a fluid. High-silver, -gold, -arsenic, and -antimony contents are restricted to the zone below the paleoground-water table.

Vapor transport and deposition of mercury above the ground-water table is common in many active hydrothermal systems (White, 1955, 1967, 1980). Significant vapor transport of $H_2S(g)$ also occurs above the ground-water table when $H_2S(g)$, $Hg^0(g)$, Cl(g), and other volatile elements are boiled off from the hydrothermal system. Oxidation of $H_2S(g)$ by atmospheric oxygen leads to deposition of native sulfur, and mercury vapor reacts with sulfur to form cinnabar. Hydrolysis of native sulfur forms sulfuric acid, which subjects the host rock to acid alteration that results in an alteration assemblage of cristobalite, opaline silica, kaolinite, alunite±quartz, commonly termed acid-leached rock (White and Roberson, 1962). The "sulfurous type" of mercury deposit originally proposed by Bailey and Phoenix (1944) is formed in this chemical environment, as is the upper part of the "opalite-type" mercury deposit. The sulfur in many opalite-type deposits, however, has been removed by surface waters during weathering of these deposits. The lower part of opalite-type mercury deposits forms below the ground-water table where silicification can be pervasive along particularly permeable strata. These opalite-type deposits are distinguished from those formed above the ground-water table by the absence of vapor-deposited minerals and the presence of hydrothermal sulfides.

Cinnabar deposited from a vapor above the ground-water table is chemically pure. The trace-element characteristics of cinnabar deposited from a vapor, as compared to cinnabar deposited from a fluid, are discussed in the following section. Below the ground-water table,

mercury is transported as native mercury in solution (Varekamp and Buseck, 1984) or as a mercury bisulfide complex (Dickson and Tunell, 1967). The various mercury transport mechanisms are summarized by Rytuba (1985). The high solubility of Hg^0 and mercury-sulfide complexes, even at low temperatures, results in deposition of cinnabar in the upper part of the hydrothermal system and at the surface in hot-spring sinter. Ore elements transported along with mercury in the hydrothermal fluid are incorporated into the cinnabar mineral structure during deposition of cinnabar. Cinnabar deposited from a fluid is generally chemically impure and contains significant contents of trace elements.

In areas where volcanic activity precedes or is contemporaneous with the development of a hot-spring system, the distribution of mercury will be complex and reflect both vapor-deposited and fluid-deposited mercury. When volcanic activity precedes development of a hot-spring system, a mercury flux from degassing magma will spread outward into the country rock to develop a broad mercury anomaly having highest mercury contents immediately above the magma source (fig. 2*A*). Varekamp and Buseck (1986) summarized the magnitude of the mercury flux for passively degassing magmas and active volcanoes. The subsequently developed hydrothermal system will be superimposed on the mercury anomaly related to magma degassing. Mercury will be remobilized, concentrated in the hydrothermal system, and deposited in the upper level of the hot-spring system from a fluid phase and above the ground-water table from a vapor phase (fig. 2*B*). Lowering of the paleoground-water table during the waning stage of hydrothermal activity will expose previously deposited hypogene ore to volatiles boiling off from the residual hydrothermal fluid. Oxidation and alteration of the hypogene ore will occur at the same time that mercury is transported and deposited from the vapor phase. The overprinting of this late stage of vapor-deposited mercury on earlier hypogene ore is common in many hot-spring-related deposits. The geochemical distribution of mercury in hot-spring systems is therefore complex and reflects the cumulative effect of multiple events developed over the duration of volcanic and hydrothermal activity.

TRACE-ELEMENT CONTENT OF VAPOR- AND FLUID-DEPOSITED CINNABAR

Cinnabar can incorporate significant amounts of trace elements in its mineral structure. These elements include silver, arsenic, gold, copper, molybdenum, lead, tin, antimony, and zinc. Cinnabar deposited from a fluid transporting these elements will contain varying amounts of an element depending on the concentration of the element in the fluid phase. Cinnabar is an effective monitor of whether a fluid is carrying a particular element, such as silver or gold, even if the chemical and (or) physical conditions do not cause silver or gold to precipitate at the level or time of cinnabar deposition. In contrast, cinnabar deposited from a vapor is chemically pure and has very low contents of trace elements. The trace-element content of cinnabar can be used to distinguish between vapor-deposited cinnabar and fluid-deposited cinnabar.

Cinnabar mineral separates from 28 different mercury deposits in Nevada were analyzed by quantitative spectrographic analysis. Data for five mercury deposit types—opalite, limestone-hosted, clastic sediment-hosted, mafic volcanic-hosted, and metamorphic-hosted—are listed in table 1.

Cinnabar deposited from a vapor occurs in two deposit types: opalite and clastic sediment-hosted. Vapor-deposited cinnabar separates have very low concentrations of trace elements (in ppm): Ag (<0.70), As (≤ 20), Au (≤ 0.5), Cu (≤ 70), Mo (≤ 7), Pb (≤ 30), Sb (≤ 15), Sn (≤ 15), and Zn (≤ 200).

In contrast, cinnabar deposited from a hydrothermal fluid occurs in all five mercury deposit types and is characterized by high concentrations of antimony, greater than 150 ppm, and (or) arsenic, greater than 100 ppm. All cinnabar samples having high antimony contents contain from 1 to 300 ppm silver, and if arsenic content is high, gold is characteristically present in the range of 0.5 to 1 ppm. Base-metal contents in fluid-deposited cinnabar are generally in the same range as vapor-deposited cinnabar except for cinnabar having high silver content (>5 ppm). In these samples either lead, zinc, or copper exceeds 300 ppm. Tin and molybdenum values are comparable to those in vapor-deposited cinnabar except for two opalite-type deposits containing high tin (70–150 ppm) and molybdenum (20–50 ppm).

Trace-element analysis of cinnabar may prove useful in precious-metal exploration where identification of the paleoground-water table is important in defining the level at which precious metals are deposited. Chemically pure cinnabar indicates that the samples are from the zone of vapor transport and deposition and that precious-metal deposition occurred at a lower level. Analysis of fluid-deposited cinnabar could indicate whether silver and (or) gold were present in the hydrothermal solution as well as indicate the concentration of precious metals. The presence of appreciable silver and gold in cinnabar but not in the host rock indicates that these elements were deposited either above the level of cinnabar deposition or laterally away from the cinnabar in cases where fluid flow was confined to an aquifer. Systematic sampling of cinnabar from various levels indicates the direction of fluid flow because trace-element content decreases as fluids move from the source area. Trace-element analysis of cinnabar separates is more effective in geochemical prospecting than whole-rock analysis because the whole-rock chemistry records the cumulative effects of the mineralization event as it developed through time.

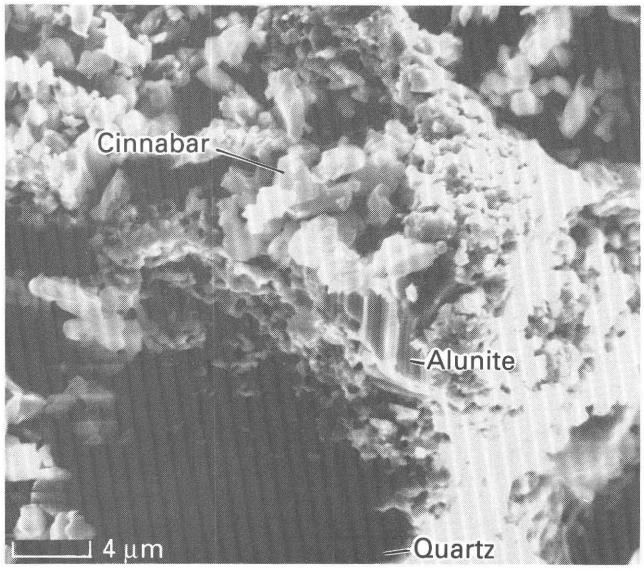

Figure 3. Cinnabar from the Nody prospect adjacent to and above the Paradise Peak ore zone. Assemblage consists of vapor-deposited cinnabar, with alunite and quartz (occurrence type 1).

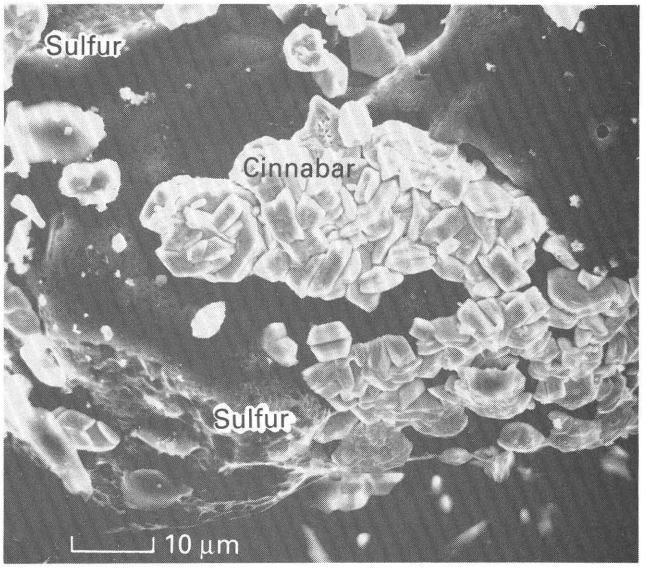

Figure 4. Vapor-deposited cinnabar and native sulfur overprinted on earlier hypogene ore, Paradise Peak deposit (occurrence type 2).

MERCURY IN THE PARADISE PEAK MINE

The Paradise Peak mine, located 14 km south of Gabbs, Nev., began production in 1986. With reserves of 1.1 million oz of gold and 30 million oz of silver, the deposit ranks seventh in gold reserves in the United States. It is the second largest producer of mercury in the United States. Mercury production averages about 1 metric ton (29 flasks) per month, and reserves are estimated to be about 3,000 flasks. More recent estimates suggest mercury production could increase to 800 to 2,600 flasks per year (Carrico, 1986).

The deposit has characteristics similar to those of many hot-spring-type gold deposits. The ore is hosted by pervasively silicified ash-flow tuff and andesite of mid-Tertiary age. Above the ore zone, the tuff is altered to an assemblage of alunite, kaolinite, and quartz. Gold is present as the native element, and silver occurs primarily as cerargyrite, acanthite, and native silver (Thomason, 1986; John and others, 1989). Within the deposit, mercury occurs in several phases and in several different environments, which include (1) cinnabar in association with kaolinite and alunite above the ore horizon, (2) cinnabar associated with sulfur in the ore zone, (3) corderoite as an oxidation product of stibnite in the ore zone, and (4) cinnabar containing appreciable silver in the ore zone.

Prior to discovery of the Paradise Peak gold deposit, sporadic exploration work occurred on the property, principally in the area around the Nody mercury prospect. The prospect occurs just above the gold ore zone and consists of sparse disseminations of cinnabar (occurrence type 1) in volcanic rock completely altered to kaolinite, alunite, and quartz (fig. 3). Sulfur is present in vugs within the more silicified rock. The occurrence is typical of cinnabar deposits formed in hot-spring systems above the ground-water table through vapor transport of mercury. The cinnabar is chemically pure and contains no gold or silver, either in the cinnabar or in acid-leached host rock. Interestingly, the shaft within the old mercury prospect was stopped just 12 m above the gold ore zone.

Within the gold ore zone, cinnabar occurs with native sulfur (occurrence type 2) in cavities that occur within the silicified tuff. Crystals of chemically pure cinnabar, up to 10 μm in diameter, are disseminated throughout the native sulfur (fig. 4). The cinnabar-sulfur assemblage formed late in the paragenetic sequence as evidenced by its presence only in cavities developed within previously silicified and mineralized tuff. The presence of sulfur and chemically pure cinnabar indicates that deposition occurred from a vapor. During the waning stage of the hydrothermal system, the paleoground-water table was lowered, exposing hypogene ore to vapor boiling off from the hydrothermal fluid. Mercury vapor and $H_2S(g)$ were transported through the few remaining spaces present in the silicified tuff. Oxidation of $H_2S(g)$ by atmospheric oxygen resulted in deposition of native sulfur, which reacted with mercury vapor to form cinnabar. The process is identical to that which formed cinnabar in occurrence type 1 except that it is overprinted on an earlier hypogene mineralization deposited from a hydrothermal fluid.

The major occurrence of mercury in the ore zone is as corderoite, occurrence type 3. Corderoite, $Hg_3S_2Cl_2$, is an extremely rare mineral, previously recognized only at two other localities: the McDermitt mercury mine, Nev., where

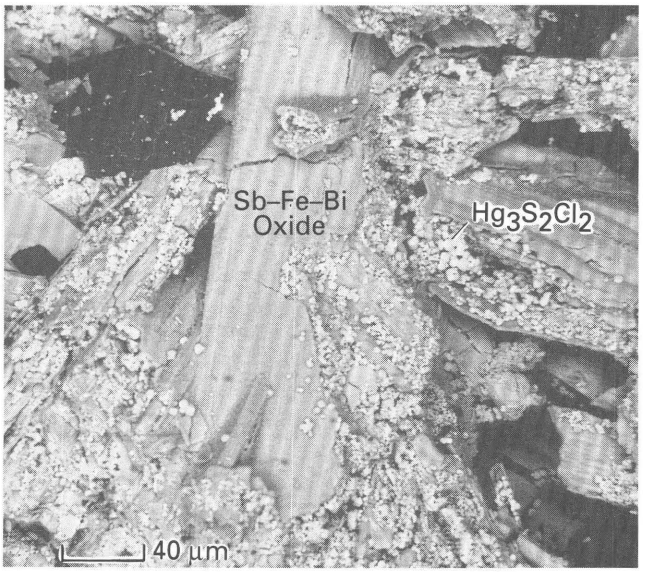

Figure 5. Antimony-iron-bismuth pseudomorphs after bismuthian stibnite. White crystals are corderoite, $Hg_3S_2Cl_2$ (occurrence type 3).

it is the main ore mineral, and at the Aizak mercury prospect in Tuva, U.S.S.R. (Vasil'ev and others, 1984). The corderoite at Paradise Peak occurs in association with an Sb-Bi-Fe oxide (an unnamed new mineral), which typically forms as pseudomorphs after stibnite (fig. 5). The corderoite occurs as isometric, dodecahedron crystals ranging from 1 to 5 in diameter (fig. 6*A*), which are identical to those present at the McDermitt mine (fig. 6*B*). The Sb-Bi-Fe-oxide is an oxidation product of stibnite that was deposited along fractures and in vugs with quartz during the early phase of hypogene mineralization. The stibnite contains appreciable bismuth in solid solution (Thomason, 1986) and mercury, indicating that both these elements were present in the ore-forming solution. During oxidation of the stibnite, mercury was released and reacted with native sulfur and $Cl_2(g)$ to form corderoite. Oxidation of the stibnite occurred during the waning stage of the hydrothermal activity when the paleoground-water table was lowered exposing the hypogene ore to atmospheric oxygen and $Cl_2(g)$ boiling off from the hydrothermal fluid.

The fourth occurrence type consists of silver-bearing cinnabar intergrown with quartz in the ore zone (fig. 7) and is quite rare. The cinnabar occurs as crystals up to 2 µm in diameter. The molecular ratio of silver to mercury in the cinnabar is variable and is as high as 1. The presence of silver in the cinnabar and its association with quartz indicate that it was deposited from a hydrothermal fluid rather than a vapor.

In summary, a variety of mercury phases occur at the Paradise Peak mine. During the hypogene stage of mineralization, mercury was deposited with stibnite in solid solution and as cinnabar containing variable amounts of

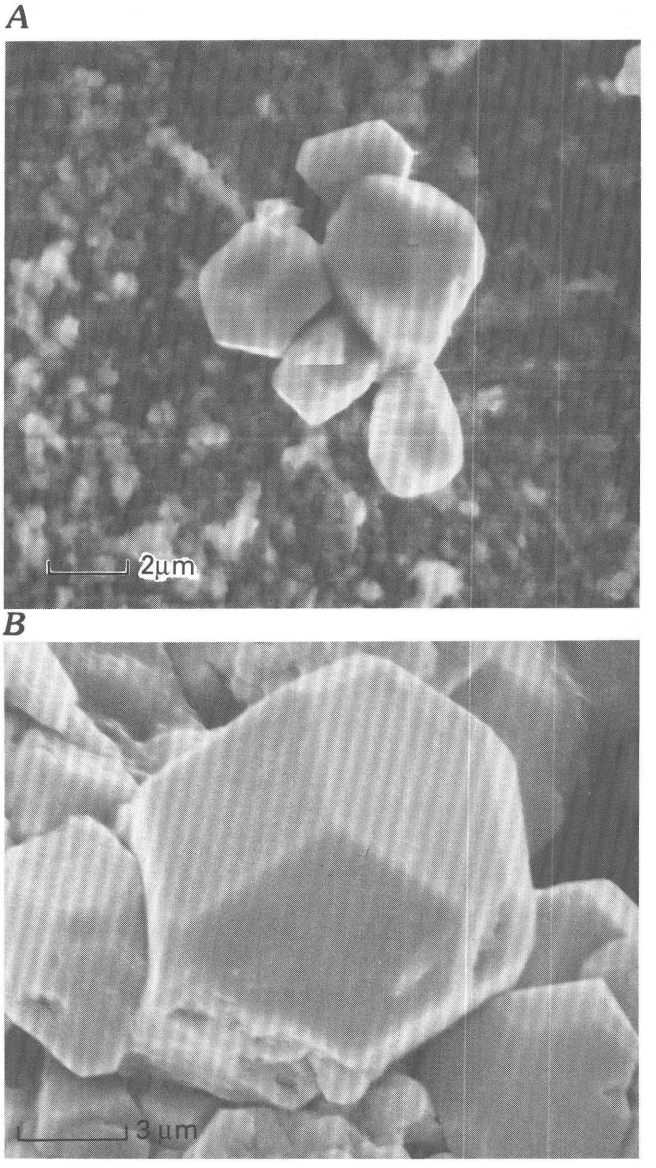

Figure 6. *A*, Isometric dodecahedron crystals of corderoite from Paradise Peak deposit. *B*, Corderoite from the McDermitt mercury deposit (occurrence type 3).

silver. During the waning stage of hydrothermal activity, lowering of the paleoground-water table exposed hypogene ore to vapor $H_2S(g)$ and Cl(g), $Hg^0(g)$ boiling off from the remaining hydrothermal fluid. Oxidation of $H_2S(g)$ resulted in the formation of native sulfur, which reacted with mercury vapor to form chemically pure cinnabar. Oxidation of stibnite released mercury, which reacted with native sulfur and chlorine vapor to form corderoite.

Mercury occurrences in the Paradise Peak deposit are an excellent example of the diverse processes that typically deposit mercury in epithermal gold systems. The distribution of mercury in these deposits reflects the

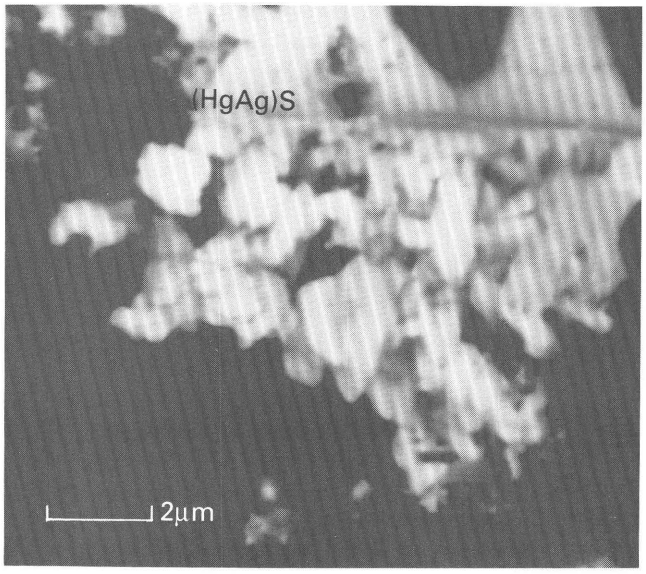

Figure 7. Silver-bearing cinnabar in association with quartz, Paradise Peak deposit (occurrence type 4). Darker gray cinnabar crystals contain highest Ag:Hg.

cumulative effect of these processes. Because only some stages of mercury deposition occur concurrently with gold or silver deposition, the use of whole-rock mercury for analysis in geochemical exploration should be done with caution.

REFERENCES

Bagby, W.C., and Berger, B.R., 1985, Comparative anatomy of sediment-hosted epithermal precious-metal deposits, *in* Berger, B.R., and Bethke, P.M., eds., Geology and geochemistry of epithermal systems: Reviews in Economic Geology, v. 2, p. 169–202.

Bailey, E.H., and Phoenix, D.A., 1944, Quicksilver deposits in Nevada: University of Nevada Bulletin, v. 30, no. 5, 206 p.

Berger, B.R., 1982, The geological attributes of Au-Ag-base metal epithermal deposits, *in* Erickson, R.L., ed., Characteristics of mineral deposit occurrences: U.S. Geological Survey Open-File Report 82–795, p. 119–126.

———1985, Geologic-geochemical features of hot-spring precious-metal deposits, *in* Tooker, E.W., ed., Geologic characteristics of sediment- and volcanic-hosted disseminated gold deposits—Search for an occurrence model: U.S. Geological Survey Bulletin 1646, p. 47–54.

Berger, B.R., and Eimon, P.I., 1983, Conceptual models of epithermal precious metal deposits, *in* Shanks, W.C., ed., Cameron volume on unconventional mineral deposits: American Institute of Mining, Metallurgical and Petroleum Engineers, p. 191–205.

Buchanan, L.J., 1981, Precious metal deposits associated with volcanic environments in the southwest, *in* Dickinson, W.R., and Payne, W.D., eds., Relations of tectonics to ore deposits in the southern cordillera: Arizona Geological Society Digest, v. 14, p. 237–261.

Carrico, L.C., 1986, Mercury: U.S. Bureau of Mines Minerals Yearbook, v. 1, p. 683–689.

Dickson, F.W., and Tunell, G., 1967, Mercury and antimony deposits associated with active hot-springs in the western United States, *in* Ridge, J.D., ed., Ore deposits of the United States, 1933–1967, Graton-Sales volume: American Institute of Mining, Metallurgical and Petroleum Engineers, v. 2, p. 1673–1701.

Henley, R.D., and Ellis, A.J., 1983, Geothermal systems ancient and modern—A geochemical review: Earth-Science Reviews, v. 19, p. 1–50.

John, J.A., Thomason, R.E., and McKee, E.H., 1989, Geology and potassium-argon geochronology of late Cenozoic volcanism, tectonism, and precious-metal mineralization in Paradise Peak mine area west-central Nevada: Economic Geology, v. 84, p. 631–649.

Radtke, A.S., 1985, Geology of the Carlin gold deposit, Nevada: U.S. Geological Survey Professional Paper 1267, 124 p.

Rytuba, J.J., 1985, Geochemistry of hydrothermal transport and deposition of gold and sulfide minerals in Carlin-type gold deposits, *in* Tooker, E.W., ed., Geologic characteristics of sediment- and volcanic-hosted disseminated gold deposits—Search for an occurrence model: U.S. Geological Survey Bulletin 1646, p. 27–34.

Thomason, R.E., 1986, Geology of the Paradise Peak gold/silver ore deposit, Nye County, Nevada, *in* Tingley, J.V., and Bonham, H.F., eds., Precious-metal mineralization in hot spring systems, Nevada-California: Nevada Bureau of Mines and Geology Report 41, p. 90–92.

Varekamp, J.C., and Buseck, P.R., 1984, The speciation of Hg in hydrothermal systems, with application for ore deposition: Geochimica et Cosmochimica Acta, v. 48, p. 177–185.

———1986, Global mercury flux from volcanic and geothermal sources: Applied Geochemistry, v. 1, p. 65–73.

Vasil'ev, V.I., Pal'chick, N.A., and Grechischev, O.K., 1984, Lavrentievite and Arkazite—New natural mercury sulfohalides: Geologiya i Geofizika, v. 25, no. 7, p. 54–73.

Vikre, P.G., 1985, Precious-metal vein systems in the National district, Humboldt County, Nevada: Economic Geology, v. 80, no. 2, p. 360–393.

White, D.E., 1955, Thermal springs and epithermal ore deposits: Economic Geology, 50th Anniversary Volume, p. 99–154.

———1967, Mercury and base-metal deposits with associated thermal and mineral waters, *in* Barnes, H.L., ed., Geochemistry of hydrothermal ore deposits: New York, Holt, Rinehart, and Winston, Inc., p. 575–631.

———1980, Steamboat Springs geothermal area: Society of Economic Geologists Epithermal Deposits Field Conference, 1980, Field Trip Guidebook, p. 44–51.

———1981, Active geothermal systems and hydrothermal ore deposits, *in* Skinner, B.J., ed.: Economic Geology, 75th Anniversary Volume, p. 392–423.

White, D.E., and Roberson, C.E., 1962, Sulphur Bank, California, a major hot-spring quicksilver deposit: Geological Society of America Buddington Volume, p. 397–428.

Chapter E

Nickel—Mineralogy and Chemical Composition of Some Nickel-Bearing Laterites in Southern Oregon and Northern California

By MICHAEL P. FOOSE

U.S. GEOLOGICAL SURVEY BULLETIN 1877

CONTRIBUTIONS TO COMMODITY GEOLOGY RESEARCH

CONTENTS

FIGURES

TABLES

Nickel—Mineralogy and Chemical Composition of Some Nickel-Bearing Laterites in Southern Oregon and Northern California

By Michael P. Foose

Abstract

The mineralogy and chemistry of 109 samples from 11 nickel-bearing laterites located in southern Oregon and northern California were determined. The laterites are primarily composed of serpentine, chlorite, goethite, and maghemite. Some contain additional minor amounts of smectite, quartz, talc, hornblende, orthopyroxene, and tremolite. Smectite (possibly nontronite) occurs only in laterites located on hillslopes and appears to be restricted to areas where ground water may have been enriched in SiO_2 and MgO from downslope flow across bedrock. Nickel content of the laterites averages 0.64 weight percent but varies between 0.45 and 1.4 weight percent; cobalt averages 0.06 weight percent and ranges between 0.03 and 0.15 weight percent. Neither nickel nor cobalt has predictable distributions. In contrast, patterns made by major elements follow trends defined by relatively simple chemical models. Calculated net changes in laterite chemistry indicate that the mobility of components is, from most depleted to least, MgO, SiO_2, nickel, MnO, Fe_2O_3, and cobalt. These calculations also show that only a few of the laterites have significant amounts of net enrichment in either nickel or cobalt.

INTRODUCTION

The United States is import-dependent for a number of important commodities, among which are nickel and cobalt. Several potentially important domestic deposits containing these elements have been identified. Of these, the most important are the magmatic sulfides in the Stillwater Complex (Montana) and the Duluth Complex (Minnesota), the sediment-hosted and strata-bound Cu-rich sulfides and arsenides of the Blackbird deposit (Idaho), Mississippi Valley-type lead deposits (southeast Missouri), and the nickel-bearing laterites in Oregon and northern California (Foose, 1991). Although one of these, a nickel laterite located near Riddle, Oreg., was recently mined (fig. 1), none of these deposits are currently in production.Other nickel-bearing laterites occur in southern Oregon and northern California, and several of these have recently been examined as potential additional sources of nickel and byproduct cobalt. This study looks at some of the mineralogical and chemical features associated with several of these occurrences.

GENERAL SETTING

The nickel laterite deposits in Oregon and northern California occur over ophiolites that are part of several different accreted terranes. As a result of the accretionary processes by which these terranes were affixed to the western margin of the United States, these ophiolitic rocks now form subparallel belts that range in age from Paleozoic (easternmost) to upper Jurassic (westernmost) (Irwin, 1977). Subsequent to emplacement, many of these ophiolitic bodies were exposed to extensive weathering that resulted in formation of laterites. There is some uncertainty as to the exact age of weathering. Most probably occurred during the Miocene formation of the Klamath peneplain (Diller, 1902). Some weathering, however, was much younger, as shown by the occurrence of laterite on Pleistocene terraces (Hotz, 1964; Moring, oral commun., 1986). Subsequently, most laterites have been uplifted and dissected so that many now occur on plateaus or as cappings on ridges and saddles and as transported debris on sides of hills and in valleys.

Nickel laterites similar to these are a common product of tropical weathering of ultramafic rocks. They, in fact, constitute the world's largest land-based resource of nickel (Chamberlain, 1986). The features associated with these deposits have been reviewed by a number of authors, most notably Trescases (1975), Evans and others (1979), and Golightly (1981). Features typical of laterite profiles from this area are reported as follows: Upper parts of laterite profiles consist of an extensively leached iron-rich zone (limonitic zone) that is dark reddish brown in color; iron oxide pellets locally occur near the profile top. This reddish zone grades downward into a yellow-brown zone (saprolitic

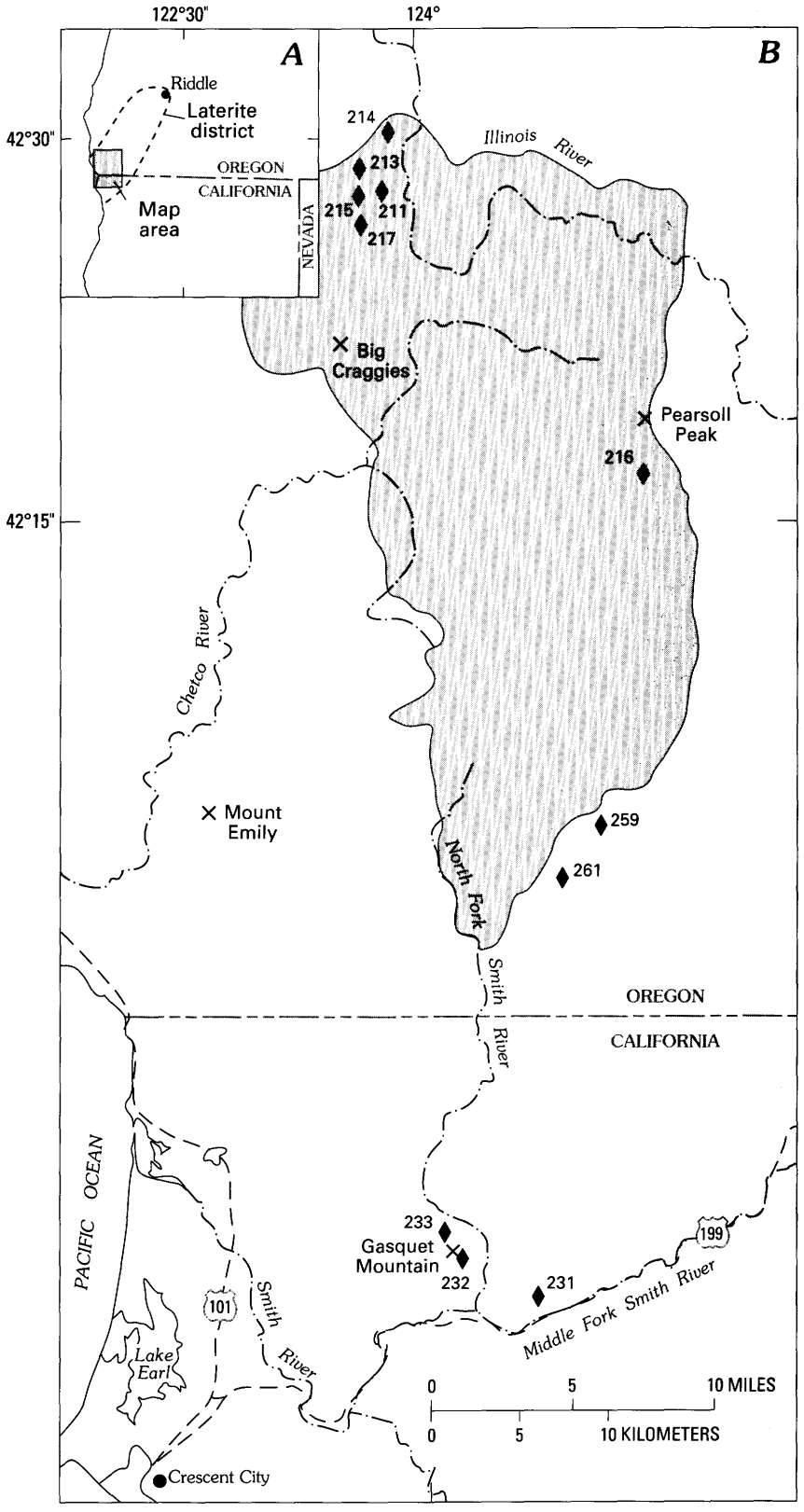

Figure 1. *A*, Approximate area of the northern California-southern Oregon laterite district (dashed boundary). *B*, Sample sites (solid diamonds). Shaded area represents approximate boundary of the Kalmiopsis Wilderness area.

zone) in which there commonly are pieces of partly weathered peridotite and in which the degree of preservation of relict bedrock structures increases with depth. The saprolite zone grades into greenish-brown weathered peridotite and then into fresh peridotite or serpentine (Hotz, 1964; Ramp, 1978).

In some laterites, nickel occurs in the lower saprolitic zone as a solid solution replacement of magnesium in a variety of secondary magnesium silicates (mostly serpentine, talc, and chlorite). These nickel-magnesium silicates are referred to as the "garnierite group" (Faust, 1966) and form what are commonly known as either saprolite or silicate ores. Nickel content of these ores typically is between 2 and 3 percent. In contrast, nickel in the overlying limonitic zone occurs mostly in goethite and rarely exceeds 2 percent. Significant amounts of cobalt also occur in many laterites and are associated mostly with manganese oxides (asbolite) that are concentrated in the lower part of the limonitic soil zone.

In Oregon and northern California, laterites having an extensively developed nickel-bearing silicate zone are known to occur only near Riddle, Oreg. Saprolite is present in other deposits but generally does not contain significant amounts of garnierite-type mineralization. The reason for the apparent restriction of higher grade nickel ores to the Riddle area is not clear, but Hotz (1964) speculates that rocks associated with this deposit may have had a longer weathering history. As a result of its higher nickel grades, the deposit near Riddle was the first to be developed.

In addition to its relatively greater nickel content, the ores at Riddle also contain relatively high amounts of silica and magnesium. As a result of this composition, refining must be done by pyrometallurgical processes (Canterford, 1975). The product was ferronickel containing about 49 percent nickel; cobalt was not recovered separately. In contrast, the lower SiO_2 and MgO contents of limonitic ores commonly allow them to be refined by a variety of hydrometallurgical techniques, many of which enable recovery of both nickel and cobalt. Specific processes designed to extract both nickel and cobalt from the relatively low grade laterites in northern California and Oregon have been developed and tested (Siemens and others, 1975; Duyvesteyn and others, 1979; Kukura and others, 1979), and, for this reason, several of these deposits have been evaluated as possible domestic sources of both nickel and cobalt.

SAMPLE DESCRIPTION AND TREATMENT

Samples from several laterite deposits were collected as part of a program to evaluate the mineral resources of the Kalmiopsis Wilderness (Page and others, 1982; fig. 1). Sample sites were both within or near the wilderness area and from an adjacent area, near Gasquet Mountain, Calif. This latter area contains several laterite deposits that may be commercially usable. Samples from the Gasquet Mountain area were collected from prospect pits in which profiles as thick as 7 m were exposed. In contrast, other samples were collected with a hand auger and, because of the limitations of this device, seldom penetrated more than 2 to 3 m of laterite. In eight cases, this amount of penetration was sufficient to sample profiles that exhibited all the features found in the more completely exposed pits as well as to show the same features that have been described for other laterites in this region (Hotz, 1964; Ramp, 1978). Samples collected from these eight locations as well as those taken from the exploration pits provide the material discussed in this report.

One hundred laterite samples and nine rock samples were analyzed for nickel, cobalt, copper, and 10 major oxides. Results are given in table 1. In addition, the mineralogy of samples was determined by X-ray diffraction. Samples were ground to less than 325 mesh and then pressed into circular wafers. Wafers were made by placing the ground material on a layer of boric acid and methyl cellulose, a compound added to provide strength. This mixture was compressed in a hydraulic press for at least 30 seconds at a pressure of 10,000 pounds per square inch. Wafers were then exposed to CuK_{α_1} radiation by using a 1.0° beam slit, a 0.1° detection slit, a crystal monochrometer, and a proportional counter detector. The samples were scanned between 2° and 60° 2θ at a rate of 1/2° 2θ/minute.

In order to resolve some ambiguous mineralogical identifications, several samples received further treatment. Splits from these were suspended in water and then allowed to settle onto porcelain tiles, a procedure which oriented the clay-size fraction. Four X-ray diffraction patterns, between 2° and 18° 2θ, were made of the clay fraction; first, after the samples had been air dried; second, after the samples were treated with ethylene glycol (EG) for at least 1 hour; third, after the samples had been heated to 350 °C for at least 1 hour; and fourth, after heating the samples to 550 °C for at least one hour.

This procedure enables the distinction of smectite from chlorite and vermiculite and the distinction of serpentine from kaolinite. Mineral identification is based on the following responses (Grim, 1968; Hathaway, unpublished report):

Upon treatment with EG, the 14-Å peak of smectite expands to 17 Å, while the 14-Å peaks of chlorite and (or) vermiculite are essentially unchanged.

Upon heating to 350 °C, the 14-Å peak of smectite collapses to 10 Å, while the chlorite and (or) vermiculite 14-Å peak is unchanged.

Upon heating to 550 °C, the 14-Å peak of chlorite may increase in intensity, the 14-Å peak of vermiculite collapses to 10 Å, and the 7-Å peak of serpentine remains stable, while the 7-Å peak of kaolinite is usually destroyed.

Table 1. Analyses from 11 laterites

[Locations of profile sample numbers are shown in figure 1; depth is in meters below surface. Nickel, cobalt, and copper are given in parts per million (J.S. Wahlberg, J. Baker, and J. Taggart, analysts). Mineralogy was determined by X-ray diffraction; numbers represent qualitative estimates of relative

Site/Sample number	Sample depth (m)	Sample type	Chlorite	Serpentine	Goethite	Maghemite	Quartz	Smectite	Talc	Ortho-pyroxene	Tremolite	Horn-blende
211–1	0.23	red-brown	11	0.0	12	2.0		0.0				
211–2	.38	gray-yellow	13	8.0	10	1.5		.0				
211–3	.64	gray-yellow	13	17	8.0	2.0		3.0				
211–4	.92	gray-yellow	15	16	8.0	8.0		3.0				
211–5	1.22	gray-yellow	9.5	42	7.0	8.0		3.5				
211–6	1.53	gray-yellow	6.5	62	6.0	10		5.0				
211–7	1.83	gray-green	7.0	46	6.0	8.5		2.5				
211–8	2.14	gray-green	7.5	54	5.0	9.0		5.0				
211–9		rock										
213–1	.15	red-brown	15	4.0	11.5	1.0	11	.0	2.0	4.0	3.0	
213–2	.31	red-brown	15	4.0	12.5	1.0	13	1.5	2.5	3.5	3.5	
213–3	.61	green-gray	11	4.0	12.5	5.0	8.5	3.5	2.5	3.0	2.5	
213–4	.92	black	6.5	2.5	12.5	8.0	3	5.0	2.0	1.5	.0	
213–5	1.22	black	6.5	2.5	11.5	7.5	3	4.0	.0	1.5	.0	
213–6	1.53	yellow-green	6.0	3.5	8.0	14	2	7.5	.0	.0	.0	
213–7	1.88	green-black	5.0	8.0	6.0	13	4	7.5	.0	.0	.0	
213–8		rock										
214–1	.15	red-brown	10	.0	14	7.0	5	.0	4.0			11
214–2	.31	red-brown	11	10	10	11	4	.0	4.5			10
214–3	.61	yellow-green	6.0	46	11	8	3	4.0	.0			4.0
214–4	.92	yellow-green-black	5.0	75	3.5	10	2	5.0	.0			.0
214–5	1.22	green-black	6.5	65	4.5	7.0	1	2.5	.0			4.5
214–6	1.37	green-black	7.5	72	4.0	7.0	1	2.0	.0			3.0
214–7		rock										
215–1	.15	red-brown	16	1.5	10	2.5	23	4.0	6.0			2.5
215–2	.31	red-brown	15	2.5	10	2.5	22.5	5.0	6.0			2.0
215–3	.61	dark-red-brown	19	.0	10	2.5	23	5.0	7.5			4.5
215–4	.92	yellow-green	11	3.0	11	.0	15	6.0	9.5			5.5
215–5	1.22	yellow-green	12	.0	14	.0	10.5	8.0	8.0			7.0
215–6		rock										
216–1	.15	red-brown	40	7.5	14	3.0	7.5	.0	70			7.5
216–2	.31	red-brown	44	5.0	14	6.0	4.0	.0	75			9
216–3	.61	yellow-brown	55	2.5	16	6.0	3.5	5.5	82			10
216–4	.92	yellow-brown	43	3.5	10	3.5	4.5	5.0	57			7
216–5	1.22	yellow-brown	47	4.0	12	1.5	5.0	5.0	65			11
216–6		rock										
217–1	.15	dark-red-brown	5.0	4.0	12	6.0		2.5				
217–2	.31	red-brown	7.0	4.5	12	6.0		4.5				
217–3	.61	green-gray	6.5	42	12	13		3.5				
217–4	.92	green-gray	9.5	59	6.0	11		5.0				
217–5	1.22	green-gray	5.5	58	5.0	12		2.0				
217–6	1.53	green-gray	6.0	100	6.0	13		2.0				
217–7		rock										
231–1	.46	red-yellow	9.0	43	9.0	2.0	10					
231–2	.87	yellow-brown	43	4.0	12	.0	3.0					
231–3	1.20	red-brown	12	20	11	3.0	11					
231–4	1.55	red-brown	8.5	10	10	.0	13					
231–5	2.01	red-brown	8.5	11	12	.0	16					
231–6	2.32	red-brown	7.5	20	10	.0	16					
231–7	2.62	red-brown	8.5	3.0	12	1.0	13					
231–8	2.93	red-brown	7.0	81	10	3.5	11					
231–9	3.23	yellow-brown	8.0	86	9.5	3.5	12					
231–10	3.54	yellow-brown	8.0	6.0	10	.0	12					
231–11	3.84	yellow-brown	6.0	5.0	12	2.0	10					
231–12	4.15	yellow-brown	6.5	8.0	12	2.5	10					
231–13	4.45	yellow-brown	.0	4.0	9.5	2.5	7.5					

and were determined by flame atomic absorption (M. Doughten, analyst). Major oxides are in weight percent and were determined by X-ray spectroscopy mineral abundance and are proportional to X-ray peak height as discussed in the text. LOI, loss on ignition; <, less than; IS, insufficient sample]

Ni (ppm)	Co (ppm)	Cu (ppm)	SiO_2 (wt. %)	Al_2O_3 (wt. %)	Fe_2O_3 (wt. %)	MgO (wt. %)	CaO (wt. %)	Na_2O (wt. %)	K_2O (wt. %)	TiO_2 (wt. %)	P_2O_5 (wt. %)	MnO (wt. %)	LOI (wt. %)
6800	1000	130	15.1	14.2	41.0	10.1	0.16	<0.2	<0.02	0.28	<0.1	0.42	13.76
8300	1600	95	20.8	9.0	37.6	12.9	.55	<.2	<.02	.11	<.1	.58	13.61
8800	1300	77	27.1	8.1	30.8	15.3	.37	<.2	<.02	.06	<.1	.33	14.11
8300	1100	80	25.5	9.3	33.2	12.3	3.17	<.2	<.02	.22	<.1	.38	12.72
8000	940	82	27.2	6.9	29.9	17.3	1.13	<.2	<.02	.11	<.1	.35	13.88
8600	830	80	27.9	4.9	30.5	18.4	.70	<.2	<.02	.08	<.1	.37	13.82
8800	800	72	26.6	5.0	33.0	17.2	.55	<.2	<.02	.09	<.1	.43	13.38
9700	660	52	29.2	4.4	29.7	18.5	.65	<.2	<.02.	.08	<.1	.37	13.99
2500	130	28	40.4	2.1	8.4	37.1	2.08	<.2	<.02	.03	<.1	.17	9.19
4900	700	130	14.7	12.6	48.3	4.8	.28	<.2	.11	.48	<.1	.60	11.40
4900	700	110	18.6	12.8	43.9	5.0	.37	<.2	.15	.64	<.1	.64	12.28
5200	640	130	14.4	10.0	54.1	3.2	.27	<.2	.13	.32	<.1	.44	12.15
5700	1100	120	15.3	7.9	53.7	5.0	.40	<.2	.07	.21	<.1	.10	11.94
6200	1100	120	18.4	6.6	51.6	3.0	.31	<.2	.05	.14	<.1	1.07	14.29
6000	760	110	24.0	7.2	43.9	4.3	1.01	<.2	.05	.20	<.1	.90	14.99
7500	570	75	27.8	4.5	37.8	9.2	.83	<.2	.03	.09	<.1	.92	15.02
3800	140	10	40.3	.8	8.6	37.7	.43	<.2	<.02	<.02	<.1	.16	10.86
4800	440	40	16.6	8.7	51.7	4.8	1.11	<.2	.09	.40	.1	.35	13.69
5200	540	37	17.8	6.7	51.7	6.3	.90	<.2	.06	.29	<.1	.41	12.88
6800	390	23	26.8	4.5	36.0	15.8	.59	<.2	.05	.19	<.1	.42	13.36
6300	360	23	28.8	3.9	31.6	17.9	.54	<.2	.04	.16	<.1	.41	15.20
5400	370	25	26.3	5.3	35.8	14.7	.86	<.2	.06	.24	<.1	.44	14.10
5000	340	23	28.3	4.9	32.5	16.5	.81	<.2	.07	.23	<.1	.41	14.21
4700	160	10	38.7	.4	8.8	36.8	.07	<.2	<.02	<.02	<.1	.20	13.62
1100	190	120	21.2	23.0	33.2	2.2	.26	<.2	.26	.90	.1	.28	16.52
1100	180	120	22.4	22.8	33.0	1.8	.19	<.2	.27	1.01	.1	.28	15.71
1100	180	120	24.1	23.1	31.6	2.4	.35	<.2	.31	1.02	.1	.24	14.84
1200	140	100	25.0	22.5	29.7	2.8	.37	<.2	.18	.89	<.1	.01	15.14
1300	160	90	22.3	21.6	33.2	3.2	.61	<.2	.15	.79	<.1	.11	15.46
260	56	10	42.4	16.3	9.1	8.5	16.50	.4	.03	.88	<.1	.16	4.64
5700	530	110	27.1	5.4	34.9	11.8	1.23	.3	.07	.25	<.1	.51	11.30
5600	620	120	25.0	5.0	38.2	11.9	1.27	.3	.06	.23	<.1	.43	8.32
5900	540	120	30.5	5.0	33.6	12.4	1.15	.4	.07	.20	<.1	.39	10.59
6400	530	80	32.2	3.7	31.1	14.5	.90	<.2	.04	.14	<.1	.38	11.46
6500	440	100	34.2	4.4	29.1	14.7	1.50	.3	.05	.26	<.1	.33	10.84
3000	140	44	38.9	1.2	9.8	36.9	.59	<.2	<.02	<.02	<.1	.14	11.02
8400	710	100	8.6	6.5	58.0	3.4	.74	<.2	.03	.11	<.1	1.42	15.08
7000	630	85	16.8	5.9	52.9	3.1	1.97	<.2	.03	.10	<.1	.64	13.76
6900	460	60	30.0	3.1	30.5	19.2	1.10	<.2	<.02	.04	<.1	.44	13.22
7000	330	60	34.7	2.0	21.9	24.0	2.00	<.2	<.02	<.02	<.1	.29	12.30
6400	330	60	34.7	1.8	20.1	27.6	1.15	<.2	<.02	<.02	<.1	.27	12.39
5900	320	230	35.3	1.7	18.6	29.7	.57	<.2	<.02	<.02	<.1	.23	12.41
6800	120	12	38.9	.6	8.5	35.6	.12	<.2	<.02	<.02	<.1	.14	13.92
3700	450	75	17.1	12.7	47.1	4.5	.08	<.2	.13	.66	.1	.56	13.20
4500	600	92	14.7	13.0	52.6	2.6	<.02	<.2	.15	.51	<.1	.37	10.99
4600	450	82	16.2	14.2	50.5	1.9	<.02	<.2	.17	.65	.1	.36	11.20
4000	450	85	17.2	14.5	49.4	1.9	.03	<.2	.20	.69	.1	.37	10.75
3500	380	87	15.5	13.6	47.9	3.8	<.02	<.2	.09	.52	<.1	.42	13.49
3400	310	82	16.0	15.2	50.1	1.8	<.02	<.2	.20	.68	.1	.39	11.18
3700	300	85	15.6	15.1	50.4	1.5	<.02	<.2	.19	.67	.1	.35	11.51
3400	350	60	17.5	13.8	47.9	4.2	<.02	<.2	.17	.62	<.1	.37	11.41
3200	460	62	16.9	13.3	48.4	4.3	<.02	<.2	.16	.60	<.1	.38	11.10
3800	300	82	13.8	13.9	53.4	1.8	<.02	<.2	.15	.61	.1	.37	10.34
4000	290	75	12.9	13.9	53.3	2.1	<.02	<.2	.12	.57	.1	.36	11.68
4400	260	75	13.0	13.8	53.1	1.7	<.02	<.2	.13	.53	<.1	.33	11.60
4200	260	72	11.8	12.9	56.1	1.6	<.02	<.2	.11	.49	<.1	.35	10.79

Table 1. Analysis from 11 laterites—Continued

Site/Sample number	Sample depth (m)	Sample type	Chlorite	Serpentine	Goethite	Maghemite	Quartz	Smectite	Talc	Ortho-pyroxene	Tremolite	Horn-blende
231–14	4.76	yellow-brown	4.5	0.0	10	4.5	8.5					
231–15	5.06	yellow-brown	7.5	.0	11	5.0	9.0					
231–16	5.37	yellow-brown	9.0	.0	11	4.0	8.5					
231–17	5.67	yellow-brown	4.5	.0	12	7.0	8.0					
231–18	5.98	yellow-brown	1.5	.0	13	8.5	2.0					
231–19	6.28	yellow-brown	6.5	.0	14	8.0	4.0					
231–20	6.59	yellow-brown	5.5	.0	13	7.5	2.5					
232–1	.31	red-brown	6.0	.0	12	3.0	16		7.0			2.0
232–2	.61	red-brown	6.5	1.5	11	4.0	15		6.0			3.0
232–3	1.22	red-brown	5.0	.5	12	2.0	16		7.5			4.0
232–4	1.53	red-brown	7.0	1.5	11	2.5	18		3.0			1.5
232–5	1.83	red-yellow	4.5	.0	13	.0	13		8.0			3.0
232–6	2.14	red-yellow	2.0	.0	18	.0	10		5.5			1.5
232–7	2.44	red-yellow	2.5	.5	8.0	4.5	10		5.5			2.5
232–8	2.75	red-yellow	5.0	.0	13	1.5	12		5.0			1.5
232–9	3.05	red-yellow	3.5	.0	15	3.5	5.0		3.5			1.5
232–10	3.36	red-yellow	2.5	.0	14	18	2.0		.0			.0
232–11	3.66	red-yellow	2.5	.0	12	7.0	4.0		3.5			2.0
232–12	3.97	red-yellow	5.5	.0	12	2.5	15		6.5			4.0
232–13	4.27	red-yellow	7.5	1.5	11	3.0	14		6.0			1.5
232–14	4.58	red-yellow	4.0	.0	12	1.5	11		5.5			2.0
233–1	.31	red-brown	.0	.0	22	3.0		.0	4.5	.0		.0
233–2	.61	red-brown	.0	.0	20	2.0		.0	9.5	.0		.0
233–3	1.22	red-brown	5.0	.0	18	2.0		.0	13	.0		.0
233–4	1.53	yellow-brown	7.0	7.0	16	2.0		.0	12	.0		.0
233–5	1.83	yellow-brown	12	30	15	2.0		.0	13	11		2.5
233–6	2.14	yellow-brown	16	40	14	4.0		.0	13	.0		3.0
233–7	2.44	yellow-brown	9.0	50	13	8.5		2.0	3.5	.0		3.0
233–8	2.75	yellow-brown	5.0	33	16	4.0		.0	5.5	.0		2.0
233–9	3.05	yellow-brown	4.5	20	13	3.0		.0	3.5	2.0		3.0
233–10	3.36	yellow-brown	4.0	15	13	5.5		.0	1.5	1.0		1.5
233–11	3.66	yellow-brown	7.5	20	9.5	10.5		.0	1.5	4.0		2.5
233–12	3.97	yellow-brown	2.5	10	14	6.5		.0	3.0	9.5		2.5
233–13		rock										
259–1	.15	red-brown	25	.0	11	7.0	8.0		5.5			10
259–2	.31	red-brown	16	8.5	16	3.0	5.0		5.5			2.0
259–3	.61	yellow-red	12	47.5	13	5.0	4.0		5.0			5.0
259–4	.92	yellow-red	9.0	100	10	6.0	4.5		5.5			4.0
259–5	1.22	yellow-brown	10.5	100	10	7.0	2.0		5.0			5.0
259–6	1.53	yellow-brown	8.0	100	9	7.0	2.0		11			1.0
259–7	1.83	yellow-brown	6.0	100	8	7.0	2.0		15			4.0
259–8	2.14	yellow-brown	6.0	100	8	9.0	1.0		6.5			6.0
259–9		rock										
261–1	.15	red-brown	.0	.0	13	9.0			.0			.0
261–2	.31	red-brown	.0	.0	14	9.0			.0			.0
261–3	.61	red-brown	3.5	.0	13	11			.0			.0
261–4	.92	gray-brown	2.0	.0	13	11			.0			.0
261–5	1.22	gray-brown	3.0	.0	13	9.5			5.5			.0
261–6	1.53	yellow-brown	8.0	25	13	11			1.5			.0
261–7	1.83	yellow-brown	6.5	20	12	9.0			3.0			2.0
261–8	2.14	yellow-brown	3.0	18	14	13			3.0			1.0
261–9	2.44	yellow-brown	2.0	100	11	14			2.5			2.0
261–10		rock										

Ni (ppm)	Co (ppm)	Cu (ppm)	SiO_2 (wt. %)	Al_2O_3 (wt. %)	Fe_2O_3 (wt. %)	MgO (wt. %)	CaO (wt. %)	Na_2O (wt. %)	K_2O (wt. %)	TiO_2 (wt. %)	P_2O_5 (wt. %)	MnO (wt. %)	LOI (wt. %)
5200	340	55	13.7	10.5	58.8	1.8	<0.02	<0.02	0.15	0.38	<0.1	0.39	8.22
5000	480	57	15.3	11.6	56.6	1.7	<.02	<.2	.22	.43	<.1	.44	9.01
5400	470	60	15.1	10.8	57.6	1.8	<.02	<.2	.19	.43	<.1	.48	8.84
6300	660	62	10.7	8.9	63.6	1.8	<.02	<.2	.12	.28	<.1	.51	8.09
6100	860	67	6.5	7.8	69.4	1.8	<.02	<.2	.05	.14	<.1	.56	7.72
5700	2000	77	11.6	9.7	62.5	2.4	<.02	<.2	.11	.24	<.1	.78	7.92
5700	1500	97	14.1	10.9	56.1	3.5	<.02	<.2	.11	.25	<.1	.83	9.45
5300	720	70	23.2	11.2	41.4	4.7	.46	<.2	.21	.52	.1	.70	11.85
5200	700	70	24.0	11.4	41.0	4.5	.47	<.2	.23	.55	.1	.70	12.30
5800	720	70	23.5	10.5	42.6	4.7	.55	<.2	.21	.50	.1	.65	11.51
3900	510	87	28.1	13.2	35.7	4.7	.44	<.2	.30	.69	.1	.73	11.32
5700	910	80	22.1	10.0	44.3	4.8	.55	<.2	.15	.43	.1	.76	11.68
5500	600	63	10.4	7.0	60.2	2.6	.19	<.2	.05	.17	<.1	.36	13.65
6100	1000	70	20.3	11.3	46.4	3.3	.32	<.2	.15	.53	.1	.85	11.15
6100	570	63	21.6	11.1	45.5	3.4	.31	<.2	.25	.50	.1	.45	11.10
7900	630	85	9.9	10.2	58.3	1.5	.06	<.2	.15	.28	.1	.28	13.54
6200	480	110	2.5	5.2	77.6	.7	<.02	<.2	<.02	.06	<.1	.18	8.36
6400	660	80	8.4	6.7	68.0	1.9	.13	<.2	.08	.18	<.1	.37	9.01
5800	760	67	23.0	11.1	43.1	4.1	.44	<.2	.20	.53	.1	.63	11.16
5800	720	65	22.9	10.9	43.4	4.5	.46	<.2	.18	.51	.1	.61	10.85
7000	1000	72	16.1	9.8	51.9	3.7	.27	<.2	.16	.37	.1	.57	11.95
7300	630	70	5.1	5.9	66.1	1.7	<.02	<.2	.03	.11	<.1	.39	15.59
7200	760	70	4.0	5.3	67.8	1.4	<.02	<.2	<.02	.07	<.1	.37	15.49
7000	1200	57	7.4	5.2	65.3	2.9	.12	<.2	.03	.07	<.1	.49	13.20
9200	1300	57	10.0	4.5	63.1	4.0	.25	<.2	<.02	.04	<.1	.65	13.05
13000	700	63	21.0	3.2	48.2	10.2	1.07	<.2	<.02	.03	<.1	.57	11.68
13000	1000	53	17.4	3.4	52.9	8.6	.66	<.2	<.02	<.02	<.1	.87	11.62
11000	1000	71	11.4	3.0	66.6	5.2	.38	<.2	<.02	<.02	<.1	1.09	8.60
14000	880	43	21.3	2.9	48.5	10.9	.88	<.2	<.02	<.02	<.1	.97	10.60
14000	920	68	24.2	3.4	44.8	12.4	.99	<.2	<.02	<.02	<.1	.78	9.00
5500	440	97	IS	IS	IS	IS	IS	IS	IS	IS	IS	IS	IS
16000	1100	98	IS	IS	IS	IS	IS	IS	IS	IS	IS	IS	IS
15000	840	63	19.2	3.0	50.3	9.9	.72	<.2	<.02	<.02	<.1	.90	11.04
6200	110	14	41.2	.6	9.3	39.1	.54	<.2	<.02	<.02	<.1	.13	8.15
4300	400	72	23.9	14.2	32.7	10.2	1.67	<.2	.19	.45	<.1	.57	12.46
5900	410	120	17.8	13.8	42.1	6.8	.59	<.2	.12	.34	<.1	.39	13.84
5400	430	95	19.4	12.0	40.3	9.1	.83	<.2	.09	.29	<.1	.50	13.05
4800	430	72	24.6	9.9	32.8	14.7	.56	<.2	.08	.26	<.1	.64	12.69
5000	300	60	27.6	8.6	28.6	18.2	1.20	<.2	.06	.22	<.1	.40	11.96
4300	260	45	31.6	6.8	23.1	21.7	.76	<.2	.04	.16	<.1	.39	12.02
4400	250	35	33.6	5.4	20.3	24.7	.77	<.2	<.02	.11	<.1	.34	11.64
5000	250	20	35.8	4.1	18.6	26.1	.64	<.2	<.02	.08	<.1	.34	10.89
2100	100	10	39.4	1.8	8.4	36.5	.98	<.2	<.02	<.02	<.1	.14	11.28
8100	1200	120	3.9	7.7	66.4	1.1	.08	<.2	.06	.13	<.1	.76	13.91
8800	950	110	3.7	8.3	67.4	.8	.04	<.2	.05	.13	<.1	.66	13.61
8100	1200	100	3.2	8.0	70.8	.9	<.02	<.2	.04	.11	<.1	.78	11.38
10000	2700	65	3.2	5.0	74.1	.9	.03	<.2	<.02	.08	<.1	1.44	10.65
13000	2000	45	4.1	4.2	73.0	1.2	.05	<.2	<.02	.07	<.1	1.20	10.41
14000	1800	55	5.7	4.7	68.2	2.0	.27	<.2	<.02	.06	<.1	1.17	12.76
12000	1200	95	7.7	6.4	63.6	2.7	.72	<.2	<.02	.06	<.1	.94	12.28
11000	1200	100	7.7	6.5	65.9	2.8	.57	<.2	<.02	.05	<.1	1.05	11.30
10000	950	70	12.1	5.6	58.9	8.2	.17	<.2	<.02	<.04	<.1	.92	10.22
2700	170	10	40.3	.8	9.2	41.5	.71	<.2	<.02	<.02	<.1	.21	6.48

Table 2. Mineralogical and chemical summary

Relative change in mineral abundance with increasing sample depth[1]

Site	Serpentine	Chlorite	Goethite	Maghemite	Smectite	Quartz	Talc	Horn-blende	Ortho-pyroxene	Tremolite
211	Inc	Dec	Dec	Inc	Inc					
213	Inc	Dec	Dec	Inc	Inc	Dec	Dec		Dec	Dec
214	Inc	Dec	Dec	Inc	Inc	Dec	Dec	Dec		
215	NC	Dec	NC	Dec	Inc	Dec	Dec	Inc		
216	NC	NC	NC	NC	Inc	NC	Dec	Inc		
217	Inc	NC	Dec	Inc	NC					
231	Dec	Dec	NC	Inc		Dec				
232	Inc	NC	NC	NC		Dec	NC	NC		
233	Inc	Inc	Dec	Inc			Dec	Inc	Inc	
259	Inc	Dec	Dec	Inc		Dec	Inc	NC		
261	Inc	Inc	Dec	Inc			Inc	Inc		

Bedrock mineralogy[2]

Site	Serpentine	Chlorite	Olivine	Ortho-pyroxene	Clino-pyroxene	Maghemite	Goethite	Talc	Horn-blende	Magnetite	Tremolite
211	x	x	x		x					x	
213	x	x		x							x
214	x					x					
215		x					x	x	x		
216	x	x	x			x	x	x	x		
217	x	x				x					
233	x		x	x				x			
259	x	x				x	x		x		
261	x		x			x					

Trends in laterite chemistry with increasing depth[1]

Site	MgO	SiO_2	Fe_2O_3	Al_2O_3	TiO_2	CaO	Ni	Co	MnO	Cu
211	Inc	Inc	Dec	Dec	Dec	Inc	Inc	Dec	NC	Dec
213	Inc	Inc	Dec	Dec	Dec	Inc	Inc	Inc	Inc	Dec
214	Inc	Inc	Dec	Dec	Dec	NC	NC	Dec	Inc	Dec
215	Inc	NC	NC	NC	NC	Inc	Inc	Dec	Dec	Dec
216	Inc	Inc	Dec	Dec	Dec	NC	Inc	Dec	Dec	Dec
217	Inc	Inc	Dec	Dec	Dec	NC	Dec	Dec	Dec	Dec
231	NC	NC	Inc	Dec	Dec	NC	Inc	Inc	Inc	NC
232	NC	NC	NC	NC	NC	NC	Inc	NC	NC	NC
233	Inc	Inc	Dec	Dec	Dec	Inc	Inc	NC	Inc	NC
259	Inc	Inc	Dec	Dec	Dec	NC	NC	Dec	Dec	Dec
261	Inc	Inc	Dec	Dec	Dec	Inc	Inc	NC	Inc	Dec

[1]Inc, increase; Dec, decrease; NC, no change.
[2]x indicates presence of mineral.

The abundance of a mineral in these samples is, in part, reflected by the intensity of its X-ray diffraction peaks. Peak intensity is, however, also dependent on other factors, such as degree of crystallinity, orientation, and interferences. As a result, obtaining quantitative mineral modes from diffraction data is an extremely difficult task (Grim, 1968) and was not done for these samples. An attempt was made, however, to qualitatively estimate mineral abundances within each of the 11 laterite profiles. These estimates were made by measuring the height above background of each mineral's most intense reflection. Mineral abundance estimates derived from X-ray diffraction data most often are made by measuring the area under peaks. Although less accurate, measurement of peak height has also been shown to be closely related to mineral abundance (Gibbs, 1965).

The mineralogical and chemical data for the 11 profiles are presented in table 1 and are partly summarized in tables 2 and 3. The X-ray traces and plots of mineralogical and chemical data from two profiles (sites 216 and 233) are given in figures 2 and 3 as further illustration of the approach used in this study.

LATERITE MINERALOGY

The mineralogy of these laterite profiles is relatively simple (table 2). All contain serpentine, chlorite, goethite, and maghemite. Additional phases that are present in some samples, but not all, are smectite, quartz, talc, and hornblende. No attempt was made to further identify the smectite, but on the basis of the iron-rich composition of

Table 3. Range of laterite compositions

[Mean values are computed on untransformed data (arithmetic (Ar.) means) and on log-transformed data (geometric (Gm.) means). Sd., standard deviations. Numbers in parentheses indicate number of samples analyzed]

Site		Ni (ppm)	Co (ppm)	SiO_2 (percent)	MgO (percent)	Fe_2O_3 (percent)	Al_2O_3 (percent)	MnO (percent)
211	Min.	6,800	660	15.1	10.1	29.7	4.4	0.33
(8)	Max.	9,700	1,600	29.2	18.5	41.0	14.2	.58
	Ar. mean	8,413	1,029	24.9	15.3	33.2	7.7	.40
	Sd.	827	303	4.7	3.1	4.1	3.2	.08
	Gm. mean	8,375	993	24.5	14.9	33.0	7.2	.40
	Sd.	1.1074	1.327	1.25	1.25	1.12	1.49	1.19
213	Min.	4,900	570	14.4	3.0	37.8	4.5	.10
(7)	Max.	7,500	1,100	27.8	9.2	54.1	12.8	1.07
	Ar. mean	5,771	796	19.0	4.9	47.6	8.8	.67
	Sd.	920	216	5.1	2.0	6	3.1	.33
	Gm. mean	5,712	773	18.5	4.6	47.3	8.3	.55
	Sd.	1.1644	1.294	1.29	1.44	1.14	1.46	2.25
214	Min.	4,800	340	16.6	4.8	31.6	3.9	.35
(6)	Max.	6,800	540	28.8	17.9	51.7	8.7	.44
	Ar. mean	5,583	407	24.1	12.7	39.9	5.7	.41
	Sd.	791	74	5.4	5.6	9.3	1.8	.03
	Gm. mean	5,539	402	23.5	11.3	39.0	5.5	.41
	Sd.	1.1471	1.184	1.28	1.77	1.25	1.34	1.08
215	Min.	1,100	140	21.2	1.8	29.7	21.6	.01
(5)	Max.	1,300	190	25.0	3.2	33.2	23.1	.28
	Ar. mean	1,160	170	23.0	2.5	32.1	22.6	.18
	Sd.	89	20	1.5	.5	1.5	.6	.12
	Gm. mean	1,157	169	23.0	2.4	32.1	22.6	.12
	Sd.	1.0780	1.130	1.07	1.25	1.05	1.03	4.15
216	Min.	5,600	440	25.0	11.8	29.1	3.7	.33
(5)	Max.	6,500	620	34.2	14.7	38.2	5.4	.51
	Ar. mean	6,020	532	29.8	13.1	33.4	4.7	.41
	Sd.	409	64	3.7	1.4	3.5	.7	.07
	Gm. mean	6,009	529	29.6	13.0	33.2	4.7	.40
	Sd.	1.0698	1.130	1.14	1.11	1.11	1.16	1.18
217	Min.	5,900	320	8.6	3.1	18.6	1.7	.23
(6)	Max.	8,400	710	35.3	29.7	58.0	6.5	1.42
	Ar. mean	6,933	463	26.7	17.8	33.7	3.5	.55
	Sd.	838	170	11.3	11.8	17.4	2.2	.45
	Gm. mean	6,893	439	23.8	12.6	30.2	3.0	.44
	Sd.	1.1249	1.425	1.78	2.89	1.65	1.83	1.98
231	Min.	3,200	260	6.5	1.5	47.1	7.8	.33
(20)	Max.	6,300	2,000	17.5	4.5	69.4	15.2	.83
	Ar. mean	4,490	559	14.3	2.4	54.2	12.5	.45
	Sd.	966	441	2.7	1	5.9	2.1	.14
	Gm. mean	4,394	467	14.0	2.3	54.0	12.3	.43
	Sd.	1.2351	1.732	1.25	1.45	1.11	1.20	1.30
232	Min.	3,900	480	2.5	.7	35.7	5.2	.18
(14)	Max.	7,900	1,000	28.1	4.8	77.6	13.2	.85
	Ar. mean	5,907	713	18.3	3.5	50.0	10.0	.56
	Sd.	908	163	7.5	1.3	11.9	2.2	.20
	Gm. mean	5,840	696	15.9	3.1	48.8	9.7	.52
	Sd.	1.1727	1.252	1.92	1.74	1.25	1.30	1.56
233	Min.	5,500	440	4.0	1.4	44.8	2.9	.37
(10)*	Max.	16,000	1,300	24.2	12.4	67.8	5.9	1.09
	Ar. mean	11,017	898	11.7	6.7	57.4	4.0	.71
	Sd.	3626	245	7.4	4.1	9.2	1.1	.25
	Gm. mean	10,414	864	12.0	5.3	56.7	3.8	.66
	Sd.	1.4355	1.351	1.9	2.23	1.18	1.31	1.47
259	Min.	4,300	250	17.8	6.8	18.6	4.1	.34
(8)	Max.	5,900	430	35.8	26.1	42.1	14.2	.64

Table 3. Range of laterite compositions—Continued

[Mean values are computed on untransformed data (arithmetic (Ar.) means) and on log-transformed data (geometric (Gm.) means). Sd., standard deviations. Numbers in parentheses indicate number of samples analyzed]

Site		Ni (ppm)	Co (ppm)	SiO_2 (percent)	MgO (percent)	Fe_2O_3 (percent)	Al_2O_3 (percent)	MnO (percent)
	Ar. mean	4,888	341	26.8	16.4	29.8	9.3	.45
	Sd.	567	84	6.5	7.4	8.8	3.8	.11
	Gm. mean	4,860	332	26.1	14.8	28.6	8.6	.44
	Sd.	1.1202	1.286	1.29	1.65	1.36	1.57	1.27
261	Min.	8,100	950	3.2	.8	58.9	4.2	.66
(9)	Max.	14,000	2,700	12.1	8.2	74.1	8.3	1.44
	Ar. mean	10,556	1,467	5.7	2.3	67.6	6.2	.99
	Sd.	2118	585	3	2.4	4.7	1.5	.25
	Gm. mean	10,371	1,380	5.1	1.7	67.4	6.1	.96
	Sd.	1.2204	1.428	1.6	2.15	1.07	1.28	1.28
All	Min.	1,100	140	2.5	.7	18.6	1.7	.01
profiles	Max.	16,000	2,700	35.8	29.7	77.6	23.1	1.44
(98)**	Ar. mean	6,575	704	18.5	7.3	45.7	8.8	.53
	Sd.	3032	439	8.6	7.1	14.2	4.9	.27
	Gm. mean	5,864	593	16.3	4.8	44.3	7.7	.47
	Sd.	1.6800	1.813	1.84	2.61	1.40	1.78	1.86
All	Min.	3,200	250	2.5	.7	18.6	1.7	.10
profiles	Max.	16,000	2,700	35.8	29.7	77.6	15.2	1.44
except 215	Ar. mean	6,860	732	18.3	7.6	46.4	8.0	.55
(93)***	Sd.	2835	433	8.7	7.1	14.2	3.8	.27
	Gm. mean	6,387	633	16.0	5.0	45.1	7.2	.51
	Sd.	1.4454	1.704	1.86	2.64	1.40	1.70	1.58

* Data for Ni and Co based on 12 samples; all other data are from 10 samples.

** Data for Ni and Co based on 100 samples; all other data are from 98 samples.

*** Data for Ni and Co based on 95 samples; all other data are from 93 samples.

these laterites and the yellow-green color of some clay-rich samples, it is reasonable to assume that they are nontronitic. Only two profiles contain orthopyroxene, and only one has small amounts of tremolite.

The bedrock mineralogy is also simple and consists predominantly of serpentine, with lesser amounts of chlorite, olivine, and maghemite. Additionally, clino- and orthopyroxene, talc, goethite, hornblende, tremolite, and magnetite occur in some samples. The bedrock at site 215, however, differs markedly in composition from the other rock samples as it is composed predominantly of hornblende, chlorite, talc, and goethite and contains little or no serpentine.

There are three mineralogical associations that are worth noting. First, all soil profiles that contain hornblende also have talc. Although talc typically is derived from the weathering of pyroxenes (Boeglin and others, 1983), the association noted here may indicate that in these samples some talc results from the alteration of hornblende. Second, tremolite occurs only in one of the two samples containing orthopyroxene, perhaps indicating that it is an alteration of orthopyroxene. Third, samples having smectite occur only in the northern part of the area sampled, within the boundaries of the Kalmiopsis Wilderness (fig. 1). A possible explanation for this distribution is presented later.

Within most profiles, mineralogy changes systematically. In general, serpentine, maghemite, smectite, and hornblende increase with depth. Conversely, goethite, chlorite, talc, and quartz are usually most abundant toward the surface. Notable exceptions to these trends occur in samples from sites 215, 216, 231, and 232 (table 2).

As previously mentioned, the profile at site 215 formed over a hornblende-rich bedrock that is compositionally distinct from the serpentine-rich rocks associated with the base of the other profiles. As a result, little serpentine is present in the profile from site 215, and evidently most of the other mineralogical trends present in the other profiles also did not develop. The samples from site 215 are also markedly lower in nickel than those which formed over ultramafic bedrock (1,100–1,300 ppm vs. 3,200–16,000 ppm).

The profiles from sites 216, 231, and 232, which also do not show the systematic mineralogical trends of the other profiles, have been slumped and mixed. Sites 216 and 232 both are in landslide masses and have evidently been so completely homogenized that any initial vertical change in mineralogy has been eliminated. The profile for site 231 is also from a landslide but has apparently retained some component of its original profile. Increases in serpentine and maghemite and decreases in goethite and chlorite are observed to a depth of about 3.2 m, but below this depth

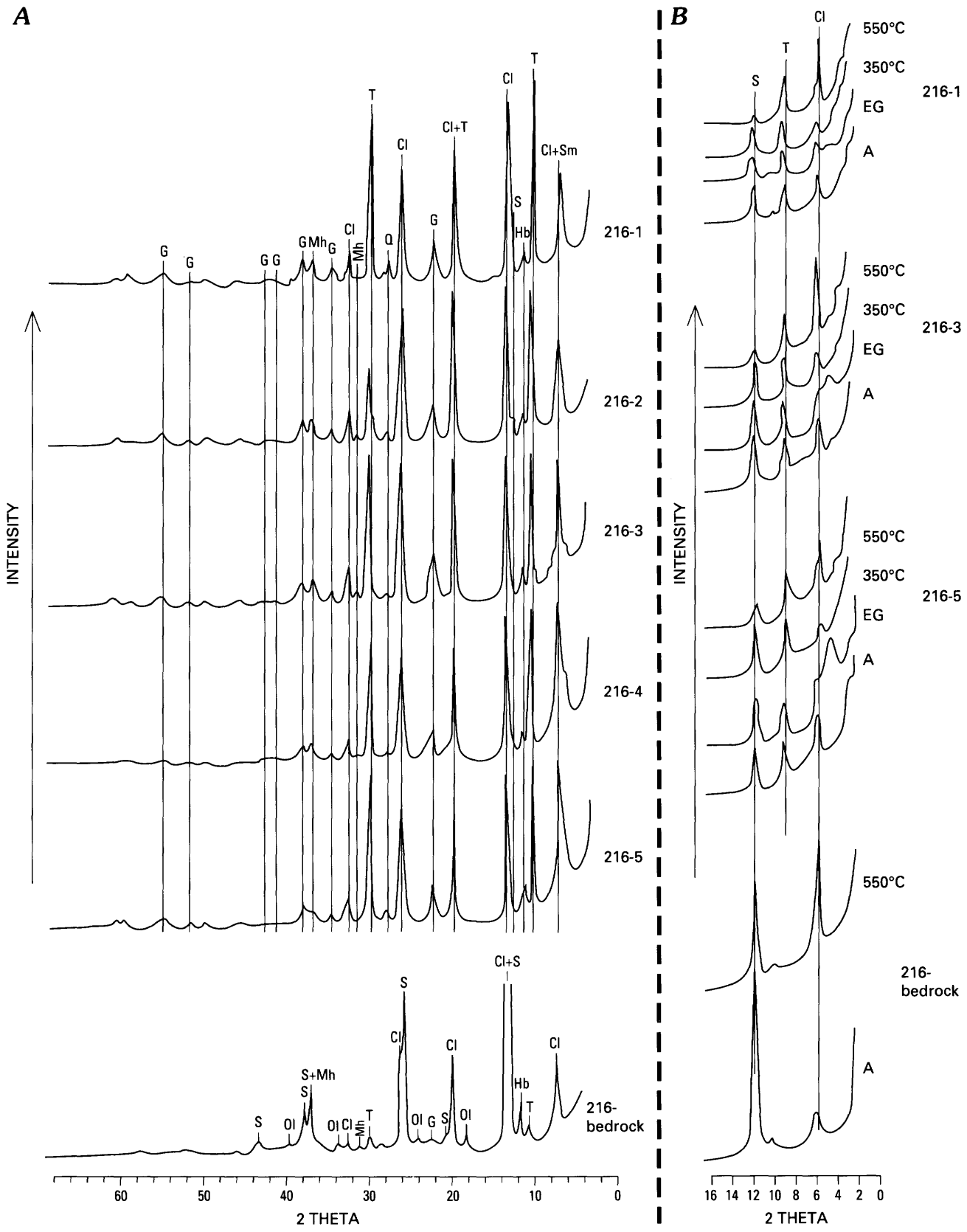

Figure 2. X-ray mineralogy and chemistry for profile from site 216. *A*, Hand-smoothed X-ray diffraction patterns. (Abbreviations: Cl, chlorite; S, serpentine; G, goethite; Mh, maghemite; Q, quartz; Sm, smectite; T, talc; Ol, olivine; Hb, hornblende.) *B*, Diffraction patterns of samples settled from water onto porcelain tiles and then dried in air (A), treated with ethylene glycol (EG), heated to 350 °C, and heated to 550 °C. *C*, Qualitative vertical variations in mineral abundances. *D*, Vertical variations in profile chemistry. *E*, Net change in Ni, Co, SiO_2, Fe_2O_3, MgO, and MnO calculated assuming Al_2O_3 is constant. Method of calculation discussed in text.

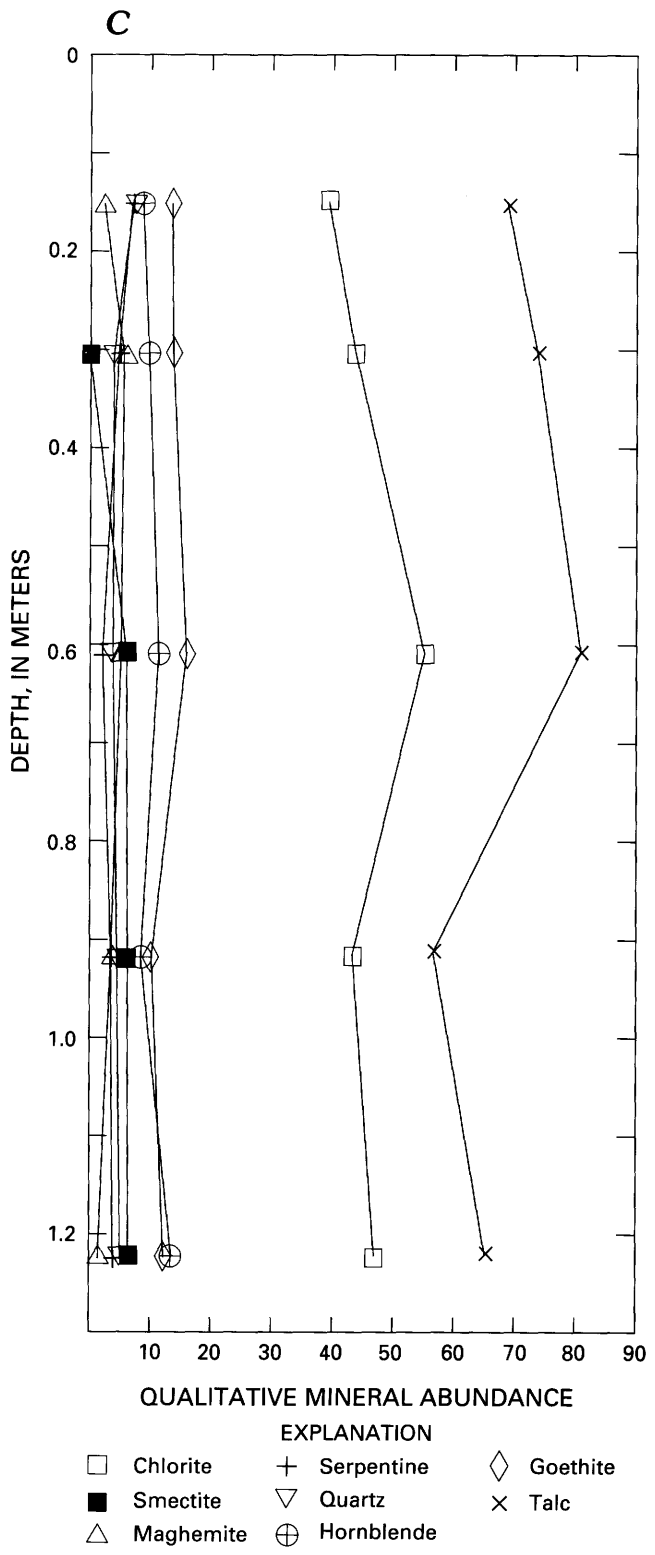

Figure 2. Continued.

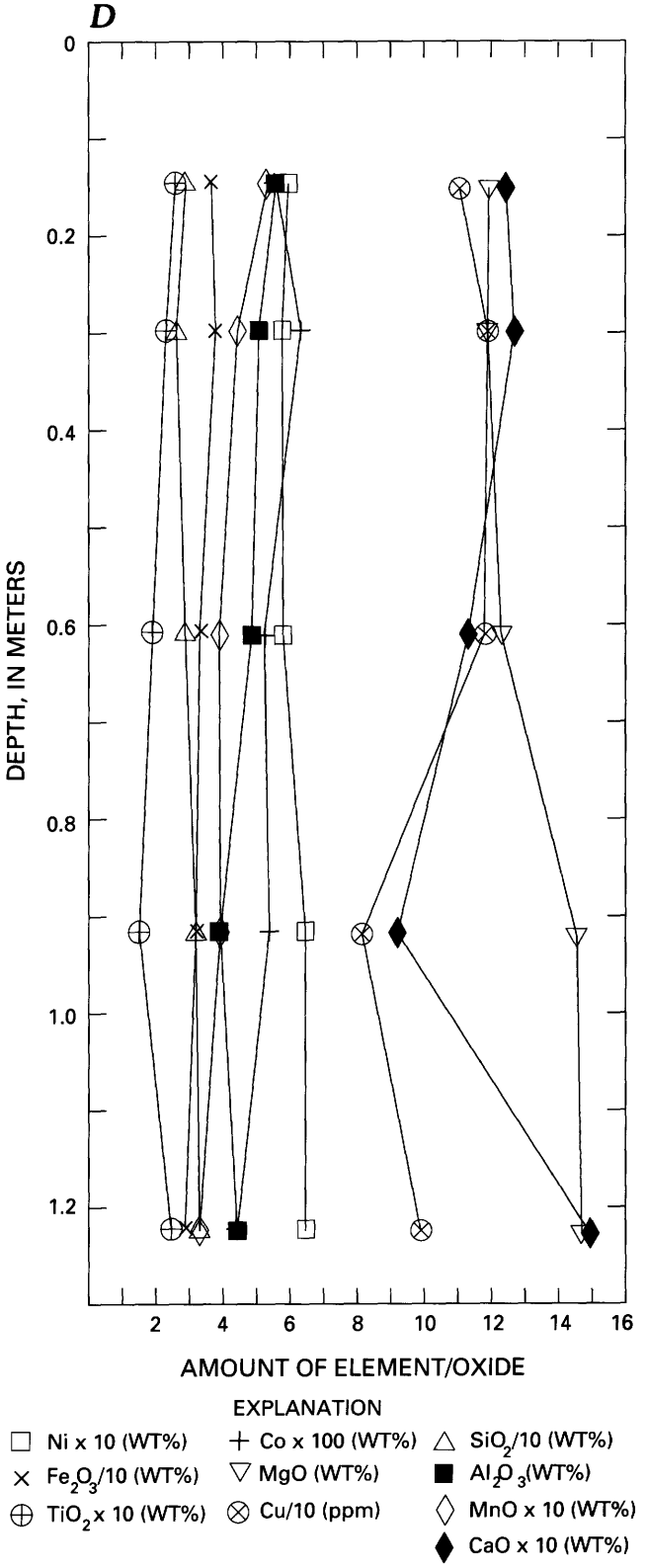

Figure 2. Continued.

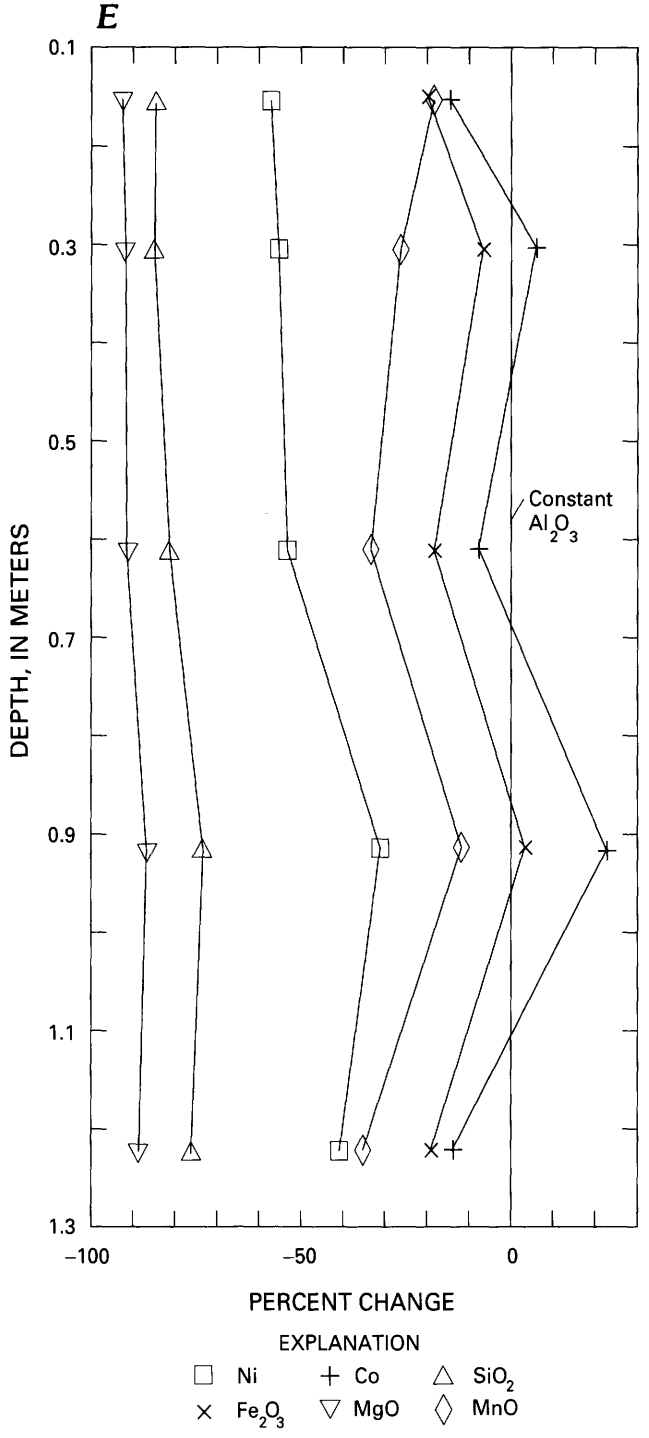

Figure 2. Continued.

there is little discernible change in relative mineral abundances. The abrupt change at 3.2 m occurs where two profiles have been juxtaposed; the upper part has the mineral zonation typical of most of the other profiles and has apparently moved over a material that either had been previously homogenized or over a material in which there was relatively little mineralogical variation.

CHEMICAL VARIATIONS

Data for SiO_2, Fe_2O_3, and Al_2O_3 most closely approximate normal distributions and, therefore, may best be characterized by arithmetic means. Data for Ni, Co, MgO, and MnO, however, approximate lognormal distributions, and for these elements the geometric mean (average value of the log-transformed data) provides a better measure of the central tendency of these data. Table 3 gives the arithmetic and geometric means, the maximum and minimum values, and standard deviations of these elements.

With the exception of samples from site 215, geometric means of Ni and Co are 6,387 ppm and 633 ppm (range of means are 4,394 to 10,414 ppm for Ni and 332 to 1,380 ppm for Co). Abundance of SiO_2 (arithmetic mean of 18.3; range of 5.7 to 29.8 percent) and MgO (geometric mean of 5.0; range of 1.7 to 14.9 percent) is directly related to mineralogy, the greatest amounts occurring in profiles that have the largest relative amounts of serpentine (or talc, in the case of profile 216). Similarly, abundance of Fe_2O_3 (arithmetic mean 46.4, range of 29.8 to 67.6 percent) increases as the amount of goethite increases.

The range in composition of these laterites agrees with those reported in a survey of laterites occurring in this area (Ramp, 1978) and also in specific studies of the Red Flats (Libbey and others, 1947; Hundhausen and others, 1954), Pine Flat, and Diamond Flat (Benson, 1963) deposits. These compositions also fit the category defined by Chandra and Ruud (1976) as transitional between high-iron nickeliferous limonite deposits and high-silica serpentinous ores. Some of these profiles are similar to compositions that have been used to test the recovery of nickel and cobalt by a variety of hydrometallurgical processes (Siemens and others, 1975; Duyvesteyn and others, 1979; Kukura and others, 1979).

Those profiles that have changes in mineralogy also show systematic changes in chemistry (table 2). Among profiles that are largely undisturbed, there are consistent depth-related increases in MgO and SiO_2 content and decreases with depth in Fe_2O_3, Al_2O_3, and TiO_2 content. Changes associated with CaO, MnO, and nickel, which generally increase with depth, and copper, which generally decreases with depth, are less consistent. Cobalt, in contrast, exhibits neither a predictable increase nor decrease with depth. Most of these chemical trends are also present in the disturbed profile at site 216. However, these trends are not found in the other disturbed profiles (231 and 232) and appear not to be developed at site 215.

As expected, many of these oxides show reasonably consistent correlations (table 4). Particularly good positive correlations are noted between MgO and SiO_2, which could be expected as both oxides are associated with serpentine and increase downward from the leached upper part of the laterite profile to the higher concentrations found in the

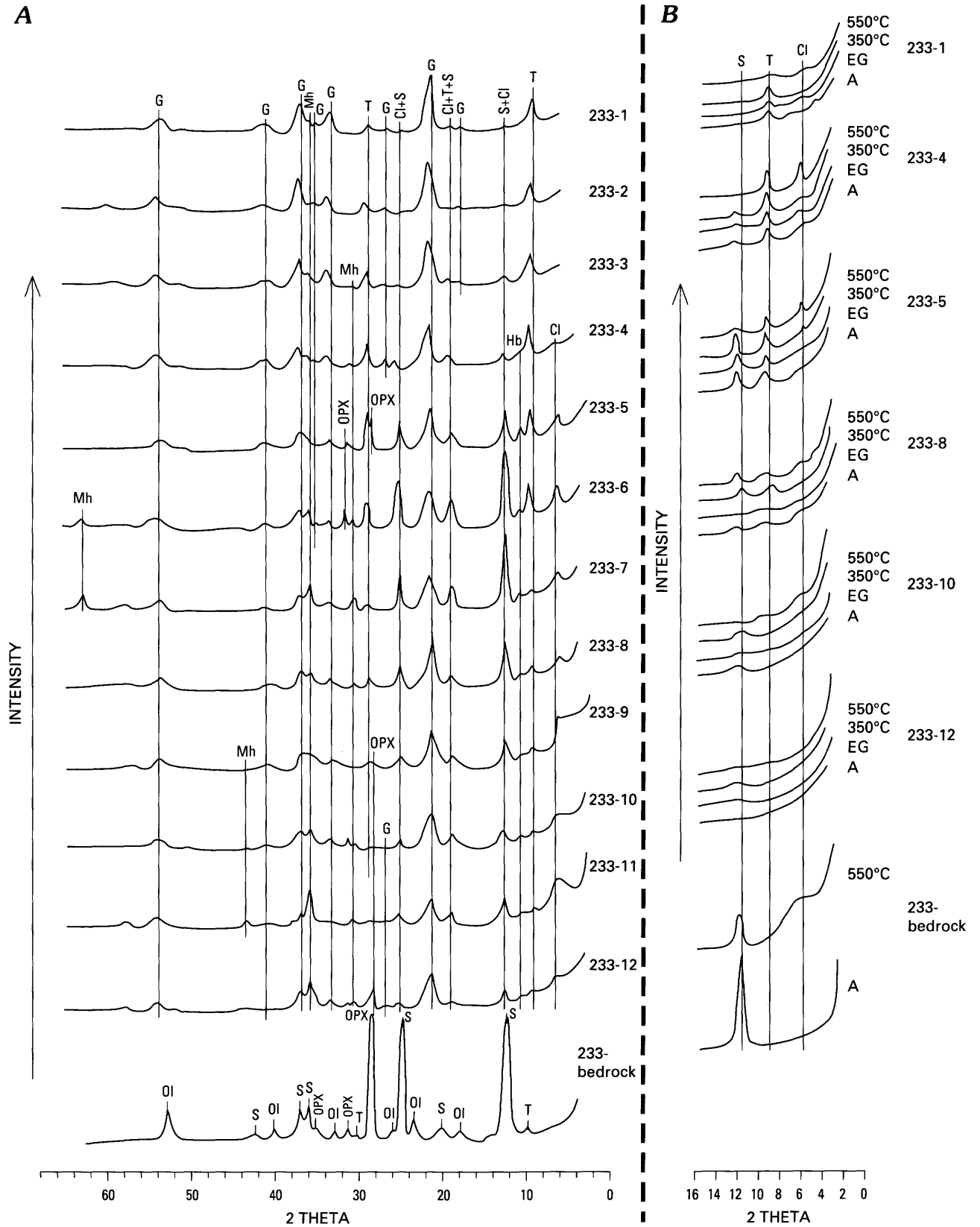

Figure 3. X-ray mineralogy and chemistry for profile from site 233. *A*, Hand-smoothed X-ray diffraction patterns. (Abbreviations: Cl, chlorite; S, serpentine; G, goethite; Mh, Maghemite; T, talc; Ol, olivine; Opx, orthopyroxene.) *B*, Diffraction patterns of samples settled from water onto porcelain tiles and then dried in air (A), treated with ethylene glycol (EG), heated to 350 °C, and heated to 550 °C. *C*, Qualitative vertical variations in mineral abundances. *D*, Vertical variations in profile chemistry. *E*, Net change in Ni, Co, SiO_2, Fe_2O_3, MgO, and MnO calculated assuming Al_2O_3 is constant. Method of calculation discussed in the text.

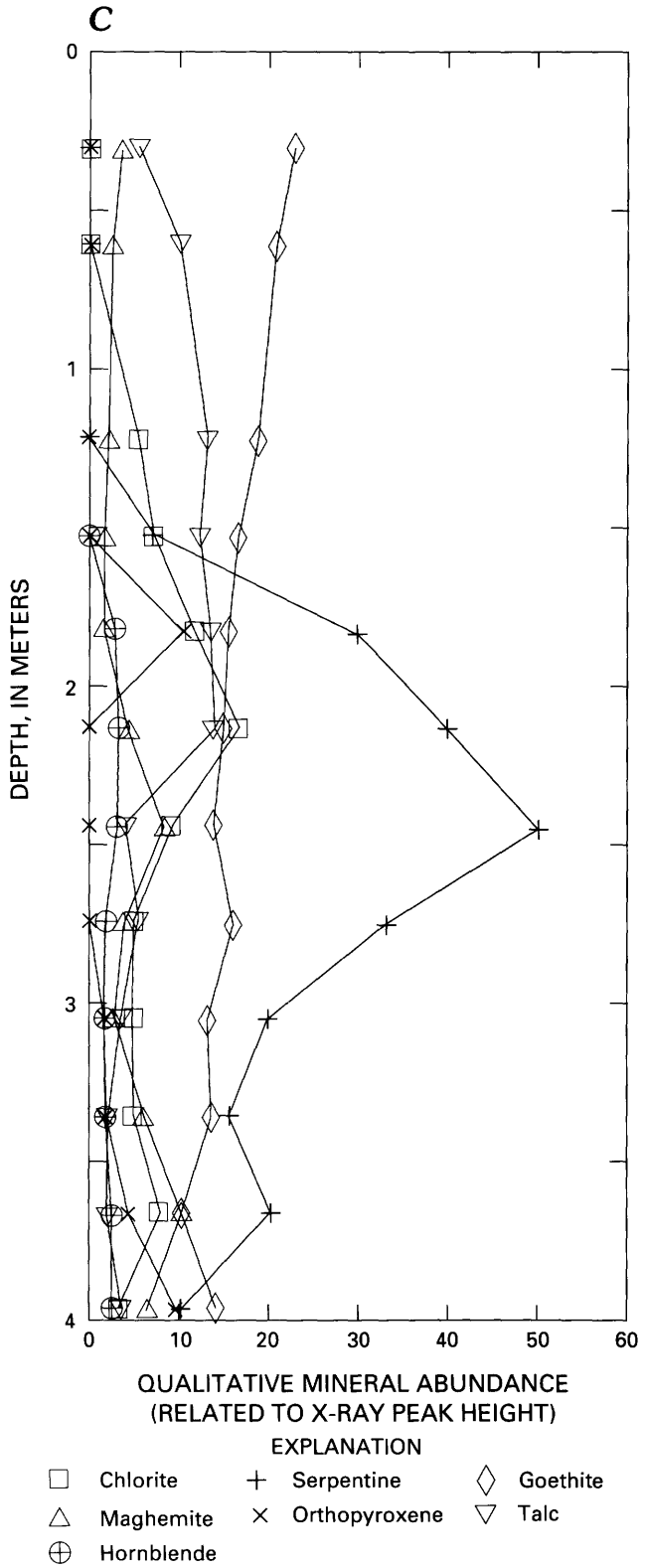

Figure 3. Continued.

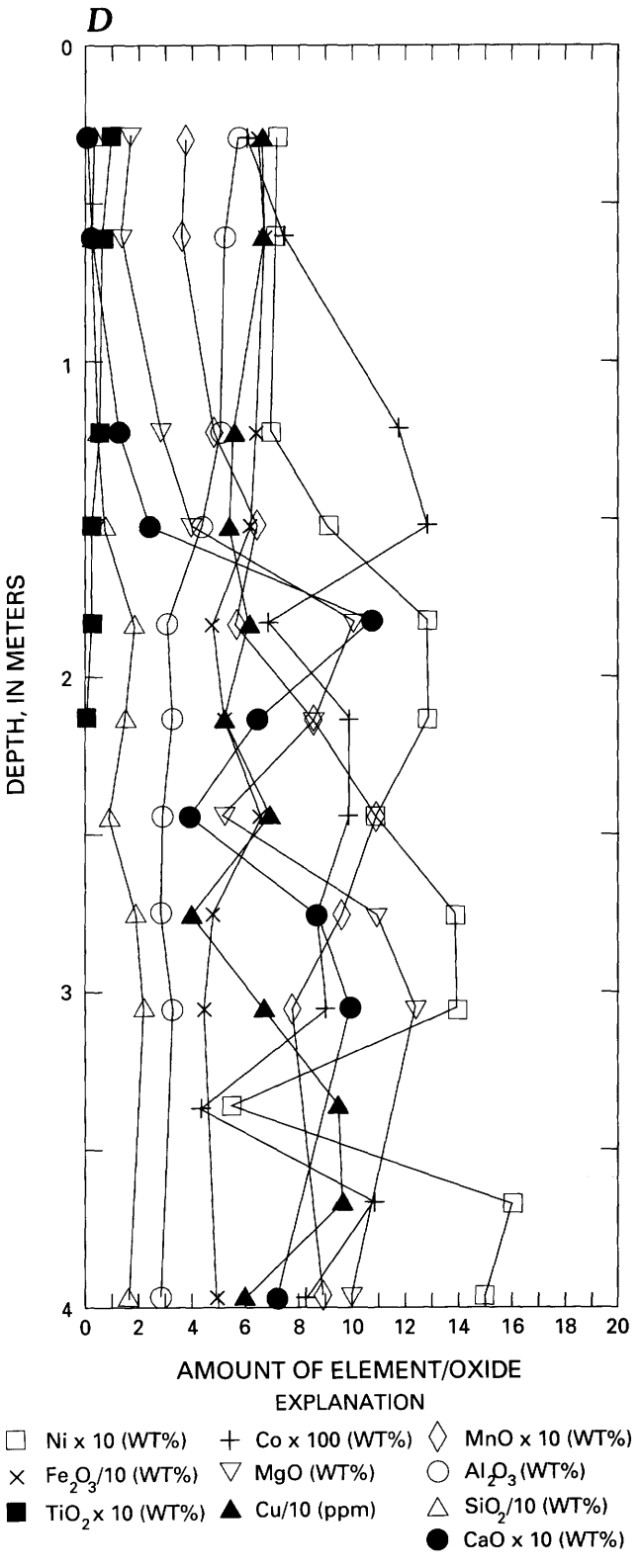

Figure 3. Continued.

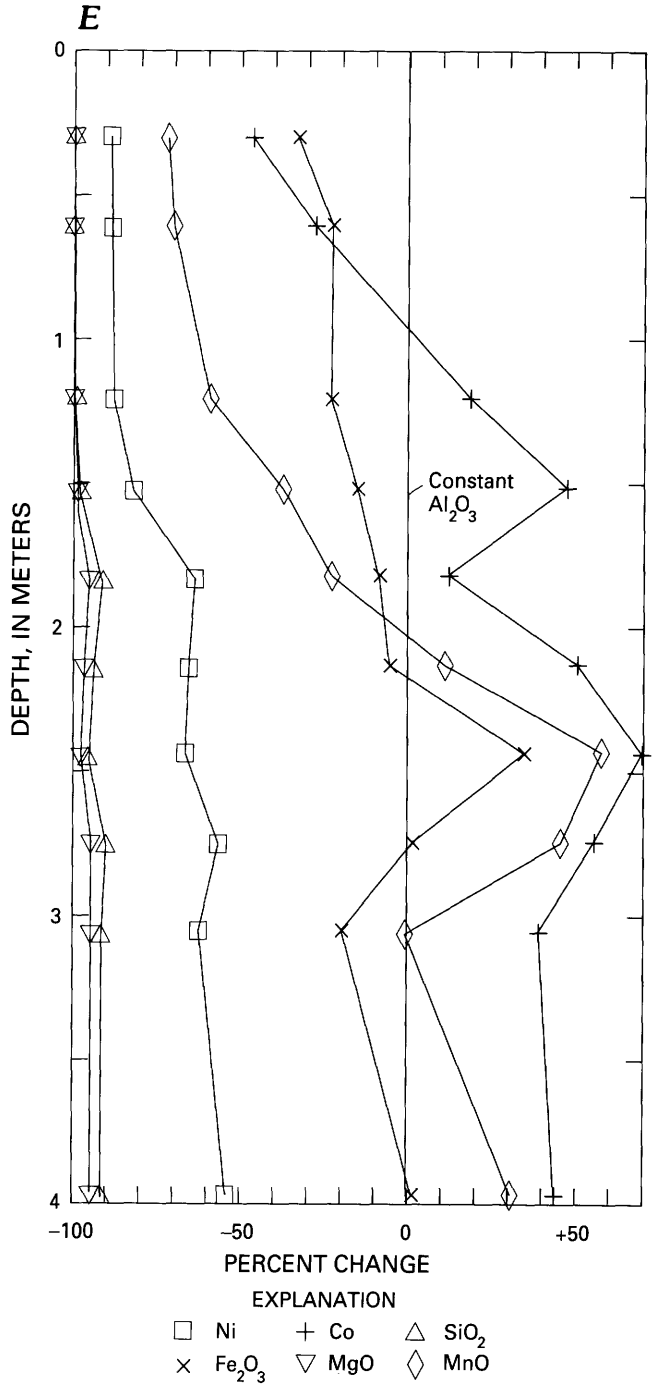

Figure 3. Continued.

parent rock. However, the correlations for several of the profiles are not as high as expected, and a plot of these data reveals at least two different trends (fig. 4). The first of these is defined by samples from profiles 213, 215, 231, and 232 (dashed line; fig. 4), while samples from the remaining profiles define a second curve.

DISCUSSION

The distribution of major oxides appears to follow trends predicted by relatively simple models. Golightly (1981) shows that the depth-related change in the concentration of an element (x) that is leached during lateritic weathering may be modeled by

$$C_x = C_{x_o} \cdot (1 - e^{-A_x \cdot d}) \quad (1)$$

where:

C_x is the concentration of element x in the laterite,
C_{x_o} is the initial concentration of element x,
A_x is a constant related to the solubility of the element, and
d is the depth.

Similarly, the relationship between two oxides (x and y) may be expressed as:

$$1/A_y \cdot \ln[1-(C_y/C_{y_o})] = 1/A_x \cdot \ln[1-(C_x/C_{x_o})] \quad (2)$$

or

$$C_y = C_{y_o} - C_{y_o} \cdot e^{[(A_y/A_x) \cdot \ln(1-(C_x/C_{x_o}))]}. \quad (3)$$

The solid curve in figure 4 represents the solution to equation 3 for bedrock concentrations of SiO_2 and MgO, respectively, of 39 and 37 weight percent. A value of 2 was assigned for the constant A_y/A_x and was chosen to produce a curve which fit the data. Actual solubility values for A_x and A_y are not known and in fact will change with different weathering conditions. The ratio used here, however, is consistent with the observed greater mobility of MgO relative to SiO_2 and also approximates the extreme ends of the relative mobility scale given by Trescases (1975) in which the mobility of magnesium is given as 1.0, while that of silicon ranges between 0.5 and 1.0.

Similar complexities are observed in the relation between MgO and Fe_2O_3 (fig. 5). Samples from profiles 213, 215, 231, and 232 again do not lie on the exponential curve made by samples from the other profiles. The fitting of a theoretically derived curve to the pattern made by these data is, however, not as straightforward as in the previous case. Both MgO and SiO_2 are removed during weathering, and equation 3 is designed to accommodate the leaching of such oxides. Iron, on the other hand, is residually enriched in the laterite, and its behavior is, therefore, not directly predicted by the leaching model (eq. 3).

By making certain assumptions, however, the above model may be simplified and redesigned to approximate variations in Fe_2O_3. First, Fe_2O_3 and Al_2O_3 are considered to be the only two major oxides not leached from the laterite and, therefore, are residually enriched in the upper part of the profile. This assumption is supported by the trends shown in table 2. Second, because all other oxides are removed during weathering, they may be lumped together and treated as the "leached component" and modeled by equation 1 as:

$$C_{lc} = C_{lc_o} - C_{lc_o} \cdot e^{-A_{lc} \cdot d} \quad (4)$$

Table 4. Correlation of abundance of elements, oxides, and minerals

[Numbers with asterisk give correlation at the 1-percent confidence level; numbers without asterisk give correlation at the 5-percent confidence level; blanks are not significantly correlated at the 5-percent confidence level. Correlations were made by using data that either fit a normal distribution or that were transformed to be normally distributed. Values for SiO_2, Fe_2O_3, Al_2O_3, goethite, and serpentine are normally distributed; data for MgO, MnO, TiO_2, Ni, and Co are lognormally distributed and were transformed]

Site	SiO_2 vs. log MgO	Log MgO vs. Fe_2O_3	SiO_2 vs. Al_2O_3	Fe_2O_3 vs. Al_2O_3	Fe_2O_3 vs. log MnO	Al_2O_3 vs. log TiO_2	Log Co vs. log Ni	Log Ni vs. SiO_2	Log Ni vs. Fe_2O_3	Log Ni vs. log MgO	Log Ni vs. log MnO	Log Co vs. SiO_2	Log Co vs. Fe_2O_3	Log Co vs. log MgO	Log Co vs. log MnO	Goethite vs. Fe_2O_3	Log MgO vs. serpentine
211	0.89*	−0.88*	−0.91*	0.84*		0.79		0.86*	−0.76	0.77						0.91*	0.95*
213		−.77				.99*		.8								.8	.88*
214	.99*	−.98*	−.94	.91*		.98*			−.68			−0.87	0.9*	−0.83		.78	.96*
215															0.96*		
216	.9	−.9						.95*	−.95*	.99*			.91				
217	.96*	−.98*	−.99*	.99*	0.95*	.99*		−.83	.81	−.79	0.91*	−.97*	.98*	−0.96*	.96*	.87	.94*
231		−.45	.72*	−.89*	.49	.92*	.64*	−.68*	.88*		.6*		.52		.9*	.53	.74*
232	.93*	−.93*	.91*	−.94*	−.89*	.95*		−.6	.53						.62		
233	.97*	−.91*		.92*		.96*		.94*	−.88*	.95*	.81*					.72*	
259	.97*	−.97*	−.93*	.91*		.97*						−.92*	.92*	−.88*	.81	.94*	.83*
261	.99*	−.83*				.65					.67		.77		.86*		.99*
All.....	.84*	−.81*			.37*	.82*	.75*	−.2	.33*		.6*	−.44*	−.52*		.63*	.56*	.71*

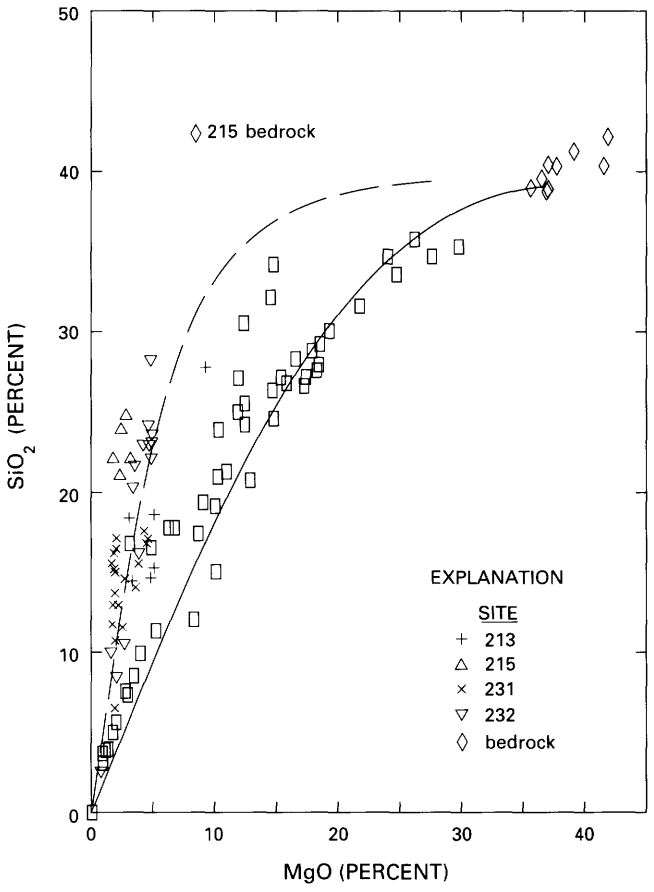

Figure 4. Plot of MgO vs. SiO_2 contents. Rectangles, All laterites except those from sites 213, 215, 231, and 232. Solid curve, Curve calculated to fit data represented by rectangles. Dashed line, Curve calculated to fit data from sites 213, 215, 231, and 232. See text for discussion.

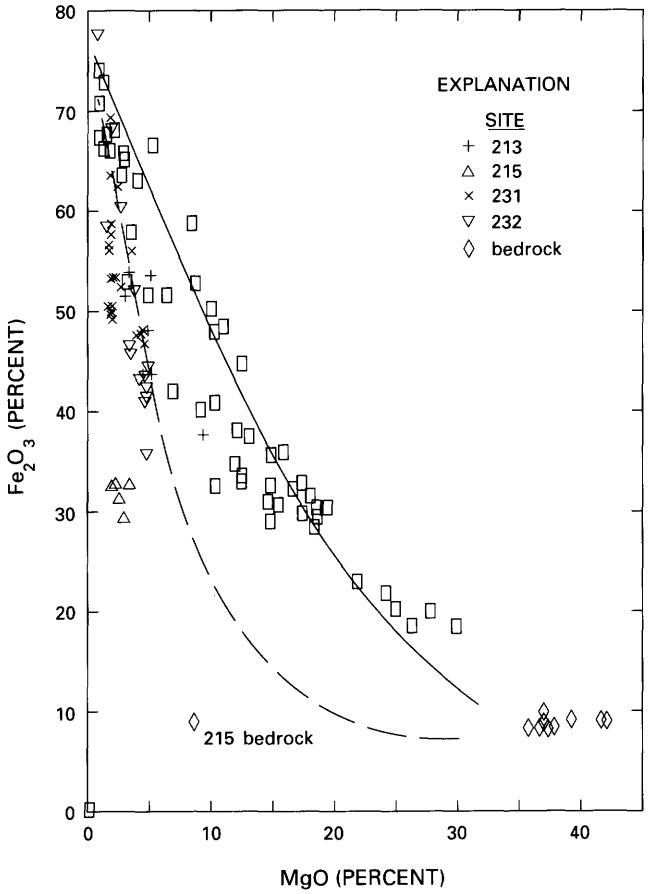

Figure 5. Plot of Fe_2O_3 vs. MgO contents. Rectangles, All laterites except those from sites 213, 215, 231, and 232. Solid curve, Curve calculated to fit data represented by rectangles. Dashed line, Curve calculated to fit data from sites 213, 215, 231, and 232.

where C_{lc_o} and C_{lc} denote original and subsequent concentrations of the "leached component." Since the concentration of the residual component (rs) is

$$C_{rs}=100-C_{lc},$$

equation 4 may be rewritten as

$$C_{rs}=C_{rs_o}+(100-C_{rs_o})\cdot e^{-A_{lc}\cdot d}. \quad (5)$$

When combined with equation 3, the variation of the residual components (rs_o denotes original residual component) with MgO may be stated as

$$C_{rs}=C_{rs_o}+(100-C_{rs_o})\cdot e^{(A_{lc}/A_{MgO})\cdot(\ln(1-(C_{MgO}/C_{MgO_o})))}. \quad (6)$$

Finally, the concentration of Fe_2O_3 may be modeled by assuming that the $Fe_2O_3/(Fe_2O_3+Al_2O_3)$ ratio is 0.79, a value consistent with the data in table 1. The concentration of Fe_2O_3 (C_{Fe}) is then given by

$$C_{Fe}=0.79\cdot[C_{rs_o}+(100-C_{rs_o})\cdot e^{(A_{lc}/A_{MgO})\cdot(\ln(1-(C_{MgO}/C_{MgO_o})))}]. \quad (7)$$

The curve derived from this relation is plotted in figure 5 (solid line) and provides a reasonable fit to the curved distribution of points, especially considering the assumptions that have been made.

The models given above, however, apparently fail to reproduce the relations found in profiles for sites 213, 215, 231, and 232. The fact that profiles for sites 231 and 232 have evidently been mechanically mixed does little to explain their different patterns; the chemical patterns in another disturbed profile, those at site 216, for example, are modeled quite well. Also, the above equations depend only on the local chemical equilibrium between components and not on the ordering of the samples. Thus these patterns should not be affected by mechanical mixing.

The most striking feature shared by all four of these profiles is a relatively large abundance of quartz (table 1). This abundance of quartz is also indicated by the vertical distribution of SiO_2 (table 2). In other profiles, SiO_2 clearly increases with depth. However, in these four profiles, quartz is most abundant at the top of the profile and results in high SiO_2 values that tend to offset the downward increase in SiO_2 due to increases in abundance of other silicate minerals. As a result, SiO_2 in profiles for sites 215, 231, and 232 shows no vertical change, while only a minor increase in SiO_2 occurs at site 213.

Golightly (1981) showed that the solubility of most magnesium silicate minerals found in laterites decreases with increasing pH. In contrast, the solubility of quartz is relatively independent of pH, while goethite has a solubility minimum at a pH of approximately 8. These relations indicate that in ground waters with relatively high pH, SiO_2 will mostly be used up in the formation of the relatively insoluble secondary magnesium-bearing silicates. However, as ground-water pH decreases and the solubility of these magnesium-bearing phases increases, SiO_2 is more likely to precipitate as quartz. The presence of quartz may thus be a useful pH indicator in some laterites (Golightly, 1981). The large amounts of quartz in profiles from sites 213, 215, 231, and 232, therefore, most likely indicate more acidic ground water at these four locations than at the other sample sites.

In terms of equation 3, the increase in solubility of magnesium-silicates with respect to quartz as pH decreases will be expressed by increases in values of A_{Si}/A_{Mg}. The dashed line in figure 4 was calculated by using a larger value for this constant than was used in calculating the solid curve (6 vs. 2). The result is a reasonable fit to the MgO-SiO_2 data for the quartz-rich samples. Similar reasoning indicates that decreases in ground-water pH should also be accompanied by increases in the term A_{lc}/A_{MgO} given in equation 7. Figure 5 shows the result of increasing this constant from 2 (solid curve) to 5 (dashed line).

Since the MgO-SiO_2 and MgO-Fe_2O_3data from these four profiles lie mostly on the nearly linear portion of these two dashed curves, it is not clear how accurately these equations fit the data, but it is clear that the observed data are consistent with behavior predicted by equations 3 and 7. It also should be noted that the curves in figures 4 and 5 are based on an ultramafic parent rock composition, while, to be treated accurately, the data for profile 215 should be fitted to curves defined by their different parent rock chemistry.

As previously discussed, smectite is found only in the northernmost sample sites (fig. 1). Although the precise compositions of these minerals are not known, inference based on comparison with other laterites suggests that they should be nontronitic. The stability of some magnesium-bearing silicates common in laterites as well as that of magnesium-bearing nontronite from laterites in New Caledonia (Trescases, 1975) is plotted in figure 6. This plot is derived from the dissolution reaction for these minerals, which, in the case of serpentine, may be written as

$$Mg_3Si_2O_5(OH)_4+6H^+=3Mg^{++}+2H_4SiO_4+H_2O, \quad (8)$$

which has an equilibrium constant (Kd) of

$$Kd=29.5=3\log[Mg^{++}]+2\log[H_4SiO_4]+6pH. \quad (9)$$

Reorganization of equation 9 as

$$3(\log[Mg^{++}]+2pH)=29.5-2\log[H_4SiO_4] \quad (10)$$

enables direct construction of figure 6.

This plot shows that waters having a concentration of Mg^{++} and SiO_2 represented by point A will not precipitate talc or Mg-bearing nontronite. However, an increase in concentration of Mg^{++} and (or) SiO_2 may result in first the formation of talc (B) and then talc and nontronite (C). In most instances, smectite occurs only in poorly drained profiles where ground waters may be enriched in cations

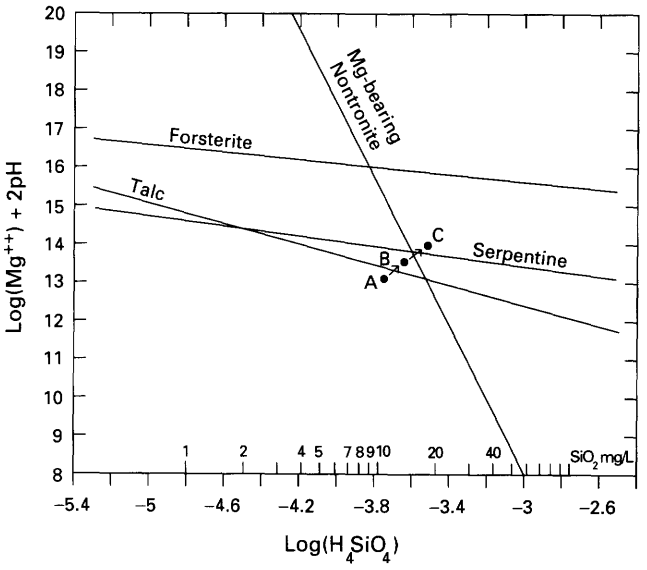

Figure 6. Stability of some minerals found in laterites plotted as log (Mg^{++}) + 2pH vs. log (H_4SiO_4). A, B, and C represent three possible ground-water compositions. Methods of calculation are discussed in text. Data are from Trescases (1975), Golightly (1981), and Boeglin and others (1983).

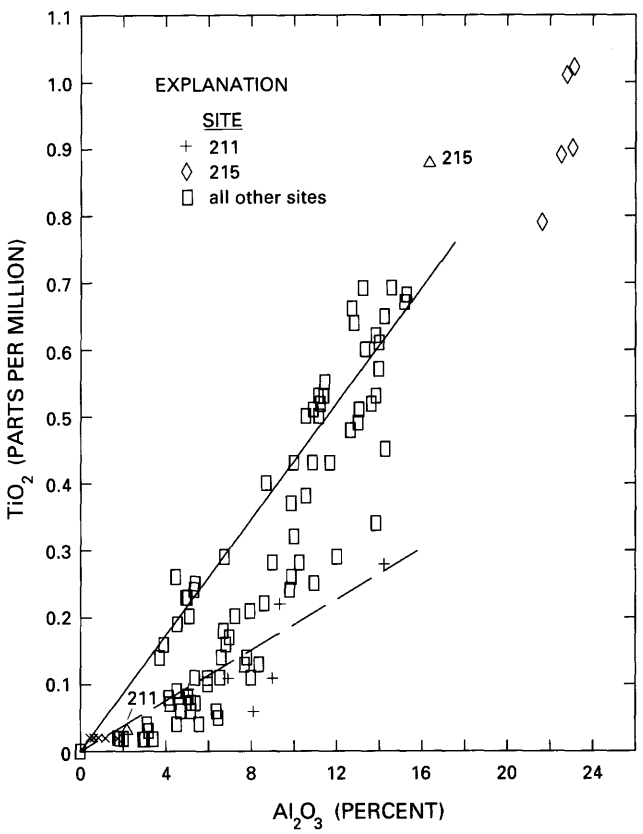

Figure 7. Plot of Al_2O_3 vs. TiO_2 contents. Labeled triangles show values for bedrock at sites 211 and 215. X (values near origin) shows Al_2O_3 values for samples in which TiO_2 was below the detection limit of 0.02 weight percent. Solid line represents best fit to all data shown by rectangles; dashed line shows best fit for data from site 211.

through prolonged interactions with the bedrock (Golightly, 1981).

In these laterite profiles, however, the smectite-bearing profiles all occur on slopes in the topographically rugged Kalmiopsis Wilderness. Laterite profiles without smectite are situated on relatively level terraces or plateaus. Both environments are extremely well drained and, therefore, would normally not be expected to have smectite. However, study of laterites in New Caledonia (Trescases, 1975) shows that ground waters on hillslopes are enriched in SiO_2 and Mg^{++} as a result of their movement down through laterite and across the bedrock that makes the hilltops. As a result, laterites on hillslopes typically contain smectite, while those from flatter, well-drained areas do not. The distribution of smectite in these laterite profiles is in accord with these observations.

Three main conclusions may be drawn from the above discussion. First, the distribution of major oxides in these laterites follows patterns predicted by relatively simple mathematical models. Second, laterite mineralogy suggests that the pH of ground waters in four of these profiles was significantly more acidic than in others. This conclusion is consistent with the different patterns that MgO, SiO_2, and Fe_2O_3 make in these profiles. Third, ground waters moving down hillslopes apparently became enriched in Mg^{++} and SiO_2 and, as a result, precipitated smectite.

Relations between many of the other oxides in these laterites appear to be somewhat less complex. Good inter-element correlations are observed between Al_2O_3 and TiO_2 (table 4) and define a nearly linear trend (fig. 7). Both these oxides are among the least mobile, and their nearly linear relation suggests that they are being residually enriched in about the same relative proportions as in the bedrock. Most bedrock values of TiO_2 are below limits of analytical detection (table 1). However, TiO_2 in bedrock from site 211 was detected, and its ratio with Al_2O_3 is similar to those ratios in the overlying laterites (fig. 7). The best-fit line through the TiO_2-Al_2O_3 data (with values from profiles 213 and 215 excepted) indicates a TiO_2/Al_2O_3 ratio of 0.05. This value is near the middle of the range commonly observed in ultramafic rocks from ophiolite complexes (Coleman, 1977).

Correlation between Fe_2O_3 and Al_2O_3 varies from strongly positive to highly negative (table 4; fig. 8). Many studies have shown that aluminum substitutes for iron within goethite, and it is therefore reasonable to assume that this substitution has occurred in cases where highly positive correlations of these elements are found. Not surprisingly, the profiles having the highest positive correlations (214,

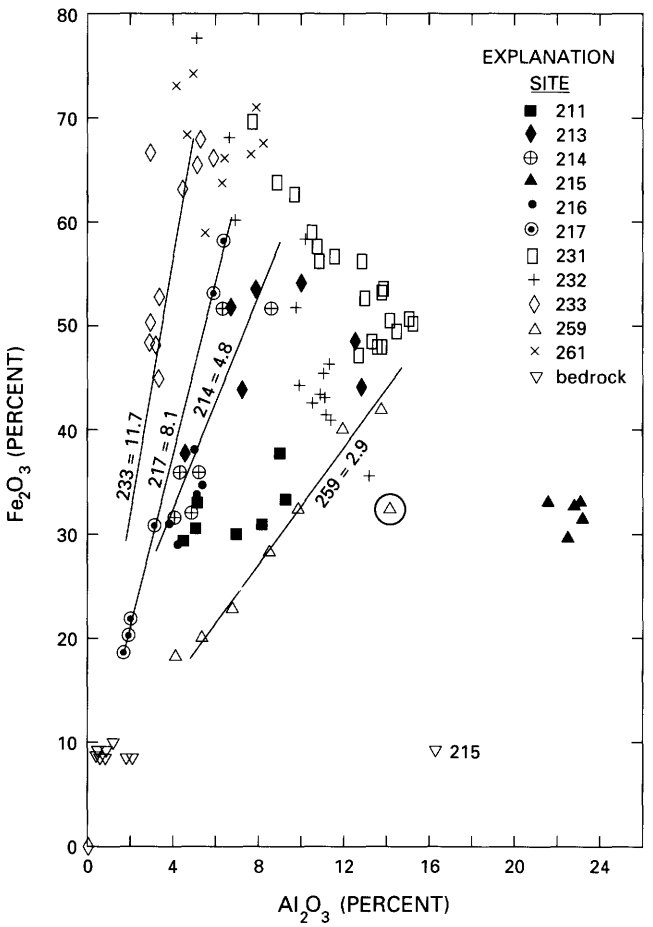

Figure 8. Plot of Al_2O_3 vs. Fe_2O_3 contents. Best-fit lines and slopes are given for data from sites 233, 217, 214, and 259. (Note: Best-fit calculations for site 259 did not include data from circled open triangle. This datum, which was from the first sample in the profile, fell off the general trend of the other points and was considered to be anomalous.)

217, 233, and 259) are also those that appear to have proportionately the smallest amounts of other aluminum-bearing phases. Best-fit lines through data from these profiles indicate that the Fe_2O_3/Al_2O_3 ratios vary between 2.9 to 11.7. Natural goethite may contain up to 33 mole percent aluminum (Schwertmann, 1983), corresponding to an Fe_2O_3/Al_2O_3 ratio of 3.1 or greater. With the exception of site 259, these data are within the range of natural goethites. The linear distribution of data from each of these sites suggests that the Al content of goethite varies between sites but remains relatively constant within a single profile. Conversely, poor or negative Al_2O_3-Fe_2O_3 correlations occur mostly in profiles where chlorite and (or) hornblende are relatively abundant.

Simple models, however, do not appear to explain the distribution of nickel and cobalt in these profiles. To a large extent, the absence of simple controls on the distribution of these trace elements is due to their ability to reside in a number of different minerals. In general, nickel increases with depth in these laterites, a relation consistent with that observed in many other laterites and attributable to the dissolution of nickel in the upper parts of the profile and reprecipitation in the lower parts where ground-water pH increases. Cobalt, in contrast, shows no consistent trend and, in fact, highest values commonly occur in middle parts of profiles. With the exception of a relatively small correlation in profile 231, significant correlation of cobalt and nickel does not occur within individual profiles (table 4), thus confirming the independent behavior of nickel and cobalt. Interestingly, analyses of the data from all profiles result in a significant correlation of cobalt and nickel. A plot of cobalt and nickel (fig. 9) clearly shows that this correlation results from superimposing data from independent populations.

The correlation data (table 4), however, does show that nickel occurs in two distinct associations. In the first (profiles 211, 213, 216, and 233), it is directly related to SiO_2. Most of these also show a positive correlation with MgO and a negative relation with Fe_2O_3; in the second (profiles 217, 231, and 232), nickel correlates with Fe_2O_3. Because Fe_2O_3 and MgO generally have high positive correlations, respectively, with abundances of goethite and serpentine (table 4), the nickel in profiles 211, 213, 216, and 233 probably occurs mostly as a substitution in serpentine, while nickel in 217, 231, and 232 is in goethite.

There is, in contrast, no evidence of cobalt being associated with silicate minerals. Instead, cobalt is mostly positively correlated with either Fe_2O_3 (profiles 214, 216, 217, 231, 259, and 261) or MnO (215, 217, 231, 232, 259, and 261). Fe_2O_3 and MnO generally vary together (profiles 217, 231, 259, and 261), and therefore it is not usually possible to determine if cobalt is mostly in goethite or in manganese oxides. That cobalt may occur within both phases is shown where significant correlation occurs with only Fe_2O_3 or MnO. For example, in profiles 214 and 216, cobalt is significantly positively correlated with Fe_2O_3 and not with MnO. In these profiles it is, therefore, likely that cobalt is hosted by goethite. Conversely, in profile 215 and 232, cobalt is significantly correlated with MnO and not with Fe_2O_3, indicating that cobalt probably is in manganese oxides.

The preceding discussion of laterite chemistry provides no information as to the net gain or loss of chemical constituents during laterite formation. One way to estimate absolute changes in laterite chemistry is to compare element abundances with those of a constituent that is assumed to be unchanged. For the purposes of this study, Al_2O_3 has been used not only because it is known to be quite immobile (Golightly, 1981) but also because it is sufficiently abundant to be measured relatively accurately. The percentage net change in concentration of an element (C_x) relative to Al_2O_3 is calculated as

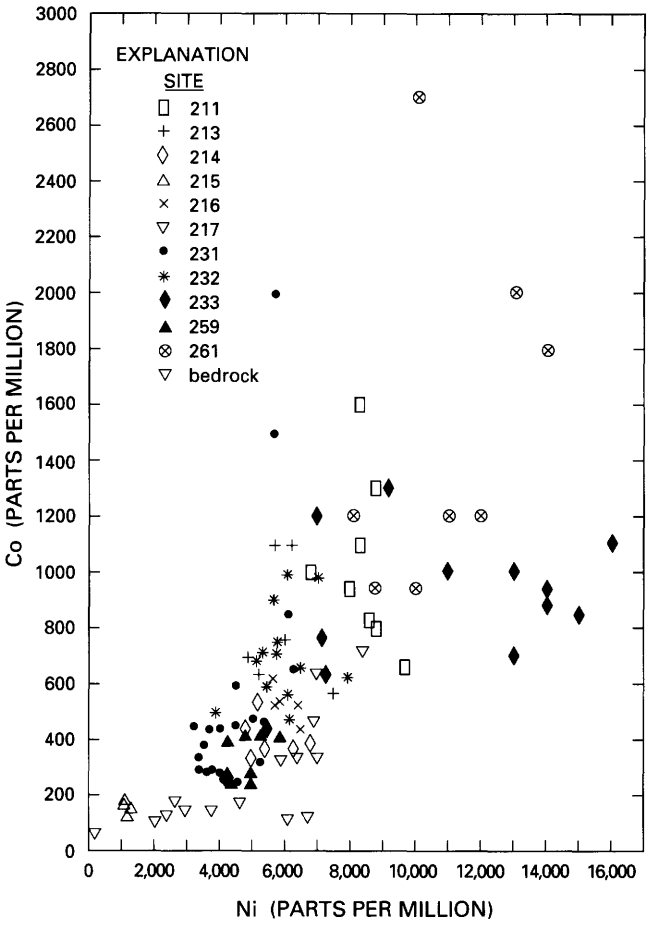

Figure 9. Plot of nickel vs. cobalt contents.

$$C_x=[(X_s/X_p)\cdot(Al_2O_3)_p/(Al_2O_3)_s)-1]\cdot 100 \quad (11)$$

where X_s and $(Al_2O_3)_s$ are the values of component x and Al_2O_3 in laterite, and X_p and $(Al_2O_3)_p$ are those values in the parent rock. Percentage net changes in six constituents based on this equation are given in table 5; variations in profiles 216 and 233 are plotted in figures 2 and 3.

The trends in net compositional change are similar in most profiles. With the exception of the mineralogically and chemically distinct profile 215, most profile averages show an ordering from most depleted component to least of MgO, SiO_2, Ni, MnO, Fe_2O_3, and Co. Exceptions occur in profile 211, where the average MnO value is more depleted than the nickel value, and in profiles 214, 231, and 259, where the average cobalt values are just slightly more depleted than the averages for Fe_2O_3. These profiles almost all show an overall loss of all their major components, with enrichments only evident in profiles 211 (Co, Ni, Fe_2O_3), 233 (Co), and 261 (Co, Fe_2O_3). In contrast to these profiles, values from sample site 215 differ significantly. Significant enrichments occur in average values of nickel, Fe_2O_3, and cobalt, with nickel showing the largest amounts of enrichment.

The most surprising feature of these patterns is the absence of consistent and significant increases in nickel. Hotz (1964) conducted a similar study using data from the Riddle laterite deposit and from laterite on Eight Dollar Mountain (located 15 km east of Pearsoll Peak; fig. 1). In both profiles, nickel was found to be the most enriched component, with net gains commonly exceeding 120 percent. Cobalt and iron also typically showed net increases. The general order of enrichment determined by Hotz was, from most depleted to most enriched, MgO, SiO_2, Mn, Fe, Co, and Ni. With the exception of nickel, this sequence is similar to the one found in these laterites.

CONCLUSIONS

Ten of the eleven laterites studied formed over serpentinized peridotite and, in general, are mineralogically and chemically similar. All contain serpentine, chlorite, goethite, and maghemite. Profiles located on hillslopes also have smectite. Quartz, talc, hornblende, orthopyroxene, and tremolite are additional components of some laterites. Within profiles that have not been physically disrupted, the least soluble minerals (mostly goethite) are most abundant at tops of profiles, and the more soluble phases generally increase with depth.

Mean values of major chemical constituents in these 10 profiles are nickel, 0.64 weight percent; cobalt, 0.063 weight percent; SiO_2, 18.3 weight percent; MgO, 5.0 weight percent; Fe_2O_3, 46.4 weight percent; Al_2O_3, 8.0 weight percent; and MnO, 0.51 weight percent. Amounts of MgO and Fe_2O_3 generally directly reflect abundance, respectively, of serpentine and goethite. These compositions are similar to those of other laterites described from this area.

The profile at site 215 differs from the others in having formed over a hornblende-rich parent rock. These laterites are also distinguished by having relatively large amounts of quartz, chlorite, and talc and by low values of MgO and nickel (having mean values of 2.4 and 0.11 weight percent, respectively).

The restriction of smectite to laterites located on hillslopes results from local variations in ground-water chemistry. Precipitation of smectite is favored by high concentrations of SiO_2 and MgO in ground water, but the excellent drainage present in these laterites tends to prevent enrichment in these components. As a result of downslope flow over serpentine, however, waters on hillsides locally have dissolved enough SiO_2 and MgO to precipitate smectite.

The distribution of MgO, SiO_2, and Fe_2O_3 in these laterites appears to follow trends predicted by the relatively simple equation:

Table 5. Net change in laterite composition

[Calculations made assuming no change in Al_2O_3, as discussed in text; whole-rock values from site 233 were used to calculate values for profiles 231 and 232. IS, insufficient sample]

Site sample number	Sample depth (m)	Percent change					
		Ni	Co	SiO_2	Fe_2O_3	MgO	MnO
211–1 . . .	0.23	–59.8	13.8	–94.5	–27.6	–96.0	–63.5
211–2 . . .	.38	–22.4	187.8	–88.0	5.1	–91.9	–20.2
211–3 . . .	.64	–8.6	159.6	–82.6	–4.5	–89.3	–49.6
211–4 . . .	.92	–25.0	91.1	–85.7	–10.4	–92.5	–49.5
211–5 . . .	1.22	–2.5	120.4	–79.5	8.9	–85.8	–37.2
211–6 . . .	1.53	47.4	173.6	–70.4	56.2	–78.7	–6.7
211–7 . . .	1.83	47.0	156.9	–72.5	64.6	–80.6	5.6
211–8 . . .	2.14	85.2	142.3	–65.5	69.4	–76.2	3.9
213–1 . . .	.15	–91.9	–68.7	–97.7	–64.7	–99.2	–76.5
213–2 . . .	.31	–92.0	–69.1	–97.2	–68.4	–99.2	–75.3
213–3 . . .	.61	–89.1	–63.7	–97.2	–49.9	–99.3	–78.2
213–4 . . .	.92	–85.0	–21.4	–96.2	–37.3	–98.7	–93.8
213–5 . . .	1.22	–80.4	–5.8	–94.5	–27.8	–99.0	–19.8
213–6 . . .	1.53	–82.7	–40.4	–93.5	–43.7	–98.7	–38.2
213–7 . . .	1.88	–65.4	–28.5	–87.9	–22.6	–95.7	.9
214–1 . . .	.15	–95.3	–87.3	–98.0	–72.9	–99.4	–91.9
214–2 . . .	.31	–93.4	–79.9	–97.3	–65.0	–99.0	–87.8
214–3 . . .	.61	–87.1	–78.3	–93.8	–63.6	–96.2	–81.3
214–4 . . .	.92	–86.3	–76.9	–92.4	–63.2	–95.0	–79.0
214–5 . . .	1.22	–91.2	–82.4	–94.8	–69.0	–97.0	–83.2
214–6 . . .	1.37	–91.3	–82.7	–94.0	–69.9	–96.3	–83.3
215–1 . . .	.15	199.8	140.5	–64.6	158.3	–81.7	24.0
215–2 . . .	.31	202.5	129.8	–62.2	159.0	–84.9	25.1
215–3 . . .	.61	198.5	126.8	–59.9	144.8	–80.1	5.8
215–4 . . .	.92	234.4	81.1	–57.3	136.2	–76.2	–95.5
215–5 . . .	1.22	277.3	115.6	–60.3	175.0	–71.6	–48.1
216–1 . . .	.15	–57.5	–15.2	–84.4	–20.5	–92.8	–18.4
216–2 . . .	.31	–55.2	6.3	–84.6	–6.7	–92.3	–26.3
216–3 . . .	.61	–53.2	–8.2	–81.3	–18.6	–92.0	–33.7
216–4 . . .	.92	–30.8	22.8	–73.2	2.6	–87.3	–12.0
216–5 . . .	1.22	–40.9	–14.3	–76.0	–19.3	–89.1	–35.7
217–1 . . .	.15	–88.3	–43.7	–97.9	–34.8	–99.1	–3.5
217–2 . . .	.31	–89.2	–44.9	–95.5	–34.4	–99.1	–52.0
217–3 . . .	.61	–79.7	–23.3	–84.6	–27.9	–89.2	–37.1
217–4 . . .	.92	–68.1	–14.8	–72.3	–19.8	–79.1	–35.8
217–5 . . .	1.22	–67.6	–5.3	–69.3	–18.2	–73.3	–33.6
217–6 . . .	1.53	–68.4	–2.7	–66.9	–19.8	–69.6	–40.1
231–1 . . .	.46	–97.4	–82.0	–98.2	–77.6	–99.5	–81.0
231–2 . . .	.87	–96.9	–76.5	–98.5	–75.6	–99.7	–87.7
231–3 . . .	1.20	–97.1	–83.9	–98.4	–78.5	–99.8	–89.1
231–4 . . .	1.55	–97.5	–84.2	–98.4	–79.4	–99.8	–89.0
231–5 . . .	2.01	–97.7	–85.8	–98.5	–78.7	–99.6	–86.7
231–6 . . .	2.32	–98.0	–89.6	–98.6	–80.1	–99.8	–88.9
231–7 . . .	2.62	–97.8	–89.9	–98.6	–79.9	–99.9	–90.0
231–8 . . .	2.93	–97.8	–87.1	–98.3	–79.1	–99.6	–88.5
231–9 . . .	3.23	–97.8	–82.4	–98.3	–78.0	–99.5	–87.7
231–10 . .	3.54	–97.5	–89.0	–98.7	–76.8	–99.8	–88.5
231–11 . .	3.84	–97.4	–89.4	–98.7	–76.9	–99.8	–88.8
231–12 . .	4.15	–97.1	–90.4	–98.7	–76.8	–99.8	–89.7
231–13 . .	4.45	–97.1	–89.7	–98.8	–73.8	–99.8	–88.3
231–14 . .	4.76	–95.5	–83.5	–98.2	–66.2	–99.8	–84.0
231–15 . .	5.06	–96.1	–78.9	–98.2	–70.6	–99.8	–83.7
231–16 . .	5.37	–95.5	–77.8	–98.1	–67.8	–99.8	–80.9
231–17 . .	5.67	–93.6	–62.4	–98.4	–57.0	–99.7	–75.4
231–18 . .	5.98	–92.9	–43.5	–98.9	–46.0	–99.7	–68.9
231–19 . .	6.28	–94.7	4.5	–98.4	–61.3	–99.6	–65.5
231–20 . .	6.59	–95.3	–29.9	–98.2	–68.9	–99.5	–67.2
232–1 . . .	.31	–95.7	–67.3	–97.2	–77.7	–99.4	–73.1
232–2 . . .	.61	–95.9	–68.7	–97.1	–78.3	–99.4	–73.5
232–3 . . .	1.22	–95.0	–65.1	–97.0	–75.5	–99.4	–73.3
232–4 . . .	1.53	–97.3	–80.3	–97.1	–83.7	–99.5	–76.2
232–5 . . .	1.83	–94.8	–53.5	–97.0	–73.2	–99.3	–67.1
232–6 . . .	2.14	–92.9	–56.0	–98.0	–47.7	–99.5	–77.7
232–7 . . .	2.44	–95.1	–54.9	–97.6	–75.2	–99.6	–67.6
232–8 . . .	2.75	–95.0	–73.9	–97.4	–75.3	–99.6	–82.5
232–9 . . .	3.05	–93.0	–68.6	–98.7	–65.5	–99.8	–88.2
232–10 . .	3.36	–89.1	–52.6	–99.3	–9.1	–99.8	–84.9
232–11 . .	3.66	–91.3	–49.5	–98.3	–38.3	–99.6	–76.0
232–12 . .	3.97	–95.3	–65.1	–97.2	–76.6	–99.5	–75.6
232–13 . .	4.27	–95.2	–66.4	–97.1	–76.0	–99.4	–75.9
232–14 . .	4.58	–93.6	–48.1	–97.8	–68.1	–99.5	–75.0
233–1 . . .	.31	–88.9	–45.9	–98.8	–32.7	–99.6	–71.7
233–2 . . .	.61	–87.8	–27.4	–99.0	–23.2	–99.6	–70.1
233–3 . . .	1.22	–87.8	18.2	–98.0	–23.8	–99.2	–59.2
233–4 . . .	1.53	–81.5	47.1	–97.0	–15.4	–98.7	–37.8
233–5 . . .	1.83	–63.3	11.4	–91.1	–9.1	–95.4	–23.3
233–6 . . .	2.14	–65.5	49.7	–93.0	–6.1	–96.4	10.2
233–7 . . .	2.44	–66.9	69.7	–94.8	34.0	–97.5	56.5
233–8 . . .	2.75	–56.4	54.5	–90.0	.9	–94.6	44.1
233–9 . . .	3.05	–62.8	37.8	–90.3	–20.5	–94.8	–1.2
233–10 . .	3.36	IS	IS	IS	IS	IS	IS
233–11 . .	3.66	IS	IS	IS	IS	IS	IS
233–12 . .	3.97	–54.8	42.5	–91.3	1.2	–95.3	29.2
259–1 . . .	.15	–74.0	–49.3	–92.3	–50.8	–96.5	–48.4
259–2 . . .	.31	–63.4	–46.5	–94.1	–34.9	–97.6	–63.7
259–3 . . .	.61	–61.4	–35.5	–92.6	–28.3	–96.3	–46.4
259–4 . . .	.92	–58.3	–21.5	–88.6	–29.0	–92.6	–16.5
259–5 . . .	1.22	–50.0	–37.0	–85.3	–28.7	–89.5	–40.0
259–6 . . .	1.53	–45.9	–31.3	–78.8	–27.6	–84.3	–26.4
259–7 . . .	1.83	–29.5	–15.9	–71.3	–19.0	–77.2	–18.3
259–8 . . .	2.14	4.5	9.8	–60.1	–3.1	–68.6	6.6
261–1 . . .	.15	–68.3	–25.5	–99.0	–23.8	–99.7	–61.8
261–2 . . .	.31	–68.1	–45.3	–99.1	–28.3	–99.8	–69.3
261–3 . . .	.61	–69.4	–28.1	–99.2	–21.6	–99.8	–62.2
261–4 . . .	.92	–40.0	157.3	–98.7	30.5	–99.7	11.1
261–5 . . .	1.22	–7.1	126.9	–98.0	53.0	–99.4	10.2
261–6 . . .	1.53	–10.6	82.5	–97.6	27.8	–99.2	–4.0
261–7 . . .	1.83	–43.5	–10.2	–97.6	–12.1	–99.2	–43.1
261–8 . . .	2.14	–48.8	–11.4	–97.6	–10.0	–99.2	–37.2
261–9 . . .	2.44	–46.0	–18.6	–95.6	–6.7	–97.1	–36.2

$$C_y = C_{y_o} - C_{y_o} \cdot e^{[(A_y/A_x) \cdot \ln(1-(C_x/C_{x_o}))]} \quad (12)$$

where:

C_x and C_y are the concentration of components x and y in the laterite,

C_{x_o} and C_{y_o} are the initial concentration of x and y, and

A_x and A_y are constants related to the solubility of x and y.

Trends fitted by this equation and its derivatives for profiles 213, 215, 231, and 232 differ from those in the other laterites. These four profiles contain relatively large amounts of quartz, which commonly is a mineralogical indicator of relatively acidic ground waters. The shift in the major element trends in these four profiles from those in the other laterites is consistent with the presence of ground water having a lower pH.

The distribution of other oxides reveals a variety of relations. Good positive correlation exists between abundance of Al_2O_3 and TiO_2. Both are relatively immobile and appear to be residually enriched in about the same proportions as occur in the parent rock. Al_2O_3 and Fe_2O_3, in contrast, are strongly positively correlated in goethite-rich laterites, but not in laterites having large amounts of aluminum-bearing minerals. It is probable that, where positively correlated, most of the aluminum occurs as a substitution for iron in goethite. Fairly constant Al_2O_3/Fe_2O_3 ratios occur in the goethite-rich profiles and indicate a uniformity of goethite compositions within individual laterites. Nickel in some profiles is positively correlated with Fe_2O_3, indicating that it occurs in goethite; in other laterites, nickel is mostly present in serpentine as shown by its good correlation with MgO. Cobalt, on the other hand, apparently occurs primarily in either goethite or in manganese oxides, but in most profiles its host phase could not actually be determined.

Calculations of net changes in laterite chemistry show that loss of chemical components during weathering generally occurs in a well-defined order. This sequence is, from most depleted to most enriched, MgO, SiO_2, Ni, MnO, Fe_2O_3, and Co. The observed net chemical changes in these deposits differ from those observed in the adjacent laterite on Eight Dollar Mountain and the deposit at Riddle, Oreg., in two ways. First, nickel is the most enriched component in those deposits. Second, the large amounts of net enrichment in nickel and cobalt observed at Eight Dollar Mountain and at Riddle were not found in the laterites studied here.

REFERENCES

Benson, W.T., 1963, Pine Flat and Diamond Flat nickel-bearing laterite deposits, Del Norte County, Calif.: U.S. Bureau of Mines Report of Investigations 6206, 19 p.

Boeglin, J.L., Melfi, A.J., Nahon, D., Paquet, H., and Tardy, Y., 1983, Early formed mineral paragenesis in the deep zones of supergene ores in lateritic weathering, *in* Melfi, A.J., and Carvalho, A., eds., Lateritisation processes—Proceedings of the 2nd International Lateritisation Seminar on Lateritisation Processes: Sao Paulo, Brazil, p. 71–88.

Canterford, J.H., 1975, The treatment of nickeliferous laterites: Minerals Science and Engineering, v. 7, p. 3–17.

Chamberlain, P.G., 1986, Nickel, *in* U.S. Bureau of Mines, Mineral Commodity Summaries 1986: Washington, D.C., p. 108–109.

Chandra, D., and Ruud, C.O., 1976, Characterization study of domestic nickeliferous laterites by electron optical and X-ray techniques: U.S. Bureau of Mines Open File Report 95–76, 58 p.

Coleman, R.G., 1977, Ophiolites: New York, Springer-Verlag, 229 p.

Diller, J.S., 1902, Topographic development of the Klamath Mountains: U.S. Geological Survey Bulletin 196, 69 p.

Duyvesteyn, W.P., Wicker, G.R., and Doane, R.E., 1979, An omnivorous process for laterite deposits, *in* Evans, D.J.I., Shoemaker, R.S., and Veltman, H., eds., International laterite symposium: New York, Society of Mining Engineers of the American Institute of Mining, Metallurgical and Petroleum Engineers, p. 553–570.

Evans, D.J.I., Shoemaker, R.S., and Veltman, H. , eds., 1979, International laterite symposium: New York, Society of Mining Engineers of the American Institute of Mining, Metallurgical and Petroleum Engineers, 688 p.

Faust, G.T., 1966, The hydrous nickel-magnesium silicates—The garnierite group: American Mineralogist, v. 51, p. 279–298.

Foose, M.P., 1991, Deposits containing nickel, cobalt, chromium, and platinum-group elements in the United States, *in* The geology of North America—Economic geology: Geological Society of America, v. P–2, p. 87–102.

Gibbs, R.J., 1965, Error due to segregation in quantitative clay mineral X-ray diffraction mounting techniques: American Mineralogist, v. 50, p. 741–751.

Grim, R.E., 1968, Clay mineralogy: New York, McGraw-Hill Book Co., 596 p.

Golightly, J.P., 1981, Nickeliferous laterite deposits, *in* Skinner, B.J., ed., Economic Geology 75th Anniversary Volume: p. 710–735.

Hotz, P.E., 1964, Nickeliferous laterites in southwestern Oregon and northwestern California: Economic Geology, v. 59, no. 3, p. 355–396.

Hundhausen R.J., McWilliams, J.R., and Banning, L.H., 1954, Preliminary investigation of the Red Flats nickel deposit, Curry County, Oregon: U.S. Bureau of Mines Report of Investigations 5072, 19 p.

Irwin, W.P., 1977 , Ophiolitic terranes of California, Oregon, and Nevada, *in* Coleman, R.G. and Irwin, W.P., eds., North American ophiolites: Oregon Department of Geology and Mineral Industries Bulletin 95, p. 75–92.

Kukura, M.E., Stevens, L.G., and Auck, Y.T., 1979, Development of the UOP process for oxide silicate ores of nickel and cobalt, *in* Evans, D.J.I., Shoemaker, R.S., and Veltman, H., eds., International laterite symposium: New York, Society of Mining Engineers of the American Institute of Mining, Metallurgical and Petroleum Engineers, p. 527–552.

Libbey, F.W., Lowry, W.D., and Mason, R.S., 1947, Nickel-bearing laterite, Red Flats, Curry County, Oregon: Ore Bin, v. 9, no. 3, p. 19–27.

Page, N.J, Miller, M.S., Grimes, D.J., Leinz, R.W., Blakely, R.W., Lipin, B.R., Foose, M.P., and Gray, F., 1982, Mineral resource potential map of the Kalmiopsis Wilderness, southwestern Oregon: U.S. Geological Survey Miscellaneous Field Studies Map MF–1240–E, scale 1:62,500.

Ramp, L., 1978, Investigations of nickel in Oregon: Oregon Department of Geology and Mineral Industries Miscellaneous Paper 20, 68 p.

Schwertmann, U., 1983, The role of aluminium in iron oxide systems, *in* Melfi, A.J., and Carvalho, A., eds., Lateritisation processes—Proceedings of the II International Seminar on Lateritisation Processes: University of Sao Paulo, Brazil, p. 65-68.

Siemens, R.E., Good, P.C., and Stickney, W.A., 1975, Recovery of nickel and cobalt from low-grade domestic laterites: U.S. Bureau of Mines Report of Investigations 8027, 14 p.

Trescases, Jean-Jacques, 1975, L'evolution geochimique supergene des roches ultrabasiques en zone tropicale—Formation des gisements nickeliferes de Nouvelle-Caledonia: Memoires O.R.S.T.O.M., no. 78, 259 p.

Chapter F

Platinum-Group Elements—Occurrences in the Bethlehem Porphyry Copper Deposits, Highland Valley, British Columbia

By NORMAN J PAGE, JOSEPH A. BRISKEY, and LEUNG MEI

U.S. GEOLOGICAL SURVEY BULLETIN 1877

CONTRIBUTIONS TO COMMODITY GEOLOGY RESEARCH

CONTENTS

FIGURES

TABLES

Platinum-Group Elements—Occurrences in the Bethlehem Porphyry Copper Deposits, Highland Valley, British Columbia

By Norman J Page, Joseph A. Briskey, *and* Leung Mei

Abstract

Samples of unaltered and of altered and mineralized rocks from the Bethlehem porphyry copper deposits, and from the host Guichon Creek batholith, are analyzed for platinum-group elements. Iridium and ruthenium are not detected at levels of 20 ppb (parts per billion) and 100 ppb, respectively. On the average, altered and mineralized rocks are slightly enriched in palladium, platinum, and rhodium compared to unaltered and unmineralized rocks. Within the group of relatively unaltered and mineralized rocks, the younger phases have slightly higher platinum concentrations, and with the altered and mineralized rocks, the palladium content tends to increase from the propylitic to the potassic zone. Highly mineralized rocks tend to have higher concentrations of the three platinum-group elements. The highest palladium, platinum, and rhodium contents are 17, 14, and 411 ppb; however, most contents average near 1, 2, and 0.6 ppb for palladium, platinum, and rhodium, respectively.

INTRODUCTION

Platinum-group elements (PGE) are known to occur in porphyry copper systems, but their concentrations and distributions are generally unknown. Ageton and Ryan (1970) estimated that copper ores average about 1 troy ounce of PGE per 6,000 short tons of ore or 5.7 ppb (parts per billion). Information for many individual deposits is limited. On the basis of Eilers' (1913) analyses of blister copper, the Bingham porphyry copper deposit probably contains platinum and palladium in the ore at some low concentration. He found 0.0034 oz/ton platinum (106.3 ppb) and 0.0118 oz/ton palladium (405 ppb) in the blister copper. Smith (1976) reported that ore from the porphyry copper deposits near Ely, Nev., in the Robinson mining district, contained an average of 0.0004 oz/ton palladium (14 ppb) and 0.0001 oz/ton platinum (3.4 ppb). Studies in the Iron Canyon area, Nev., which is on the northeast outermost fringes of the Copper Canyon porphyry system, show that palladium was detected in 137 of 270 rock samples analyzed. The palladium had an average concentration of 3.4 ppb, and the highest concentration was 20 ppb (Carlson and others, 1976; Theodore and others, 1976; Page and others, 1978). Palladium in rocks from Iron Canyon classified as granitic porphyries had an average of 3 ppb and a maximum of 7 ppb. Recently, some PGE data from alkaline-rock-hosted porphyry copper systems have become available (Finch and others, 1983; Mutschler and others, 1984). Some of these systems were estimated to have 100 to 300 ppb palladium and 10 to 500 ppm platinum in copper-sulfide concentrates. Eckle (1949) identified PGE in the La Plata district in Colorado; Werle and others (1984) reported 1,900 to 2,300 ppb palladium and 2,900 to 3,900 ppb platinum in copper-sulfide concentrates from the alkaline Allard stock of the La Plata district. The rocks from which these concentrates were derived would have much lower amounts of platinum-group elements.

Samples of unaltered and of altered and mineralized rocks from the Bethlehem porphyry copper deposits, and from the host Guichon Creek batholith, were analyzed with the following goals in mind: (1) to perform a reconnaissance survey of the levels of PGE concentration present in a calc-alkaline porphyry system, (2) to evaluate whether documentable changes occur in PGE concentration during alteration and mineralization, and (3) to investigate the potential of PGE geochemistry in suggesting sources for metals in porphyry systems. The Bethlehem porphyry copper deposits, 400 km by highway northeast of Vancouver, B.C., are near the center of the 202- to 205-m.y.-old Guichon Creek batholith. This batholith is a concentrically zoned, chemically primitive, calc-alkaline pluton that intrudes oceanic assemblages and island-arc lithologies (Briskey and Bellamy, 1976; Briskey, 1980; Briskey and others, 1981). This communication will review briefly the geologic setting as background for the PGE geochemistry, present the analytical techniques and analyses for platinum-group elements, and give a preliminary evaluation of the significance of those results.

ACKNOWLEDGMENTS

The authors are grateful to the former Bethlehem Copper Corporation, to its vice president for exploration, Henry G. Ewanchuk, and to Cominco Limited for supporting this and other detailed studies of the Bethlehem deposits. Numerous discussions of the geology of the deposits with William J. McMillan, Pantellis P. Tsaparas, Michael B. Jones, Robert A. Schmuck, James M. Allen, and especially Cyrus W. Field were invaluable and are sincerely appreciated. Cyrus W. Field, William J. McMillan, Ted G. Theodore, and Dennis P. Cox critically reviewed and improved the manuscript. This study was in part supported by grants from the Geological Society of America and from Sigma Xi.

GEOLOGIC SETTING

Within the Intermontane belt of the Canadian Cordillera, the Upper Triassic Guichon Creek batholith intrudes island-arc lithologies of the Upper Triassic to perhaps Middle Jurassic Nicola Group (McMillian, 1978). The Nicola Group is shown as Upper Triassic volcanic and sedimentary rocks in figure 1. The batholith (fig. 1) is a concentrically zoned calc-alkaline pluton, which contains major intrusive phases that become progressively younger and change in composition from quartz diorite and diorite of the peripheral hybrid (border) phase; through quartz diorite and granodiorite of the Guichon variety; to granodiorites of the Chataway variety, the Bethlehem phase, and the Skeena variety; to a core of granodiorite and quartz monzonite of the Bethsaida phase (McMillan, 1976, 1978). The mineralogy and texture of these units are typical of many calc-alkaline suites of the Coast Plutonic Complex of British Columbia, and of island-arc and continental-marginal-arc tectonic settings (Briskey and others, 1981).

The Bethlehem deposits formed along an irregular intrusive contact separating two major plutonic units of the Guichon Creek batholith (fig. 2*A*). Older Guichon variety granodiorite is intruded by younger Bethlehem phase granodiorite that forms a digitated northward-elongated apophysis along which is also localized a porphyry dike swarm that is most closely related in time and space with the ore deposits. Intrusive breccias; dacite porphyry dikes; small masses of "granite," granodiorite, and porphyritic quartz latite; dikes of silicic aplite; faults and fractures; and hydrothermal mineralization and alteration all are localized along digitations in the contact of the apophysis.

Hydrothermal alteration generally has a zonal development within the ore deposits, with the distribution of epidote and secondary biotite forming a roughly concentric zonal pattern (Briskey and others, 1981). Epidote defines the peripheral zone of propylitic alteration, and secondary biotite the central potassic alteration core. In between is an area dominated by white mica and chlorite that is equivalent to phyllic alteration. Significant hydrothermal alteration is restricted to the immediate areas of orebodies; only propylitic and zeolite assemblages extend beyond the limits of conspicuous copper sulfide minerals.

Hypogene metallic minerals in the Bethlehem deposits include chalcopyrite, bornite, pyrite, specularite, molybdenite, and minor magnetite and chalcocite. In the Jersey deposit, and probably in the Huestis and Iona deposits, there is a zonation of iron-bearing metallic minerals (Briskey and Bellamy, 1976). Vein-controlled specularite occurs peripheral to pyrite, each forming crudely concentric zones about a bornite-rich core. Though chalcopyrite is most abundant within the outer limits of the pyrite zones, it occurs throughout the deposits. Low-grade copper mineralization coincides with the pyrite halo, and high-grade copper occurs in the bornite-rich core. Molybdenite is distributed sporadically and is commonly peripheral to the central parts of ore zones. The copper content of unaltered Guichon and Bethlehem granodiorite in the vicinity of the deposits is 223 and 25 ppm, respectively, and the average content increases inward to the potassic zone where analyzed samples average 5,200 and 3,200 ppm, respectively (Briskey, 1980). Thus, type of alteration roughly corresponds to the copper content of the rock. Characteristics of the hypogene metallic mineral assemblage include (1) low total sulfide content (average <2 volume percent), (2) sparse pyrite (average <1 volume percent in the halo zone, and (3) high bornite to chalcopyrite ratios (>1) in the bornite-rich core.

Details of mineralogy, petrology, geochemistry, and geology that supplement this brief description are given by Briskey and Bellamy (1976), Briskey (1980), and Briskey and others (1981).

ANALYTICAL METHODS AND RESULTS

Analyses of platinum-group elements were performed (1) on grab and composite samples of unaltered rocks representing the major phases of the batholith and (2) on unaltered, altered, and mineralized grab samples from the porphyry copper systems. Sample descriptions and analytical results for palladium, platinum, and rhodium are given in table 1. Locations of individual rock samples are shown on figures 1 and 2.

The samples were analyzed for platinum, palladium, and rhodium by using a fire assay preconcentration with gold wire extraction (Haffty and others, 1977) followed by a graphite furnace atomic absorption technique (Simon and others, 1978; Page and others, 1980). The samples were analyzed in two groups. Detection limits for one group were 0.1, 1.0, and 0.1 ppb of palladium, platinum, and rhodium,

Table 1. Palladium, platinum, and rhodium analyses and description of samples from the Guichon Creek batholith and the Bethlehem porphyry copper deposits, British Columbia

[Sample numbers used by Briskey (1980) are in parentheses. Samples preceded by asterisks are composite samples. Analysts: L. Mei and M. Doughten]

Field number	Pd	Pt	Rh	Sample description
	Parts per billion			
Major plutonic units of Guichon Creek batholith				
*GB–5 (25)	1.3	<1	0.2	Bethsaida phase.
*GB–1 (23)	1	<1	.3	Skeena variety.
GB–2–72 (30)	.7	<1	.1	Witches Brook phase.
*GB–2 (19)	.6	<1	.2	Bethlehem phase-Highland Valley phase.
*GB–7 (11)	1.5	<1	<.5	Chataway variety.
*GB–6 (9)	1.6	<1	<.5	Guichon variety.
*GB–3 (1)	.5	1	<.5	Hybrid (border) phase.
Weakly altered and weakly mineralized dikes and small intrusive masses from the Bethlehem porphyry property				
J–B21–30 (64)	<0.5	<1	<0.5	Dacite porphyry.
J–X39–23 (54)	1	1.6	<.5	Do.
BTH–8–70 (52)	.55	1	<.5	Do.
J–D0–18 (50)	<.5	<1	<.5	Do.
BTH–4–70 (56)	.7	<1	<.5	Do.
J–F13–65 (66)	.65	<1	<.5	Dacite porphyry.
J–D39–8 (78)	<.5	1.9	<.5	K-feldspar-rich aplite.
J–I–53 (74)	<.5	1.8	<.5	K-feldspar-poor aplite.
BTH–27–72 (47)	<.5	1	<.5	Granite.
BTH–28–72 (45)	.7	1	<.5	Granodiorite.
H–4533–17 (43)	.95	2.4	<.5	Porphyritic quartz latite.
H–HR–7 (17)	1.1	<1	<.1	Bethlehem phase.
J–E9–80 (16)	.4	<1	<.1	Do.
J–B233–175 (35)	1	<1	<.5	Bethlehem porphyry.
H–5033–2 (38)	<.1	<1	.5	Bethlehem leucophase.
BTH–11–72 (7)	.95	1	<.5	Guichon variety.
J–D24–2 (5)	1	<1	<.5	Do.
J–X18–80 (6)	1.6	1.5	.6	Leucocratic Guichon variety.
Altered and mineralized rocks from the Bethlehem porphyry property				
J–D30–70 (88)	0.9	2	<0.5	Propylitically altered Bethlehem phase.
J–C12–45 (86)	<.5	<1	<.5	Do.
J–X14–50 (84)	1.2	<1	<.5	Propylitically altered Guichon variety.
J–2–5 (81)	.75	<1	<.5	Do.
J–E1–65D (106)	.85	<1	.5	Phyllically altered Bethlehem phase.
J–B29–230 (111)	.6	<1	<.5	Do.
J–B234–106 (113)	1	1.5	8	Do.
J–B234–192 (114)	1	1.4	.85	Do.
J–B234–291 (115)	.5	1.5	.5	Do.
J–B52–153 (102)	1.7	1.6	.75	Phyllically altered Guichon variety.
J–B18–367 (100)	1.8	1.6	<.5	Do.
J–X33–0 (99)	.75	2	<.5	Do.
J–R2–9 (93)	2	2.1	<.5	Do.
J–R0–40 (92)	2.2	2.3	<.5	Do.
H–4533–6 (116)	<.5	1.5	<.5	Potassically altered Bethlehem phase.
J–U6–45 (126)	<.5	1.5	<.5	Do.
J–B235–500 (127)	.52	.3	<.5	Do.
J–B235–922 (128)	.7	1.5	<.5	Do.
J–X45–7 (121)	2.8	2	<.5	Potassically altered Guichon variety.
J–B35–956 (122)	<.5	<1	<.5	Do.
Vein samples from the Bethlehem porphyry property				
J–E2–28B (140)	17	14	4.1	Bornite with minor chalcopyrite.
J–E2–28C (141)	<.5	<1	<.5	Chalcopyrite with minor bornite.

respectively. For the other group, the technique has detection limits of 0.5, 1.0, and 0.5 ppb for palladium, platinum, and rhodium under optimum conditions, which are dependent on sample size; smaller samples have higher detection limits. At the 1-ppb level, precision is about ±30 percent for platinum, and at the 0.5-ppb level is ±20 percent and ±50 percent for palladium and rhodium, respectively. Samples J–RO–40, J–X45–7, and J–E2–28B were analyzed for iridium and ruthenium by the method of Haffty and others (1980), but neither element was found above the limits of detection (20 ppb for iridium and 100 ppb for ruthenium).

The analyses in table 1 are all near or below detection limits for the three elements analyzed. Only one sample, from a bornite-rich vein (J–E2–28B), contains more than 10 ppb each of palladium and platinum. Averages for all samples, excluding qualified values and the bornite-rich vein, are 1.06±0.54 ppb palladium, 1.63±0.44 ppb platinum, and 0.48±0.27 ppb rhodium. The averages for all samples have standard deviations less than the levels of precision reported for each element near the mean. Consequently, these low concentration levels emphasize the tentativeness and possibly speculative nature of the following discussions.

DISCUSSION

The calc-alkaline Guichon Creek batholith, which contains the Bethlehem porphyry copper deposits, was emplaced in an oceanic island-arc terrane. The concentration levels of platinum-group elements in rocks from the batholith and the deposits are low, near the limits of detection. The presence of small amounts of these elements is consistent with, and predictable from, limited data on their presence in other porphyry copper systems described earlier. The averages and standard deviations for different groupings of the samples are given in table 2. These

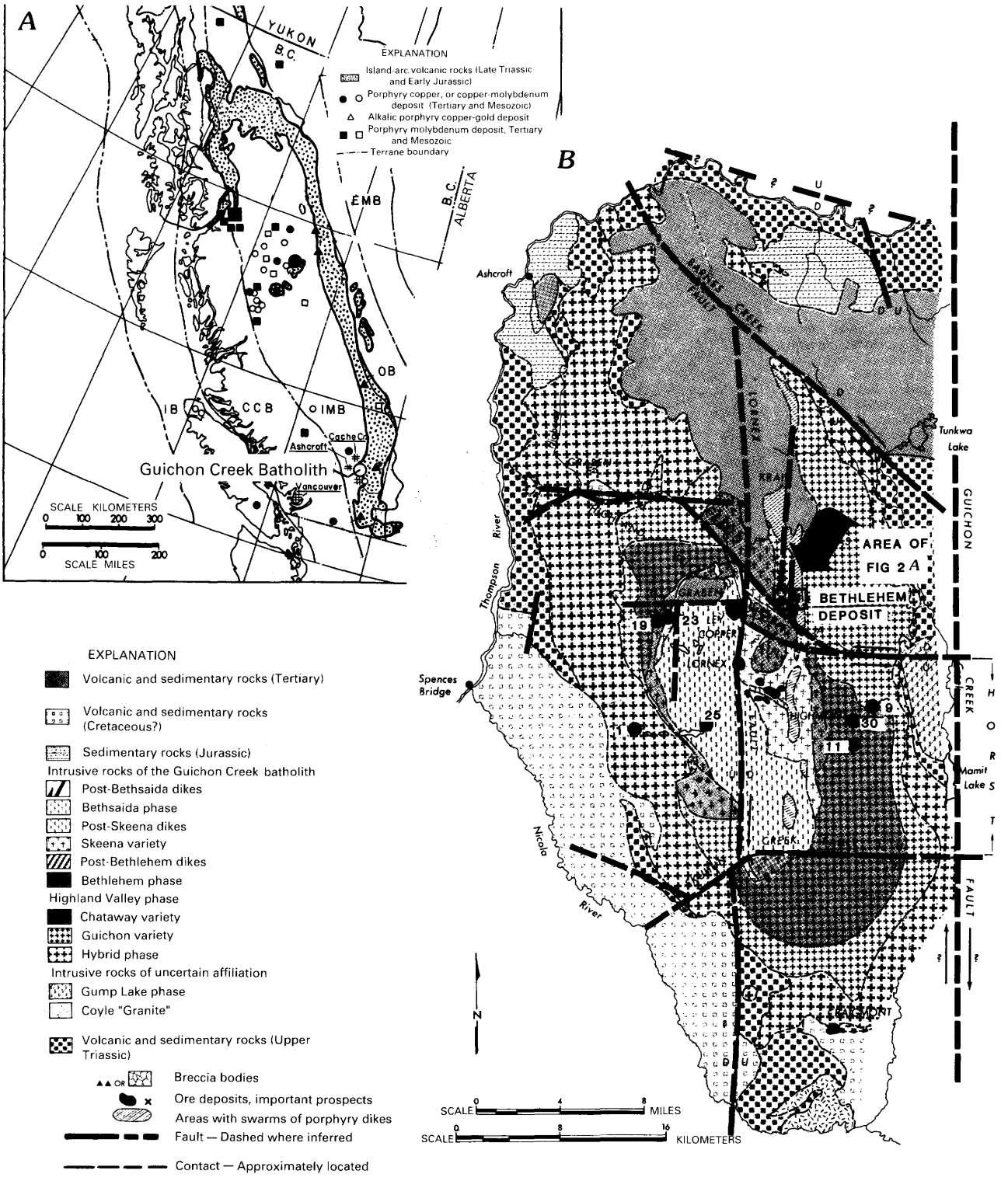

Figure 1. Location of the Guichon Creek batholith and the Bethlehem porphyry copper-molybdenum deposits in the southern part of the Canadian Cordillera. *A*, Distribution of porphyry deposits in petrotectonic belts, and Upper Triassic and Lower Jurassic island-arc volcanic and related rocks (shaded). IB, Insular belt; CCB, Coast crystalline belt; IMB, Intermontane belt; OB, Omineca belt; EMB, Eastern marginal belt. Modified from Christopher and Carter (1976), McMillan (1976), and Barr and others (1976). *B*, Geologic map of the Guichon Creek batholith showing the locations of samples analyzed for platinum-group elements, and showing the location of figure 2*A*. After McMillan (1976). Numbers refer to samples, which are described in table 1.

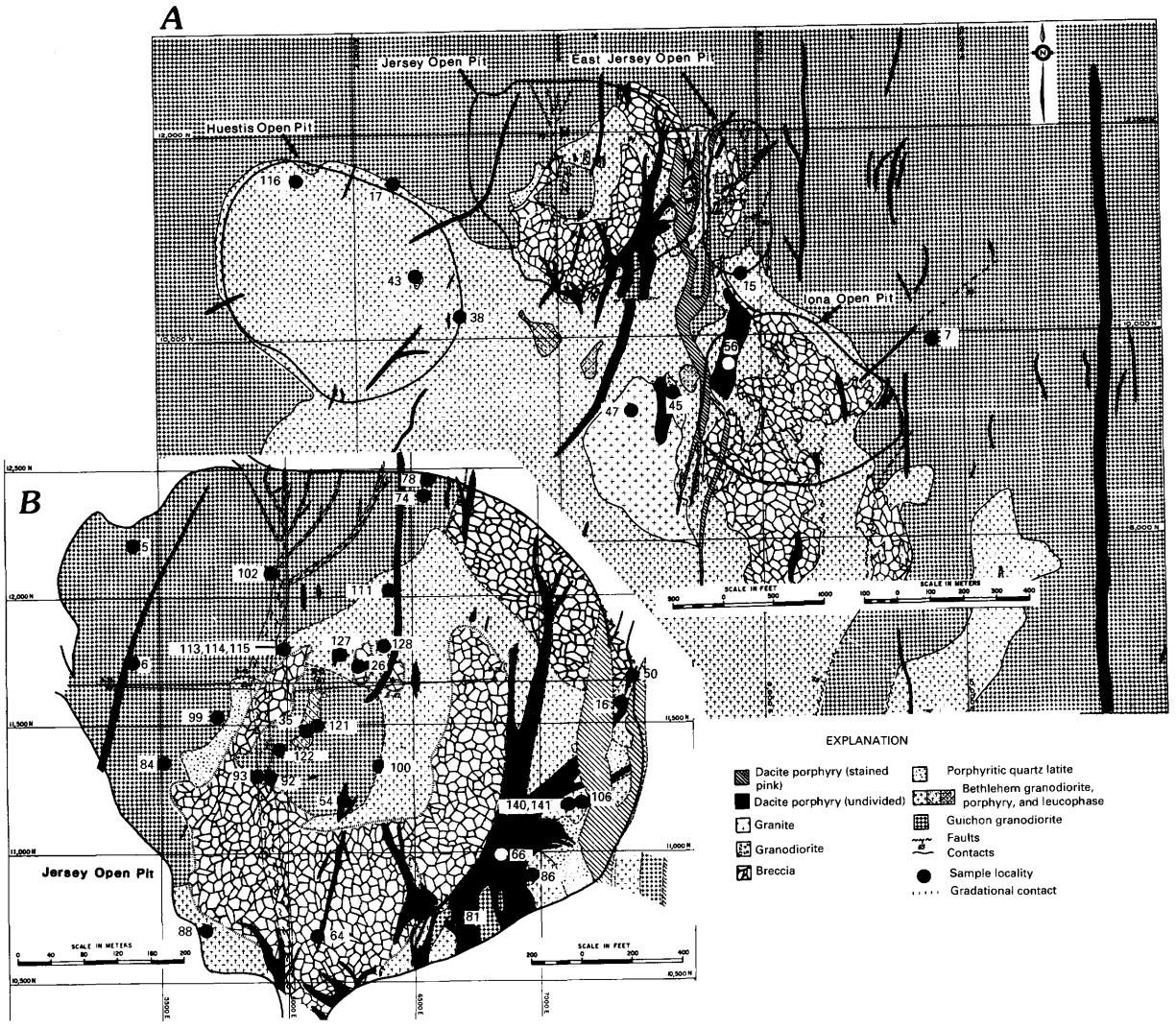

Figure 2. Geology of the Bethlehem deposits showing the locations of samples analyzed for platinum-group elements. *A*, Map of the deposits. *B*, Detailed map of the Jersey open pit. After Briskey and others (1981). Numbers refer to samples, which are described in table 1.

groupings are based on petrologic and mineralogic characteristics of the rocks. Average PGE values for these groups suggest that altered and mineralized rocks are slightly enriched in palladium, platinum, and rhodium compared to relatively unaltered and unmineralized rocks. However, only the averages for platinum and rhodium are significantly different at the 5-percent level based on the pooled estimate of the standard deviations. Within the group of relatively unaltered and unmineralized rocks, the younger phases have slightly higher average platinum concentrations than the Bethlehem phase or Guichon variety, but the Guichon variety has slightly higher palladium concentrations. Neither of these comparisons are significantly different at the 5-percent level. Altered rocks have about the same average concentrations of platinum and perhaps rhodium in the propylitic, phyllic, and potassic zones. Average palladium content appears to increase from the propylitic to the potassic zone, but these differences are not statistically significant. Within the phyllic zone, the average palladium content is higher in altered rocks of the Guichon variety than in those of the Bethlehem phase, and the difference is significant at the 5-percent level. Highly mineralized rocks tend to have higher concentrations of the three platinum-group elements. Comparison of platinum±palladium content with copper content (reported in Briskey, 1980) of the altered and mineralized rocks suggests that those rocks containing copper above about 8,000 ppm also contain platinum±palladium greater than 3 ppb. The average platinum±palladium contents of the three alteration zones are roughly equivalent, 2.95 to 3.09 ppb. Changes appear to occur in PGE concentrations during alteration and mineral-

Table 2. Average, standard deviation, and number of analyses of samples containing detectable palladium, platinum, and rhodium in mineralogic and petrologic groupings of the Guichon Creek batholith and Bethlehem porphyry copper deposits

[Unaltered rocks include major plutonic units of the Guichon Creek batholith, as well as weakly altered and weakly mineralized rocks from the Bethlehem porphyry property. Younger phases include the Skeena variety, Witches Brook phase, Bethsaida phase, dacite porphyry, aplite, granite, granodiorite, and porphyritic quartz latite. The averages for the Guichon variety include the analyses of Bethlehem porphyry, and the averages for the Guichon variety include the analyses of leucocratic Guichon variety. Average (x), standard deviation (σ), and number (n). —, no data]

Group	Palladium			Platinum			Rhodium		
	x	σ	n	x	σ	n	x	σ	n
Unaltered rocks	0.94	0.36	19	1.42	0.50	10	0.28	0.19	5
Younger phases	.84	.24	9	1.53	.55	7	.2	—	3
Bethlehem phase	.78	.33	4	<1	—	5	.35	—	2
Guichon variety	1.29	.36	4	1.25	.35	2	.6	—	1
Altered and mineralized rocks	1.20	.69	16	1.77	.33	14	.68	.17	5
Propylitic	.95	.23	3	2.0	—	1	<.5	—	4
Phyllitic	1.24	.62	10	1.75	.33	8	.68	.17	5
Bethlehem phase	.79	.23	5	1.47	.06	3	.66	.19	4
Guichon variety	1.69	.56	5	1.92	.31	5	.75	—	1
Potassic	1.33	1.27	3	1.76	.37	5	<.3	—	6
Veins	17	—	1	14	—	1	4.1	—	1

ization, but with the limited amount of data, it is not possible to document these changes reliably.

Chondrite-normalized PGE ratios have been used to compare different groups of rocks including those from ophiolites, komatiites, and stratiform layered intrusions (Naldrett, 1981; Page and others, 1982). Generally, chromitites from ophiolites show negative slopes, komatiites flat slopes, and layered intrusions positive slopes. Figure 3 shows chondrite-normalized ratios for palladium, platinum, and rhodium for rocks from the Guichon Creek batholith and Bethlehem porphyry deposits. Bornite from veins has the highest ratios; relatively unaltered and unmineralized rocks, the lowest; and altered and mineralized rocks, intermediate ratios. Superimposed on the diagram is the field of ophiolitic chromitites, which represents different worldwide occurrences and ages. Komatiites and stratiform layered intrusions tend to have higher chondrite-normalized ratios of palladium, platinum, and rhodium, and thus are not shown. Although altered and unaltered rocks and mineralized and unmineralized rocks from the batholith and the deposits have lower chondrite-normalized ratios than ophiolitic chromitites, their overall negative-sloping character allows speculation that these patterns represent platinum-group elements picked up by the calc-alkaline magmas as they traversed through oceanic crust and island-arc volcanic lithologies, which perhaps include serpentinized ultramafic rocks of ophiolitic affinity. Nevertheless, the platinum-group element data are missing the iridium and ruthenium values necessary to define complete trends, and the data are too limited to firmly support such a conclusion.

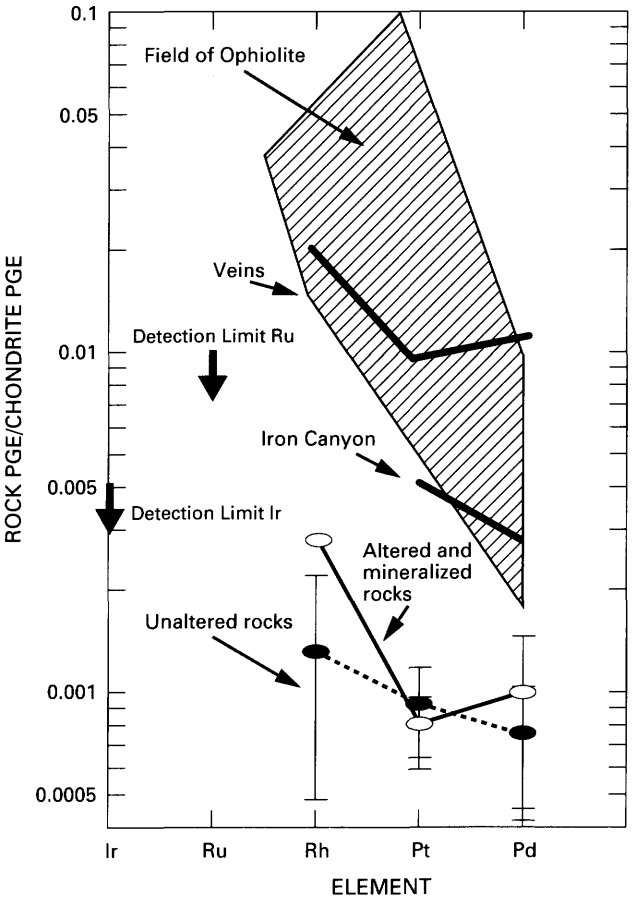

Figure 3. Chondrite-normalized ratios for palladium, platinum, and rhodium averages for the sample groupings defined in table 2 from the Guichon Creek batholith and the Bethlehem porphyry deposits. Field of ophiolites from Page and others (1985); Iron Canyon from Page and others (1978); averages and standard deviation from table 2; chrondite-normalizing values are the same as used by Page and others (1982). PGE, platinum-group element.

Unknown mechanisms or processes in PGE metal transport in porphyry copper systems may be the explanation for the observed patterns.

In summary, (1) the platinum-group elements are present in calc-alkaline porphyry copper systems almost at levels that can be investigated by the methods used; (2) these elements appear to show changes in concentration with respect to petrogenetic, alteration, and mineralization processes in porphyry copper systems; and (3) accumulation of adequate platinum-group element data from numerous systems may help determine source areas of metals in some magmatic hydrothermal copper deposits.

REFERENCES

Ageton, R.W., and Ryan, J.P., 1970, Platinum-group metals, *in* Mineral facts and problems: U.S. Bureau of Mines Bulletin 650, p. 653–669.

Barr, D.A., Fox, P.E., Northcote, K.E., and Preto, V.A., 1976, The alkaline suite porphyry deposits—A summary, *in* Sutherland Brown, A., ed., Porphyry deposits of the Canadian Cordillera: Canadian Institute of Mining and Metallurgy Special Volume 15, p. 359–367.

Briskey, J.A., Jr., 1980, Geology, petrology, and geochemistry of the Jersey, East Jersey, Huestis, and Iona porphyry copper-molybdenum deposits, Highland Valley, British Columbia: Corvallis, Oregon, Oregon State University, Ph.D. dissertation, 399 p.

Briskey, J.A., Jr., and Bellamy, J.R., 1976, Bethlehem Copper's Jersey, East Jersey, Huestis, and Iona deposits, *in* Sutherland Brown, A., ed., Porphyry deposits of the Canadian Cordillera: Canadian Institute of Mining and Metallurgy Special Volume 15, p. 105–119.

Briskey, J.A., Jr., Field, C.W., and Bellamy, J.R., 1981, Geology, petrology, and geochemistry of the Jersey, East Jersey, Huestis, and Iona porphyry copper-molybdenum deposits, Highland Valley, British Columbia: U.S. Geological Survey Open-File Report 81–355, p. 107–126.

Carlson, R.R., Venuti, P.E., Page, N.J, and Theodore, T.G., 1976, Descriptions and chemical analyses of 270 rocks and soils analyzed for platinum-group metals from the Iron Canyon area, Lander County, Nevada: U.S. Geological Survey Open-File Report 76–524, 32 p.

Christopher, P.A., and Carter, N.C., 1976, Metallogeny and metallogenic epochs for porphyry mineral deposits in the Canadian Cordillera, *in* Sutherland Brown, A., ed., Porphyry deposits of the Canadian Cordillera: Canadian Institute of Mining and Metallurgy Special Volume 15, p. 64–71.

Eckle, E.B., 1949, Geology of the ore deposits of the La Plata district, Colorado: U.S. Geological Survey Professional Paper 219, 179 p.

Eilers, A., 1913, Rare metals in blister copper: American Institute of Mining Engineers Transactions, v. 47, p. 217–218.

Finch, R.J., Ikramuddin, M., Mutschler, F.E., and Shannon, S.S., Jr., 1983, Precious metals in alkaline suite porphyry copper systems, western North America: Geological Society of America Abstracts with Programs, v. 15, no. 6, p. 572.

Haffty, Joseph, Haubert, A.W., and Page, N.J, 1980, Determination of iridium and ruthenium in geological samples by fire assay and emission spectrograph: U.S. Geological Survey Professional Paper 1129A–I, p. G1–G4.

Haffty, Joseph, Riley, L.B., and Goss, W.D., 1977, A manual on fire assaying and determination of the noble metals in geological materials: U.S. Geological Survey Bulletin 1445, 58 p.

McMillan, W.J., 1976, Geology and genesis of the Highland Valley ore deposits and the Guichon Creek batholith, *in* Sutherland Brown, A., ed., Porphyry deposits of the Canadian Cordillera: Canadian Institute of Mining and Metallurgy Special Volume 15, p. 85–104.

———1978, Notes and legend to accompany preliminary map no. 30—Geology of the Guichon Creek batholith: British Columbia Ministry of Mines and Petroleum Resources, 17 p.

Mutschler, F.E., Griffin, M.E., Stevens, S.D., and Shannon, S.S., Jr., 1984, Precious metal deposits related to alkaline igneous rocks in the North American Cordillera: Geological Society of American Abstracts with Programs, v. 16, no. 6, p. 606.

Naldrett, A.J., 1981, Platinum-group element deposits, *in* Cabri, L.J., ed., Platinum group elements, mineralogy, geology, recovery: Canadian Institute of Mining and Metallurgy Special Volume 23, p. 197–231.

Page, N.J, Banerji, P.K., and Haffty, Joseph, 1985, Characterization of the Sukinda and Nausahi ultramafic complexes, Orissa, India, by platinum-group element geochemistry: Precambrian Research, v. 30, p. 27–41.

Page, N.J, Cassard, Daniel, and Haffty, Joseph, 1982, Palladium, platinum, rhodium, ruthenium, and iridium in chromitites from the Massif du Sud and Tiebaghi Massif, New Caledonia: Economic Geology, v. 77, no. 6, p. 1571–1577.

Page, N.J, Myers, J.S., Haffty, Joseph, Simon, F.O., and Aruscavage, P.J., 1980, Platinum, palladium, and rhodium in the Fiskenaesset complex, southwestern Greenland: Economic Geology, v. 75, no. 6, p. 907–915.

Page, N.J, Theodore, T.G., Venuti, P.E., and Carlson, R.R., 1978, Implications of the petrochemistry of palladium at Iron Canyon, Lander County, Nevada: U.S. Geological Survey Journal of Research, v. 6, no. 9, p. 107–114.

Simon, F.O., Aruscavage, P.J., and Moore, R.. 1978, Determination of platinum, palladium, and rhodium in geologic spectroscopy using electrothermal atomization [abs.]: American Chemical Society, National Meeting, 176th, Miami Beach, Florida, September 11–14, 1978.

Smith, R.M., 1976, Mineral resources, pt. 2 of Geology and mineral resources of White Pine County, Nevada: Nevada Bureau of Mines and Geology Bulletin 85, p. 36–105.

Theodore, T.G., Venuti, P.E., Page, N.J, and Carlson, R.R., 1976, Maps showing distribution of palladium and other elements in rocks at Iron Canyon, Lander County, Nevada: U.S. Geological Survey Miscellaneous Field Studies Map MF–790, 2 sheets.

Werle, J.L., Ikramuddin, Mohammed, and Mutschler, F.E., 1984, Allard stock, La Plata Mountains, Colorado—An alkaline rock-hosted porphyry copper-precious metal deposit: Canadian Journal of Earth Sciences, v. 21, p. 630–641.

Chapter G

Platinum-Group Elements—Occurrences in Gold Deposits in Nevada, Oregon, and Idaho

By NORMAN J PAGE, WILLIAM C. BAGBY, RAUL J. MADRID, and BARRY C. MORING

U.S. GEOLOGICAL SURVEY BULLETIN 1877

CONTRIBUTIONS TO COMMODITY GEOLOGY RESEARCH

CONTENTS

FIGURE

TABLES

Platinum-Group Elements—Occurrences in Gold Deposits in Nevada, Oregon, and Idaho

By Norman J Page, William C. Bagby, Raul J. Madrid, *and* Barry C. Moring

Abstract

Mineralized and unmineralized rock samples, selected in a reconnaissance fashion from carbonate-hosted gold-silver, hot-spring gold-silver, epithermal gold, hot-spring mercury, and hot-spring manganese-tungsten deposits in Nevada, Oregon, and Idaho are analyzed for platinum, palladium, and rhodium. Average values of platinum range from 1.6 to 23 parts per billion (ppb), and average values of palladium range from less than 1 to 4 ppb. These averages are highly biased by the large proportion of unmineralized rock included in the samples. All except hot-springs manganese-tungsten deposits contain detectable amounts of platinum (<1.0 ppb) and palladium (0.5 ppb). Higher palladium contents tend to correlate with higher gold contents. Data are too sparse to speculate on the origin or genesis of the platinum-group elements in these deposits or to evaluate the possible resources in these deposit types. The range of concentrations of the platinum-group elements is remarkably limited considering the diversity of the samples analyzed.

INTRODUCTION

A geochemical survey of platinum-group elements (PGE) in Nevada, Oregon, and Idaho was initiated because of the reported occurrence of these metals associated with gold in a few widely spread and geographically significant hydrothermal deposits. Platinum and palladium occurrences have been previously recognized in placer and lode gold deposits from Nevada. Platinum-group elements have been produced from porphyry copper deposits in Nevada and Utah and in hydrothermal systems elsewhere (Quiring, 1962; Mertie, 1969; Blair and others, 1977). Samples of placer gold from the Iron Canyon area (Theodore and Roberts, 1971), the Natomas placer (Theodore and Blake, 1975), and lode gold from the east orebody of the Copper Canyon porphyry copper deposit (Theodore and Blake, 1975) contained between 2 and 100 parts per million (ppm) palladium. Followup studies by Carlson and others (1976), Theodore and others (1976), and Page and others (1978) indicated that about half of 270 samples of rocks analyzed from the Iron Canyon mine area in Nevada contained measurable amounts of palladium that averaged 3.4 ppb.

Other notable occurrences of platinum-group elements associated with gold include deposits in Arizona, British Columbia, and Brazil. In the Lost Basin-Gold Basin mining districts in northwestern Arizona, lode gold samples from the Golden Gate mine, Senator mine, and a prospect northwest of the Golden Hill mine contained traces of palladium as determined by semiquantitative spectrographic analyses, and a sample from the Senator mine contained traces of platinum (Antweiler and Campbell, 1982). Page, Briskey, and Mei (this volume) summarize the PGE contents in porphyry copper deposits and present PGE analyses for the Bethlehem porphyry copper deposits. Abundant palladium (as much as 2.5 metric tons, or t) along with gold has been produced from the Serra Pelada gold mine in Brazil (Engineering and Mining Journal, 1986). Some nuggets of gold at Serra Pelada have concentrations of as much as 10 percent palladium (Dayton and Sassos, 1985).

The occurrence of platinum-group elements in the above deposits suggested the possibility that other gold deposits might also contain significant amounts of platinum-group elements. Based on this limited background of previous investigations, 65 grab samples of mineralized and unmineralized rocks were collected from various types of lode gold deposits and analyzed for platinum-group elements. The deposits from which the samples were obtained include carbonate-hosted gold-silver, hot-springs gold-silver, epithermal gold, hot-springs mercury, and hot-springs manganese-tungsten deposits.

Due to the reconnaissance nature of the sampling, and the lack of a clear geologic context for many of the samples, this report should be considered preliminary. This study investigates the PGE resources in lode gold deposits and the utility of the platinum-group elements in assessing the genesis of the various types of gold deposits. The latter aspect has been discussed in Page and Talkington (1984) and may prove useful in the future when more PGE data are available for lode gold deposits. In this report, our purpose is to introduce analytical data, to discuss the significance of the PGE contents, and to suggest further lines of research.

GEOLOGIC SETTING

The deposits sampled occur in a number of diverse stratigraphic and structural settings of the Basin and Range province of the Western Cordillera (fig. 1). These settings are described below to illustrate their diversity,which, it will be shown, appears to have had a limited effect on the range of PGE concentrations in rocks analyzed in this study. This area has been the site of repeated deformation, plutonism, and widespread volcanism during much of Phanerozoic time.

During the Paleozioc, oceanic rocks of the Roberts Mountains and Golconda allochthons were emplaced over the continental shelf during the late Devonian Antler and latest Permian Sonoma orogenies, respectively (Roberts and others, 1958). The continental-rise and deeper water strata that form these allochthons were deposited in complex basins developed west of, and adjacent to, depositional sites of the continental shelf. The predominantly chert-sandstone-greenstone and subordinate carbonate stratigraphy of these allochthons record sedimentologic and structural events that tie them to the North American craton (Miller and others, 1984) and, specifically, to similar events recorded within the coeval, largely carbonate rocks of the continental shelf. Thus, the Paleozoic allochthonous rocks in Nevada differ from rocks of similar compositions in the accreted terranes of the Sierra Nevada and Klamath Mountains, which do not display stratigraphic ties with rocks of the continental margin.

These rocks in Nevada are covered by those of Upper Paleozoic age that composed the continental shelf and were deposited on the allochthons and the earlier Paleozoic continental shelf. These rocks, termed the Overlap Assemblage (Roberts and others, 1958) and the Foreland Basin deposits (Poole and Sandberg, 1977), occur as far east as western Utah and extend as far north as the Pioneer Mountains in Idaho.

The early Mesozoic is characterized by the presence of basinal and shelf strata that discontinuously covered much of western Nevada and portions of north-central Nevada. Late Jurassic, Cretaceous, and Early Tertiary plutons intruded these and earlier Paleozoic rocks throughout the region.

The predominance of extensional tectonics in the Basin and Range province developed as early as Eocene time but culminated during the Miocene (Stewart, 1984). Widespread volcanism accompanied this extensional tectonism in three major episodes: late Eocene to middle-late Oligocene, early to middle Miocene, and post-late-middle Miocene.

Isotopic studies by Kistler and Peterman (1978), Farmer and DePaolo (1983), and Kistler (1983) suggest that the Precambrian basement is present beneath the area studied and extends as far west as central Nevada (fig. 1). Overlying this basement are the Paleozoic carbonate rocks of the continental shelf and the allochthonous rocks.

Paleozoic rocks are the hosts for the vast majority of the sediment-hosted gold-silver deposits of the region. Other epithermal deposit types are hosted in volcanogenic sedimentary and volcanic rocks or are associated with plutonism.

DEPOSITS SAMPLED

Several types of deposits were sampled. These included carbonate-hosted gold-silver, hot-spring mercury, hot-spring gold-silver, hot-spring manganese-tungsten, and epithermal gold. The terminology follows that of Cox and Singer (1986).

Carbonate-hosted gold-silver deposits, also known as sediment-hosted disseminated gold, Carlin-type, or invisible gold, contain assemblages of native gold$\pm$ arsenic-bearing pyrite$\pm$barite$\pm$stibnite$\pm$realgar$\pm$orpiment $\pm$arsenopyrite$\pm$cinnabar$\pm$fluorite and are usually associated with silicification. These minerals, together with silica, selectively replace thin-bedded silty or argillaceous, and sometimes carbonaceous, limestone or dolostones (Bagby and Berger, 1985; Berger, 1985; Tooker, 1985; Madrid and Bagby, 1986a). Such deposits are of high tonnage (median=5.1 million metric tons) and relatively low-grade gold compared to other types (median = 2.5 g/t) with gold-to-silver ratios generally greater than 1 (Bagby, 1984; Bagby and Berger, 1985). The sediment-hosted gold deposits appear to have formed between the late Cretaceous and the inception of Basin and Range faulting during the Miocene (Madrid and Bagby, 1986b). Data suggest that perhaps they were formed primarily during the Oligocene, but more absolute dates are needed to narrowly constrain the episode of mineralization. Structural relations associated with sediment-hosted deposits indicate that mineralization is spatially associated with high-angle normal faulting.

Hot-spring mercury deposits contain assemblages of cinnabar$\pm$native mercury$\pm$pyrite$\pm$minor marcasite that are disseminated in, and on, fractures in siliceous sinters and associated breccias of fossil hot-springs systems. They have a median tonnage of 9,500 metric tons (Rytuba, 1986). These deposits generally occur in Miocene and post-Miocene rocks and are associated in part with volcanism.

Gold resources that range from about 200 to over 300 million grams (300 t) and with ore that grades 1 to 15 g/t gold occur in hot-spring gold-silver deposits (Tooker, 1985). These deposits consist of assemblages of native gold $\pm$pyrite$\pm$stibnite$\pm$realgar, or arsenopyrite$\pm$sphalerite$\pm$ chalcopyrite$\pm$fluorite, or silver-selenide, or telluride$\pm$ pyrite in crustified banded veins, stockworks, breccias, or disseminated in subaerial rhyolitic to andesitic volcanic centers. They are related to shallow geothermal systems (Berger, 1985).

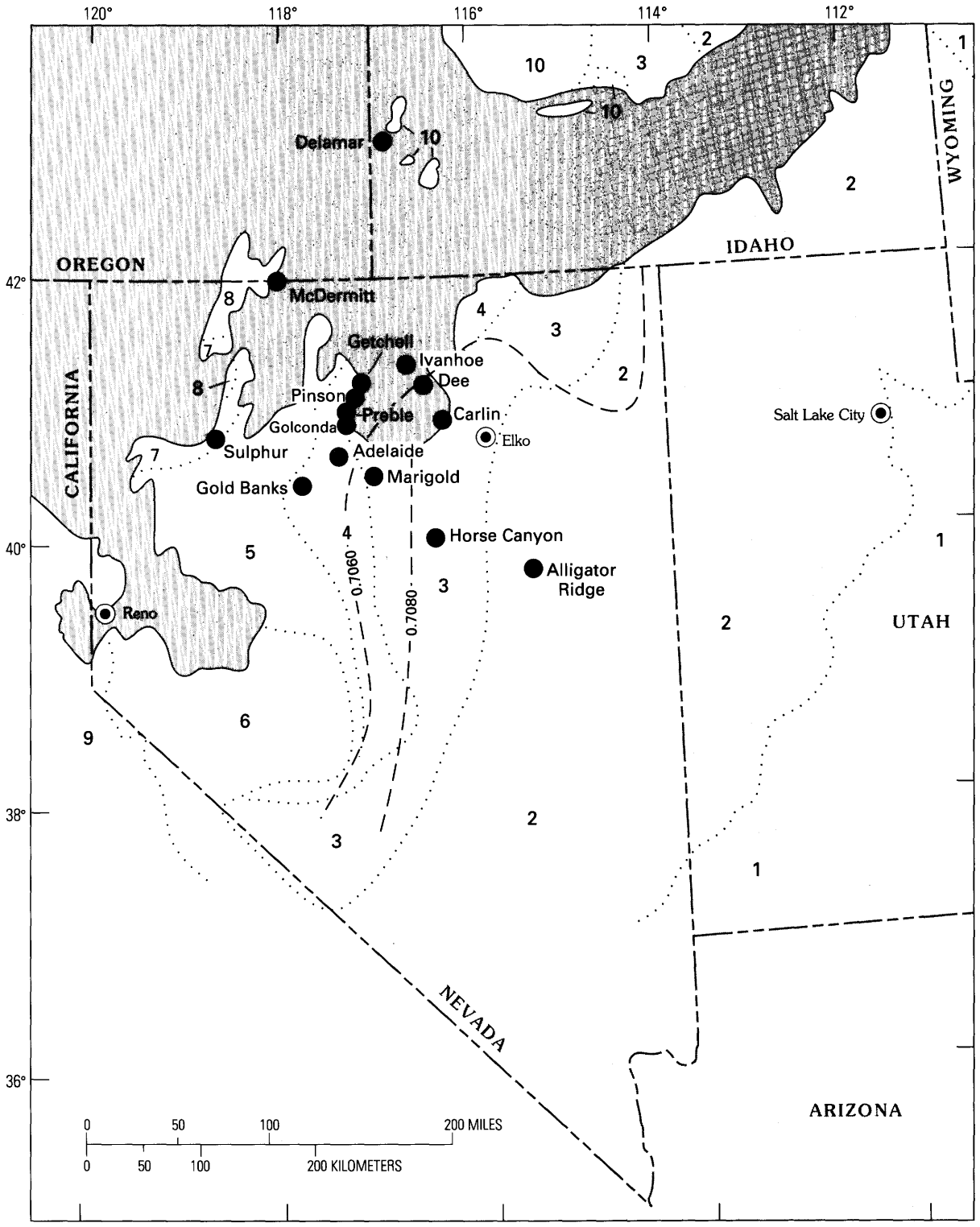

Figure 1. Locations of deposits (solid circles) in Nevada and adjacent parts of neighboring States from which rocks were analyzed for platinum, palladium, and rhodium; geologic host terranes; and inferred Precambrian basement. Terranes (separated by dotted lines) after Silberling and others (1984) are (1) cratons, (2) miogeoclinal cratonal shelf, (3) Roberts Mountains, (4) Golconda, (5) Mesozoic overlap, (6) Walker Lane, (7) Jackson, (8) Black Rocks, (9) Sierra Nevada batholith, and (10) Idaho batholith. Shaded ares is postaccretion volcanic cover; dashed lines are 0.7060 and 0.7080 initial strontium lines from Kistler (1983) and Farmer and DePaolo (1983), respectively.

The term "epithermal gold deposit type" is used here in a broad sense to include assemblages of native gold, precious-metal-bearing tellurides and sulfosalts, and base-metal sulfides. These assemblages are present in vuggy quartz veins and breccias within zones of argillic and silicic alteration that are related to felsic to intermediate volcanic rocks.

ANALYTICAL TECHNIQUES

Rock samples were collected as grab samples from outcrops that represent ore and unmineralized rocks. The samples are probably not as representative of a larger mass as would be other types of samples, such as channel samples, concentrates, or tailings. Sample locations and descriptions are given in table 1.

The samples were analyzed for platinum, palladium, and rhodium by using a fire-assay preconcentration with gold wire extraction (Haffty and others, 1977) followed by a graphite furnace atomic absorption technique (Simon and others, 1978; Page and others, 1980). The samples were analyzed in two groups. Detection limits for one group were 0.5, 1.0, and 0.5 ppb for palladium, platinum, and rhodium, respectively. For the other group, detection limits were 1, 10, and 1 ppb for palladium, platinum, and rhodium, respectively. At the 1-ppb level, precision is about ±30 percent for platinum, and at the 0.5-ppb level, precision is ±20 percent and 50 percent for palladium and rhodium, respectively. Samples, except those from the Preble deposit, were analyzed for gold, arsenic, and antimony by atomic absorption techniques. The method of O'Leary and Meier (1984) was used for gold and has a lower limit of detection of 0.05 ppm; modifications of Viets's (1978) technique were used for arsenic and antimony with lower limits of detection of 5 and 2 ppm, respectively. Mercury was analyzed by a thermally released mercury-gold amalgam/atomic absorption method modified from Vaughn and McCarthy (1964) and McNerney and others (1972) and has detection limits of 0.02 ppm. The samples from the Preble deposit were analyzed by quantitative emission spectroscopy with lower limits of detection of 0.1 or 0.2 and 1 or 2 ppm for gold and arsenic, antimony, and mercury, respectively. The limit of detection depends on how carefully the plates are read.

Table 1 presents the results. Rhodium was detected only in one sample and therefore is not reported in table 1. Iridium and ruthenium were analyzed in samples having prefixes 84BM by a fire-assay spectrographic technique (Haffty and others, 1980) with detection limits of 20 and 100 ppb for iridium and ruthenium, respectively. Iridium and ruthenium were not detected in any of the samples.

DISCUSSION OF RESULTS

Platinum-Group-Element Occurrences and Resources

During mining for gold from deposits in the area under consideration, samples are not commonly analyzed for platinum-group elements. Thus, as a resource, the potential for the various platinum-group elements is virtually unknown for the deposit types sampled for this report. The concentrations of palladium and platinum reported in table 1 for the rock samples are not high; however, very few of these samples represent the higher grade gold ores of the deposits considered. Of the 15 samples analyzed for gold, only 4 contain gold greater than 0.2 ppm (table 1). These four samples also contain palladium in the range of 2.2 to 3.8 ppb, which is high relative to all other samples. If higher grade ore samples are enriched in platinum-group elements, then the potential for those elements as a resource may be significant. The arsenic, antimony, and mercury are common trace elements associated with gold in carbonate-hosted gold deposits. In table 1, high values of palladium and platinum correspond to the higher values of arsenic and mercury. Although the number of samples is insufficient to establish statistical limits and constraints, the rough correspondence suggests that future analyses should also include rocks containing these gold-associated elements.

Detailed sampling across the major gold orebodies of each of these deposit types will be necessary to establish abundances of the platinum-group elements for resource assessment. Table 2 summarizes the palladium and platinum data now available in the deposit types sampled. The numbers of samples with detectable concentrations of palladium and platinum are limited; however, they indicate that these elements are present in the gold and mercury epithermal environments. The samples from the Preble deposit (table 1) were collected from a wide area relative to the orebody. Emphasis was placed on those samples that displayed various degrees of hydrothermal alteration, and these show consistent PGE values. Table 3 summarizes concentration data for palladium and platinum in carbonate-hosted hot-spring deposits. These data are heavily biased by the amount of information from the Preble deposit (table 1). Only a few background rock samples were analyzed for platinum-group elements, and they appear to display average PGE concentrations slightly lower than concentrations for the altered rocks. Therefore, a systematic sampling program of the unaltered host rocks of the orebodies should be conducted to establish threshold values for PGE in ore and to assess the background values of the host rocks.

Table 1. Platinum and palladium analyses of rocks from hydrothermal deposits in Nevada, Oregon, and Idaho

[Locations are shown on figure 1. Rhodium was analyzed in all samples but was not detected at 0.5 ppb except in samples as noted. Analysts: C. Gent for Pt, Pd, and Rh by fire assay-atomic absorption; Chris Heropoulous for Au, As, Sb, and Hg by emission spectrograph; Randy Hill for Au, As, Sb, and Hg by atomic absorption. *, contains 1 ppb Rh]

Sample	Location	Pd (ppb)	Pt (ppb)	Au (ppm)	As (ppm)	Sb (ppm)	Hg (ppm)	Lithology and description
Carbonate-hosted gold-silver deposits								
*84ARM 1	Alligator Ridge	5	<1					Altered shale with disseminated gold.
84ARM 2	do.	<1	<2					Carbonaceous shale.
4CA001C	Carlin	2.2	1					Surface massive jasperoid west ore zone.
CA003A	do.	2.0	<1					Arsenical carbonaceous ore.
CA004B	do.	.6	<1					Jasperoid, east wall of main pit.
CAR830B	do.	.5	<1					Limestone, fresh Roberts Mountains Formation.
4CA002C	do.	2.8	3					Dike in northwest structure, south wall of main pit.
BCB305	Dee	3.2	<1	3	130	66	0.34	Silicified siltstone.
4DE007A	do.	<.5	<1					Silicified, brecciated, veined siltstone.
BC8302	do.	<.5	<1	.2	50	92	.48	Silicified ore-grade rock.
4DE003A	do.	4.8	1					Dike, andesitic.
19MAU83	Getchell	4	<10					Carbonaceous ore.
GE001B	do.	1.4	<1					Quartz vein in Osgood Pluton.
GEDD4A	do.	.6	<1					Dike, andesitic.
OP001A	do.	.6	<1					Fresh granodiorite.
OP001A	do.	.8	<1					Vein quartz in Osgood Pluton.
16MAU83	Pinson	5	<10					Gold ore.
PN8302	do.	3.6	1	2.9	1,800	110	80	A zone jasperoid.
PN003B	do.	1.4	<1					Altered silty bed near dike.
25MAU83	Preble	1	<10					Jasperoid breccia.
PS1017–4	do.	1.8	1					Jasperoid with some calcite.
4PRO10C	do.	1	<1	<.2	40	53	<2	Jasperoid.
4PRO14D	do.	.4	<1					Do.
4PRO24B	do.	2.4	1	<.1	30	3	1.5	Do.
4PRO15D	do.	2.0	1					Do.
4PR022B	do.	.8	1	<.2	2.4	<2	<2	Limestone, unaltered.
RM-17A	do.	1.6	<1	<.2	6.3	<2	<2	Limestone.
RM-12A	do.	2.6	3					Dolomitized limestone.
4PRO15A	do.	2.2	<1					Dolomite vein.
4PRO21A	do.	1.1	4	<.2	25	44	<2	Carbonaceous phyllite, weakly altered.
4PR016A	do.	1.3	1	<.2	2.2	<2	<2	Phyllite, unaltered
RM 13B	do.	2.8	<1					Clay-altered phyllite.
4PRO14G	do.	2.6	<1	<.1	70	70	20	Do.
4PRO12A	do.	2.2	<1	1.5	70	70	20	Silicified phyllite.
RM-15	do.	1.6	<1					100 percent clay-altered phyllite.
P-001A	do.	1.4	1					Stockwork quartz veins.
4PRO14E	do.	1.4	<1	<.1	100	10	2	Quartz vein.
4PRO12C	do.	3.8	2	1	150	70	10	Do.
4PRO12N	do.	.6	<1	<.1	30	1.5	1	Do.
4PRO16B	do.	.6	<1	<.1	<1	<1	<1	Quartz vein, metamorphic.
RM-8A	do.	1	<1					Quartz veins in fault zone.
PR003A	do.	1.2	<1					Altered intermediate compositions dike.
84BM15	Horse Canyon	<.5	<1					Limestone.
84BM16	do.	<.5	<1					Dike rock with sulfides.
84BM1	Ten Mile	<.5	<1					Altered siltstone with sulfides.
Hot-spring gold-silver deposits								
6MAU83	Delamar	<1	<10					Altered porphyritic rhyolite.
7MAU83	do.	<1	<10					Do.
8MAU83	do.	<1	<10					Altered vitrophyre.
12MAU83	do.	<1	<10					Altered porphyritic rhyolite.
13MAU83	do.	<1	<10					Volcanic breccia.

Table 1. Platinum and palladium analyses of rocks from hydrothermal deposits in Nevada, Oregon, and Idaho—Continued

Sample	Location	Pd (ppb)	Pt (ppb)	Au (ppm)	As (ppm)	Sb (ppm)	Hg (ppm)	Lithology and description
Hot-spring gold-silver deposits—Continued								
84BM25	Ivanhoe district	<.5	<1					Mineralized tuff.
84BM26	do.	<.5	<1					Mineralized basalt.
84BM27	do.	<.5	<1					Do.
84BM28	do.	<.5	<1					Mineralized sinter.
2MAU83	Sulfur	<1	23					Chalcedonic sinter.
Epithermal gold deposits								
84BM3	Adelaide	<.5	<1					Sinter.
84BM4	do.	2.0	2.0					Altered rock.
84BM5	do.	.9	3.0					Dolomite.
84BM22	Marigold mine	1.6	<1					Mineralized veins.
Hot spring mercury deposits								
84BM7	Gold Banks	2.7	<1					Altered sedimentary rock.
84BM8	do.	.5	<1					Mineralized sinter.
3MAU83	McDermitt	2.0	13					Cinnabar ore.
4MAU83	do.	<1	16					Tailings from retorted mercury ore.
Hot-spring manganese-tungsten deposits								
20MAU83	Golconda	<1	<10					Manganese-rich sinter.

Table 2. Summary of palladium and platinum analyses in rocks from five types of gold deposits

[$\bar{X}$=average; σ=standard deviation; n=number of samples above detection limits; n.a.=not applicable]

Element deposit type	Palladium, ppb			Platinum, ppb		
	$\bar{x}$	σ	n	$\bar{x}$	σ	n
Carbonate-hosted Au-Ag	1.93	1.28	40	1.57	1.02	14
Hot-spring Au-Ag	<1	n.a.	0	23	n.a.	1
Epithermal Au	1.50	n.a.	3	2.5	n.a.	2
Hot-springs Hg	1.73	n.a.	3	14.5	n.a.	2
Hot-springs Mn-W	<1	n.a.	0	<10	n.a.	0

Table 3. Summary of palladium and platinum analyses of various rocks from carbonate-hosted gold-silver deposits

[$\bar{X}$=average; σ=standard deviation; n=number of samples above detection limit; n.a.=not applicable]

Element rock type	Palladium, ppb			Platinum, ppb		
	$\bar{x}$	σ	n	$\bar{x}$	σ	n
Ore	4.0	1.41	4	<1	n.a.	0
Jasperoid	1.67	1.02	9	1	n.a.	5
Quartz veins	1.35	1.04	8	1.33	n.a.	3
Granitic rocks and dikes	1.8	2.02	4	2.0	n.a.	2
Altered and unaltered siltstones, shales, phyllites	2.03	.78	8	2.5	n.a.	2
Limestone and dolomite	1.54	.89	5	2.0	n.a.	2

Relations of Platinum-Group Elements to the Origin of the Deposit Types

Igneous activity may serve as a source of metals, as a heat source for the development of ore deposits, and perhaps as the responsible agent for the formation of structures along which many deposits are formed. For most of the deposit types presented here, igneous activity has been invoked to explain the presence of the gold and associated elements, even though no clear links have been established. Certainly, there appears to be some relation between igneous activity and the formation of the hot-spring, epithermal, and carbonate-hosted deposit types. There is oxygen isotopic evidence (Taylor, 1979; Radtke and others, 1980) that demonstrates that the waters associated with the ore stage in most epithermal and carbonate-hosted deposits may have been predominantly meteoric. Despite this, buried plutons at depth are commonly invoked to explain both the heat source and the source of the metals and fluids for all epithermal types. It is clear, however, that cause and effect for the source fluids is not well documented and that faulting alone may penetrate sufficiently hot reservoirs at depth, without invoking directly related plutonism.

The depth of penetration of the faults associated with gold deposits in the study area is not well known, but a depth of 11 to 14 km may be a common penetration depth for most high-angle normal faults in the region. These depths are great enough so that tapping of rocks heated by the prevailing geothermal gradient is possible, particularly in this area where the continental crust is thin. Fluids that circulated within these deep fault zones may have affected the complete stratigraphic section. The rock types so affected potentially range from Precambrian basement to

those presently exposed at the surface in the region. Presently, most of the large, sediment-hosted gold-silver deposits are hosted by Paleozoic rocks that were derived from, and overlie, a common Precambrian basement.

The samples in table 1 display values that, with some exceptions (those for Sulfur and McDermitt), show a limited overall range. This result is surprising, inasmuch as the samples span a wide range in compositions, ages, and alteration and the ages of mineralization for the deposits span a considerable time period. Thus, this result may reflect a consistent overall background value for platinum-group elements in the host rocks, a common source for the platinum-group elements, or common factors in the fluid compositions that affected the host rocks. The range in values may also be an artifact of the sampling without proper geologic context. PGE contents seem to be independent of rock type. Correlation of PGE and gold-arsenic contents suggests that both are dependent on the intensity of hydrothermal activity or on the composition of the hydrothermal fluids.

Page and Talkington (1984) defined differences in the patterns of PGE occurrence relative to their occurrence in chondrite. Relative enrichments of palladium, platinum, and rhodium reflect their mantle source rock. This relation could have been used to establish sources for the platinum-group elements found associated with the gold deposits of this study had the samples contained high enough PGE concentrations to adequately depict the necessary source-dependent PGE patterns.

REFERENCES CITED

Antweiler, J.C., and Campbell, W.L., 1982, Implications of the compositions of lode and placer gold, *in* Theodore, T.G., Blair, W.N., and Nash, J.T., eds., Preliminary report on the geology and gold mineralization of the Gold Basin-Lost Basin Mining districts, Mohave County, Arizona: U.S. Geological Survey Open-File Report 85–1052, p. 245–263.

Bagby, W.C., 1984, Sediment-hosted disseminated gold deposits in Nevada—A review of their geologic characteristics [abs.]: Geological Society of America Abstracts with Programs, v. 16, no. 6, p. 434.

Bagby, W.C., and Berger, B.R., 1985, Geologic characteristics of sediment-hosted, disseminated precious-metal deposits in the western United States, *in* Berger, B.R., and Bethke, P.M., eds., Geology and geochemistry of epithermal systems: Reviews in Economic Geology, Society of Economic Geologists, v. 2, p. 169–202.

Berger, B.R., 1985, Geologic-geochemical features of hot-spring precious-metal deposits, *in* Tooker, E.W., ed., Geologic characteristics of sediment- and volcanic-hosted disseminated gold deposits—Search for an occurrence model: U.S. Geological Survey Bulletin 1646, p. 47–53.

Blair, W.N., Page, N.J, and Johnson, M.G., 1977, Map and list of reported occurrences of platinum-group metals in the continental United States: U.S. Geological Survey Miscellaneous Field Studies Map MF–861, scale 1:5,000,000, 2 sheets.

Carlson, R.R., Venuti, P.E., Page, N.J, and Theodore, T.G., 1976, Descriptions and chemical analyses of rocks and soils analyzed for platinum-group metals from the Iron Canyon area, Lander County, Nevada: U.S. Geological Survey Open-File Report 76–524, 32 p.

Cox, D.P., and Singer, D.A., eds., 1986, Mineral deposit models: U.S. Geological Survey Bulletin 1693, 379 p.

Dayton, S.H., and Sassos, M.P., 1985, Carajas, a new district, new mines and a big future: Engineering and Mining Journal, v. 186, no. 11, p. 24–31.

Engineering and Mining Journal, 1986, In Latin America, Brazil, Serra Pelada: Engineering and Mining Journal, v. 187, no. 1, p. 56.

Farmer, G.L., and DePaolo, D.J., 1983, Origin of Mesozoic and Tertiary granite in the Western United States and implications for pre-Mesozoic crustal structure, pt. 1, Nd and Sr isotopic studies in the geocline of the northern Great Basin: Journal of Geophysical Research, v. 88, no. B4, p. 3379–3401.

Haffty, Joseph, Haubert, A.W., and Page, N.J, 1980, Determination of iridium and ruthenium in geological samples by fire assay and emission spectrograph: U.S. Geological Survey Professional Paper 1129–A–I, p. G1–G4.

Haffty, Joseph, Riley, L.B., and Goss, W.D., 1977, A manual on fire assaying and determination of the noble metals in geological materials: U.S. Geological Survey Bulletin 1445, 58 p.

Kistler, R.W., 1983, Isotope geochemistry of plutons in the northern Great Basins, *in* The role of heat in the development of energy and mineral resources in the northern Basin and Range Province: Geothermal Resources Council Special Report, No. 13, 383 p.

Kistler, R.W., and Peterman, Z.E., 1978, Reconstruction of crustal blocks of California on the basis of initial strontium isotopic compositions of Mesozoic granitic rocks: U.S. Geological Survey Professional Paper 1071, 17 p.

Madrid, R.J., and Bagby, W.C., 1986a, Vein paragenesis in selected sediment-hosted gold deposits in north-central Nevada: Geological Society of America Abstracts with Programs, v. 18, no. 5, p. 393.

———1986b, Structural alignment of sediment-hosted gold deposits in north-central Nevada: An example of inherited fabrics: Geological Society of America Abstracts with Programs, v. 18, no. 5, p. 394.

McNerney, J.J., Buseck, P.R., and Hanson, R.C., 1972, Mercury detection by means of thin gold film: Science, v. 178, p. 611–612.

Mertie, J.B., Jr., 1969, Economic geology of the platinum metals: U.S. Geological Survey Professional Paper 630, 120 p.

Miller, E.L., Holdsworth, B.K., Whiteford, W.B., and Rodgers, D., 1984, Stratigraphy and structure of the Schoonover sequence, northeastern Nevada: Implication for Paleozoic plate-margin tectonics: Geological Society of America Bulletin, v. 95, p. 1063–1076.

O'Leary, R.M., and Meier, A.L., 1984, Analytical methods used in geochemical exploration: U.S. Geological Survey Circular 948, p. 51–55.

Page, N.J, Myers, J.S., Haffty, Joseph, Simon, F.O., and Aruscavage, P.J., 1980, Platinum, palladium, and rhodium in the Fiskenaesset complex, southwestern Greenland: Economic Geology, v. 75, no. 6, p. 907–915.

Page, N.J, and Talkington, R.W., 1984, Palladium, platinum, rhodium, ruthenium and iridium in peridotites and chromitites from ophiolite complexes in Newfoundland: Canadian Mineralogist, v. 22, p. 137–149.

Page, N.J, Theodore, T.G., and Venuti, P.E., 1978, Implications of the petrochemistry of palladium at Iron Canyon, Lander County, Nevada: U.S. Geological Survey Journal of Research, v. 6, no. 1, p. 107–114.

Poole, F.G., and Sandberg, C.A., 1977, Mississippian paleogeography and tectonics of the western United States, *in* Stewart, J.H., Stevens, C.H., and Fritsche, A.E., eds., Paleozoic Paleogeography Symposium 1: Society of Economic Paleontologists and Mineralogists, Pacific Section, Symposium 1, p. 67–85.

Quiring, H., 1962, Die Metallischen Rohstoffe, ihre Lagerungsverhältnisse und ihre wirtschaftliche Bedeutung—Platinmetalle: Stuttgart, Ferdinand Enke, v. 16, 288 p.

Radtke, A.S., Rye, R.O., and Dickson, F.W., 1980, Geology and stable isotope studies of the Carlin gold deposit, Nevada: Economic Geology, v. 75, no. 5, p. 641–672.

Roberts, R.J., Hotz, P.E., Gilluly, James, and Ferguson, H.G., 1958, Paleozoic rocks of north-central Nevada: American Association of Petroleum Geologists Bulletin, v. 42, no. 12, p. 2813–2857.

Rytuba, J.J., 1986, Descriptive model of hot-spring Hg, *in* Cox, D.P., and Singer, D.A., eds., Mineral deposit models: U.S. Geological Survey Bulletin 1693, p. 178.

Silberling, N.J., Jones, D.L., Blake, M.C., Jr., and Howell, D.G., 1984, Part C—Lithotectonic terrane map of the western conterminous United States, *in* Silberling, N.J., and Jones, D.L., eds., Lithotectonic terrane maps of the North American Cordillera: U.S. Geological Survey Open-file Report 84–523, p. C1–C43.

Simon, F.O., Aruscavage, P.J., and Moore, R., 1978, Determination of platinum, palladium, and rhodium in geologic spectroscopy using electrothermal atomization [abs.]: American Chemical Society National Meeting, 176th, Miami Beach, Fla., September 11–14, 1978.

Stewart, J.H., 1984, Geology of Nevada: Nevada Bureau of Mines Special Publication 4, 136 p.

Taylor, H.P., 1979, Oxygen and hydrogen isotope relationships in hydrothermal mineral deposits, *in* Barnes, H.L., ed., Geochemistry of hydrothermal ore deposits: New York, Wiley-Interscience, p. 236–277.

Theodore, T.G., and Blake, D.W., 1975, Geology and geochemistry of the Copper Canyon porphyry copper deposit and surrounding area, Lander County, Nevada: U.S. Geological Survey Professional Paper 798–B, 86 p.

Theodore, T.G., and Roberts, R.J., 1971, Geochemistry and geology of deep drill holes at Iron Canyon, Lander County, Nevada, *with a section on* Geophysical logs of drill hole DDH–2 *by* C.J. Zablocki: U.S. Geological Survey Bulletin 1318, 32 p.

Theodore, T.G., Venuti, P.E., Page, N.J, and Carlson, R.R., 1976, Maps showing geochemical distribution of palladium and other elements in rocks at Iron Canyon, Lander County, Nevada: U.S. Geological Survey Miscellaneous Field Studies Map MF–790.

Tooker, E.W., ed., 1985, Geologic characteristics of sediment- and volcanic-hosted disseminated gold deposits—Search for an occurrence model: U.S. Geological Survey Bulletin 1646, 150 p.

Vaughn, W.W., and McCarthy, J.H., Jr., 1964, An instrumental technique for the determination of submicrogram concentrations of mercury in soils, rocks and gas, *in* Geological Survey Research 1964: U.S. Geological Survey Professional Paper 501–D, p. D123–D127.

Viets, J.G., 1978, Determination of silver, bismuth, cadmium, copper, lead, and zinc in geologic materials by atomic absorption spectrometry with tricaphylylmethyl ammonium chloride: Analytical Chemistry, v. 50, p. 1097–1101.

Chapter H

Sand and Gravel—An Enormous Offshore Resource within the U.S. Exclusive Economic Zone

By S. JEFFRESS WILLIAMS

U.S. GEOLOGICAL SURVEY BULLETIN 1877

CONTRIBUTIONS TO COMMODITY GEOLOGY RESEARCH

CONTENTS

FIGURES

TABLE

Sand and Gravel—An Enormous Offshore Resource within the U.S. Exclusive Economic Zone

By S. Jeffress Williams

Abstract

The U.S. Geological Survey (USGS), in collaboration with other Federal and State agencies and academic groups, is actively conducting geologic and geophysical studies in continental margin areas within the Exclusive Economic Zone (EEZ) of the United States. Some of the USGS projects have as objectives the location and evaluation of marine sand and gravel resources and the interpretation of the origins of the deposits. Results from these studies show that many extremely large deposits are located close to expanding metropolitan areas, which have a need for aggregate materials for construction, and near developed coastal areas, where beach replenishment may be used to mitigate coastal erosion. Offshore deposits are likely to be commercially mined when conventional deposits onshore are depleted or are no longer available because of land-use and environmental limitations. The latest estimates of onshore and offshore resources compared with the annual sand and gravel consumption in the United States suggest that anticipated national needs can be easily satisfied for the foreseeable future.

The Nation's largest offshore sand and gravel deposits are found on the Atlantic continental margin and offshore Alaska, because these regions have large continental shelf areas that were affected by glacial processes and sea-level fluctuations that favor deposition and preservation of large sand bodies. Sand and limited volumes of gravel are also present on the U.S. Pacific Continental Shelf and on the narrow insular shelves around the Hawaiian Islands, Puerto Rico, and the U.S. Virgin Islands. Sand is also present throughout much of the Gulf of Mexico, but it is nearshore and tends to be fine grained and often mixed with muddy or organic detritus as well as carbonate shell material.

INTRODUCTION

The stability and economic well-being of the United States are dependent to a large degree on the mineral resources contained within its boundaries or available from reliable foreign sources. Although the Nation is self-sufficient in many minerals, much attention has focused recently on shortages and the uncertain supply of some strategic or critical minerals.

In 1983, Presidential declaration of an Exclusive Economic Zone (EEZ) around the United States and its territories and possessions established the Nation's sovereign right to explore, conserve, and manage all resources within the EEZ, an area extending seaward 200 nautical miles around all the coasts. The EEZ proclamation more than doubled the national domain by adding over 3 billion acres (figs. 1 and 2) of submerged continental margin (Ballard and Bischoff, 1984) to the U.S. territorial area.

The economically important resources identified within the EEZ include fisheries, oil and gas, and metallic and nonmetallic minerals. Recent new scientific discoveries of metallic minerals at deep-ocean plate boundaries in the Atlantic and Pacific Oceans have directed attention to the potential of all marine minerals. Sand and gravel, however, probably constitute the most widespread and immediately useful nonenergy mineral resource contained in offshore areas (Emery and Uchupi, 1984; McKelvey, 1986).

In general, onshore sand and gravel resources are still plentiful across the conterminous United States, and average unit prices are less than $5 per ton; however, metropolitan areas such as Boston, New York, Los Angeles, San Francisco, San Juan, and Honolulu are already experiencing shortages in local supply and a resulting increase in cost. For example, prices in the New York metropolitan area can reach $25 per ton, and a recent U.S. Bureau of Mines (1987) report states that both New York City and Boston, Mass., have immediate potential as markets for development of offshore mining of sand and gravel resources. Because transportation is a primary component in the price of sand and gravel, the use of marine sand and gravel is becoming increasingly attractive to cities having port facilities. Barge transport is often considerably less expensive and less disruptive than rail or truck haul, and offshore mining may offer land-use and environmental advantages over onshore mining (Williams, 1986).

Several foreign nations such as the United Kingdom, the Netherlands, Denmark, and Japan already have well-established marine-mining industries and derive nearly 20 percent of their sand and gravel requirements from nearshore mining. The Dutch, in particular, have a highly

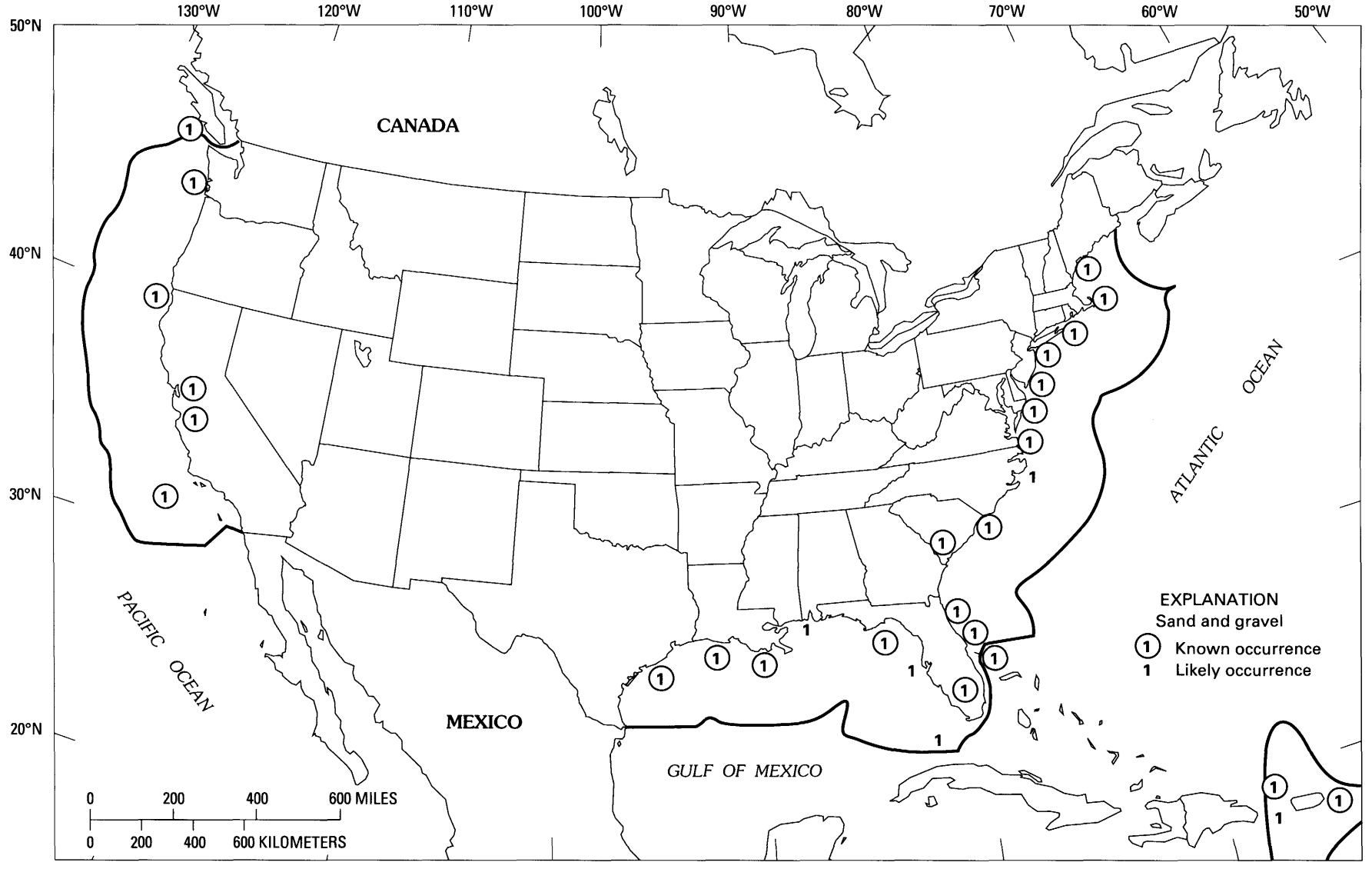

Figure 1. Occurrence of marine sand and gravel in the Exclusive Economic Zone for the conterminous United States (modified from Williams, 1986).

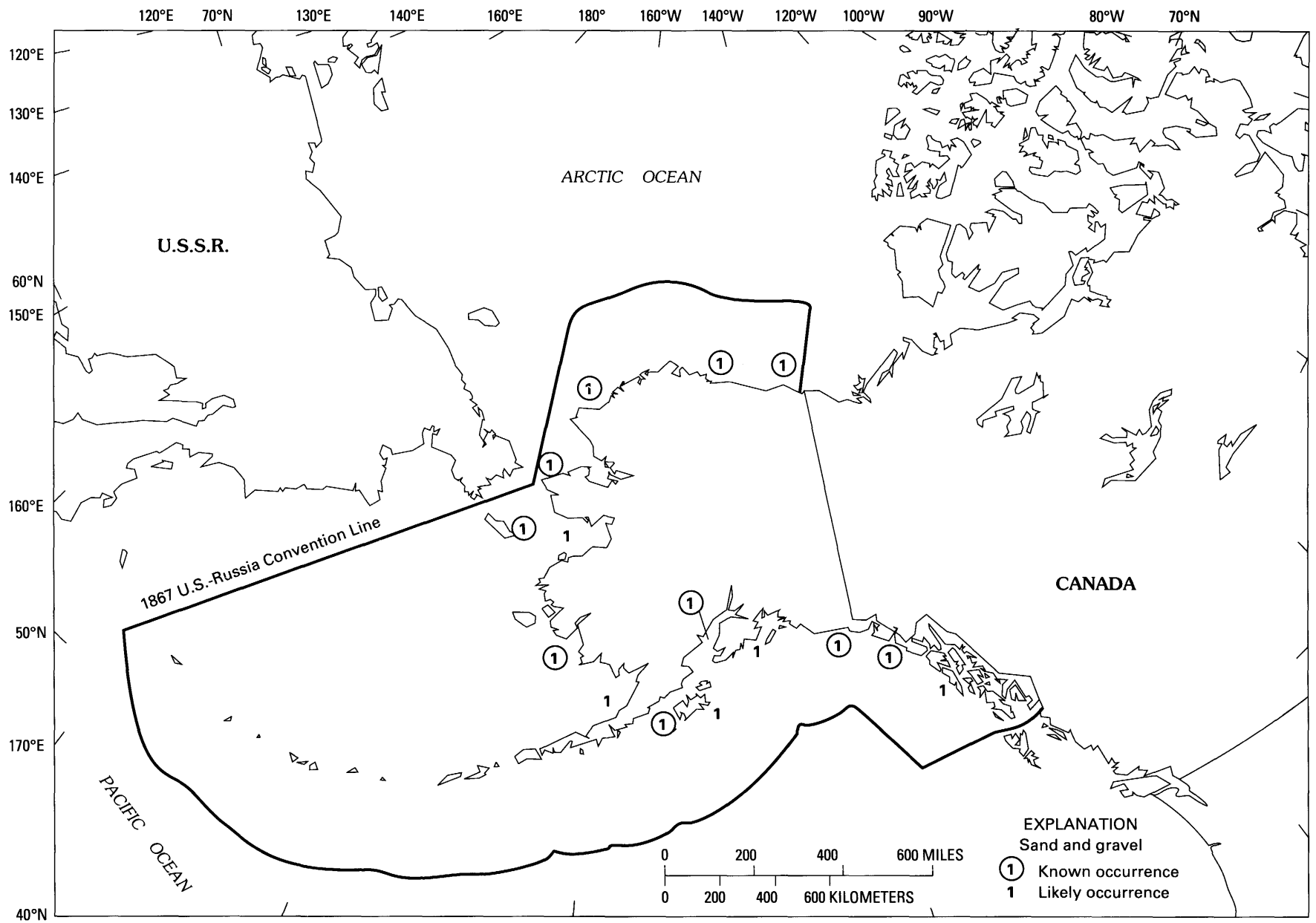

Figure 2. Occurrence of marine sand and gravel in the Exclusive Economic Zone for Alaska (modified from Williams, 1986).

developed dredging technology to operate in the North Sea. Today, commercial viability of large-scale dredging worldwide appears to be restricted to water depths of less than approximately 40 m (Cruickshank and Hess, 1975) and maximum economic haul distances of approximately 150 km, although distances can be greater depending upon the local factors affecting the cost of barge transport (Manheim and Hess, 1981; U.S. Bureau of Mines, 1987).

The practical limit for sand and gravel resource assessments is the continental shelf edge, nominally at 200-m depths. However, current dredging technology and economics further concentrate the focus on sand and gravel resources to inner shelf regions landward of about 40-m depths (Williams, 1986). This region will be the major focus of this paper. Descriptions of specific areas are based on resource studies completed. Other areas not mentioned have not been studied in sufficient detail, but future exploration is likely to show that they contain sizable resources as well.

GRADES AND SPECIFICATIONS

The terms "sand" and "gravel" denote grain-size classes of granular sediments that often occur together in the same deposit but in highly variable proportions due to the processes of formation, transport, and deposition. Both sand and gravel are composed of diverse rock types; however, the major constituent is quartz, with secondary amounts of feldspar, iron oxides, and heavy minerals. According to the widely used Udden-Wentworth classification, sand is material between 0.63 and 2 mm (4 to -1 phi units), retained on a No. 230 sieve. Gravel is material in the range of 2 mm to 64 mm. Sand and gravel used as aggregate in concrete for construction and road building often have very specific grain size, sorting, shape, and chemical characteristics (Tepordei, 1987).

Selection of sand used as fill for beach replenishment and restoration is dependent upon the physical properties of the native beach sediments and on the intended use of the beach after fill operations are completed (Duane, 1969). Ideally, the borrow material should be similar in grain size, sorting, and composition to the native sediments. Matching the composition of the native beach with borrow sand is also important. Sands having a large proportion of calcium carbonate fragments are likely to be broken and abraded relatively quickly if placed on high-energy quartz beaches.

PRESENT AND FUTURE USES

Prior to the buildup of metropolitan areas and the construction of concrete road systems, demand for sand and gravel was limited, and mining and production were small. However, steadily increasing requirements for large volumes have made sand and gravel the third largest (behind cement and crushed stone) U.S. nonfuel mineral industry. The most recent (1986) U.S. production figures from Tepordei (1987) show that domestic production of construction sand and gravel was 837 million short tons, valued at $2.6 billion. Production of industrial sand and gravel for 1986 totaled 28.5 million tons, valued at $360 million. In terms of marine minerals, even though construction sand and gravel have a low unit price (average $3.20 per ton, Tepordei, 1987), they are the second most valuable marine mineral (behind oil and gas) mined at the seabed (Emery and Uchupi, 1984; McKelvey, 1986).

Most sand and gravel production is from onshore sources and is intended primarily for construction, mainly as aggregate in concrete and as road-base material and earth fill. Lesser amounts are utilized in specialty applications such as glass making, as foundry sand for metal casting, and by the abrasives industry. In Alaska, sand and gravel from onshore and offshore are used to construct islands on which to locate facilities associated with exploration and recovery of hydrocarbons. The islands, which are built in nearshore areas in water depths not exceeding 20 m, enable year-round drilling. To date, approximately 10 million cubic meters of sand and gravel have been mined in the North Slope region for island construction (Molnia, 1979).

Since the early 1950's, use of sand as fill to replenish eroded beaches has become more widespread, both to enhance the recreational assets and to lessen storm damage due to waves and storm-surge flooding (Duane, 1969). More than 40 beach restoration projects in the United States have been completed. The Federal projects alone used more than 59 million m^3 of sand fill. For environmental reasons and to obtain sand of optimum texture at the lowest cost, marine or estuarine sources have been used in most nourishment projects.

Recent scientific evidence suggests that sea level around the world could rise 70 cm in the next 100 years due to climate warming brought on by the buildup of atmospheric carbon dioxide and other gases released as a consequence of human activities (Revelle, 1983). Natural sea-level rise, which has averaged 15 to 20 cm over the past century, is a primary factor in coastal erosion; consequently, these forecasts of accelerated rise for the near future are reason for concern. In coastal areas where engineering solutions are deemed economically feasible, construction of protective beaches and dikes is going to require many millions of tons of fill material. Offshore areas may be a logical source of such large volumes of sand and gravel.

EXPLORATION METHODS AND EQUIPMENT

The procedures for locating and assessing sand and gravel on the seabed generally begin with high-resolution seismic-reflection profiling by use of equipment towed from

survey vessels. Seismic analog records are formed by echos from subbottom strata and are similar to geologic cross sections. These records are useful in determining the subbottom stratigraphy and structure and for mapping buried features such as fluvial and tidal-inlet channels. Another tool, high-resolution sidescan sonar equipment, focuses a broad acoustic beam across a swath of seabed to define the small-scale relief (shoals, bedforms) and variations in seabed texture. The latest of these automated systems include computer-assisted recorders that adjust for the slant-range distortion. These data can be used to produce photolike images of the seabed when sonograms from parallel ship tracks are fit into a mosaic (Williams, 1982).

Grab samples of sea-floor sediment are useful in confirming interpretations from seismic and sidescan sonar data regarding sediment composition and are helpful in identifying promising sites worthy of deeper sampling by cores. Vibratory coring equipment (pneumatic, hydraulic, and electric) is relatively inexpensive to operate and has been used successfully since the early 1960's for recovering long and relatively undisturbed cores of granular sediment. Pneumatic vibracores are limited to water depths of about 100 m, but hydraulic and electric vibracores are more versatile for deep-water sampling and can operate to at least shelf-edge depths (200 m). Cores as long as 6 m are routinely taken, and recovery of 10 to 12 m of sediment can be accomplished by using water-jetting techniques with the vibracore (Meisburger and Williams, 1981).

A variety of electronic positioning equipment is available to accurately determine the horizontal location of bottom and subbottom features detected during the geophysical and sediment-sampling surveys. Microwave systems are desirable for nearshore surveys because of their high (± 3 m) accuracy. For longer range surveys, LORAN-C is widely used, and automated and very accurate global positioning systems are becoming more widely available.

MARINE GEOLOGIC SETTINGS

The occurrence, sedimentary character, and distribution of sand and gravel on the continental shelves are the result of a combination of glaciofluvial, marine, and estuarine processes that affected the continental shelves many times during Pleistocene and Holocene times, periods spanning the past 1.6 million years (Field and Duane, 1976). The following factors from Williams (1986) are major influences on the geologic framework and geomorphologic character of the U.S. continental margin: (1) Four or more major glacial advances in northern latitudes of the Atlantic and Pacific regions transported massive volumes of sediment from continental areas to coastal plain regions, parts of which are now submerged continental shelves. (2) Growth and decay of continental glaciers due to climate change and isostatic adjustments due to glacial loading and unloading have caused worldwide and local fluctuations in sea level in the range of 100 to 150 m. These fluctuations caused repeated transgressions and regressions of the coast across the shelves. (3) Meltwater-enlarged streams and rivers drained glacial terrains and transported large volumes of terrestrial sediment onto exposed shelf areas during Pleistocene sea level lowstands. (4) Tectonic changes, especially along the U.S. Pacific margin, altered land elevations, which affected the gradients of streams and their capacity to transport sediments to the coast and onto the shelf.

Atlantic Province

On the U.S. Atlantic continental margin, the EEZ encompasses very large continental shelf areas as well as portions of the slope and rise (fig. 1). The northern region from Maine to Long Island, N.Y., experienced at least four glacial advances and associated marine transgressions during the Quaternary period. Numerous geologic studies (Schlee and Pratt, 1970; Trumbull, 1972; Schlee, 1973) show that thick sequences of glaciofluvial outwash sand and gravel deposits are present throughout much of the region, resulting in enormous resources estimates (Manheim, 1972). Although sand and gravel may be plentiful, the deposits are likely to vary considerably in textural properties, and muddy sediments are occasionally mixed with or overlie sand and gravel deposits (Schlee, 1973).

Gravel is most abundant north of lat 40° N. To the south, gravel distribution is patchy and limited to areas where exposed ancestral river channels and deltas are subject to marine erosion and winnowing processes. The most promising sand and gravel deposits are associated with glacial depositional features such as moraines, outwash plains, and glaciofluvial deltas (Duane and Stubblefield, 1986). Several moraines and deltas offshore Maine and Massachusetts are described by Oldale and others (1983) and Oldale (1985). High-quality aggregate associated with such glacial landforms has been identified around Massachusetts Bay (Schlee and others, 1973) and Nantucket. Identified resources of offshore sand and gravel (table 1) appear sufficient to supply the New England market well into the future (Manheim and Hess, 1981).

The New York City metropolitan area is one of the major markets for sand and gravel in the United States. Large sand and gravel deposits on the inner shelf and along the south shore of Long Island (Williams and Duane, 1974; Schlee and Sanko, 1975) and in more restricted areas of Long Island Sound (Williams, 1981) have great potential for use as commercial aggregate and as sand fill to replenish the eroded coast along the south shore of Long Island (Williams, 1976). Offshore resources are judged to be in excess of 10 billion m^3 (Williams, 1976), enough to meet

Table 1. Estimates of sand and gravel resources within the U.S. Exclusive Economic Zone

[Modified from Williams,1986]

Province	Volume (cubic meters)
Atlantic	
Maine-Long Island	340 billion
New Jersey-South Carolina	190 billion
South Carolina-Florida	220 billion
Gulf of Mexico	269 billion
Caribbean	
Virgin Islands	46 million
Puerto Rico	170 million
Pacific	
Southern California	30 billion
Northern California-Washington	Insufficient data
Alaska	160 billion
Hawaii	19 billion

the needs of Metropolitan New York for many centuries at current consumption rates. The middle Atlantic Shelf region, from New Jersey to South Carolina, is south of the direct influence of Pleistocene glaciation, but the area received large volumes of clastic terrigenous sediment when sea level was lower and the ancestral Delaware, Susquehanna, Potomac, and Roanoke Rivers had much larger sediment discharges than do their present-day counterparts. The largest sand deposits are present in the relict deltas, located where the rivers intersected paleoshorelines, and in the filled fluvial channels that transect the shelf. The many prominent capes along the coast are regions of abundant sand supply as well, and their associated shoals are promising sites for future exploration.

Linear shoals are common sea-floor features, particularly on the continental shelf off New Jersey and the Delmarva Peninsula. The shoals, which are as much as 10 m thick and hundreds of meters wide, extend for tens of kilometers (Duane and others, 1972). Seismic profiles and cores show most of these shoals are composed of clean medium-to-coarse sand, texturally similar to the onshore beaches they abut (Field, 1980). Some of the shoals may represent relict barrier spits and islands drowned in place by the late Holocene transgression; however, geologic evidence suggests the majority formed in the nearshore region by coastal hydraulic processes reworking existing sand bodies, such as relict deltas and ebb-tide shoals. With sea-level rise, the coast migrates landward, and the shoals become detached from the shoreface (Field and Duane, 1976).

Individual shoals, many containing millions of cubic meters of sand, appear to be highly suitable borrow sources for beach-fill projects. At present, several linear shoals offshore Maryland are being evaluated as sand sources for replenishment of the beaches at Ocean City, Md. (Kerhin and Williams, 1987). With regard to the sand budget of the adjacent coast, the environmental effects of dredging the shoals are cause for concern, but these effects can be minimized if sand is removed from several shoals that are well seaward of the zone of active littoral processes.

Even though more information is available for estimating sand and gravel resources along the Atlantic EEZ than for anywhere else, these resource estimates vary greatly depending upon the assumptions made and the degree of extrapolation from limited, often widely spaced data. Manheim and Hess (1981) have estimated as much as 830 billion m^3 of sand and gravel are present on the shelf based on average thicknesses of 5 m. Current scientific knowledge, however, suggests that the sedimentologic character of the shelf is much more complex. Gravel is limited and patchy in distribution, and sand is widespread, but the greatest thicknesses are found in discrete bodies. North of lat 40° N., thicknesses of sand and gravel may exceed 5 m; however, this thickness is too optimistic an average for other areas. Probably the most reliable estimate of sand and gravel for the Atlantic shelf is 750 billion m^3 (table 1), but this estimate is likely to increase when additional areas are surveyed. Estimates will be further refined as the U.S. Geological Survey and several State Geological Surveys, including those in Maine, Connecticut, Maryland, Virginia, Florida, and Louisiana, complete cooperative studies aimed at evaluating sand and gravel deposits within their respective territorial waters.

Gulf of Mexico

The Gulf of Mexico Continental Shelf from the Florida peninsula to the Mexico border is an enormous area in which little attention has been focused on sand and gravel resources (fig. 1). Like the Atlantic Shelf, the Gulf of Mexico Shelf owes most of its geomorphological character and shallow sedimentary stratigraphy to Quaternary sea-level fluctuations and the resulting transgressions and regressions of the coast. In the central Gulf of Mexico, the Mississippi River has been a dominant influence on the composition and distribution of clastic sediments. Ancestral channels of the Mississippi River have shifted position over time, each channel building large deltaic complexes that are fronted by sandy barrier islands. When the channels change position, the coastal barriers and abandoned deltas erode and migrate landward, leaving blanket-type sand deposits and linear shoals having relief of 5 to 10 m (Berryhill and others, 1985). Among those off Louisiana are the Chandeleur Islands and their associated sand sheet, the Isles Dernieres and associated Ship and Outer Shoals, and Trinity and Tiger Shoals.

Over the past 8 years, the Louisiana Geological Survey has cooperated with the U.S. Geological Survey to carry out geophysical and coring surveys over parts of the Louisiana Shelf to identify and map the geometry of sand bodies. Plans are now underway by the State to use offshore

sand to nourish three different coastal areas to test the effectiveness of constructing beach fills to mitigate the serious erosion and land-loss problems in coastal Louisiana.

Surveys of limited extent in Florida, Louisiana, and Texas, aimed at mapping and characterizing nearshore sand bodies for beach nourishment, have been conducted by the U.S. Army Corps of Engineers over the past decade. These surveys have focused on nearshore areas of St. Petersburg and Panama City, Fla., Grand Isle, La., and Galveston and Corpus Christi, Tex. All but the Galveston coast have been nourished in the decade. Williams and others (1979) identified five potential sites offshore Galveston where relict channels and deltas contain an estimated 63 million m^3 of mostly muddy fine sand, but so far no dredging of material for use in beach replenishment has taken place.

Caribbean Province

Exclusive Economic Zones have also been established for the U.S. Virgin Islands and Puerto Rico. The Virgin Islands and Puerto Rico are part of a volcanic island-arc complex exhibiting narrow insular shelves and abrupt shelf breaks at about 100 m below sea level. Terriginous sediments are most abundant close to shore, where modern and ancient rivers deposited marine deltas. The sediments, which exhibit a reduction in grain size, become mixed with carbonate and organic material away from the river mouths. Both Puerto Rico and the Virgin Islands are experiencing severe shortages of sand and gravel for concrete aggregate as well as sand of suitable texture for replenishment of eroded beaches. In some areas, onshore sources of sand are so limited that the beaches and dunes have been mined. These practices occurred for many years until recently and have altered the esthetic beauty and natural protection of the beach and have aggravated coastal erosion.

In the early 1970's, the beaches of the Virgin Islands were recognized as a valuable natural resource that attracted tourists, and mining along the coast was prohibited. Until 1977, except for illegal sand extraction from the beaches at night, the Virgin Islands' primary sand source was Puerto Rico, where sand from river channels and deltas was mined and shipped at a cost of approximately $\$16/m^3$ (Hubbard and others, 1981). This practice was halted by the Commonwealth when the rivers were recognized as the source for most of the sand on the coast. Once the environmental effects of mining the shore and onland sites were known, both countries began to investigate the feasibility of mining offshore sand bodies.

In the late 1970s, the U.S. Geological Survey conducted surveys to inventory sand on the insular shelves of the U.S. Virgin Islands. Holmes (1978) reports several promising sand prospects and estimated that one sand body off the southwest coast of St. Thomas contains 30 million m^3 of fine sand, and another, a shoal near Buck Island, is calculated to contain 12 million m^3 of sand. Recent surveys offshore St. Croix have identified two major sand bodies on the broad southern shelf (table 1). A site on its eastern shelf contains almost 4 million m^3. Seismic-reflection data suggest that sand thicknesses of 17 m are present over a broad area west of Sand Point (Hubbard and others, 1981); however, long sediment cores are needed in conjunction with the seismic profiles in order to estimate actual sand volumes.

The narrow shelves on all these islands lack large sand bodies, apparently because the dominant coastal processes transport sand offshore into the deeper basins. These processes are aided by several submarine canyons that funnel sand seaward into deep water. Additional seismic and coring surveys are necessary before potential deposits can be evaluated in other parts of the U.S. Virgin Islands. Areas with naturally high biogenic sand productivity may be especially promising for mining, although no studies have been done to determine rates of production of carbonate sands.

Puerto Rico requires about 7 million m^3 of construction sand in addition to the large volumes of fill needed to mitigate beach erosion. Present onshore supplies are very limited. Cooperative efforts by the U.S. Geological Survey and the Department of Natural Resources of Puerto Rico over the past decade have identified three offshore sand bodies in water depths shallower than 16 m (Grove and Trumbull, 1978, and Rodriguez, 1984). The best prospects are off Cabo Rojo on the southwest coast and at the Escollo de Arenas deposit. Their total volume of 170 million m^3 could supply the anticipated need of Puerto Rico for over two decades. Present field surveys are directed at studying the broad insular shelf off eastern Puerto Rico, and preliminary results indicate a high potential for additional large volumes of sand (Rodriguez, 1984).

Pacific Province

The major commercial requirements for sand and gravel in the U.S. Pacific region are in southern California for construction aggregate and fill for beach nourishment; in Alaska, to serve in construction of manmade islands for hydrocarbon exploration and production; and in Hawaii, where shortages are such that local prices for construction-quality sand reach $\$50/m^3$ (Ballard and Bischoff, 1984).

The tectonically active U.S. Pacific margin has a comparatively narrow continental shelf, limiting the deposits recoverable by present dredge technology. The narrowness of the shelf and its unrestricted exposure to Pacific storms result in much larger waves than on the Atlantic or Gulf of Mexico coasts, thereby constricting the periods during which dredges can operate safely.

Geophysical and coring surveys off southern California, summarized by California Department of Boating and Waterways (1983), show that sand, generally fine-grained, and some gravel are present in narrow zones parallel to the coast. Most sand and gravel occur as relict blanket, deltaic, and stream-valley fill deposits in the offshore extensions of some major rivers. Large and economically significant deposits are present on the shelf off San Diego, San Pedro, and Santa Monica (fig. 1). Some of these deposits are of limited extent and occur in basins bounded by bedrock cropping out at the seabed, whereas other deposits are of currently marginal value because of muddy overburden sediments several meters thick. Various studies have yielded estimates of 30 billion m^3 of sand and gravel resources for southern California. However, only about 10 billion m^3 are located within depths of 30 m below sea level, and some of the deposits may be too fine for use as either beach fill or construction sand (California Department of Boating and Waterways, 1983).

The distribution of surficial sediments at the seabed for the rest of the California, Oregon, and Washington Shelf is known only to a limited degree, but even less information is available on the shallow stratigraphy and sedimentary character. Preliminary work indicates several high-potential deposits are present off central Washington, proximal to markets in Portland, Oreg., and Seattle, Wash. Oregon has recently released a map of the EEZ of its coast that includes resource information on sand, gravel, and other commodities (Gray and Kulm, 1985).

The U.S. Geological Survey has studied the geologic character and modern processes of much of Alaska's coasts and shelves. Many of these efforts have been summarized by Peter Stauffer (written commun., 1986), who describes the occurrence, distribution, and estimated volumes of sand and gravel on the Alaska Shelf (fig. 2). Sediments there are highly variable because of Alaska's complex geologic history and the dominant influence of seasonal ice and glacial erosion and deposition. Gravel is abundant in many regions. The largest sand and gravel deposits are contained in moraines at the coast or on the seabed where waves and currents have winnowed and removed the fine-grained sediment, leaving a coarse lag deposit (Molnia, 1979).

Many of the barrier islands and spits in Alaska contain large volumes of gravel, but most are now cut off from their sediment sources. Mining could harm sensitive areas and increase coastal erosion. Also, many of the offshore areas of Alaska exhibit complex topography that includes deltas and fields of sand ridges containing large volumes of sand. Peter Stauffer (written commun., 1986) reports the Yukon River delta and associated sand bodies alone contain an estimated 70 billion m^3. Buried stream channels in nearshore shelf areas also contain large volumes of coarse sand. The effects of mining these deposits may come closest to duplicating the natural process where sea ice gouges troughs or furrows in the seabed that are subsequently filled by shelf sediments. If Alaska's construction growth and oil exploration continue, demand for sand and gravel is likely to be high. And while onshore resources are large and widespread, the high transportation costs and lack of roads may favor offshore mining to meet future commercial demands.

Many parts of the Hawaiian Islands suffer severe shortages of suitable sand and gravel for reasons similar to those in the U.S. Virgin Islands and Puerto Rico. Demand is great for construction-quality aggregate, and beach nourishment is a method preferred by the State for mitigating erosion of the recreational beaches that are so important to the economy of Hawaii (Dollar, 1979). Sand from onshore pits can cost $\$50/m^3$, but some of the islands do not have enough sand to meet demands at any price. The offshore areas may offer a logical alternative. Several geophysical and sediment sampling surveys have identified pockets of sand along the narrow insular shelves (Moberly and others, 1975). Much of the material is a mixture of volcanic detritus and calcareous sand; the most promising deposits are relict Pleistocene shore terraces, drowned by the Holocene transgression. One such source area is off Penguin Bank, 35 km from Honolulu in 50-m to 60-m water depths. It contains an estimated 270 million m^3 of sand (Campbell and others, 1970). Other such banks and buried ancestral stream valleys containing potentially valuable sand may exist offshore. Additional site-specific studies to locate and evaluate these features will help in assessing Hawaii's sand resources.

ENVIRONMENTAL EFFECTS

Environmental concerns have been a major deterent to implementation of marine mining in the United States, even when suitable deposits are present and where the economic factors are favorable. A number of the environmental studies carried out over the past decade and summarized by Naqui and Pullen (1982) show that the impact of dredging depends largely on the local geologic and biologic conditions. Dredging effects are most detrimental where proportions of fine-grained sediment are high and where the dredging is close to nonmobile benthic communities, because the muds can reduce light transmission and smother organisms. This situation could be a problem in reef areas of southern Florida and for many of the islands in the Caribbean and Pacific.

Dredging can also affect the environment by exposing a different substrate or by causing substantial changes in the seabed topography from removal of large volumes of sand. Dredging in areas with mobile fauna produces no apparent long-term ill effects, and in cases where sediment elutriation releases organics into the water column, the effects actually may be beneficial. Most long-term environmental damages can be avoided by careful planning prior to dredging, by the use of proper dredging equipment, and by

close monitoring of the dredge site and adjacent areas during the operation (Naqui and Pullen, 1982).

Dredging too close to coastal areas is likely to remove sand from the active sediment budget and alter wave and current patterns, changes that can eventually increase erosion. The volume of sand along the coast and the morphology of nearshore areas are influenced by wave and current conditions. If sand is dredged too close to shore, the shore profile will shift as sand moves seaward from the shore to fill the dredge holes. These problems can be avoided if dredging is limited to relict sand bodies, which are no longer connected to littoral processes, or to areas where natural sediment input is great enough to compensate for losses due to dredging. These safeguards may require dredging farther offshore, which will increase costs, but the alternatives will accelerate coastal erosion and property damage and may ultimately be far more costly.

CONCLUSIONS

Sand and gravel deposits are abundant and widespread resources within much of the U.S. Exclusive Economic Zone. Their volume and proximity to market areas make them potentially the most valuable and immediately useful nonenergy commodity within U.S. offshore areas. Some deposits are already competitive with onshore deposits for uses such as beach replenishment and manmade island construction. Other deposits could be competitive within the next decade, especially near urban areas such as Boston, New York, Los Angeles, San Juan, and Honolulu, where nearby onshore deposits are depleted or where land use and environmental laws constrain mining. Dredging technology is now available for the mining of sand and gravel in water depths to 40 m with little long-term environmental harm, and private industry appears willing to pursue marine mining if suitable leasing provisions are established by Federal and State governments.

REFERENCES CITED

Ballard, R.D., and Bischoff, J.L. 1984, Assessment and scientific understanding of hard minerals in the EEZ, *in* Symposium proceedings—A national program for the assessment and development of the mineral resources of the United States Exclusive Economic Zone: U.S. Geological Survey Circular 929, p. 185–208.

Berryhill, H.L., Moslow, T.F., Penland, S., and Suter, J.R., 1985, Shelf and shoreland sands—Northwest Gulf of Mexico: American Association Petroleum Geologists, Continuing education short course, chaps. 1–11.

California Department of Boating and Waterways, 1983, Study of Quaternary shelf deposits (sand and gravel) of southern California: Report FR 82–11, Sacramento, Calif., 75 p.

Campbell, J.F., Coulbourn, W.T ., Moberly, R., and Rosendahl, B.R., 1970, Reconnaissance sand inventory off Leeward Oahu: University of Hawaii Sea Grant Program, Technical Report 70–2, 47 p.

Cruickshank, M.J., and Hess, H.D., 1975, Marine sand and gravel mining: Oceanus, fall issue, p. 32–44.

Dollar, S.J., 1979, Sand mining in Hawaii: University of Hawaii Sea Grant Program, Technical Paper 79–1, 106 p.

Duane, D.B., 1969, Sand inventory program—A study of New Jersey and northern New England coastal waters: Shore and Beach, p. 12–16.

Duane, D.B., Field, M.E., Meisburger, E.P., Swift, D.J.P., and Williams, S.J., 1972, Lineral shoals on the Atlantic Inner Continental Shelf, Florida to Long Island, *in* Swift, D.J.P., Duane, D.B. and Pilkey, O.H., eds., Shelf sediment transport—Process and pattern: Stroudsburg, Pa., Dowden, Hutchinson, and Ross, p. 447–498.

Duane, D.B., and Stubblefield, W.L., 1986, Sand and gravel resources, U.S. Atlantic Continental Shelf, *in* Grow, J.A., and Sheridan, R.E., eds., Decade of North America Geology—Atlantic Continental Margin: Boulder, Colo., v. I–Z, p. 481–500.

Emery, K.O., and Uchupi, E., 1984, The geology of the Atlantic Ocean: New York, Springer-Verlag, 1050 p.

Field, M.E., 1980, Sand bodies on coastal plain shelves—Holocene record of the U.S. Atlantic Inner Shelf off Maryland: Journal of Sedimentary Petrology, v. 50, p. 505–528.

Field, M.E., and Duane, D.B., 1976, Post-Pleistocene history of the United States Inner Continental Shelf—Significance to origin of barrier islands: Geological Society of America Bulletin, v. 87, p. 691–702.

Gray, J.J., and Kulm, L.D., 1985, Mineral resources map, offshore Oregon: Oregon Department Geology and Mineral Industries, Map GMS–37.

Grove, K.A., and Trumbull, J.V.A., 1978, Surficial geologic maps and data on three potential offshore sand sources on the insular shelf of Puerto Rico: U.S. Geological Survey Miscellaneous Field Studies Map MF–1017.

Holmes, C.W., 1978, Virgin Islands sand resource study: U.S. Geological Survey Open-File Report 78–919, 49 p.

Hubbard, D.K., Sadd, J.L., Miller, A.I., Gill, I.P., and Dill, R.F., 1981, The production, transportation, and deposition of carbonate sediments on the insular shelf of St. Croix, U.S. Virgin Islands: West Indies Laboratory, Fairleigh Dickinson University, Technical Report MG–1, 45 p.

Kerhin, R.T., and Williams, S.J., 1987, Surficial sediments and late Quaternary sedimentary framework of the Maryland Inner Continental Shelf, *in* American Society of Civil Engineers Coastal Sediments 87 Conference Proceedings: New Orleans, La., p. 2126–2140.

Manheim, F.T., 1972, Mineral resources off the northeastern coast of the United States: U. S. Geological Survey Circular 669, 28 p.

Manheim, F.T., and Hess, H.D., 1981, Offshore hard mineral resources around the U.S. continental margins: Offshore Technology Conference, 13th Proceedings, v. 4, p. 129–138.

McKelvey, V.E., 1986, Subsea mineral resources, Chapter A *in* Mineral and petroleum resources of the ocean: U.S. Geological Survey Bulletin 1689, 106 p.

Meisburger, E.P., and Williams, S.J., 1981, Use of vibratory coring samplers for sediment surveys: Coastal Engineering Research Center, Technical Aid 81–9, 18 p.

Moberly, R., Campbell, J.F., and Coulbourn, W.T., 1975, Offshore and other sand resources for Oahu, Hawaii: University of Hawaii Sea Grant Program, Technical Report 75–3, 63 p.

Molnia, B.F., 1979, Sand and gravel resources of the continental shelf off Alaska: Appendix 4 to OCS Mining Policy Phase II Task Force, Program feasibility document, OCS hard mineral leasing, 70 p.

Naqui, S.M., and Pullen, E.J., 1982, Effects of beach nourishment and borrowing on marine organisms: Coastal Engineering Research Center, Miscellaneous Report 82–14, 43 p.

Oldale, R.N., 1985, Upper Wisconsinan submarine end-moraines off Cape Ann, Massachusetts: Quaternary Research, v. 24, p. 187–196.

Oldale, R.N., Wommack, L.E., and Whitney, A.B., 1983, Evidence for a post glacial low relative sea-level stand in the drowned delta of the Merrimack River, western Gulf of Maine: Quaternary Research, v. 19, p. 325–336.

Revelle, R., 1983, Probable future changes in sea level resulting from increased atmospheric CO_2, *in* Changing climate: Washington, D.C., National Academy Press, chap. 8, p. 433–448.

Rodgriguez, R.W., 1984, Submerged sand resources of Puerto Rico, *in* Clark, S.H., ed., U.S. Geological Survey highlights in marine research: U.S. Geological Survey Circular 938, p. 57–63.

Schlee, J.S., 1973, Atlantic Continental Shelf and Slope of the United States sediment texture of the northeastern part: U.S. Geological Survey Professional Paper 529–L, 64 p.

Schlee, J., Folger, D.W., and O'Hara, C.J., 1973, Bottom sediments on the continental shelf off the northeastern United States—Cape Cod to Cape Ann, Massachusetts: U.S. Geological Survey Miscellaneous Geological Investigation Map I–746.

Schlee, J., and Pratt, R.M., 1970, Atlantic Continental Shelf and Slope of the United States— Gravels of the northeastern part: U. S. Geological Survey Professional Paper 529–H, 39 p.

Schlee, J., and Sanko, P., 1975, Sand and gravel: New York Sea Grant Institute, New York Bight Atlas Monograph 21, 26 p.

Tepordei, V.V., 1987, Sand and gravel, *in* Mineral Commodity Summaries 1987: U.S. Bureau of Mines, p. 136–137.

Trumbull, J.V.A., 1972, Atlantic Continental Shelf and Slope of the United States—Sand-size fraction of bottom sediments, New Jersey to Nova Scotia: U.S. Geological Survey Professional Paper 529–K, 45 p.

U.S. Bureau of Mines, 1987, An economic reconnaissance of selected sand and gravel deposits in the U.S. Exclusive Economic Zone: U.S. Bureau of Mines Open-File Report 3–87, 113 p.

Williams, S. J., 1976, Geomorphology, shallow subbottom structure, and sediments of the Atlantic Inner Continental Shelf off Long Island, New York: Coastal Engineering Research Center, Technical Paper 76–2, 123 p.

———1981, Sand resources and geological character of Long Island sound: Coastal Engineering Research Center, Technical Paper 81–3, 65 p.

———1982, Use of high resolution seismic reflection and side-scan sonar equipment for offshore surveys: Coastal Engineering Research Center, Technical Aid 82–15, 22 p.

———1986, Sand and gravel deposits within the United States Exclusive Economic Zone—Resource assessment and uses: Offshore Technology Conference, 18th Proceedings, p. 377–386.

Williams, S.J., and Duane, D.B., 1974, Geomorphology and sediments of the inner New York Bight Continental Shelf: Coastal Engineering Research Center, Technical Memorandum No. 45, 83 p.

Williams, S.J., Prins, D.A., and Meisburger, E.P., 1979, Sediment distribution, sand resources, and geologic character of the inner continental shelf off Galveston County, Texas: Coastal Engineering Research Center, Miscellaneous Report 79–4, 159 p.

Chapter I

Tungsten—Geology and Resources of Deposits in Southeastern China

By JAMES E. ELLIOTT

U.S. GEOLOGICAL SURVEY BULLETIN 1877

CONTRIBUTIONS TO COMMODITY GEOLOGY RESEARCH

CONTENTS

FIGURES

TABLE

Tungsten—Geology and Resources of Deposits in Southeastern China

By James E. Elliott

Abstract

The People's Republic of China is the largest producer of tungsten in the world with an annual production of about 15,000 metric tons of contained tungsten, approximately a third of the world's total production. In addition, it is estimated that more than 40 percent of world's tungsten reserves are in China. Nearly all of China's tungsten deposits are located in the southeastern part of the country, a region that was a complex continental margin from Middle Proterozoic to at least Late Cretaceous time. The complex geology is the result of sedimentation that was interrupted by several periods of folding, faulting, metamorphism, and igneous activity.

Most of China's tungsten production comes from wolframite-bearing quartz-vein systems such as those at the Xihuashan and Dajishan mines; these mines have operated since the early 1900's. During the last 35 years, important skarn deposits have also been discovered; these include the Shizhuyuan W-Sn-Mo-Bi deposit, the largest tungsten deposit in the world. Other important kinds of deposits include disseminated, stockwork or porphyry, greisen, and strata-bound. Most of the deposits have complex mineralogy, and most mines produce a variety of byproducts in addition to tungsten. The most common of these are tin, molybdenum, and bismuth. Other commodities such as copper, lead, zinc, niobium, tantalum, beryllium, and rare earth elements are also important.

Nearly all of the tungsten deposits are closely related to highly evolved, felsic, high-silica granites of Jurassic or Cretaceous age. These probably formed by anatexis of continental crust, which was made up of metasedimentary and older felsic igneous rocks that were enriched in tungsten and associated metals. The partial melting of continental crust and the generation of granitic magmas occurred as a result of westward-directed subduction during the middle and late Mesozoic.

INTRODUCTION

Since the early 1900's, when tungsten first became important to the industrial countries in North America and Europe, China has been a major supplier of this strategic commodity to world markets. At present, China continues to dominate the tungsten market as the world's leading producer of tungsten, accounting for approximately one-third of the world's production in 1985. Until about 1949, most of the tungsten production was from small mines worked by local villagers and farmers by hand with little mechanization. Most of these workings were on surface outcrops of veins and in shallow underground workings along the veins. Since the founding of the People's Republic of China in 1949, the exploration, development, and mining of tungsten have been organized and directed by government agencies. Many districts having numerous small mines were consolidated and developed as large mechanized tungsten mines with centralized milling facilities. In addition, systematic exploration since about 1960 has resulted in the discovery of many new deposits, several of which have not yet reached full production status.

Until recently, information on the geology and resources of tungsten in China was very sparse and fragmentary. Prior to about 1982, the few geologic reports available were generally based on information obtained prior to 1949. Since 1982, however, there has been a rapid increase in the knowledge of the geology and mineral resources of China as a result of visits by western geologists to China, the publication of Chinese-authored reports in English, and international conferences and symposia held in China. Nevertheless, information on tungsten mines and deposits is still very limited because many aspects of the geology, production, reserves, and even accurate locations of deposits are still considered to be confidential by Chinese government agencies. Some of the most valuable and accurate data on the resources and geology of tungsten in China are the result of personal visits to important mines and districts by western geologists.

During 1984 several U.S. Geological Survey (USGS) geologists participated in an exchange with geologists from the Chinese Academy of Geological Sciences. Part of this exchange consisted of visits to major tungsten mines and districts in China by three of the USGS geologists. The major deposits visited included the Shizhuyuan deposit in the Dongpo ore field, Hunan province; the Xihuashan and

Piaotang mines in the Dayu district, Jiangxi province; and the Dajishan mine, Jiangxi province. During these visits, a great deal of information was gained on geology and mineral deposits of these areas, and a limited amount of resource and production data was obtained. The descriptions of the geology and resources of these deposits are based principally on information obtained during these 1984 visits.

GEOLOGIC SETTINGS OF TUNGSTEN DEPOSITS

Nearly all of the important tungsten deposits of China are located in southeastern China, mostly in the provinces of Jiangxi, Hunan, and Guangdong (fig. 1; table 1). This region of approximately 800 by 800 km is roughly equivalent in area to that of the combined States of California and Nevada. Other deposits in China are located in the Fujian, Guangxi, and Yunnan provinces. Many of the largest and most productive deposits, both present and past, are located in the relatively small, mountainous region of Nanling, which lies in southern Jiangxi, southeastern Hunan, and northern Guangdong provinces. The principal tungsten deposits are quartz vein, stockwork or disseminated, and skarn types (table 1). Greisen and strata-bound deposits also occur. Most of the tungsten mines produce a variety of byproducts; the most common are tin, molybdenum, and bismuth.

The regions in which most of the tungsten deposits are found are geologically complex; sequences of Proterozoic and Paleozoic clastic and carbonate-rich sedimentary rocks have been repeatedly folded and faulted and intruded by plutonic rocks of several ages. The deposits are closely associated with highly evolved, leucocratic granites that show enrichment in many lithophile elements and are generally of Yanshanian (Jurassic and Cretaceous) age.

Tectonics and Structure

The region of southeastern China where most of the tungsten deposits are found is called the South China Accretionary Fold Belt (Zhang and others, 1984) and is also called the East China Continental Margin Domain (Yang and others, 1986). It consists of two fold zones, the Xianggui and Min-Yue, separated by the Jien'ou Uplift (Yang and others, 1986). This region has been a complex continental margin since the middle Proterozoic and was subjected to repeated magmatism, folding, and faulting during the Paleozoic and Mesozoic eras.

From Late Proterozoic (Sinian) through Silurian time, the region was a passive continental margin along the eastern border of the Yangtze craton, where sequences of flysch, graywacke, carbonates, and minor volcanic rocks accumulated (Zhang and others, 1984). Near the end of the early Paleozoic, these strata were folded, metamorphosed, and intruded by granitic plutons forming the Caledonian basement (Yang and others, 1986). Shallow marine and terrestrial sedimentary rocks, including carbonates, were deposited during the late Paleozoic and Triassic. Following the Triassic, the Mesozoic Circum-Pacific volcanic belt began to take form and evolve. As part of that belt, this region was subjected to major episodes of folding, faulting, and igneous activity. The Mesozoic marked the end of large-scale marine transgressions and the start of active westward-directed subduction in south China (Yang and others, 1986). Profuse magmatic activity during the Jurassic and Cretaceous periods (Yanshanian) was accompanied by the formation of deposits of tungsten, tin, molybdenum, and other metals throughout most of southeastern China.

Association with Granitoid Rocks

Granitoid rocks of southeastern China have been classified into two major types: (1) transformation or crustal and (2) syntexis or transitional (Xu and others, 1982). The former rocks are highly evolved granites with greater than 70 percent SiO_2; low CaO, MgO, TiO_2, and total Fe; and high Na_2O and K_2O. These granites are similar to S-type or ilmenite-type granites and are thought to be formed by the melting of continental crust. They are commonly associated with tungsten, tin, niobium, and tantalum deposits. The syntexis granitoids have compositions ranging from quartz diorite to monzonite and SiO_2 generally ranging from 56 to 70 percent. They are similar to I-type or magnetite-type granitoids and are thought to be formed by mixing of magma from the upper mantle with continental crust. Some tungsten and many copper and molybdenum deposits are associated with syntexis granitoid plutons.

The granites that are genetically linked to most of the tungsten deposits are strikingly similar to specialized tin or S-type granites described in many other parts of the world and are also similar to Climax-type granites of the Western United States. They differ from most of the granitic rocks of the Cordilleran region of North America that occur with skarn tungsten deposits in California, Nevada, Montana, and northwestern Canada. These Cordilleran granitic rocks are generally more mafic, have lower silica contents, and are less evolved than the Chinese tungsten granites; they have been interpreted as variably contaminated I-type granites (Newberry and Swanson, 1985).

DESCRIPTION OF DEPOSITS

Most of the China's tungsten production, past and present, is from wolframite-bearing quartz-vein deposits that occur both within granite plutons (endocontact deposits) and in the metasedimentary rocks adjacent to granite bodies (exocontact deposits). Since the 1960's, however,

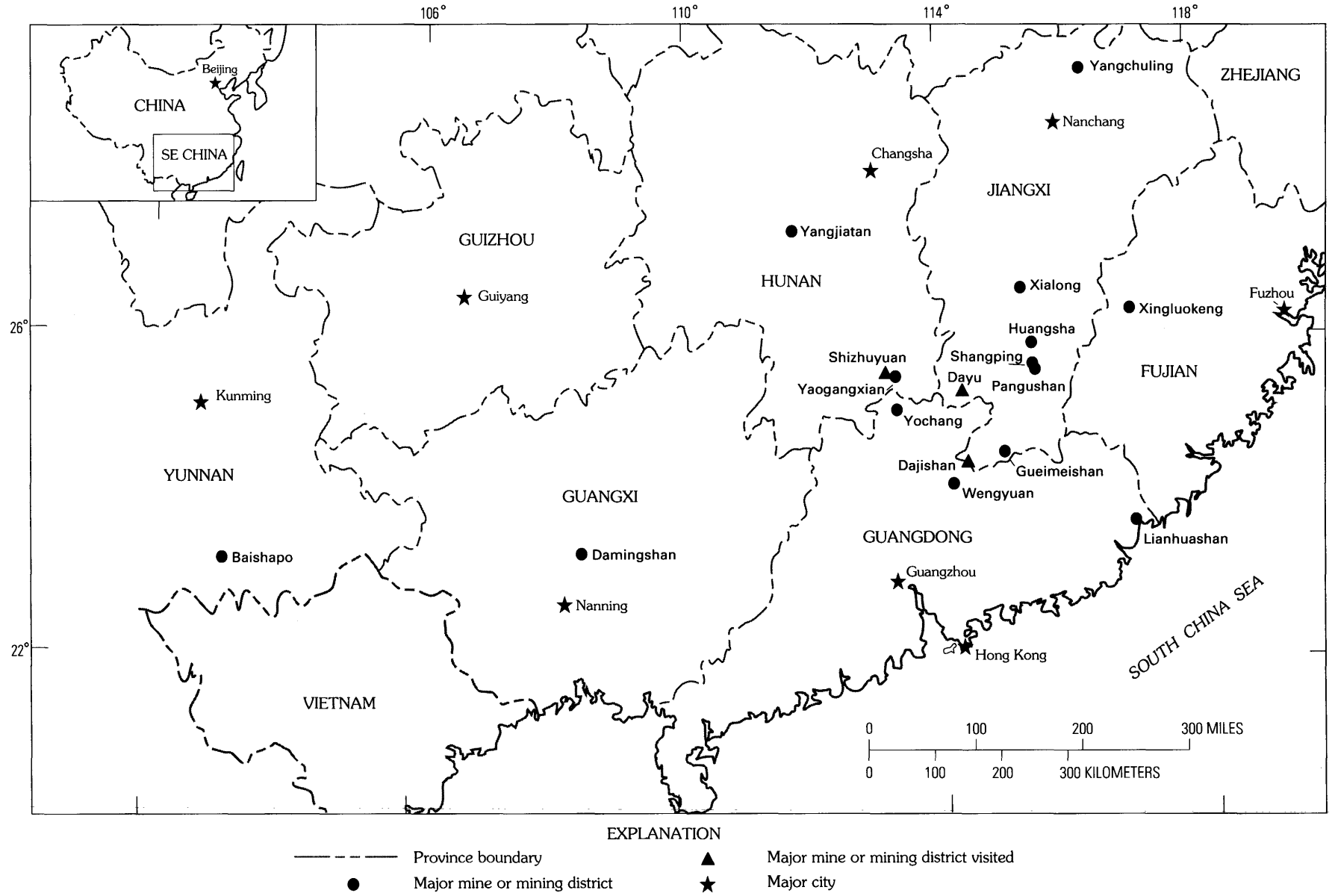

Figure 1. Locations of major tungsten mines and districts in southeastern China. Xihuashan and Piaotang mines are located in Dayu district.

Table 1. Deposit types, lithologies, and ages of host and associated igneous rocks and the references for mines and districts shown in figure 1

Name	Province	Deposit type	Age and lithology of host rocks	Age and lithology of associated igneous rocks	References
Xingluokeng	Fujian	Porphyry/stockwork/ vein.	Jurassic granite; Devonian hornfels.	Jurassic granite	Liu, 1982.
Lianhuashan.....	Guangdong	Porphyry/stockwork	Cretaceous quartz porphyry; Early Jurassic sandstone.	Cretaceous quartz porphyry.	Lu, 1985; Bai and others, 1983; Tan, 1983; Li and others, 1982.
Wengyuan	----do.----	Vein	Jurassic granite; Devonian sandstone.	Jurassic granite	Li and Wang, 1955.
Yochang	----do.----	----do.----	Jurassic granite; Permian sandstone, shale.	----do.----	Do.
Damingshan	Guangxi	Stratiform/stockwork/ vein.	Devonian sandstone, shale.	Cretaceous granite	Ma, 1982; Wan, 1982.
Shizhuyuan	Hunan	Stockwork/skarn/ greisen.	Devonian limestone	Jurassic granite	Wang and others, 1982.
Yangjiatan	----do.----	Vein	Paleozoic metasedimentary rocks.	Mesozoic granite	Carter and Kiilsgaard, 1983.
Yaogangxian	----do.----	Vein/skarn	Devonian sandstone	Jurassic granite	Wang and others, 1930.
Dajishan	Jiangxi	Vein/disseminated	Cambrian phyllite, slate, sandstone.	----do.----	Li and Wang, 1955; Shi and Hu, 1986; Chang, 1974.
Dayu (includes Xihuashan and Piaotang)	----do.----	Vein/stockwork	Jurassic granite; Cambrian sandstone, phyllite, slate.	----do.----	Wu and Mei, 1982; Wang and Zhou, 1982.
Gueimeishan	----do.----	----do.----	Cambrian, Ordovician quartzite, phyllite.	----do.----	Hsu, 1943.
Huangsha	----do.----	Vein	Cambrian quartzite, slate.	----do.----	Chen and Hu, 1982; Xia and others, 1982.
Pangushan	----do.----	Vein/stockwork	Devonian sandstone	----do.----	Hsu, 1943; Cai and others, 1982.
Shangping	----do.----	Vein	Proterozoic, Cambrian phyllite, quartzite.	----do.----	Hsu, 1943.
Xialong	----do.----	----do.----	Proterozoic, Cambrian phyllite, quartzite.	----do.----	Do.
Yangchuling	----do.----	Porphyry/stockwork	Jurassic granodiorite porphyry.	Jurassic granodiorite porphyry.	Yan and others, 1980.
Baishapo	Yunnan	Skarn/vein/placer	Triassic limestone	Cretaceous granite	Anstett and others, 1985.

many other kinds of tungsten deposits have been discovered in China, and these deposits will become increasingly important as sources of tungsten. These kinds of deposits include skarn, stockwork or porphyry, greisen, disseminated, and strata-bound.

During October 1984, four major tungsten deposits in southeastern China were visited by the author and two other USGS geologists. These visits were arranged by members of the Chinese Academy of Geological Sciences, Ministry of Geology and Mineral Resources, as part of an exchange between that agency and the USGS. This exchange was focused on the study and comparison of environments of ore deposition and the genesis of deposits of tungsten, tin, niobium, and tantalum in southeastern China and the Western United States. The Chinese deposits visited included the Shizhuyuan deposit, Hunan province; the Xihuashan and Piaotang deposits in the Dayu district, Jiangxi province; and the Dajishan deposit, Jiangxi province (fig. 1). These represent a variety of deposit types including quartz-vein, skarn, stockwork, greisen, and disseminated. Large mines are present at two of these deposits, Xihuashan and Dajishan, and these mines have a long history of production; the Shizhuyuan and Piaotang deposits are being developed for production.

Shizhuyuan Mine

Shizhuyuan is the largest known tungsten deposit in the world with an estimated 627,000 metric tons of contained WO_3 (Anstett and others, 1985). It was discovered in the 1950's in southeastern Hunan province (fig. 1). Other mines in the district produce copper, lead, and zinc. Shizhuyuan is presently being mined on a small scale and is being developed as a large mine-mill complex that will produce up to 5,000 tons per day (Ye Qingtong, oral commun., 1984).

The deposit is hosted by argillaceous limestone of Late Devonian age in the contact zone of the Qianlishan granite stock of Jurassic (Early Yanshanian) age (Wang and others, 1982). The stock is composite, consisting of at least four phases of granite, granite porphyry, and quartz porphyry, which are highly evolved and peraluminous, have silica contents of greater than 70 percent, and are enriched in tin, tungsten, molybdenum, and bismuth.

The deposit is large and complex; it occurs above the contact between the stock and the overlying metasedimentary rocks and dips to the east (fig. 2). The body of mineralized rock is about 1,000 m long (north-south), 600 to 800 m wide (east-west), and generally 200 to 300 m thick with a maximum thickness of about 500 m (Wang and others, 1982). The deposit has been subdivided into four zones based on kind and grade of ore (fig. 2):

Zone I—The uppermost zone, 50 to 220 m thick, consists of a stockwork of cassiterite-sulfide-quartz veins in marble.

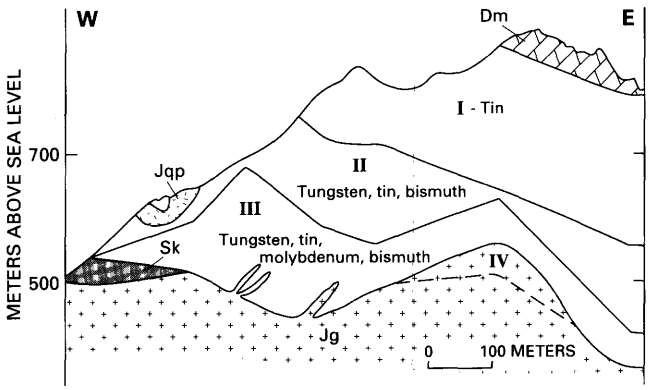

Figure 2. Generalized cross section through the Shizhuyuan deposit showing ore zones I to IV (explanation in text). Other units are Dm, Devonian dolomitic marble; Jqp, Jurassic quartz porphyry; Jg, Jurassic granite and porphyritic granite; Sk, skarn with subeconomic concentrations of ore minerals. Modified from unpublished data of Chinese Academy of Geological Sciences.

The veins are closely spaced and generally less than 1 cm thick. The average grade of tin is about 0.17 percent, but tungsten, molybdenum, and bismuth are very low, each usually less than 0.05 percent.

Zone II—Below the tin-bearing stockwork zone is a zone in which garnet skarn has selectively replaced favorable beds within the marble. The skarn layers are lenticular to stratiform and contain scheelite, cassiterite, molybdenite, bismuthinite, and various beryllium minerals in addition to calc-silicate minerals, such as garnet and pyroxene, and quartz. The number and thickness of the skarn layers increase downward toward the granite contact; unreplaced marble is rare or absent in the lower part of the zone. This zone is 10 to 150 m thick and contains approximately 0.21 percent tungsten, 0.15 percent tin, 0.02 percent molybdenum, and 0.10 percent bismuth.

Zone III—Adjacent to the granite stock is a zone that consists of complex pyroxene-garnet-sulfide skarn cut by a stockwork of quartz veins. These veins range in thickness from a few centimeters to about 0.5 m and increase in number toward the granite contact; close to the contact they commonly exceed 50 percent by volume of the contact zone. Most of the ore minerals are contained in these veins, although the skarn also contains significant concentrations of tungsten and other metals. Both wolframite and scheelite occur in the veins, but scheelite is the principal tungsten-bearing mineral in the skarn between the veins. This zone ranges in thickness from 40 to 200 m and contains the highest grades of tungsten, molybdenum, and bismuth. The approximate grades are 0.50 percent tungsten, 0.12 percent molybdenum, 0.18 percent bismuth, and 0.09 percent tin.

Zone IV—In places the mineralization is found below the granite-skarn contact forming an ore zone in greisenized,

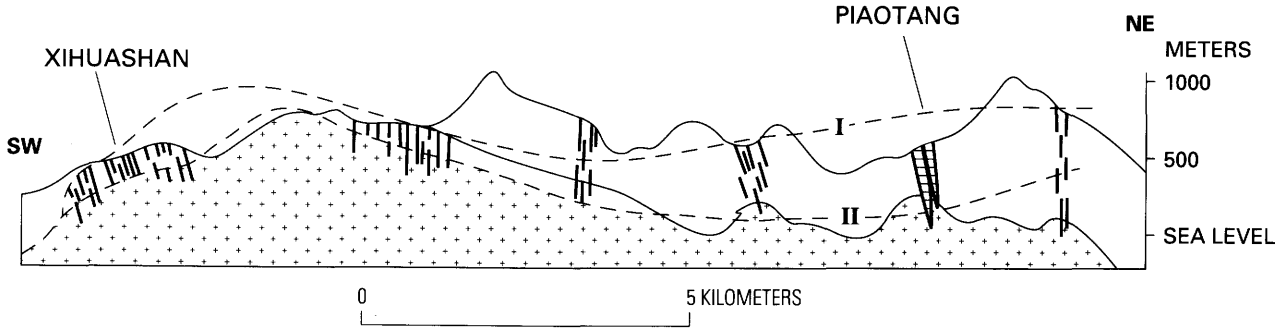

Figure 3. Generalized longitudinal section through the Xihuashan and Piaotang tungsten deposits in the Dayu district. Other vein systems are indicated by heavy lines. I, upper limits of ore zones; II, lower limits of ore zones. Modified from Yang and Lu (1982). Patterned area is granite batholith. Unpatterned area is sedimentary and metamorphic rocks.

silicified granite. This type is relatively thin and discontinuous, usually less than a few meters thick. Ore grades are similar to those in zone III.

Strong metal zonation is evident in zones I to III. Tin is highest in zone I and decreases toward the granite contact. Tungsten, molybdenum, and bismuth all increase toward the granite contact. Tungsten is less than 0.05 percent in zone I and increases to about 0.5 percent in zone III. Molybdenum and bismuth show similar increases from zones I to III.

Xihuashan Mine

The Xihuashan mine is the largest mine in the Dayu district (fig. 1) and is the most famous tungsten mine in China, having a history of production dating back to 1908. Prior to 1949, the area was mined by many individuals in surface and shallow underground workings. Since 1949, the mining has been conducted by the government through the development of a large underground mine and a mill for processing of the ore (Zhou Yuzhen, oral commun., 1984).

In 1984, the Xihuashan mine was producing at a rate of 3,000 metric tons (t) of ore per day and 2,500 t of tungsten concentrate (containing 65 percent WO_3) per year. Molybdenum, tin, and bismuth are also recovered as byproducts. Since 1960, when centralized, large-scale mining and milling began, the mine has produced about 75,000 t of tungsten concentrate. The ore reserves in 1984 were 110,000 t of WO_3 (87,232 t contained tungsten) (Zhou Yuzhen, oral commun., 1984).

The deposit consists of a system of wolframite-quartz veins in the southwest part of the Xihuashan stock of Jurassic age, which has intruded Late Proterozoic and Cambrian metasedimentary rocks. The stock is exposed over an area of about 24 km^2 and is composite; four stages of biotite granite plus a stage of granite porphyry are recognized. All granitic stages are highly evolved; they are high in silica content (74–76 percent SiO_2) and are enriched in many trace elements. Each of the four stages of biotite granite is accompanied by alteration and mineralization; these vary in intensity and type of metals. The Xihuashan mineralized zone occupies about 6.5 km^2 of the stock; granites of the first two stages are the principal types exposed in the mine workings; these are closely related to the economic mineralization in the mine.

The Xihuashan mine is an endocontact deposit in which the wolframite-quartz veins occur near the top and around the periphery of the stock (fig. 3). They pinch out rapidly where they cross the contact into the metasedimentary rocks. The mineralized zone consists of more than 650 veins arranged in three sets of steeply dipping parallel veins. The veins have an average thickness of 0.4 m (maximum of 3.6 m) and length of 150 m (maximum of 1,075 m). The orebodies in the veins show vertical zoning in the kind and concentration of ore minerals and in the style of alteration. The vertical extent of orebodies in each set of veins is commonly about 250 m (Zhou Yuzhen, oral commun., 1984).

Piaotang Mine

The Piaotang mine, also in the Dayu district, is located about 13 km northeast of the Xihuashan mine (fig. 3). It is an exocontact deposit hosted by Cambrian metasedimentary rocks in the contact zone and above a granite cupola. It was discovered in 1918 but has been mined only in small-scale operations, mainly in surface and shallow-underground workings. In 1984, the mine was being developed for production, and a mill was under construction. The principal products of this operation will be tungsten and tin, but molybdenum, bismuth, copper, lead, zinc, beryllium, niobium, tantalum, and other commodities are planned byproducts (Wu Chang Zhu, oral commun., 1984).

Whereas Xihuashan is a large-vein deposit, Piaotang is a small-vein deposit. Most veins at Piaotang are too thin to be mined individually, and orebodies consist of many

small, closely spaced veins. These veins occur within a mineralized zone that trends northeast, is more than 1.3 km long, and is more than 500 m from the surface to the deepest levels that were affected by mineralization. From top to bottom, the zone shows systematic variations in the number and thickness of veins, from the "thread-vein" subzone at the top to the "big vein" subzone at the bottom. The No. 1 or thread vein subzone consists of many closely spaced veinlets (three to eight veinlets per meter, about 0.5 to 3 cm thick). The No. 5 or big vein subzone, occurring at the level of the granite-metasediment contact, consists of a few widely spaced veins that are 30 to 200 cm thick. The orebodies are generally found in the intermediate subzones, and the best grades are in the No. 3 or "big-veinlet vein" subzone where 2-cm to 5-cm veins are interspersed with large veins (3 to greater than 100 cm, average about 15 cm) and where the vein density is about 2.5 veins per meter. Veins constitute about 11 percent by volume of the total rock in this No. 3 subzone, which is about 200 m from top to bottom (Wu Chang Zhu, oral commun., 1984).

On the basis of crosscutting relations between alteration types and veins of different mineralogy, seven paragenetic stages have been defined at Piaotang. The earliest stage, stage 1, is contact metamorphism and silicification of the metasedimentary rocks. Where carbonate-bearing beds are present in the sequence, calc-silicate minerals have replaced the original carbonate and silicate minerals forming skarn. Stages 2 through 7 consist of sets of veins that show a progressive change in mineralogy from early stages of mainly oxides and silicates (wolframite, cassiterite, beryl, quartz), through intermediate stages of oxides, silicates, and sulfides (mainly molybdenite, chalcopyrite, sphalerite, galena, and pyrite), to late stages of sulfides, chlorite, quartz, fluorite, and carbonate minerals. Minerals of economic value are found mainly in the intermediate stages (stages 2 through 5) (Wu Chang Zhu, oral commun., 1984).

Dajishan Mine

The Dajishan mine is one of the largest producing tungsten mines in China, having a mill capacity of 3,000 t of ore per day (Wu, 1982). The average grade of ore mined is about 0.25 percent WO_3, and this value is upgraded to greater than 0.5 percent WO_3 by preconcentrating through hand and photometric sorting prior to treatment in the mill. As at Xihuashan, the principal orebodies are tungsten-bearing quartz veins. The Dajishan mine has a long history of production, having been worked for more than 60 years (Wu, 1982).

The Dajishan mine is located near the edge of a granitoid batholith of Jurassic age. Two types of deposits are exposed in the underground workings of the mine. The principal one, which is the source of most of the past and present production, consists of sets of steeply dipping parallel quartz veins hosted by Cambrian metasandstone, slate, and phyllite. A second type consists of disseminated wolframite and beryllium-bearing and niobium-tantalum-bearing minerals in albite muscovite granite that occurs as an irregularly shaped intrusive body in the lower levels of the mine (Shi and Hu, 1986) (fig. 4).

The quartz veins occur as west-trending to west-northwest-trending parallel veins that dip steeply to the northeast. Hundreds of veins have been worked in the mineralized zone that is bounded on the east and west sides by northeast-trending faults. Orebodies occur in a vertical range of over 500 m, and the mine area is underlain by a body of biotite-muscovite granite (fig. 4). Veins are variable in thickness from about 1 cm or less to about 3 m. Smaller veins (less than 1 m) contain higher grades and account for most of the economic mineralization, but some of the larger veins contain spectacular large clusters of wolframite crystals; individual crystals of up to 1 m long have been noted. A mass of nearly pure wolframite weighing about 2.5 t was taken out of one of the large veins and is now on display at the Great Hall of the People in Beijing (Teng Jian De, oral commun., 1984). The principal ore minerals are wolframite and scheelite (ratio ranges from 3:1 to 4:1). The veins also contain minor amounts of sulfide minerals and native bismuth plus a variety of silicate and oxide minerals. Molybdenum and bismuth are recovered as byproducts in the mill (Wu, 1982).

The muscovite granite body that contains the disseminated tungsten-niobium-tantalum-beryllium mineralization is exposed in the lower workings of the mine and is connected at depth with biotite-muscovite granite (fig. 4). The muscovite granite has a well-developed pegmatoid margin, and the ore minerals are contained in the interior of the granite in spheroidal to ellipsoidal masses, 10 to 100 cm in diameter, that contain up to 30 percent WO_3 plus minor amounts of beryllium-bearing and niobium-tantalum-bearing minerals. This mineralization is earlier than that found in the quartz veins, which cut the muscovite granite as well as the metasedimentary rocks (Shi and Hu, 1986).

PRODUCTION AND RESOURCES

China is the leading producer of tungsten in the world and has been a leader since the early 1900's. During the period of 1913 to 1937, China contributed about 37 percent of the world's production (Li and Wang, 1955). China's 1986 estimated production was approximately one-third of the total world production of 42,474 t of contained tungsten (Smith, 1988). China's role as a supplier of tungsten to world markets has strengthened in recent years, especially since about 1980. During the period of 1980 to 1986, the production of tungsten in China was maintained at high

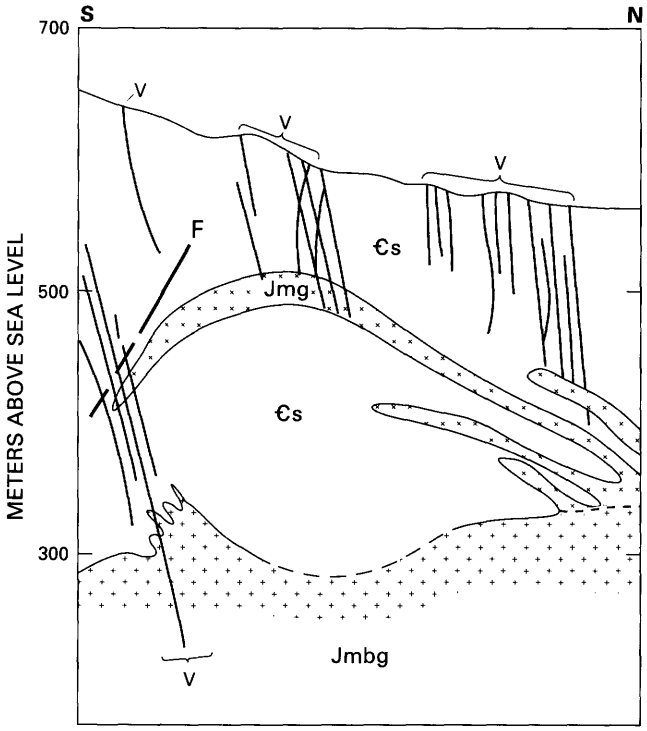

Figure 4. Generalized cross section through the Dajishan mine area. V, wolframite-quartz veins; F, fault; €s, Cambrian metasedimentary rocks; Jmg, Jurassic muscovite granite with tungsten-niobium-tantalum-beryllium ore bodies; Jmbg, Jurassic muscovite biotite granite. Dashed line indicates area where contact is approximate. Modified from Chang (1974).

levels, in the range of 12,500 to 15,000 t of contained tungsten per year (Chin, 1983; Smith, 1988). Over this same period the production by U.S. mines dropped dramatically from 2,738 t of contained tungsten in 1980 (U.S. Bureau of Mines, 1985) to 817 t in 1986 (U.S. Bureau of Mines, 1988). This drop in U.S. production is mainly the result of the fall of market prices from an average of $144 per metric ton unit WO_3 in 1980 (U.S. Bureau of Mines, 1985) to an average of $56 in 1986 (Smith, 1988).

Also during the period of 1980 to 1985, there has been a dramatic shift in the type of products produced and exported by China and corresponding changes in the importation of these products into the United States. Prior to 1980, nearly all of China's tungsten production was in the form of tungsten concentrates. Since that time, however, there has been a rapid increase in the production of value-added products such as ammonium paratungstate (APT) and tungsten oxide. As a result, a major trend in the U.S. trade patterns has been the shift from importing tungsten concentrate to importing these value-added products (Thurber, 1985). In 1980, the United States imported tungsten concentrate containing 918 t tungsten and APT with 10 t contained tungsten from China (Thurber, 1985). By 1986, the amount of tungsten in concentrate had fallen to 302 t, whereas the amount of tungsten in APT had risen to 971 t (Smith, 1988).

The aggressive production and pricing policies of Chinese producers have had a serious negative effect on both world and U.S. tungsten mining and refining industries. All of the major U.S. operations, such as the Pine Creek mine near Bishop, Calif., and the Emerson and Springer mines in Nevada, have been closed or are operating on greatly reduced schedules. Exploration for and development of tungsten deposits have virtually been discontinued in the United States. In China, however, production continues at high levels and could be increased if more deposits are put into production. For example, in 1984 the Piaotang and Shizhuyuan mines were being developed for production. Shizhuyuan is the largest known tungsten deposit in the world and, if put into production at the planned capacity of 5,000 t of ore per day, would be the largest producing mine in China (Ye Qingtong, oral commun., 1984).

Certainly much of the success that China has gained in competition with the rest of the world in tungsten marketing stems from the low cost of labor there. China's mines are labor intensive but, unlike the situation in U.S. mines, labor costs are a much lower percentage of overall operating costs. For underground mines in the United States, wages account for 44 to 64 percent of total costs, whereas in China wages for labor make up only 10 to 25 percent of the total costs (Chen, 1986). In China, the yearly wage for an underground worker is about 3,000 yuan ($937 at a rate of 3.2 yuan per dollar) versus about $30,000 per year for an underground worker in the United States (Chen, 1986). At tungsten mines and mills, these low labor rates permit hand sorting of ore prior to milling. This practice, which is prohibited by high labor costs in the United States, allows lower grade ores to be mined economically, thus prolonging the lives of many mines (Wu, 1982). At Xihuashan, for example, approximately 200 people were employed in the hand sorting of ore in 1984.

Besides being the world's leader in production, China also has a major share of the world's resources of tungsten. Recent estimates (Smith, 1988) indicate that China has reserves of 1,200,000 t of contained tungsten and a reserve base (reserves plus marginal reserves and some subeconomic resources) of 1,230,000 t contained tungsten. These reserves are 42.9 percent of the world's estimated total of 2,800,000 t contained tungsten.

SUMMARY

As the leading producer of tungsten, China dominates the world's tungsten market. Favorable factors contributing to this dominance are its large tungsten ore reserves, the low cost of labor in China, aggressive production and pricing

policies by Chinese producers, and the recent changes in government policies that promote expanded trade with market economy countries.

China's tungsten deposits are located in the southeastern part of the country in a region that is geologically complex. Many of the mines having the largest production and longest history of operation are located in the Nanling region in the southern parts of Hunan and Jiangxi provinces and the northern part of the Guangdong province. Southeastern China has been a complex continental margin since Late Proterozoic time and during the Paleozoic and Mesozoic eras the sedimentation was repeatedly interrupted by orogenic periods of faulting, folding, and igneous activity. Of greatest significance to the formation of tungsten deposits was the widespread and abundant granitic plutonism of the Jurassic and Cretaceous periods (Yanshanian). Most of the major tungsten deposits are directly associated with granitic rocks of this age.

The occurrence of so many large and productive tungsten deposits in a relatively small area of the world such as southeastern China has long been a source of controversy and questions. What is the source of the tungsten and associated metals? Is the source sedimentary or magmatic? Is the mantle of the Earth unusually enriched in tungsten in this part of the world? Are the tungsten deposits the result of a single cycle or multiple cycles of magmatism, erosion, and sedimentation?

Three principal factors seem to control the occurrence of tungsten deposits in southeastern China. They are (1) the occurrence of source rocks, mainly sedimentary, which are enriched in tungsten, (2) a favorable tectonic environment over a long period of time, and (3) a long history of cyclic and widespread granitic plutonism. Some of the oldest sedimentary units such as the Banxi Group of Late Proterozoic age (Yang and others, 1986) show appreciable enrichment in tungsten. In western Hunan province, rocks of this group contain 5 to 15 parts per million (ppm) tungsten. Even higher levels (up to about 800 ppm tungsten) have been detected in Proterozoic and Paleozoic sedimentary rocks in southeastern Hunan and southern Jiangxi provinces (Xu and others, 1982). The anomalies in the sedimentary rocks may have been inherited from an uneven distribution of tungsten in the upper mantle in the region of southeastern China. Evidence of this enrichment is seen in a range of tungsten values in mafic and ultramafic Precambrian rocks from different parts of southeastern China (Xu and others, 1982). The tectonic environment of southern China has, through a long history of sedimentation interrupted by orogenies, promoted a recycling of tungsten and associated metals through sedimentation, erosion, and magmatism into deposits of increasing degrees of enrichment over geologic time. It has also provided favorable zones for the movement of magma and hydrothermal fluids and favorable environments for the final deposition of economic deposits. Granitic plutonism, the result, in part, of the tectonic environment, has occurred periodically since Late Proterozic time. The granitoid rocks of southern China have average tungsten values of 3.6 ppm, which is about 2.4 times the clarke value (Liu and others, 1982). Studies show that the highest values are found in evolved felsic, silica-rich granites and that there is a progressive enrichment of tungsten in these granites from oldest to youngest (Liu and others, 1982). Regional variations have also been determined, and the highest value (5.2 ppm) was found in granites in the Nanling region where most of the largest and most productive tungsten mines are located (Liu and others, 1982). Tungsten deposits usually occur with the youngest granites, usually Jurassic, in the regions, such as Nanling, in which they are found. These granites are the transformation or crustal type and are enriched in tungsten and other metals such as tin, molybdenum, bismuth, niobium, and tantalum. They have formed as a result of anatexis of crustal material, either metasedimentary or felsic igneous rocks, which were previously enriched in tungsten and associated metals.

REFERENCES

Anstett, T.F., Bleiwas, D.I., and Hurdelbrink, R.J., 1985, Tungsten availability—Market economy countries; a minerals availability program appraisal: U.S. Bureau of Mines Information Circular 9025, 51 p.

Bai Yuzhen, Man Fasheng, Ni Shoubin, and Li Tong, 1983, K-Ar dating of Lianhuashan tungsten ore deposit: Geochimica, v. 6, no. 2, p. 133–139.

Cai Jianming, Liu Ruolan, and Zeng Guangsheng, 1982, Study on fluid inclusion and its relation to mineralization of Pangushan tungsten deposit, Jiangxi Province, China, *in* Hepworth, J.V., and Yu Hong Zhang, eds., Tungsten geology, Jiangxi, China: Bandung, Indonesia, ESCAP/RMRDC, p. 233–243.

Carter, W.D., and Kiilsgaard, T.H., 1983, Landsat analysis of the Yangjiatan tungsten district, Hunan Province, People's Republic of China, *in* Carter, W.D., Rowan, L.C., and Weill, G., eds., Remote sensing and mineral exploration: Advances in Space Research, v. 3, no. 3, Pergamon Press, p. 113–123.

Chang, Tsung-chen, 1974, Report on a Ta-, Nb-, W-, and Be-mineralized granite: Geochimica, v. 4, no. 12, p. 249–256.

Chen Yunhe, 1986, Selective underground mechanization: Engineering and Mining Journal, v. 187, no. 5, p. 31–33.

Chen Zunda and Hu Lisui, 1982, The geological characteristics and primary zoning of Huangsha vein-type tungsten deposit, *in* Hepworth, J.V., and Yu Hong Zhang, eds., Tungsten geology, Jiangxi, China: Bandung, Indonesia, ESCAP/RMRDC, p. 257–268.

Chin, Edmond, 1983, The mineral industry of China, *in* U.S. Bureau of Mines, Minerals Yearbook 1981, v. III, Area reports—International: Washington, D.C., U.S. Government Printing Office, p. 225–249.

Hsu, Ke-Chin, 1943, Tungsten deposits of southern Kiangsi, China: Economic Geology, v. 38, no. 6, p. 431–474.

Li, K.C., and Wang, C.Y., 1955, Tungsten, its history, geology, ore-dressing, metallurgy, chemistry, analysis, applications, and economics: New York, Reinhold Publishing Corp., 506 p.

Li Tung, Man Fasheng, Bai Yuzhen, and Ni Shoubin, 1982, Isotope geology of Lianhuashan tungsten deposit, *in* Proceedings of symposium on geology of granites and their metallogenetic relations [abs.]: Nanjing, China, p. 69–71.

Liu Wengzhang, 1982, Geological features of mineralization of the Xingluokeng tungsten (molybdenum) deposit, Fujian Province, *in* Hepworth, J.V., and Yu Hong Zhang, eds., Tungsten geology, Jiangxi, China: Bandung, Indonesia, ESCAP/RMRDC, p. 339–348.

Liu Yimao, Yang Qishun, Zhu Yunjie, and Jiang Qingsong, 1982, Tungsten abundance and its evolution in granitoid rocks of south China, *in* Hepworth, J.V., and Yu Hong Zhang, eds., Tungsten geology, Jiangxi, China: Bandung, Indonesia, ESCAP/RMRDC, p. 349–357.

Lu Huangzhang, 1985, Fluid inclusion studies of a new type of ore deposit; a porphyry tungsten occurrence in China: Geochemistry, v. 4, no. 1, p. 41–52.

Ma Linqing, 1982, The geological characteristics of Damingshan sedimentary-magmatic hydrothermal wolframite deposit, Guangxi Zhuang Autonomous Region, China, *in* Hepworth, J.V., and Yu Hong Zhang, eds., Tungsten geology, Jiangxi, China: Bandung, Indonesia, ESCAP/RMRDC, p. 375–384.

Newberry, R.J., and Swanson, S.E., 1985, Granites associated with tungsten skarns, *in* Taylor, R.P., and Strong, D.F., eds., Granite-related mineral deposits: Halifax, Nova Scotia, Canada, CIM Conference on Granite-Related Mineral Deposits, p. 197–199.

Shi Mingkui and Hu Xiongwei, 1986, The geological characteristics and genesis of the granite-hosted tungsten deposit at the Dajishan mine, Jiangxi Province, China [abs.]: Terra Cognita, v. 6, no. 3, p. 555.

Smith, G.R., 1988, Tungsten, *in* Minerals yearbook 1986, v. I: U.S. Bureau of Mines, p. 963–979.

Tan Yunjin, 1983, Geological-geochemical characteristics of Lianhuashan porphyry tungsten deposit and its origin: Geochimica, v. 6, no. 2, p. 121–132.

Thurber, W.C., 1985, China most aggressive: American Metal Market Metalworking News, Tungsten Special Issue, February 6, 1985, p. 9A, 11A.

U.S. Bureau of Mines, 1985, Mineral commodity summaries 1985: U.S. Bureau of Mines, p. 168–169.

———1988, Mineral commodity summaries 1988: U.S. Bureau of Mines, p. 172–173.

Wan Bing, 1982, The Damingshan strata-bound tungsten deposits in Guangxi Zhuang Autonomous Region, China, *in* Hepworth, J.V., and Yu Hong Zhang, eds., Tungsten geology, Jiangxi, China: Bandung, Indonesia, ESCAP/RMRDC, p. 403–412.

Wang Changlie, Xu Youzhi, Xie Ciguo, and Xu Wenguang, 1982, The geological characteristics of Shizhuyuan W-Sn-Mo–Bi deposit, *in* Hepworth, J.V., and Yu Hong Zhang, eds., Tungsten geology, Jiangxi, China: Bandung, Indonesia, ESCAP/RMRDC, p. 413–425.

Wang, H.C., Hsu, Y.T., and Hsiu, H.C., 1930, Report on the Yao Kanghsien wolframite mine, Tzehsing: Geological Survey of Hunan, Bulletin 10, Economic Geology, v. 7, p. 7–11.

Wang Zehua and Zhou Yuzhen, 1982, Major features of two-layered type mineralization in Xihuashan mine and its genetic model, *in* Hepworth, J.V., and Yu Hong Zhang, eds., Tungsten geology, Jiangxi, China: Bandung, Indonesia, ESCAP/RMRDC, p. 427–436.

Wu Weisum, 1982, Beneficiation and upgrading of tungsten ores in China, *in* Tungsten—1982, Proceedings of the Second International Tungsten Symposium, San Francisco, June 1982: London, Mining Journal Books, Ltd., p. 64–70.

Wu Yongle and Mei Yong Wen, 1982, Multi-phase intrusion and multi-phase mineralization in Xihuashan tungsten ore field, *in* Hepworth, J.V., and Yu Hong Zhang, eds., Tungsten geology, Jiangxi, China: Bandung, Indonesia, ESCAP/RMRDC, p. 437–449.

Xia Hongyuan, Liang Shuyi, Xie Weixin, and Shuai Dequan, 1982, Primary zoning of Huangsha tungsten deposit and its genesis, *in* Hepworth, J.V., and Yu Hong Zhang, eds., Tungsten geology, Jiangxi, China: Bandung, Indonesia, ESCAP/RMRDC, p. 451–461.

Xu Keqin, Hu Shouci, Sun Minzhi, Zhang Jingrong, Ye Jun, and Li Huiping, 1982, Regional factors controlling the formation of tungsten deposits in south China, *in* Hepworth, J.V., and Yu Hong Zhang, eds., Tungsten geology, Jiangxi, China: Bandung Indonesia, ESCAP/RMRDC, p. 473–488.

Yan Mei-Zhong, Wu Yong-Le, and Li Chong-You, 1980, Metallogenetic systems of tungsten in southeast China and their mineralization characteristics, *in* Ishihara, S., and Takenouchi, S., eds., Granitic magmatism and related mineralization: Mining Geology Special Issue, No. 8, pp. 215–221.

Yang Minggui and Lu Dekui, 1982, Structural characteristics, forms of arrangement and composition of the vein-type tungsten ore in Xihuashan-Piaotang district, *in* Hepworth, J.V., and Yu Hong Zhang, eds., Tungsten geology, Jiangxi, China: Bandung, Indonesia, ESCAP/RMRDC, p. 521–531.

Yang Zunyi, Cheng Yuqi, and Wang Hongzhen, 1986, The geology of China: Oxford, Clarendon Press, 303 p.

Zhang, Zh. M., Liou, J.G., and Coleman, R.G., 1984, An outline of the plate tectonics of China: Geological Society of America Bulletin, v. 95, p. 295–312.

Chapter J

Tungsten—Grades and Tonnages of Some Deposits

By W. DAVID MENZIE, GAIL M. JONES, and JAMES E. ELLIOTT

U.S. GEOLOGICAL SURVEY BULLETIN 1877

CONTRIBUTIONS TO COMMODITY GEOLOGY RESEARCH

CONTENTS

FIGURES

TABLES

Tungsten—Grades and Tonnages of Some Deposits

By W. David Menzie, Gail M. Jones, *and* James E. Elliott

Abstract

Descriptive and grade/tonnage models of ore deposits are important tools for mineral exploration, regional mineral-resource assessment, and commodity availability studies. Tungsten has been produced as a primary commodity mostly from two deposit types: scheelite-bearing skarns and wolframite-bearing quartz veins. Grade/tonnage models built with data from 36 skarn and 19 vein deposits indicate that these deposit types do not differ greatly in tonnage or grade. Half of the scheelite-bearing skarns have tonnages greater than just less than 1 million metric tons, and half of the wolframite-bearing quartz veins have tonnages that exceed 680 thousand metric tons. Although the veins have slightly smaller tonnages than the skarns, they have slightly higher grades. Half of the veins have grades that exceed 0.8 weight percent WO_3, while half the skarns have grades that exceed 0.64 weight percent WO_3. In contrast to their similarity in grades and tonnages, vein and skarn deposits differ in important characteristics including tectonic setting, environment of formation, morphology, mineralogy, and associated alteration assemblages.

Although tungsten has been produced mainly from two types of deposits, it is known to occur in a variety of geologic settings, and new types of deposits are being recognized. From the perspective of potential supply, porphyry (or stockwork) tungsten-molybdenum deposits may be an important new deposit type. Examples include the deposits at Mount Pleasant, New Brunswick, Canada; Logtung, Yukon Territory, Canada; Yangchuling, Jiangxi province, People's Republic of China; and Xingluokeng, Fujian province, People's Republic of China. These deposits are associated with composite granites and possess distinctive metals (W, Mo, Bi) and alteration assemblages. Available grade/tonnage data of these deposits range from tens to hundreds of millions of metric tons of ore containing from 0.1 to 0.3 percent WO_3.

INTRODUCTION

Descriptive and grade/tonnage models are important tools for mineral exploration and regional resource assessment. Such models are established for many types of deposits including rhyolite-hosted, replacement (exhalative?), vein, greisen, and skarn tin deposits (Reed, 1986a–c; Reed and Cox, 1986; Reed and others, 1986; Menzie and others, 1988). This paper discusses and presents grade tonnage models of scheelite-bearing skarn and wolframite-bearing quartz vein deposits, presently the most important sources of tungsten. Another deposit type—porphyry tungsten-molybdenum—may be an important source of tungsten in the future and is discussed briefly.

Tungsten has been produced as a primary commodity mainly from two deposit types, scheelite-bearing skarns and wolframite-bearing quartz veins, that occur in plutonic environments. The plutonic environment, however, is not the only geologic environment in which tungsten occurs. Others include shallow, low-temperature geologic environments such as hot springs and lake brines (Hobbs and Elliott, 1973). In addition, tungsten deposits have been identified in new environments including the shallow intrusive (porphyry), submarine volcano-sedimentary (strata-bound), and subaerial volcanic (hot springs), and the environments of formation of some previously known deposits have been reinterpreted.

TUNGSTEN SKARN DEPOSITS

Tungsten skarn deposits occur at or near contacts of carbonate rocks and calc-alkaline granitic bodies, which vary from batholithic to stock size. The composition of intrusives that are associated with skarns may vary from granodiorite to granite (Newberry and Swanson, 1985; classification based on Streckeisen, 1975), and the intrusives usually have coarse-grained, equant to porphyritic textures. The granites form from water-undersaturated, contaminated "I" type magmas, and the skarns form at relatively high pressures (Newberry and Swanson, 1985).

Tungsten skarns form at high temperatures (400–600 °C) and under relatively reducing conditions compared to many other deposit types, such as porphyry copper deposits. However, the mineralogy of skarns and the composition of calc-silicate minerals define both reduced and oxidized types (Morgan, 1975; Einaudi and others, 1981). Many tungsten skarns show a common sequence of discrete stages of formation. This sequence is (1) prograde thermal metamorphism, (2) high-temperature garnet-pyroxene-scheelite metasomatism, (3) lower temperature amphibole-biotite-

Table 1. Deposits used to construct the tungsten skarn model

Deposit name	Location	Source of data
Baily	Yukon Territory, Canada	5
Brejui	Rio Grande de Norte, Brazil	16
Calvert	Montana, U.S.A.	9
Cantung	Northwest Territories, Canada	17
Costabonne	Pyrennes, France	18
Dublin Gulch	Yukon Territory, Canada	5
Emerald-Dodger	British Columbia, Canada	1,11
Gardnerville	Nevada, U.S.A.	21
Gunmetal	do.	21
Hope Valley	California, U.S.A.	21
Iron Mountain	New Mexico, U.S.A.	21
Kara	Tasmania, Australia	13
King Island	do.	3
Lost Creek	Montana, U.S.A.	10
Lucky Mike	British Columbia, Canada	4
Mactung	Northwest Territories, Canada	4
Maykhura	U.S.S.R.	11
Molyhill	Northern Territory, Australia	13
Mount Alexander	West Australia, Australia	13
Milford	Utah, U.S.A.	6
Nevada-Massachusetts	Nevada, U.S.A.	21
Nevada Scheelite	do.	14,19
Osgood Range	do.	8
Pine Creek	California, U.S.A.	21
Quixaba	Brazil	11
Ray Gulch	Yukon Territory, Canada	5
Risby	do.	7
Salau	Ariege, France	18
Sangdong	Kan Won Province, Republic of Korea	12
Stormy Group	Yukon Territory, Canada	5
Tem Piute	Nevada, U.S.A.	20
Tyrny Auz	North Caucasus, U.S.S.R.	11
Uludag	Turkey	11,15
Victory	British Columbia, Canada	5
Yellow Pine	Idaho, U.S.A.	2
Ysxjoberg	Sweden	11

Sources of data for tungsten skarn grade/tonnage model (table 1)

1. British Columbia Department of Mines and Petroleum Resources, 1973, Geology, Exploration and Mining in British Columbia, 642 p.
2. Cook, E.F., 1956, Tungsten deposits of south-central Idaho: Idaho Bureau of Mines and Geology Pamphlet No. 108, 40 p.
3. Danielson, M.J., 1975, King Island scheelite deposits, *in* Knight, C.L., ed., Economic geology of Australia and Papua New Guinea, v. 1, Metals: The Australasian Institute of Mining and Metallurgy, Monograph Series no. 5, p. 592–598.
4. Einaudi, M.T., Meinert, L.D., and Newberry, R.J., 1981, Skarn deposits, *in* Skinner, B.J., ed., Economic Geology, 75th Anniversary Volume: p. 317–391.
5. Energy, Mines and Resources Canada, 1980, Canadian mineral deposits not being mined in 1980: Mineral Policy Sector, Internal Report MRI 80/7, 294 p.
6. Everett, F.D., 1961, Tungsten deposits in Utah: U.S. Bureau of Mines Information Circular 8014, p. 40–41.
7. Financial Times, 1986, Mining international yearbook: Essex, England, Longman Group Ltd., 547 p.
8. Hotz, P.E., and Willden, R., 1964, Geology and mineral deposits of the Osgood Mountains quadrangle, Humboldt County, Nevada: U.S. Geological Survey Professional Paper 431, 128 p.
9. Krohn, D.H., and Weist, M.M., 1977, Principal information of Montana mines: Montana Bureau of Mines and Geology, Special Publication 75,150 p.
10. Larson, L.P., Lowrie, R.L., and Leland, G.R., 1971, Availability of tungsten at various prices from resources in the United States: U.S. Bureau of Mines Information Circular 8500, 65 p.
11. Laznicka, Peter, compiler, 1973, Manifile—The University of Manitoba file of nonferrous metal deposits of the world, pt. 2: Winnipeg, University of Manitoba, Department of Earth Science, 767 p.
12. Lemmon, D.M., and Ross, D.C., 1956, Resources, chap. II, *in* Materials survey—Tungsten: U.S. Department of Commerce, Business and Defense Services Administration, compiled for the Office of Defense Mobilization, p. II-1–II-16.
13. Louthean, Ross, ed., 1986, Register of Australian mining 1984–85: Sydney, Australia, Australian Consolidated Press Ltds., 488 p.
14. Mining Congress Journal, 1979, v. 65, no. 7, p. 10, 13.
15. Mining Magazine, 1979, v. 140, no. 6, p. 501.
16. Ministero das Minas e Energia (Brazil), 1969, Relatorio Preliminar Sobre as Investigacoes Geological na Minas Breje—R.N. (Projeto Tungstenio/Molibdeno), Recife, Brazil, 53 p.
17. Pazour, D.A., 1979, Canada Tungsten to double production: World Mining, v. 32, no. 4, p. 50–54.
18. Pouit, Georges, and Fortune, Jean-Pol, 1980, Metallogenesis of Pyrenees compared with that of the Southern Massif Central: International Geological Congress, 26th, Paris 1980, Excursion 205, p. 109–161.
19. Schilling, J.H., 1964, Tungsten, *in* Mineral and water resources of Nevada: Nevada Bureau of Mines and Geology Bulletin 65, p. 155–161.
20. Wall Street Journal, 1977, Union Carbide advertisement, July 5, p. 7.
21. Proprietary data.

sulfide metasomatism, and (4) chlorite-calcite-epidote-quartz retrograde metamorphism and metasomatism (Meinert and others, 1981). Scheelite may be formed during stages 2, 3, and 4, but sulfides are generally restricted to stage 3.

The formation of skarn deposits is controlled by the shape of the contact of the intrusive rock, by the presence of favorable beds in the host rock sequence, and by structural relations of the strata to the contact (Bateman, 1965; Hobbs and Elliott, 1973). Skarns commonly form at irregularities in the contact, especially where there is an overhang of the granitic contact (Bateman, 1982). They form by the metasomatism of relatively pure marble or limestone, and their formation is enhanced where the bedding of the sedimentary rocks dips into, rather than away from, the intrusive contact. Other structures such as premineral faults and plunging troughlike features in the intrusive contact may also be important.

The grade/tonnage model of scheelite-bearing skarns is built with data from 36 deposits (table 1). The majority of the deposits are from the United States and Canada, but deposits from Australia, Brazil, France, Korea, and Sweden are also included. In most cases, the data include past production plus reserves and resources. Because it is

commonly difficult to define precisely what constitutes a skarn deposit from mineral production, reserve, and resource data, all bodies of mineralized skarn associated with the contact of a particular intrusion are considered to belong to one "deposit." Thus physically separate skarns on opposite sides of an intrusion were considered to be parts of the same deposit in order to maintain consistency in the data. Lognormal distributions fit the observed distributions of both grade and tonnage, and the two variables are not significantly correlated (r=0.06). Ninety percent of the deposits contain at least 41,000 metric tons (t), half of the deposits contain just less than 1 million t (fig. 1). Ninety percent of the skarn deposits have grades of at least 0.30 percent, half have grades of at least 0.64 percent, and 10 percent have grades of at least 1.3 percent WO_3 (fig. 1).

WOLFRAMITE-BEARING QUARTZ VEIN DEPOSITS

Wolframite-bearing quartz vein deposits are widely distributed and as recently as 1973 accounted for more than three-fourths of the world reserves of tungsten (Hobbs and Elliott, 1973). The great bulk of these reserves occur in southeastern China, the most productive region in the world for tungsten.

These deposits are similar to most lode tin deposits and many molybdenum deposits in that they are found associated with highly evolved and highly differentiated granites that can be generally classified as specialized or tin-bearing granites (Tischendorf, 1977). These granites form multiphase, composite plutons of biotite or biotite-muscovite granite. In southeastern China, the majority of wolframite-bearing quartz-vein deposits are associated with granites of the early Yanshanian (mostly Jurassic in age) period (Yan and others, 1980) that are highly enriched in tungsten, tin, niobium, and tantalum and are compositionally similar to granites associated with Climax-type molybdenum deposits (Mutschler and others, 1981) in the United States and to tin-bearing granites (Tischendorf, 1977) in many other parts of the world.

Found commonly with granite stocks or cupolas that form topographic highs or ridges of granite batholiths, these tungsten deposits occur both within the intrusive rock (endocontact) and in the adjacent metasedimentary rocks (exocontact). Wolframite-bearing quartz veins commonly are steeply dipping to vertical as at Xihuashan and Dajishan, southeastern China, but may be flat lying or subhorizontal as at Panasqueira, Portugal (Kelly and Rye, 1979).

In many exocontact deposits in China, the quartz veining shows distinctive vertical zonation in the morphology and mineralogy of the veins and veinlets (Yan and others, 1980). The upper zone consists of closely spaced abundant quartz-mica veinlets containing small, subeconomic amounts of ore minerals such as wolframite and

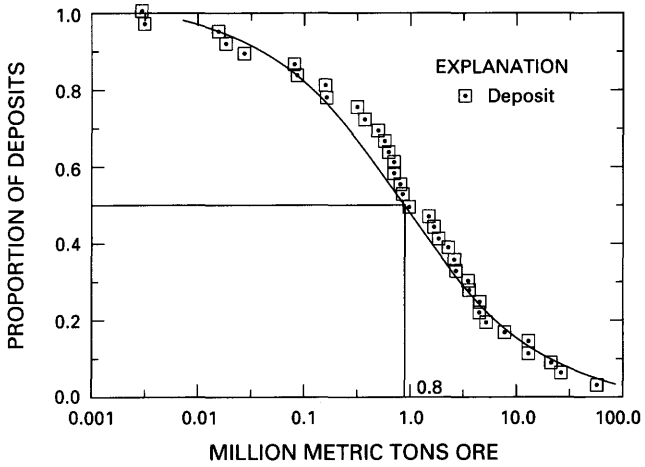

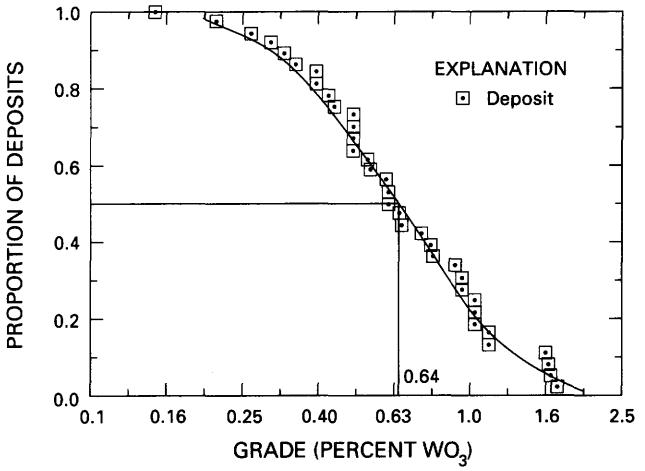

Variable	Number of deposits in the model	90%	50%	10%
Ore tonnage, in million metric tons	36	0.041	0.80	18
Average weight percent WO_3	36	0.30	0.64	1.3

Figure 1. Grade-tonnage model for tungsten skarn deposits.

cassiterite. Downward, the veinlets increase in thickness but decrease in number through an intermediate zone that contains most of the economic mineralization to a lowermost subeconomic zone of sparse, thick veins (typically 1 to 3 m) near or within the intrusion. These zoned systems also show complex parageneses in crosscutting vein relations that include silicate, oxide, sulfide, and carbonate stages (Yan and others, 1980). The silicate stage is characterized by formation of calc-silicate and other silicate minerals as skarn or hornfels in the metasedimentary rocks of the contact zone. This stage is followed by the oxide, or main ore, stage that includes most of the wolframite, scheelite,

Table 2. Deposits used to construct the wolframite-bearing quartz vein model

Deposit name	Location	Source of data
Bir Tawila	Saudi Arabia	15
Carrock Fell	England	2
Chicote Grande	Bolivia	17
Chojilla area	do.	7
Grey River	Newfoundland	8
Hamme district	North Carolina	16,5
Isla de Pinos	Cuba	11
Josefina	Argentina	3
Kami	Bolivia	1
Los Avestruces	Argentina	18
Los Condores	do.	3
Montredon	France	13
Needle Hill	Hong Kong	4
Oakleigh Creek	Tasmania	14
Panasqueira	Portugal	19
Pasto Bueno	Peru	9,12
San Martin	Argentina	3
Storeys Creek	Tasmania	6,10
Xihuashan	China	20

Sources of data for wolframite vein grade/tonnage model (table 2)

1. Ahlfeld, Federico, and Schneider-Scherbina, Alejandro, 1964, Los yacimientos minerales y hidrocarburos de Bolivia: Bolivia Ministerio de Minas y Petroleo, Servicio Geologico, Bol. no. 5 especial, 388 p.
2. Ball, T.K., Fortey, N.J., and Shepard, T.J., 1985, Mineralization at the Carrock Fell tungsten mine, N. England: Paragenetic, fluid inclusion and geochemical study: Mineralium Deposita, v. 20, p. 57–65.
3. Bundesanstalt fur Geowissenschaften und Rohstoffe, 1975, Argentina: Rohstoffwirtschaftliche Landerberichte, v. 10, 118 p.
4. Davis, S.G., 1961, Mineralogy and genesis of the wolframite ore deposit, Needle Hill mine, New Territories, Hong Kong: Economic Geology, v. 56, no. 7, p. 1238–1249.
5. Espenshade, G.H., 1947, Tungsten deposits of Vance County, North Carolina, and Mecklenburg County, Virginia: U.S. Geological Survey Bulletin 948–A, p. 1–17.
6. Financial Times, 1972, Mining international year book 1972–73: London, England, FT Business Publications Limited, 693 p.
7. ———1986, Mining international year book 1986: Essex, England, Longman Group Limited, 547 p.
8. Higgins, N.C., 1985, Wolframite deposition in a hydrothermal vein system—The Grey River tungsten prospect, Newfoundland, Canada: Economic Geology, v. 80, no. 5, p. 1297–1327.
9. Hyde, D.M., 1983, The mineral industry of Peru: Mineral yearbook 1981, v. 3, Area reports: International, p. 773–782.
10. Kingsbury, C.J.R., 1965, Cassiterite and wolframite veins of Aberfoyle and Storeys Creek, *in* McAndrew, John, ed., Geology of Australian ore deposits: Commonwealth Mining and Metallurgical Congress, Australia and New Zealand, 8th, v. 1, Melbourne, 1965, p. 506–511.
11. Li, K.C., and Wang, C.Y., 1955, Tungsten—Its history, geology, ore-dressing, metallurgy, chemistry, analysis, applications, and economics (American Chemical Society Monograph no. 94, 3d ed.): New York, Reinhold Publishing, 506 p.
12. Malaga Santolalla, Fermin, 1954, El tungsteno en el Peru: Sociedad Geologica Del Peru, Bol. 27, 186 p.
13. Pouit, Georges, and Fortune, J.P., 1980, Metallogenie comparée des Pyrenees et du sud du Massif Central—Itineraires geologiques, excursions dans "le Grand Sud-ouest," preparées dans le cadre du 26e Congres Géologique International: (Paris, Juillet 1980), Aquitaine, Languedoc, Pyrenees, Bulletin des Centres de Recherches Exploration-Production Elf-Aquitaine, Memoire no. 3, p. 381–439.
14. Register Australian Mining, 1981: Leederville, Western Australia, Lodestone Press Pty Ltd., p. 190.
15. Salpeteur, I., 1985, Geochemical dispersion from the Bir Tawilah wolfram-quartz veins in the pediplain of Saudi Arabia: The Institution of Mining and Metallurgy, Prospecting in Areas of Desert Terrain, p. 141–154.
16. U.S. Bureau of Mines, Calculated cumulative deposit production from mineral data canvass. (Individual records on microfilm files are proprietary.)
17. Valasco, Pablo, 1985, The mineral industry of Bolivia, *in* U.S. Bureau of Mines; Minerals yearbook 1983, v. 3, Area reports—International: Washington, D.C., U.S. Government Printing Office, p. 111–120.
18. Willig, C.D., and Delgado, J., 1985, South America as a source of tungsten, *in* Primary Tungsten Association: Madrid, Spain, International Tungsten Symposium, 3d, 36 p.
19. Proprietary data.
20. Estimate by author.

cassiterite, beryl, minor sulfide minerals, and lithium-bearing micas in quartz veins. Sulfide minerals, including pyrite, sphalerite, galena, and other sulfide minerals, as well as minor wolframite and cassiterite, are deposited in quartz veins during the sulfide stage. The late carbonate stage is characterized by minor amounts of tungsten- and tin-bearing minerals in fluorite-pyrite-carbonate-quartz veins.

At the most famous tungsten mine in China, Xihuashan in the Dayu district, Jiangxi province, the orebodies occur as parallel sets of several hundred steeply dipping quartz veins across a 2.5-km distance (Tanelli, 1982). Each set or zone of quartz veins has economic mineralization over vertical ranges of 250 to 300 m and shows vertical zonation in ore and alteration mineralogy (Wu and Mei, 1982). Wolframite is concentrated mostly in the middle to upper parts of the veins; sulfides are highest in the lower to middle sections; and calcite and fluorite are most abundant in the lower parts. Alteration varies from predominantly potash feldspathization in the lower parts to predominantly greisenization in the upper parts of each vein.

The grade/tonnage model of wolframite-bearing quartz veins has been built with data from 19 deposits (table 2). Although the deposits are distributed worldwide, China is represented by only one deposit even though it has the largest number of important deposits of this type. Data for many of the deposits include reserves, resources, and past production. Ninety percent of the deposits contain at least 60,000 t of ore, half contain at least 680,000 t, and 10 percent contain at least 7.7 million t (fig. 2). Figure 2 also presents the distribution of tungsten grades for WO_3 in the deposits. Ninety percent of the deposit grades exceed 0.5 percent; 50 percent exceed 0.8 percent; and 10 percent exceed 1.4 percent WO_3. Lognormal distributions fit the

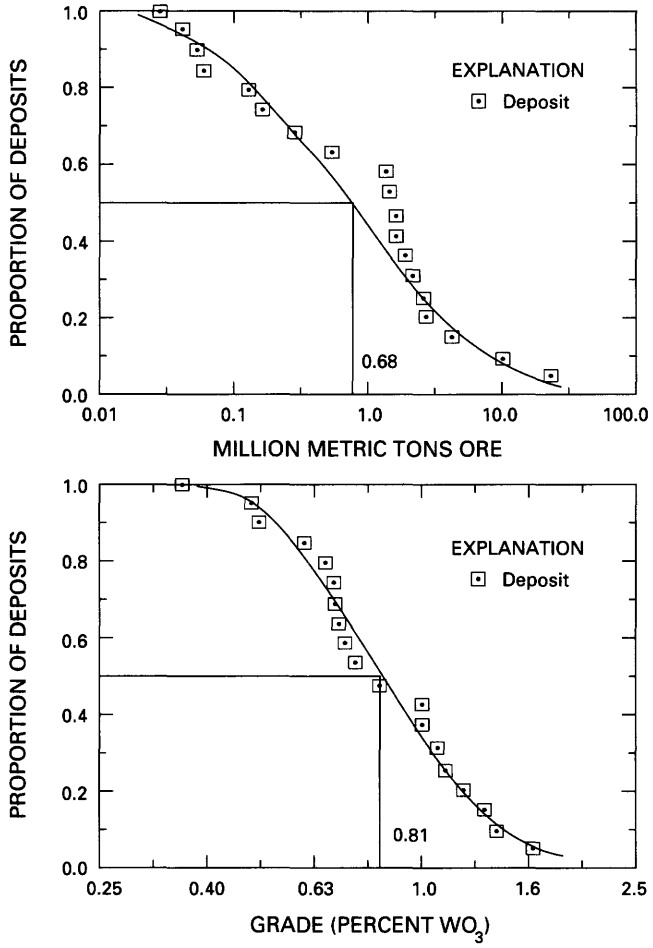

Variable	Number of deposits in the model	90%	50%	10%
Ore tonnage, in million metric tons	19	0.06	0.68	7.7
Average weight percent WO_3	19	0.52	0.81	1.4

Figure 2. Grade-tonnage model for quartz-wolframite vein deposits.

observed distributions of tonnage and grade well. The correlation coefficient ($r=-0.45$) shows a marginally significant inverse correlation between grade and tonnage at a 5-percent significance level.

PORPHYRY TUNGSTEN-MOLYBDENUM DEPOSITS

Porphyry or stockwork tungsten-molybdenum deposits (Hobbs and Elliott, 1973) represent another class of deposit; studies have been published on only a few of this type. Deposits that have been described include the Mount Pleasant deposit, New Brunwick, Canada (Parrish, 1982); the Logtung deposit, Yukon territory, Canada (Noble and others, 1984); the Yangchuling deposit, Jiangxi province People's Republic of China (Yan and others, 1980); and Xingluokeng, Fujian province, People's Republic of China (Liu, 1982).

The Xingluokeng, Yangchuling, and Logtung deposits include scheelite, wolframite, and molybdenite as disseminated grains, in veins and veinlets, and in breccia pipes in or above epizonal granitic rocks. The deposits are associated with late phases of granodiorite to granite (monzogranite) stocks. The stocks are emplaced into contact-metamorphosed clastic sedimentary rocks. The deposits show several generations of mineralization. The main ore minerals are scheelite, wolframite, and molybdenite; bismuthinite, pyrrhotite, pyrite, sphalerite, arsenopyrite, galena, and chalcopyrite are also present. Alteration assemblages include K-feldspar, biotite, quartz, sericite, and montmorillonite (Yan and others, 1980; Liu, 1982; and Noble and others, 1984).

The Fire Tower zone near Mount Pleasant consists of wolframite, molybdenite, native bismuth, sphalerite, arsenopyrite, chalcopyrite, stannite, and galena disseminated in brecciated rhyolite porphyry. The rhyolite porphyry, which changes gradationally with depth to microgranite, was emplaced into a quartz feldspar porphyry unit that probably contains both intrusive and extrusive rocks. The deposits are strongly zoned in terms of the metal content, mineralogy, and types of altered rocks (Parrish, 1982).

Grade and tonnage data are available for deposits near Mount Pleasant (Parrish, 1982) and Logtung (Noble and others, 1984). Liu (1982) presents data on grades and physical dimensions of the Xingluokeng deposit. While these data are too few to construct a grade/tonnage model, they are adequate to obtain a rough idea of the magnitude of tonnages and grades for these deposits. These few data suggest porphyry tungsten-molybdenum deposits contain from a few tens of millions to a few hundreds of millions of metric tons of ore. Grades of WO_3 probably vary from 0.1 to 0.3 percent; grades of molybdenum probably vary from about 0.01 to 0.1 percent.

DISCUSSION

Mineral deposit and grade/tonnage models are useful aids in making decisions with regard to land classification, mineral exploration, and mineral availability. Figure 3 shows three types of tungsten grade/tonnage domains derived from such models. For the tungsten skarns and wolframite-bearing quartz veins, the domain is defined by the mean plus and minus one standard deviation of the logarithms of grade and tonnage. These domains should contain about 45 percent of deposits of each type. The domain for porphyry tungsten-molybdenum deposits is an

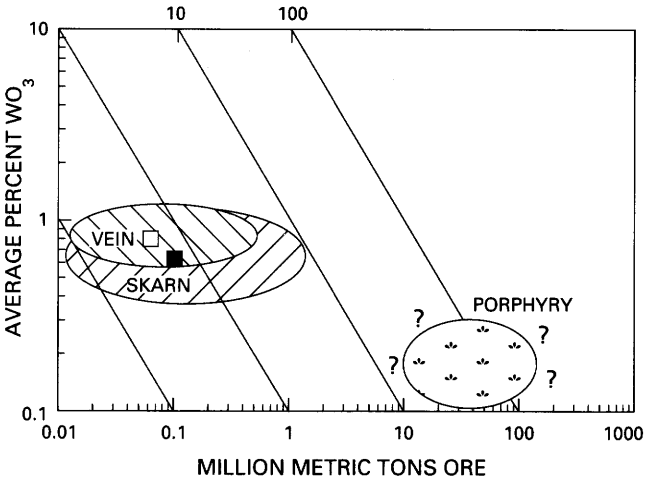

Figure 3. Grade and tonnage domains for tungsten skarn, wolframite-bearing quartz vein, and tungsten-molybdenum porphyry deposits. Domains for skarn and vein deposits are defined by the mean plus and minus one standard deviation of the logarithms of the grade and tonnage data. Domain for porphyry deposits is approximate.

approximation based upon limited data. Figure 3 shows the slight differences between skarn and vein types and the greater differences between these types and the porphyry tungsten-molybdenum deposits.

REFERENCES

Bateman, P.C., 1965, Geology and tungsten mineralization of the Bishop district, California: U.S. Geological Survey Professional Paper 470, 208 p.

———1982, Scheelite-bearing skarns of the east-central Sierra Nevada, California, U.S.A., *in* Hepworth, J.V., and Yu Hong Zhang, eds., Symposium on tungsten geology, Jiangxi, People's Republic of China, 1981, Proceedings: ESCAP/RMRDC, Bandung, Indonesia, p. 23–31.

Einaudi, M.T., Meinert, L.D., and Newberry, R.J., 1981, Skarn deposits, *in* Skinner, B.J., ed., Economic Geology, 75th Anniversary Volume: p. 139–183.

Hobbs, S.W., and Elliott, J.E., 1973, Tungsten, *in* Brobst, D.A. and Pratt, W.P., eds., United States mineral resources: U.S. Geological Survey Professional Paper 820, p. 667–678.

Kelly, W.C., and Rye, R.O., 1979, Geologic, fluid inclusion, and stable isotope studies of the tin-tungsten deposits of Panasqueira, Portugal: Economic Geology, v. 74, p. 1721–1822.

Liu Wengzhang, 1982, Geological features of mineralization of the Xingluokeng tungsten (molybdenum) deposit, Fujian Province, *in* Hepworth, J.V., and Yu Hong Zhang, eds., Symposium on tungsten geology, Jiangxi, People's Republic of China, 1981, Proceedings: ESCAP/RMRDC, Bandung, Indonesia, p. 339–348.

Meinert, L.D., Newberry, Rainer, and Einaudi, M.T., 1981, An overview of tungsten, copper, and zinc-bearing skarns in western North America, *in* Silberman, M.L., Field, C.W., and Berry, A.L. eds., Proceedings of the symposium on mineral deposits of the Pacific Northwest: U.S. Geological Survey Open-File Report 81–355, p. 303–327.

Menzie, W.D., Reed, B.L., and Singer, D.A., 1988, Grades and tonnages of some lode tin deposits, *in* Hutchinson, C.S., ed., Geology of tin deposits in Asia and the Pacific: Berlin, Springer-Verlag, p. 73–88.

Morgan, B.A., 1975, Mineralogy and origin of skarns in the Mount Morrison pendant, Sierra Nevada, California: American Journal of Science, v. 275, p. 119–142.

Mutschler, F.E., Wright, E.G., Ludington, Steve, and Abbott, J.T., 1981, Granite molybdenite systems: Economic Geology, v. 76, p. 874–897.

Newberry, R.J., and Swanson, S.E., 1985, Granites associated with tungsten skarns, *in*, Taylor, R.P., and Strong, D.F., eds., Granite-related mineral deposits: Halifax, Nova Scotia, Canada, CIM, p. 197–199.

Noble, S.R., Spooner, E.T.C., and Harris, F.R., 1984, The Logtung large tonnage, low grade W (scheelite)-Mo porphyry deposit, South-Central Yukon Territory: Economic Geology, v. 79, p. 848–868.

Parrish, I.S., 1982, The Mt. Pleasant tungsten deposit, Canada, *in* Hepworth, J.V., and Yu Hong Zhang, eds., Symposium on tungsten geology, Jiangxi, People's Republic of China, 1981, Proceedings: ESCAP/RMRDC, Bandung, Indonesia, p. 165–178.

Reed, B.L, 1986a, Replacement Sn, *in* Cox, D.P., and Singer, D.A., eds., Mineral deposit models: U.S. Geological Survey Bulletin 1693, p. 61.

———1986b, Sn veins, *in* Cox, D.P., and Singer, D.A., eds., Mineral deposit models: U.S. Geological Survey Bulletin 1693, p. 70.

———1986c, Sn greisen, *in* Cox, D.P., and Singer, D.A., eds., Mineral deposit models: U.S. Geological Survey Bulletin 1693, p. 70.

Reed, B.L., and Cox, D.P., 1986, Sn Skarns, *in* Cox, D.P., and Singer, D.A., eds., Mineral deposit models: U.S. Geological Survey Bulletin 1693, p. 58.

Reed, B.L., Duffield, W., Ludington, S.D., Maxwell, C.H. and Richter, D.H., 1986, Rhyolite-hosted Sn, *in* Cox, D.P., and Singer, D.A., eds., Mineral deposit models: U.S. Geological Survey Bulletin 1693, p. 172.

Streckeisen, A., 1975, To each plutonic rock its proper name: Earth-Science Reviews, v. 12, p. 1–33.

Tanelli, G., 1982, Geological setting, mineralogy and genesis of tungsten mineralization in Dayu district, Jiangxi (People's Republic of China)—An outline: Mineralium Deposita, v. 17, p. 279–294.

Tischendorf, G., 1977, Geochemical and petrographic characteristics of silicic magmatic rocks associated with rare-element mineralization, *in* Stemprok, M., Burnol, L., and Tischendorf, G., eds., Metallization associated with acid magmatism, v. 2: Prague, Czechoslovakia Geological Survey, p. 41–96.

Wu Yongle, and Mei Yong Wen, 1982, Multi-phase intrusion and multi-phase mineralization in Xihuashan tungsten ore field, *in* Hepworth, J.V., and Yu Hong Zhang, eds., Symposium

on tungsten geology, Jiangxi, People's Republic of China, 1981, Proceedings: ESCAP/RMRDC, Bandung, Indonesia, p. 437–449.

Yan Meizhong, Wu Yongle, and Li Chongyou, 1980, Metallogenetic systems of tungsten in southeast China and their mineralization characteristics, *in* Ishihara, Shunso, and Takenouchi, Sukune, eds., Granitic magmatism and related mineralization: Mining Geology Special Issue 8, p. 215–221.

Chapter K

Vanadium—Resources in Fossil Fuels

By GEORGE N. BREIT

U.S. GEOLOGICAL SURVEY BULLETIN 1877

CONTRIBUTIONS TO COMMODITY GEOLOGY RESEARCH

CONTENTS

TABLES

Vanadium—Resources in Fossil Fuels

By George N. Breit

Abstract

Significant amounts of vanadium are made available for commercial use as a byproduct of petroleum, while minor amounts are produced as byproducts of coal and oil shale. Depending on the future demand for fossil fuels, vanadium recovered from these sources could satisfy a substantial portion of the world's vanadium needs. Though the United States does not possess large resources of vanadiferous fossil fuels comparable to those in Venezuela, Australia, and Canada, vanadium contained in heavy oils in California and in oil shales in Montana and Kentucky may some day satisfy domestic needs.

Vanadium is variably distributed in fossil fuels. It occurs as oil-soluble organic complexes, particularly porphyrins (tetrapyrroles), and in authigenic minerals. The vanadium content of fossil fuels is related to the origin and composition of the organic matter as well as depositional conditions and diagenetic history. The origin of vanadium and mechanisms of concentration are incompletely understood, though it seems likely that the interaction of seawater and terrestrial sediments surrounding depositional basins mobilized a portion of the metal incorporated into the organic material.

INTRODUCTION

In 1985, approximately one-half of the domestic vanadium requirement of the United States was satisfied by recovery of the metal as a byproduct of petroleum processing and consumption (Hilliard, 1987). The magnitude of this production highlights the potential of vanadium produced from oil and other organic-rich geologic materials. If the projected reliance on metal-rich oils is accurate (International Petroleum Encyclopedia, 1985), the amount of byproduct vanadium could increase dramatically. Approximately 10 percent of the world's vanadium resources are contained in tar sands and petroleum (Kuck, 1985). Future energy demands may favor worldwide development of oil shales and other presently uneconomic fossil fuel resources that contain large amounts of vanadium.

In addition to petroleum, byproduct vanadium has been produced from the mining and beneficiation of iron, uranium, phosphate, and aluminum; in these deposits, the vanadium content rarely exceeds 1 percent. In the recent past, the demand for vanadium in the United States was satisfied largely by uranium ores mined on the Colorado Plateau. A large drop in the price of uranium closed most of these mines, forcing vanadium mills in the United States to rely on imported feedstocks, such as iron slags from South Africa and petroleum residues. Whereas most petroleum residues are from imported oils, development of some of the domestic heavy oil resources could satisfy a substantial portion of the United States' vanadium demand.

This paper focuses on vanadium resources contained in petroleum, coal, tar sands, and oil shale. The evaluation includes a brief review of vanadium production from and resources in these materials, a discussion of the form of the metal, and speculation on the origin of the variable amounts of vanadium in these materials. This paper is not intended as a thorough review of vanadium resources in organic-rich geologic materials but as an introduction to the importance of these materials in projecting future vanadium supplies. The important problems related to recovering the vanadium contained in these materials are not addressed.

PRODUCTION AND RESOURCES IN FOSSIL FUELS

Petroleum

Crude oils contain vanadium concentrations from less than 0.2 parts per million (ppm) to 1,400 ppm (table 1). The highest vanadium contents are generally associated with heavy oils, those having API gravity lower than 20°. Heavy oils also contain high abundances of sulfur and asphaltenes (Yen, 1975), which cause problems during refining (International Petroleum Encyclopedia, 1985). Decreasing supplies of lighter oils have favored production of these metal-rich oils, and refineries and oil production facilities have been designed to accommodate associated processing problems (Peer, 1981).

Vanadium is recovered from oil by processing ash generated in thermoelectric power plants, petroleum coke residues generated during refining of heavy oils, and residues plated onto catalysts. An estimated 3,000 metric tons (t) of vanandium (10 percent of the world's vanadium

Table 1. Range of vanadium abundances in petroleum from various locations

[Data from Whisman and Cotton, 1971; Nelson, 1972; and Kuck, 1985]

Location	Vanadium (ppm)
Abu Dhabi	<1–1.3
Australia	<1–2
Indonesia	<1
Iran	16–150
Israel	<1
Libya	0.2–28
Mexico	10–80
Nigeria	<1–4
North Sea	<1–19
Venezuela	0.3–1,400
United States	
Alaska	<1–100
Arkansas	<1–15
California	<1–400
Louisiana	<1–15
Mississippi	<1–40
Oklahoma	<1–15
Texas	0.01–15
Wyoming	<1–110

production) was recovered from these materials in 1985 (Kuck, 1987). Most of this vanadium is produced by processing ash from powerplants. Recovery of vanadium from this material was started by Long Island Light Company in 1964 (Kuck, 1985). Refineries that process heavy oils concentrate the sulfur, refractory organic compounds, and metals in a residual petroleum coke that is sometimes burned to provide process heat for the refinery. The ash generated from burning the residue commonly contains as much as 8 percent vanadium. Primary vanadium is also recovered by reprocessing catalysts used in petroleum refining. Metals and refractory organic compounds plate on the catalysts until they amount to 50 percent of the weight of the catalyst and poison the active surfaces. This occurs even in refining oils that have low metal contents. Currently, facilities in Japan and Texas produce vanadium by reprocessing catalysts, and planned increases in capacity will add the capability of producing an additional 2,300 t of vanadium per annum in the United States alone (Metals Week, 1986).

Most of the ash and petroleum coke treated for the recovery of vanadium is from vanadium-rich Venezuelan oil. Kapo (1978) estimated that the amount of vanadium annually added to the environment as pollution from the use of Venezuelan oil is equivalent to the world's consumption of vanadium. Venezuela contains the majority of the world's heavy oil resources and also contains the largest resource of vanadium in petroleum, an estimated 10 million t (Kapo, 1978). While no oil fields of comparable extent contain the consistently high vanadium contents of the Venezuelan fields, oils with greater than 50 ppm vanadium are produced in Iran and from several fields within the United States. All of these heavy oils are processed in order to remove the metals to a residual fraction prior to refining, hence beneficiating the vanadium.

Within the United States most oils contain less than 50 ppm vanadium, making them unlikely vanadium feedstocks, though residual ashes from burning even metal-poor oils commonly contain 20 weight percent vanadium (Hyden, 1961), and a few contain as much as 40 weight percent vanadium (Yen, 1975). Major heavy oil deposits in California and Alaska contain up to 400 ppm vanadium (table 1). The heavy oil fields of California contain an estimated 37 billion barrels, about 87 percent of the heavy oil resources of the conterminous United States (International Petroleum Encyclopedia, 1985). If half of the contained vanadium is recovered, 250,000 t of vanadium could be produced, enough to satisfy the domestic vanadium requirements for 50 years at our present rate of consumption. The heavy oil resources in Alaska are not defined enough to allow evaluation of their vanadium resources.

Coal

The world average vanadium content of coal is 25 ppm (Valkovic, 1983). Vanadium abundances in ashes formed by burning coals generally range from 0.01 to 0.3 weight percent (Abernathy and Gibson, 1963), though some ashes contain almost 8 percent (Reynolds, 1948). The lower values are typical for most common coals formed from subaerial plant material. However, by comparison, rare marine sapropelic (cannel) coals may contain more than 1 percent vanadium in the raw coal (Zhang, 1985).

China is the only producer of vanadium from coal. Sapropelic coals of Cambrian age in Changyang County, Hubei Province have produced vanadium since 1977 (Wang, 1980). The extent of these deposits is unknown, but their development may have influenced China's entry into the world vanadium market as an exporter. In addition to the coals in China, sapropelic coal deposits in Venezuela contain high abundances of vanadium (Kapo, 1978).

The average content of vanadium in coals in the United States is 20 ppm (Swanson and others, 1976). Values of most mined coal deposits are less than 100 ppm, though Maylotte and others (1981) describe the upper portion of a coal layer that contains up to 1,800 ppm vanadium. As far as the author is aware, none of the major coal deposits of the United States contain vanadium abundances consistently high enough for them to be considered a vanadium resource.

Vanadium-rich material burned as a substitute for coal in Peru and Argentina during World War II was actually asphaltite, a petroliferous residue. This resinous material occurs as a fracture filling and as layers in bituminous shales. Ash generated by burning this material

Table 2. Vanadium content of bitumen recovered from selected tar sands deposits

[Numbers in parantheses indicate the following references: (1) Peer, 1981; (2) Harrison and others, 1981; (3) Ondish and Suchanek, 1981; and (4) Martin and others, 1984]

Location	Vanadium (ppm)	
Canada		
Athabasca basin	180–290	(1)
United States		
Northeastern Oklahoma	14	(2)
Southern Oklahoma	200	(2)
Uinta basin, Utah	20–70	(1)
Ulvalde, Texas	126	(3)
Southern Texas	85	(4)

contained up to 14 percent vanadium, but Kett (1948) determined that these deposits were small and too discontinuous to be mined economically solely for the production of vanadium.

Tar Sands

Asphaltite deposits, particularly tar sands, are substantial vanadium resources. Although no commercial facilities are producing vanadium from these deposits at present, plans have been prepared to recover vanadium by processing ash generated from one of the operations that recovers oil from the tar sands in Alberta, Canada (Northern Miner, 1984). The tar sand deposits in Alberta are the world's largest and contain oil resources of 2 trillion barrels (Koch, 1982). The bitumen in the tar sands contains about 250 ppm vanadium, whereas the ash formed during processing has a maximum of 2.5 percent vanadium. Estimates indicate that the proposed plant could produce 850 t of vanadium per year from the 33,000 t of fly ash generated in the production of 20 million barrels of oil (Northern Miner, 1984). Plans for vanadium plants at other tar sand operations in Alberta are under study.

Measured and speculative tar sand resources in the United States contain about 53.7 billion barrels of bitumen (Lewin and Associates, 1984). The largest tar sand deposits occur in Utah, Alaska, Alabama, California, and Texas. Test production of bitumen has been done for several deposits (Marchant and Koch, 1982), though no recovery of contained metals has been described. The limited data on the vanadium contents of these bitumens indicate a range of values (table 2). The Uinta basin in Utah hosts the largest domestic tar sand deposits, about 20 billion barrels. However, the vanadium content of oil recovered from these deposits is low and is comparable to the content of the Eocene Green River Formation (table 3), the probable source rock. Deposits in California, Oklahoma, and Texas contain greater amounts of vanadium than the Utah deposits, although less than the Alberta tar sands.

Table 3. Vanadium and oil content of selected oil shales

[Numbers in parentheses designate the following references: (1) Tuttle and others, 1983; (2) Ingram and others, 1983; (3) Robl and others, 1983; (4) Desborough and others, 1981; (5) Derkey and others, 1985; (6) Glikson and others, 1985; (7) Lindner, 1983; (8) Mining Journal, 1974; and (9) Shirav and Ginzburg, 1983]

Oil shale	Vanadium (ppm)		Oil content Fischer assay (gal/ton)
United States:			
Green River Formation.	80	(1)	30 (2)
Ohio Shale	1,400	(3)	12 (3)
Heath Formation	25–8,000	(4,5)	10 (5)
Australia:			
Rundle Formation	110	(6)	26 (7)
Condor deposit	100	(6)	18 (7)
Toolebuc Formation	1,000–2,000	(6)	16 (8)
Israel:			
Ghareb Formation	110	(9)	16 (9)

Oil Shale

Vanadium contents of oil shales range from 25 to 8,000 ppm (table 3). The highest vanadium contents are contained in marine deposits; this is the same relation observed in coal deposits. A plant in Nanjing, China, is the only reported producer of vanadium from residues of processed oil shale (Kuck, 1984). The feedstock for this plant probably originated from the extensive Fushun or Maoming oil shale deposits (Wang, 1980). Although vanadium is currently produced from only one plant, plans for the coproduction of this metal from oil shale have been considered for Devonian black shales in the Eastern United States (Chase, 1980; Leventhal and Kepferle, 1982), oil shales in Estonia (Mining Magazine, 1985), and the Toolebuc Formation, in Australia (Mining Journal, 1974).

The vanadium resources of the Cretaceous Toolebuc Formation near Julia Creek, Queensland, Australia, are the world's largest such resources contained in oil shale, with average grades of 0.2 percent vanadium in the shales containing the most oil. The deposit contains an estimated 4×10^9 t of oil shale (Stewart, 1983), which may contain 8×10^6 t of vanadium. Plans were prepared for the construction of a plant to produce 10,000 t of vanadium per year along with the oil (Mining Journal, 1974).

The Mississippian Heath Formation in Montana and Devonian black shales in the Eastern United States have the greatest potential for the production of vanadium and other metals as byproducts of shale oil in the United States. The Green River Formation, the richest oil-shale deposit in the United States, is an unlikely producer since it has relatively low vanadium contents, <100 ppm (Tuttle and others,

1983). The Heath Formation covers about 7,000 km^2 of central Montana (Desborough and others, 1981). If 0.1 percent of the vanadium in the Heath Formation were recovered, it would amount to 24,000 t of vanadium (Derkey and others, 1985). Devonian black shales including the Sunbury Shale, Ohio Shale, Chattanooga Shale, and others in the East-Central United States (Robl and others, 1983) contain a huge volume of low-grade oil shale, although only a small percentage can be developed by near-surface mining. Estimates indicate that 8,000 t of vanadium could be produced annually from an operation processing 90,000 t of oil shale per day (Leventhal and Kepferle, 1982).

The production of vanadium from oil shales is likely only if the oil shale is developed by mining as opposed to in situ methods. The form of the vanadium in the shales varies, and it may not be extractable by the in situ methods capable of extracting the oil. Thus, recovery of metals from oil shale will require processing the rock after the oil is extracted.

FORM OF VANADIUM

The recovery of vanadium from the organic-rich geologic materials depends on the compound in which the metal occurs and how it is bonded. Three valences of vanadium exist under natural conditions; V(V), V(IV), and V(III) (Wanty, 1986). The chemically reducing nature of humic materials enables them to reduce V(V) to V(IV) under most pH conditions (Szalay and Szilagyi, 1967). Consistent with these data, extensive electron spin resonance and other instrumental studies indicate that most of the vanadium in natural organic compounds, such as that contained in fossil fuels, is present as VO^{2+} (Saraceno and others, 1961; Filby, 1975). The association of vanadium with organic material is due to favorable bonding characteristics of VO^{2+} with functional groups containing nitrogen, oxygen, or sulfur.

Vanadium in petroleum and tar sands is contained in an oil-soluble form including several different organic complexes, but porphyrins (tetrapyrroles) are the most abundant (Yen, 1975). The proportion of vanadium in petroleum contained in the porphyrin compounds is uncertain, but estimates range from 60 to 100 percent (Speight, 1980; Spencer and others, 1982; Crouch and others, 1983; Fish and Komlenic, 1984; Goulon and others, 1984). The porphyrins are altered molecules of chlorophyll or hemoglobin that originated in plants and animals (Baker and Louda, 1981). Four nitrogen ligands in the center of the porphyrin molecule bond with the vanadium forming a very stable complex. The stability of the structure enables it to resist breakdown at temperatures as high as 300 °C and under conditions of near-surface weathering (Lewan, 1980). Apparently, the vanadium porphyrins are bound to larger organic molecules characterized as asphaltenes (Baker and Louda, 1981), hence the metals concentrate with the refractory compounds during refining.

In oil shales and coal, vanadium also occurs in porphyrins and other organic complexes, including oxygen-rich compounds (Maylotte and others, 1981). The association of vanadium with oxygen-rich functional groups is consistent with epigenetic enrichment described in the following section. In addition to organic complexes, vanadium occurs in silicates, sulfides, and oxides. Vanadium minerals are probably the result of changes during diagenesis in which some vanadium moved from sites in the organic compounds into forming authigenic phases. One of the vanadiferous authigenic minerals in coal (Finkelman, 1981) and oil shale is roscoelite, a vanadiferous mica. Other authigenic phases include sulvanite (Cu_3VS_4) (Fan, 1983) and an unidentified iron-vanadium-titanium oxide (Desborough and Poole, 1983).

MECHANISMS OF VANADIUM ENRICHMENT

Vanadium is uniformly distributed throughout the Earth's crust; most rocks contain between 20 and 250 ppm. The high vanadium content in certain fossil fuels implies that processes that favored the accumulation of some organic material also favored the concentration of vanadium or that vanadium was extracted from migrating ground waters during diagenesis. However, many otherwise similar accumulations of organic matter lack high vanadium contents. Thus, understanding the processes and conditions under which vanadium is enriched could aid in identifying vanadium resources.

The vanadium content of fossil fuels was apparently acquired from an aqueous phase because the lithic components of the coal, oil shale, and petroleum source rocks have normal abundances of vanadium. The accumulation could have occurred during the growth of the organisms that were precursors to the organic matter, by selective extraction of vanadium by particles settling through the water column, or from pore waters during diagenesis. Solutions that may have provided the vanadium include seawater, meteoric ground water, and volcanic exhalations.

Vanadium enrichment in petroleum and coal has been considered epigenetic, the result of interaction between the organic accumulations and circulating waters (Elder, 1973). Heavy oil is generally considered to have been altered by biodegradation of "normal" petroleum (Tissot and Welte, 1984). The biodegradation is enhanced by the through flow of oxygenated ground waters, which may have also supplied the vanadium. Experimental studies, however, have shown that vanadium is not adsorbed by petroleum (Gulyayeva and Lositskaya, 1968). In addition, the constant V/Ni ratio in petroleum and source rocks indicates that the vanadium content was controlled by the source rocks and,

hence, by the depositional environment (Lewan, 1980). On the other hand, a portion of the vanadium in many coal deposits accumulated largely by interaction with ground water. Zilbermintz (1935) attributed the high vanadium contents of coals in the Ural Mountains to waters transporting vanadium that was weathered from mafic massifs containing vanadiferous magnetite deposits. The interaction of the coal macerals with the oxygenated ground waters resulted in the oxidation of the organic matter, which then adsorbed the dissolved vanadium, bonding it to the coal. With the exception of coal, most of the vanadium in fossil fuels accumulated during deposition of the organic precursors. Therefore, this discussion emphasizes characteristics of environments where organic matter accumulated.

A notable characteristic of the most vanadium-rich oil shales, petroleum accumulations, and coals, is that they are or were derived from deposits composed mostly of marine-derived organic matter. This restriction implies that seawater, the composition of marine organic matter, or indigenous organisms were somehow essential to the accumulation of vanadium. The influence of the composition of the organic matter and the abundance of vanadium were examined by Lewan (1980), who determined that the highest contents are associated with deposits that were originally plankton or algae, organisms abundant in a marine environment.

Plankton may have accumulated vanadium during their life cycle, particularly because phytoplankton contain abundant chlorophyll, the likely precursor of the porphyrins common in fossil fuels. Vanadium contents of plankton average 25 ppm (Knauss and Ku, 1983). Therefore, accumulations containing 500 ppm vanadium could form simply by loss of 95 percent of the organic constituents of the plankton. If these organisms were the pathway of metal accumulation, certain metals should be selectively concentrated because of biochemical selectivity in the living organisms. Instead, a comparison of the abundance of metals in organic-rich shales with the concentration of metals in seawater suggests enrichment factors are constant, independent of the metal considered (Holland, 1979).

The presence of vanadium in porphyrins restricts the probable conditions in which the organic matter could have accumulated and therefore is an indicator of the depositional environment of the host sediments. The porphyrins were most likely formed by modification of chlorophyll as it settled through the water column and during diagenesis (Baker and Louda, 1981). Chlorin, a demetallated form of chlorophyll (magnesium is removed) is relatively abundant in marine sediments deposited in anoxic conditions (Baker and Louda, 1981). In aerated seawater, these compounds decompose rapidly. This fact implies that much of the water column overlying the deposits was anoxic or that the organic matter settled through the water column very rapidly, before oxidation could occur. Baker and Louda (1981) also concluded that chelation of vanadium by porphyrins may not occur until shallow burial. This finding most likely indicates that vanadium was initially bound to the sediments by adsorption and weak complexes and was later redistributed during early diagenesis.

Other organisms known to concentrate vanadium, up to 5 percent on a dry weight basis, are members of the order Tunicata (Glikson and others, 1985). These sessile, benthic creatures may have once been abundant in the ocean, but it is doubtful that they could have survived in the anoxic conditions ambient during the deposition and preservation of the organic matter, and therefore they are unlikely as the sole accumulators of vanadium. Nevertheless, abundant tunicate fossils have been observed in the vanadium-rich coals in China (Zhang, 1985).

Adsorption to particle surfaces is considered the major mechanism of vanadium removal from seawater (Amdurer and others, 1983). Adsorption processes are particularly effective in environments where V(V) (the dominant valence in aerated waters) is reduced to V(IV), as observed in an estuarine environment (van der Sloot and others, 1985). Anoxic conditions favoring the preservation of porphyrins would be sufficiently reducing to convert V(V) to V(IV). Thus the accumulation of organic matter under an at least partially anoxic water column may have been required for preferential accumulation of vanadium. It is notable that several recent marine deposits of organic matter, composed mainly of plankton remains, are not particularly enriched in metals including vanadium (Nissenbaum and Swaine, 1976). The low vanadium content of these recent sediments may indicate that the overlying water columns were not sufficiently reducing or that vanadium actually accumulates by diffusion of bottom waters through the sediment over relatively long periods (Lewan, 1980).

Holland (1979) argued that the relatively constant enrichment factor of metals (including vanadium) in carbonaceous marine shales favored accumulation directly from normal seawater. The present concentration of vanadium in seawater is about 0.002 ppm (Riley and Taylor, 1972). To concentrate the vanadium in a layer of sediment to 1,000 ppm, a column of water at least 1×10^6 times the thickness of the layer is required. Therefore, waters that formed oil shales in shallow, restricted basins, such as the Heath Formation and the Toolebuc Formation (less than 50 m deep), either contained higher abundances of vanadium or were subject to the circulation of large volumes of water. The latter seems unlikely considering that both units were deposited in restricted basins.

Some researchers have suggested that the vanadium was supplied by volcanic exhalations on the sea floor. This concept is consistent with the observed vanadium enrichment near ocean ridges (Hodkinson and others, 1986; Marchig and others, 1986). Bostrom and Fisher (1971) examined the variation in vanadium abundance in the Indian Ocean and concluded that volcanogenic and terrestrial sources of vanadium were important. Nevertheless, a sub-

marine volcanogenic source for all vanadium-rich fossil-fuel accumulations is precluded by those accumulations that formed in restricted, shallow basins, apparently isolated from hydrothermal vents.

Not all marine deposits are enriched in vanadium (several oil shales and some petroleums of marine origin contain relatively low vanadium contents), implying that secondary controls within the marine environment are also important. For example, the Toolebuc Formation in Australia and the Ghareb Formation in Israel have substantially different vanadium contents (table 3) even though both were deposited in shallow cratonic basins during the Cretaceous. In addition, oils recovered from Miocene rocks in California (150 ppm V) and Venezuela (350 ppm) have significantly different vanadium contents. Both of these oils are heavy (API less than 20°), and although they have other compositional differences, the difference in vanadium abundances is particularly striking.

The variation in the vanadium abundance may be related to differences in the composition of the rocks surrounding the basin. Kapo (1978) suggested that the high vanadium content in Venezuelan oil and coal was due to a source in surrounding uplands. Wedepohl (1964) proposed that metals enriched in the bituminous shales of the Kupferschiefer originated from the dissolution of iron oxides in the red bed units surrounding the sea. Hite (1978) similarly proposed that the evaporation of seawater and the interaction of the resultant brines with clastic deposits resulted in a metal-rich brine that enriched the Permian Phosphoria Formation (locally a low-grade oil shale) in metals, including vanadium.

Fossil fuels having high vanadium contents have been deposited in variable amounts throughout geologic time; therefore, it is unsatisfying to explain the variation in the vanadium content of these deposits as the result of changes in the composition of seawater. The amount of vanadium is also apparently unrelated to specific depositional settings because carbon-rich rocks deposited in geosynclines, in cratonic basins, and in shelf environments all have high vanadium contents in some locations. As shown in this discussion, factors that controlled the vanadium contents of fossil fuels are poorly understood.

SUMMARY

Production of vanadium from fossil fuels will depend heavily on the type of materials developed to meet the world's future energy needs. Large resources of vanadium are contained in the heavy oil deposits in Venezuela, coal in China, oil shale in Australia, and tar sands in Canada. In the United States, heavy oil deposits in California and possibly those in Alaska are the most likely fossil-fuel accumulations capable of producing substantial amounts of vanadium in the future. Low-grade oil shale deposits in Montana and Kentucky could produce large amounts of vanadium, but their development seems unlikely.

Vanadium is contained in fossil fuels as oil-soluble organovanadium compounds and in minerals. The oil-soluble vanadium in petroleum can be concentrated by normal processing, generating a residue amenable for vanadium recovery. In oil shales and in coal, vanadium is also contained in minerals. The mineral residence of vanadium in oil shale will limit recovery of the metal by any in situ method of oil production.

The mechanisms that cause vanadium to accumulate in fossil fuels are not well understood. The highest abundances occur in fossil fuels that originated as organic-rich deposits in a marine environment. Evidence strongly suggests that the type of organic matter, chemical conditions in the overlying water column, and interaction of seawater with clastic sediments may have been significant with regard to the accumulation of vanadium.

The drop in the price of crude oil in the mid-1980's slowed development of more expensive, vanadium-rich fossil fuels described in this paper. However, projections of future demand indicate that these resources will be developed. Therefore, vanadium produced from fossil fuels including petroleum, tar sands, coal, and oil shale should be considered in any long-term evaluation of vanadium supplies.

REFERENCES

Abernathy, R.F., and Gibson, F.H., 1963, Rare elements in coal: U.S. Bureau of Mines Information Circular 8163, 69 p.

Amdurer, M., Adler, D., and Santschi, P.H., 1983, Studies of the chemical forms of trace elements in sea water using radiotracers, *in* Wong, C.S., Boyle, Edward, Bruland, K.W., Burton, J.D., and Goldberg, E.D., eds., Trace metals in sea water: New York, Plenum Press, p. 537–562.

Baker, E.W., and Louda, J.W., 1981, Thermal aspects in chlorophyll geochemistry *in* Bjoroy, M., and others, eds., Advances in organic geochemistry: New York, Wiley and Sons, p. 401–421.

Bostrom, Kurt, and Fisher, D.E., 1971, Volcanogenic uranium, vanadium and iron in Indian Ocean sediments: Earth and Planetary Science Letters, v. 11, p. 95–98.

Chase, C.K., 1980, The Chattanooga and other Devonian shales—The United States' largest uranium source, *in* Tarman, P.B., chairman, Synthetic fuels from oil shale: Chicago, Institute of Gas Technology, p. 547–578.

Crouch, F.W., Sommer, C.S., Galobardes, J.F., Kraus, Shmuel, Schmauch, E.H., Galobardes, Mercedes, Fatmi, Aqeel, Pearsall, Kenneth, and Rogers, L.B., 1983, Fractionations of nonporphyrin complexes of vanadium and nickel from Boscan crude oil: Separation Science and Technology, v. 18, p. 603–634.

Derkey, P.D., Abercrombie, F.N., Vuke, S.M., and Daniel, J.A., 1985, Geology and oil shale resources of the Heath

Formation, Fergus County, Montana: Montana Bureau of Mines and Geology Memoir 57, 100 p.

Desborough, G.A., and Poole, F.G., 1983, Metal concentrations in some marine black shales of the United States, *in* Shanks, W.C., ed., Cameron volume on unconventional mineral deposits: New York, American Institute of Mining, Metallurgical and Petroleum Engineers, p. 99–110.

Desborough, G.A., Poole, F.G., and Green, G.N., 1981, Metalliferous oil shales in central Montana and northeastern Nevada: U.S. Geological Survey Open-File Report 81–121, 14 p.

Elder, E., 1973, Geochemistry of inorganic trace elements in petroleum, *in* Kapo, George, ed., International symposium on vanadium and other metals in petroleum, Proceedings, v. 2, article 1: Maracaibo, Venezuela, Universidad Del Zulia, 9 p.

Fan Delian, 1983, Polyelements in the lower Cambrian black shale series in southern China, *in* Augustithis, S.S., ed., The significance of trace elements in solving petrogenetic problems & controversies: Athens, Greece, Theophrastus Publications, S.A., p. 447–474.

Filby, R.F., 1975, The nature of metals in petroleum, *in* Yen, T. F., ed., The role of trace metals in petroleum: Ann Arbor, Michigan, Ann Arbor Science Publishers, p. 31–58.

Finkelman, R.B., 1981, Modes of occurrence of trace elements in coal: U.S. Geological Survey Open-File Report 81–099, 301 p.

Fish, R.H., and Komlenic, J.J., 1984, Molecular characterization and profile identifications of vanadyl compounds in heavy crude petroleums by liquid chromatography/graphite furnace atomic absorption spectrometry: Analytical Chemistry, v. 56, p. 510–517.

Glikson, M., Chappell, B.W., Freeman, R.S., and Webber, E., 1985, Trace elements in oil shales, their source and organic association with particular reference to Australian deposits: Chemical Geology, v.53, p. 155–174.

Goulon, Jose, Retournard, Alain, Friant, Pascale, Goulon-Ginet, Chantal, Berthe, Christine, Muller, Jean-Francois, Poncet, Jean-Luc, Guilard, Roger, Escalier, Jean-Claude, and Neff, Bernard, 1984, Structural characterization by X-ray absorption spectroscopy (EXAFS/XANES) of the vanadium chemical environment in Boscan asphaltenes: Journal of the Chemical Society, Dalton Transactions, no. 6, p. 1095–1103.

Gulyayeva, L.A., and Lositskaya, I.F., 1968, Interaction between petroleum and vanadium in aqueous solutions: Geochemistry International, v. 4, p. 699–709.

Harrison, W.E., Mankin, C.J., Weber, S.J., and Curiale, J.A., 1981, Oil sand and heavy oil potential of Oklahoma, *in* Meyer, R.F., and Steele, C.T., eds., The future of heavy crude oils and tar sands, First International Conference: New York, McGraw-Hill, p. 83–89.

Hilliard, H.F., 1987, Vanadium, *in* U.S. Bureau of Mines, mineral commodity summaries 1987: Washington, D.C., U.S. Government Printing Office, p. 174–175.

Hite, R.J., 1978, Possible genetic relationships between evaporites, phosphorites and iron-rich sediments: Mountain Geologist, v. 14, no. 3, p. 97–107.

Hodkinson, R., Cronan, D.S., Glasby, G.P., and Moorby, S.A., 1986, Geochemistry of marine sediments from the Lau Basin, Havre Trough, and Tonga-Kermadec Ridge: New Zealand Journal of Geology and Geophysics, v. 29, p. 335–344.

Holland, H.D., 1979, Metals in black shales—A reassessment: Economic Geology, v. 74, no. 7, p. 1676–1680.

Hyden, H.J., 1961, Distribution of uranium and other metals in crude oils, *in* Uranium and other metals in crude oils: U.S. Geological Survey Bulletin 1100, p. 17–97.

Ingram, L.L., Ellis, J., Crisp, P.T., and Cook, A.C., 1983, Comparative study of oil shales and shale oils from the Mahogany zone, Green River Formation (U.S.A.) and Kerosene Creek Seam, Rundle Formation (Australia): Chemical Geology, v. 38, p. 185–212.

International Petroleum Encyclopedia, 1985, Heavy oil changing the face of the industry, *in* International petroleum encyclopedia 1985: Tulsa, Oklahoma, PennWell Publishing Company, p. 326–343.

Kapo, George, 1978, Vanadium—Key to Venezuelan fossil hydrocarbons, *in* Chilingarian, G.V., and Yen, T.F., eds., Bitumens, asphalts and tar sands; Developments in petroleum science no. 7: New York, Elsevier, p. 213–241.

Kett, F.F., 1948, The vanadium-bearing solid bitumens of the Argentine: The Vancorum Review, v. 6, p. 3–21.

Knauss, Kevin, and Ku, Teh-lung, 1983, The elemental composition and decay-series radionuclide content of plankton from the east Pacific: Chemical Geology, v. 39, p. 125–145.

Koch, C.A., 1982, The oil resources in tar sand deposits in the United States *in* Ball, Douglas, Marchant, L.C., and Goldburg, Arnold, eds., The IOCC monograph series—Tar sands: Oklahoma City, Oklahoma, Interstate Oil Compact Commission, p. 19–26.

Kuck, P.H., 1984, Vanadium, *in* U.S. Bureau of Mines, Minerals yearbook 1983, v.1, Metals and minerals: Washington D.C., U.S. Government Printing Office, p. 912.

———1985, Vanadium, *in* Mineral facts and problems 1985 ed.: U.S. Bureau of Mines Bulletin 675, p. 895–915.

———1987, Vanadium, *in* U.S. Bureau of Mines, Minerals yearbook 1985, v.1, Metals and minerals: Washington D.C., U.S. Government Printing Office, p. 1007–1027.

Leventhal, J.S., and Kepferle, R.C., 1982, Geochemistry and geology of strategic metals and uranium in Devonian shales of the eastern interior United States, *in* Long, G.M., dir., Synthetic fuels from oil shale II: Chicago, Institute for Gas Technology, p. 73–95.

Lewan, M.D., 1980, Geochemistry of vanadium and nickel in organic matter of sedimentary rocks: unpublished Ph.D. thesis, University of Cincinnati, 353 p.

Lewin and Associates, Inc., 1984, Major tar sand and heavy oil deposits of the United States: Oklahoma City, Oklahoma, Interstate Oil Compact Commission, 272 p.

Lindner, A.W., 1983, Geology and geochemistry of some Queensland Tertiary oil shales, *in* Miknis, F.P., and McKay, J.F., eds., Geochemistry and chemistry of oil shales: American Chemical Society Symposium Series 230, p. 97–118.

Marchant, L.C., and Koch, C.A., 1982, U.S. tar sand oil recovery projects, *in* Ball, Douglas, Marchant, L.C., and Goldburg, Arnold, eds., The IOCC monograph series—Tar sands: Oklahoma City, Oklahoma, Interstate Oil Compact Commission, p. 191–200.

Marchig, Vesna, Erzinger, Jorg, and Heinze, P.M., 1986, Sediment in the black smoker area of the East Pacific Rise (18.5°S): Earth and Planetary Science Letters, v. 79, p. 93–106.

Martin, W.L., Britton, M.W., and Harmon, R.A., 1984, Conoco's south Texas tar sands project, *in* Meyer, R.F., Wynn, J.C., and Olson, J.C., The future of heavy crude oil and tar sands, Second International Conference: New York, McGraw-Hill, p. 987–997.

Maylotte, D.H., Wong, J., St. Peters, R.L., St., Lytle, F.W., and Greegor, R.B., 1981, X-ray absorption spectroscopic investigation of trace vanadium sites in coal: Science, v. 214, no. 4520, p. 554–556.

Metals Week, 1986, Catalyst reclaimers are hot property: Metals Week, v. 57, no. 25, p.1.

Mining Journal, 1974, Queensland oil shale venture: Mining Journal (London), v. 282, no. 7228, p. 158.

Mining Magazine, 1985, Estonia's oil-shales—Their characteristics and utilization: Mining Magazine, v. 152, p. 100.

Nelson, W.L., 1972, How much metals in crude oils: Oil and Gas Journal, v. 70, no. 32, p. 48–49.

Nissenbaum, Arie, and Swaine, D.J., 1976, Organic matter-metal interactions in Recent sediments: The role of humic substances: Geochimica et Cosmochimica Acta, v. 40, p. 809–816.

Northern Miner, 1984, Recovery of vanadium from oil sands plant; the first in Canada: Northern Miner, v. 70, no. 1, p. 1.

Ondish, G.R., and Suchanek, A.J., 1981, Potential for Gulf residual HDS in upgrading very heavy crudes, *in* Meyer, R.F., and Steele, C.T., eds., The future of heavy crude oils and tar sands, first international conference: New York, McGraw-Hill, p. 663–669.

Peer, E.L., 1981, United States refineries and their adaptability to process heavy crude oil, *in* Meyer, R.F., and Steele, C.T., eds., The future of heavy crude oils and tar sands, first international conference: New York, McGraw-Hill, p. 651–654.

Reynolds, F.M., 1948, The occurrence of vanadium, chromium, and other unusual elements in certain coals: Journal of the Society of Chemical Industry, v. 67, p. 341–345.

Riley, J.P., and Taylor, D., 1972, The concentrations of cadmium, copper, iron, manganese, molybdenum, nickel, vanadium and zinc, in part of the tropical north-east Atlantic Ocean: Deep Sea Research, v. 19, p. 307–317.

Robl, T.L., Bland, A.E., Koppenaal, D.W., and Barron, L.S., 1983, Geochemistry of oil shales in eastern Kentucky, *in* Miknis, F.P. and McKay, J.F., eds., Geochemistry and chemistry of oil shales: American Chemical Society Symposium Series 230, p. 159–180.

Saraceno, A.J., Fanale, D.T., and Coggeshall, N.D., 1961, An electron paramagnetic resonance investigation of vanadium in petroleum oils: Analytical Chemistry, v. 33, p. 500–505.

Shirav, M., and Ginzburg, D., 1983, Geochemistry of Israeli oil shales, *in* Miknis, F.P., and McKay, J.F., eds., Geochemistry and chemistry of oil shales: American Chemical Society Symposium Series 230, p. 85–96.

Speight, J.G., 1980, The chemistry and technology of petroleum: New York, Marcel Dekker, 498 p.

Spencer, W.A., Galobardes, J.F., Curtis, M.A., and Rogers, L.B., 1982, Chromatographic studies of vanadium compounds from Boscan crude oil: Separation Science and Technology, v. 17, p. 797–819.

Stewart, G.N., 1983, Australia, *in* Mining annual review 1983: London, Mining Journal, p. 330–345.

Swanson, V.E., Medlin, J.H., Hatch, J.R., Coleman, S.L., Wood, G.H., Woodruff, S.D., and Hildebrand, R.T., 1976, Collection, chemical analysis and evaluation of coal samples in 1975: U.S. Geological Survey Open-File Report 76–468, 503 p.

Szalay, A., and Szilagyi, M., 1967, The association of vanadium with humic acids: Geochimica et Cosmochimica Acta, v. 31, p. 1–6.

Tissot, B.P., and Welte, D.H., 1984, Petroleum formation and occurrence (2d ed.): New York, Springer-Verlag, 699 p.

Tuttle, M.L., Dean, W.E., and Parduhn, N.L., 1983, Inorganic geochemistry of Mahogany zone oil shale in two cores from the Green River Formation, *in* Miknis, F.P., and McKay, J.F., eds, Geochemistry and chemistry of oil shales: American Chemical Society Symposium Series 230, p. 249–267.

Valkovic, Vlado, 1983, Trace elements in coal, v. 1: Boca Raton, Fla., CRC Press, 210 p.

van der Sloot, H.A., Hoede, D., Wijkstra, J., Duinker, J.C., and Nolting, R.F., 1985, Anionic species of V, As, Se, Mo, Sb, Te and W in the Scheldt and Rhine estuaries and southern Bight (North Sea): Estuarine, Coastal and Shelf Science, v. 21, p. 633–651.

Wang, K.P., 1980, China, *in* Mining annual review 1980: London, Mining Journal, p. 456–451.

Wanty, R.B., 1986, Geochemistry of vanadium in an epigenetic sandstone-hosted vanadium-uranium deposit, Henry basin, Utah: unpublished Ph.D. thesis, Colorado School of Mines, 196 p.

Wedepohl, K.H., 1964, Untersuchungen am Kupferschiefer in Nordwestdeutschland; Ein Beitrag zur Deutung der Genese bituminoser Sedimente: Geochimica et Cosmochimica Acta, v. 28, p. 305–364.

Whisman, M.L., and Cotton, F.O., 1971, Bumines data promise help in identifying petroleum-spill sources: Oil and Gas Journal, v. 69, no. 52, p. 111–113.

Yen, T.F., 1975, Chemical aspects of metals in native petroleum, *in* Yen, T.F., ed., The role of trace metals in petroleum: Ann Arbor, Michigan, Ann Arbor Science Publishers, p. 1–30.

Zhang Aiyun, 1985, The geochemistry of vanadium in the marine black rock sequence of Yangjiabao, *in* International Congress on Carboniferous Stratigraphy and Geology 10, v. 2, p. 31–42.

Zilbermintz, V., 1935, On the occurrence of vanadium in fossil coals: Comptes Rendus (Doklady) de l'Academie des Sciences de l'URSS, v. 8 no. 3, p. 117–120.

SELECTED SERIES OF U.S. GEOLOGICAL SURVEY PUBLICATIONS

Periodicals

Earthquakes & Volcanoes (issued bimonthly).
Preliminary Determination of Epicenters (issued monthly).

Technical Books and Reports

Professional Papers are mainly comprehensive scientific reports of wide and lasting interest and importance to professional scientists and engineers. Included are reports on the results of resource studies and of topographic, hydrologic, and geologic investigations. They also include collections of related papers addressing different aspects of a single scientific topic.

Bulletins contain significant data and interpretations that are of lasting scientific interest but are generally more limited in scope or geographic coverage than Professional Papers. They include the results of resource studies and of geologic and topographic investigations, as well as collections of short papers related to a specific topic.

Water-Supply Papers are comprehensive reports that present significant interpretive results of hydrologic investigations of wide interest to professional geologists, hydrologists, and engineers. The series covers investigations in all phases of hydrology, including hydrogeology, availability of water, quality of water, and use of water.

Circulars present administrative information or important scientific information of wide popular interest in a format designed for distribution at no cost to the public. Information is usually of short-term interest.

Water-Resources Investigations Reports are papers of an interpretive nature made available to the public outside the formal USGS publications series. Copies are reproduced on request unlike formal USGS publications, and they are also available for public inspection at depositories indicated in USGS catalogs.

Open-File Reports include unpublished manuscript reports, maps, and other material that are made available for public consultation at depositories. They are a nonpermanent form of publication that may be cited in other publications as sources of information.

Maps

Geologic Quadrangle Maps are multicolor geologic maps on topographic bases in 7.5- or 15-minute quadrangle formats (scales mainly 1:24,000 or 1:62,500) showing bedrock, surficial, or engineering geology. Maps generally include brief texts; some maps include structure and columnar sections only.

Geophysical Investigations Maps are on topographic or planimetric bases at various scales; they show results of surveys using geophysical techniques, such as gravity, magnetic, seismic, or radioactivity, which reflect subsurface structures that are of economic or geologic significance. Many maps include correlations with the geology.

Miscellaneous Investigations Series Maps are on planimetric or topographic bases of regular and irregular areas at various scales; they present a wide variety of format and subject matter. The series also includes 7.5-minute quadrangle photogeologic maps on planimetric bases that show geology as interpreted from aerial photographs. Series also includes maps of Mars and the Moon.

Coal Investigations Maps are geologic maps on topographic or planimetric bases at various scales showing bedrock or surficial geology, stratigraphy, and structural relations in certain coal-resource areas.

Oil and Gas Investigations Charts show stratigraphic information for certain oil and gas fields and other areas having petroleum potential.

Miscellaneous Field Studies Maps are multicolor or black-and-white maps on topographic or planimetric bases on quadrangle or irregular areas at various scales. Pre-1971 maps show bedrock geology in relation to specific mining or mineral-deposit problems; post-1971 maps are primarily black-and-white maps on various subjects such as environmental studies or wilderness mineral investigations.

Hydrologic Investigations Atlases are multicolored or black-and-white maps on topographic or planimetric bases presenting a wide range of geohydrologic data of both regular and irregular areas; principal scale is 1:24,000, and regional studies are at 1:250,000 scale or smaller.

Catalogs

Permanent catalogs, as well as some others, giving comprehensive listings of U.S. Geological Survey publications are available under the conditions indicated below from the U.S. Geological Survey, Books and Open-File Reports Section, Federal Center, Box 25425, Denver, CO 80225. (See latest Price and Availability List.)

"Publications of the Geological Survey, 1879–1961" may be purchased by mail and over the counter in paperback book form and as a set of microfiche.

"Publications of the Geological Survey, 1962–1970" may be purchased by mail and over the counter in paperback book form and as a set of microfiche.

"Publications of the U.S. Geological Survey, 1971–1981" may be purchased by mail and over the counter in paperback book form (two volumes, publications listing and index) and as a set of microfiche.

Supplements for 1982, 1983, 1984, 1985, 1986, and for subsequent years since the last permanent catalog may be purchased by mail and over the counter in paperback book form.

State catalogs, "List of U.S. Geological Survey Geologic and Water-Supply Reports and Maps For (State)," may be purchased by mail and over the counter in paperback booklet form only.

"Price and Availability List of U.S. Geological Survey Publications," issued annually, is available free of charge in paperback booklet form only.

Selected copies of a monthly catalog "New Publications of the U.S. Geological Survey" are available free of charge by mail or may be obtained over the counter in paperback booklet form only. Those wishing a free subscription to the monthly catalog "New Publications of the U.S. Geological Survey" should write to the U.S. Geological Survey, 582 National Center, Reston, VA 22092.

Note.—Prices of Government publications listed in older catalogs, announcements, and publications may be incorrect. Therefore, the prices charged may differ from the prices in catalogs, announcements, and publications.